



PHD

Inhibitors of DNA repair processes as potentiating drugs in cancer radiotherapy and chemotherapy

Watson, Corrine Yvonne

Award date:
1997

Awarding institution:
University of Bath

[Link to publication](#)

Alternative formats

If you require this document in an alternative format, please contact:
openaccess@bath.ac.uk

Copyright of this thesis rests with the author. Access is subject to the above licence, if given. If no licence is specified above, original content in this thesis is licensed under the terms of the Creative Commons Attribution-NonCommercial 4.0 International (CC BY-NC-ND 4.0) Licence (<https://creativecommons.org/licenses/by-nc-nd/4.0/>). Any third-party copyright material present remains the property of its respective owner(s) and is licensed under its existing terms.

Take down policy

If you consider content within Bath's Research Portal to be in breach of UK law, please contact: openaccess@bath.ac.uk with the details. Your claim will be investigated and, where appropriate, the item will be removed from public view as soon as possible.

Inhibitors of DNA Repair Processes as Potentiating Drugs in Cancer Radiotherapy and Chemotherapy

submitted by
Corrine Yvonne Watson
for the degree of PhD
of the University of Bath
1997

The research work in this thesis has been carried out in the School of Pharmacy and Pharmacology and in the School of Biology and Biochemistry, under the supervision of Dr Michael D. Threadgill and Dr William J. D. Whish.

COPYRIGHT

Attention is drawn to the fact that copyright of this thesis rests with its author. This copy of the thesis has been supplied on condition that anyone who consults it is understood to recognise that its copyright rests with its author and that no quotation from the thesis and no information derived from it may be published without the prior written consent of the author.

This thesis may be made available for consultation within the University Library and may be photocopied or lent to other libraries for the purposes of consultation.

Corrine Y. Watson
.....
24th May 1997
.....

UMI Number: U529548

All rights reserved

INFORMATION TO ALL USERS

The quality of this reproduction is dependent upon the quality of the copy submitted.

In the unlikely event that the author did not send a complete manuscript and there are missing pages, these will be noted. Also, if material had to be removed, a note will indicate the deletion.



UMI U529548

Published by ProQuest LLC 2013. Copyright in the Dissertation held by the Author.
Microform Edition © ProQuest LLC.

All rights reserved. This work is protected against
unauthorized copying under Title 17, United States Code.



ProQuest LLC
789 East Eisenhower Parkway
P.O. Box 1346
Ann Arbor, MI 48106-1346

UNIVERSITY OF BATH		
LIBRARY		
23	1 JUL 1997	
PHD		

511 2 S17

Abstract

The effectiveness of the treatment of cancer using radiotherapy or cytotoxic drugs is limited by lack of selectivity for cancer cells. One approach towards improving cancer therapy, therefore, is to sensitise tumour cells to the cytotoxic effects of radiotherapy and chemotherapy. This can be achieved through the inhibition of DNA repair processes. Poly(ADP-ribose) polymerase (PARP) is an abundant, chromatin-bound enzyme which is activated by binding to DNA strand-breaks and catalyses the synthesis of polymers of ADP-ribose from NAD^+ . The cellular functions of PARP are not fully understood but it appears that the enzyme is involved in DNA repair. Inhibitors of PARP may, therefore, be of use in the treatment of cancer as potentiators of radiotherapy and chemotherapy. The design and synthesis of potential inhibitors of PARP has been studied. Analogues of NAD^+ with appropriately located electrophilic side chains have been synthesised as potential irreversible inhibitors of PARP.

Several novel benzamide derivatives have been synthesised and evaluated for their effect on PARP activity. Two benzamides with electrophilic side chains have been prepared. The first, 3-chloromethylbenzamide, was a moderately potent inhibitor of PARP, causing 62% inhibition at 10.5 μM . The second, 3-(oxiran-2-yl)benzamide was a very potent PARP inhibitor, one of the most potent of its benzamide class, causing 88% inhibition of PARP activity at 9.2 μM .

Various methods of synthesis of isoquinolinones have been investigated and several novel isoquinolin-1-one derivatives have been prepared. The successful preparation of 5-bromoisquinolinone and 5-iodoisquinolinone allowed investigation of the C-metallation of isoquinolinones. 3-(1-Oxoisoquinolin-5-yl)propenoic acid was prepared using the palladium-catalysed Heck reaction. This potentially irreversible inhibitor reduced PARP activity by 81% at 11.6 μM . These results indicate the potential for the development of new, more potent PARP inhibitors.

Acknowledgements

I would like to thank Dr. Mike Threadgill for his support, encouragement and enthusiasm throughout this research project.

For the provision of NMR spectra; many thanks to Mr David Wood and Mr Harry Hartell. For mass spectral data many thanks to Mr Chris Cryer.

I wish to thank Mrs Joan Whish (School of Biology and Biochemistry) for discussions and much help with the PARP inhibitory assays. Many thanks also to Dr Bill Whish and Ms Steffi Kappus (School of Biology and Biochemistry) for discussions.

I would like to thank my postgraduate and postdoctoral colleagues in labs 3.5/3.7 for their friendship, help and advice.

I acknowledge financial support from the Royal Pharmaceutical Society of Great Britain and the Wellcome Foundation in the form of a CRISP studentship.

Finally, I would like to thank my family, especially Huw, for their love and support.

Contents

Abstract		ii
Acknowledgements		iii
Contents		iv
List of Figures Schemes and Tables		vii
Abbreviations		xiv
Chapter One	Radiotherapy	1
1.1	Mechanism of Action	1
1.1.1	Cytotoxicity	3
1.1.2	DNA Damage	4
1.2	Clinical Aspects of Radiotherapy	5
1.3	Modification of Radiation Effects	6
1.3.1	Densely Ionising Radiation	6
1.3.2	Radioprotectors	6
1.3.3	Radiosensitisers	7
Chapter Two	Poly(ADP-ribose) polymerase	11
2.1	Structural Features of Poly(ADP-ribose) Polymerase	
11		
2.1.1	The DNA Binding Domain	12
2.1.2	The Automodification Domain	13
2.1.3	The Catalytic Domain	13
2.2	Enzymatic Functions of Poly(ADP-ribose) Polymerase	15
2.2.1	ADP-Ribosylation Reactions	15
2.2.1.1	Mono(ADP-ribosyl)ation	15
2.2.1.2	Poly(ADP-ribosyl)ation	16

2.2.2	Protein Acceptors of Poly(ADP-ribose)	18
2.2.3	Regulation of Poly(ADP-ribosyl)ation	19
2.2.3.1	DNA Strand Breaks	19
2.2.3.2	Poly(ADP-ribose) Glycohydrolase (PARG)	20
2.2.3.3	Automodification	22
2.2.3.4	Histones	23
2.2.3.5	Possible Mechanisms for the Role of Poly(ADP-ribose)	
	Polymerase in DNA strand-Break Rejoining.	24
2.2.3.5.1	Histone-Shuttle Mechanism	24
2.2.3.5.2	Non-histone Mechanism	26
2.3	Consequences of Poly(ADP-ribosyl)ation in the Cell	
	and Possible Functions of PARP.	29
2.3.1	Techniques used to study PARP actions	29
2.3.2	Role of PARP in Carcinogenesis	30
2.3.3	Role of PARP in Chromosome Aberrations and Sister	
	Chromatid Exchange	31
2.3.4	Role of PARP in Gene Amplification	31
2.3.5	Role of PARP in DNA Replication	31
2.3.6	Role of PARP in Cellular Differentiation	32
2.3.7	Role of PARP in Viral Replication	32
2.3.8	Role of PARP in Apoptosis	33
2.3.9	Role of PARP in DNA repair	37
Chapter 3	Inhibitors of Poly(ADP-ribose)	
	polymerase	43
3.1	Use of Poly(ADP-ribose) Polymerase Inhibitors as	
	Chemosensitisers and Radiosensitisers	43
3.1.1	Chemosensitisation	43
3.1.2	Radiosensitisation	45
3.2	Development of Poly(ADP-ribose) Polymerase	
	Inhibitors	47

3.3	Summary of Structure Activity Relationships and Binding Predictions	61
Chapter 4	Aims of the Study	64
Chapter 5	Benzamides	67
Chapter 6	Isoquinolinones	110
Chapter 7	Biological Results	140
7.1	Introduction	140
7.2	Initial PARP Activity Assays	140
7.2.1	Benzamides	141
7.2.2	Isoquinolinones	146
7.3	PARP Assays at Various Inhibitor Concentrations	151
7.4	Assays Involving Pre-incubation of the Inhibitor with the Enzyme	155
Conclusion		162
Experimental		164
References		210
Appendix A	¹ H NMR COSY Spectra	
	4 <i>R</i> -2,2-Dimethyl-4-(1-hydroxyprop-2-enyl)-1,3-dioxolane 135	226
	3-(3-(4 <i>R</i> -2,2-Dimethyl-1,3-dioxolan-4-yl)-3-hydroxyprop-1-en-yl)isoquinolin-1-one 141 .	227
Appendix B	Methods used in the PARP activity assays	228

List of Figures, Schemes and Tables

Figures	Page
Figure 1: <i>Radicals generated in the chain reaction following interaction of ionising radiation with water and organic molecules.</i>	2
Figure 2: <i>Typical dose-response curve for the survival of irradiated cells.</i>	4
Figure 3: <i>Radioprotectors.</i>	7
Figure 4: <i>Radiosensitisers.</i>	7
Figure 5: <i>Schematic radiation dose-response curves for the effects of electron-affinic radiosensitisers and DNA repair inhibitors on hypoxic cells.</i>	9
Figure 6: <i>DNA Repair Pathways (inhibitors are shown in italics; broken lines show activation interactions).</i>	10
Figure 7: <i>Schematic view of the three functional domains of human PARP obtained by mild trypsin and papain digestion.</i>	12
Figure 8: <i>Structure of poly(ADP-ribose).</i>	17
Figure 9: <i>Structure of NAD⁺.</i>	17
Figure 10: <i>Structure of Adenosine Diphosphate (Hydroxymethyl)-pyrrolidinediol.</i>	21
Figure 11: <i>Schematic diagram to show the mechanism of histone-shuttling at DNA strand breaks by poly(ADP-ribosyl)ation.</i>	26
Figure 12: <i>Schematic diagram to show the turnover of poly(ADP-ribose) at DNA strand interruptions.</i>	28
Figure 13: <i>Possible mechanism for poly(ADP-ribosyl)ation.</i>	47
Figure 14: <i>Some early PARP inhibitors and their percentage inhibition values, as tested by Sims et al¹⁵¹</i>	48

Figure 15:	<i>Benzamide analogues and their effect on the rejoining of DNA SSB produced by MMS as tested by Sestili et al.¹⁵⁵</i>	53
Figure 16:	<i>Possible conformations of the amide group in benzamide analogues.</i>	55
Figure 17:	<i>PARP inhibitors in which the conformation of the amide group is restricted.</i>	56
Figure 18:	<i>Structure of benzamide riboside.</i>	58
Figure 19:	<i>O-Alkyloxy- and O-Benzoyloxybenzamide PARP inhibitors.</i>	59
Figure 20:	<i>Nucleoside analogues of thymidine.</i>	61
Figure 21:	<i>Schematic diagram of the PARP NAD⁺ binding site with inhibitor bound.</i>	62
Figure 22:	<i>Schematic diagram of the proposed irreversible inhibition of PARP.</i>	65
Figure 23:	<i>General structure of potential irreversible PARP inhibitors synthesised, where E is an electrophile.</i>	66
Figure 24:	<i>Target compounds. NAD⁺ analogues with a chiral centre equivalent to the anomeric carbon in NAD⁺.</i>	68
Figure 25:	<i>Prelogs Rule.¹⁸³</i>	78
Figure 26:	<i>The methylene region of the ¹H NMR spectrum of 27 (270.05 MHz, CDCl₃).</i>	84
Figure 27:	<i>Examples of Chiral Derivatising agents for NMR analysis.</i>	86
Figure 28:	<i>¹H NMR (CDCl₃, 270 MHz) of the products of the MTPA derivatisation of (i) (+)-2-acetoxy-1-(hydroxyethyl)benzonitrile 30 and (ii) (±)-2-acetoxy-1-hydroxyethyl)benzonitrile 33.</i>	90
Figure 29:	<i>¹⁹F NMR spectra for the products of MTPA derivatisation of (+)-2-acetoxy-1-(hydroxyethyl)benzonitrile 30 (a) Using (R)-MTPA. (b) Using racemic MTPA. (CDCl₃, 376.05 MHz).</i>	91

Figure 30:	<i>Geometrical isomers of the cyclic sulphite 4(S)-4-(3-cyanophenyl)-1,3,2-dioxathiolane-2-oxide 38.</i>	96
Figure 31:	<i>Structure of a diaryldialkoxysulphurane</i>	101
Figure 32:	<i>Isoquinolin-1-one targets; (a) Intermediate synthetic targets; (b) potential PARP inhibitor targets.</i>	110
Figure 33:	<i>PARP activity in the presence of 3-chloromethylbenzamide 2 at 10.5 μM.</i>	141
Figure 34:	<i>PARP activity in the presence of 3-acetylbenzamide 9 at 11.0 μM.</i>	142
Figure 35:	<i>PARP activity in the presence of 3-(2-bromoacetyl)-benzamide 44 at 10.7 μM.</i>	143
Figure 36:	<i>PARP activity in the presence of (\pm)-3-(oxiran-2-yl)benzamide 43 at 9.2 μM.</i>	143
Figure 37:	<i>PARP activity in the presence of S-(+)-3-(1,2-dihydroxyethyl)benzamide 6 at 9.4 μM.</i>	145
Figure 38:	<i>PARP activity in the presence of R-(-)-3-(1,2-dihydroxyethyl)benzamide 36 at 9.3 μM.</i>	145
Figure 39:	<i>PARP activity in the presence of S-(+)-3-(2,2-dimethyl-1,3-dioxolan-4-yl)benzamide 4 at 10.0 μM.</i>	146
Figure 40:	<i>PARP activity in the presence of 5-bromoisquinolinone 62 at 11.2 μM.</i>	147
Figure 41:	<i>PARP activity in the presence of 5-iodoisquinolinone 63 at 8.0 μM.</i>	148
Figure 42:	<i>PARP activity in the presence of 1-oxoisquinoline-5-carboxylic acid 89 at 13.2 μM.</i>	148
Figure 43:	<i>PARP activity in the presence of 3-(1-oxoisquinolin-5-yl)propenoic acid 125 at 11.6 μM.</i>	149

Figure 44:	<i>PARP activity in the presence of various concentrations of 3-chloromethylbenzamide 2.</i>	152
Figure 45:	<i>PARP activity in the presence of 3-acetylbenzamide 9 as a function of concentration.</i>	153
Figure 46:	<i>PARP activity in the presence of 5-iodoisoquinolinone 63 as a function of concentration.</i>	153
Figure 47:	<i>PARP activity in the presence of 5-bromoisoquinolinone 62 as a function of concentration.</i>	154
Figure 48:	<i>PARP activity in the presence of 1-oxoisoquinoline-5-carboxylic acid 89 as a function of concentration.</i>	155
Figure 49:	<i>PARP activity in the presence of 3.9 μM 3-chloromethylbenzamide 2. (a) 1 minute pre-incubation. (b) 15 minutes pre-incubation. (c) 30 minutes pre-incubation.</i>	157
Figure 50:	<i>PARP activity in the presence of 2.8 μM (\pm)-3-(oxiran-2-yl)benzamide 43. (a) 1 minute pre-incubation. (b) 15 minutes pre-incubation. (c) 30 minutes pre-incubation.</i>	158
Figure 51:	<i>PARP activity in the presence of 5.1 μM 3-(1-oxoisoquinolin-5-yl)propenoic acid 125. (a) 1 minute pre-incubation. (b) 15 minutes pre-incubation. (c) 30 minutes pre-incubation.</i>	160

Schemes

Scheme 1	67
Scheme 2	69
Scheme 3	70
Scheme 4	70
Scheme 5	71
Scheme 6	72

Scheme 7	73
Scheme 8	73
Scheme 9	74
Scheme 10	75
Scheme 11	76
Scheme 12	76
Scheme 13	77
Scheme 14	79
Scheme 15	79
Scheme 16	80
Scheme 17	80
Scheme 18	81
Scheme 19	82
Scheme 20	83
Scheme 21	83
Scheme 22	85
Scheme 23	88
Scheme 24	88
Scheme 25	92
Scheme 26	93
Scheme 27	94
Scheme 28	95
Scheme 29	96
Scheme 30	97
Scheme 31	98
Scheme 32	98
Scheme 33	100
Scheme 34	101
Scheme 35	102
Scheme 36	103

Scheme 37	103
Scheme 38	104
Scheme 39	104
Scheme 40	105
Scheme 41	106
Scheme 42	106
Scheme 43	107
Scheme 44	108
Scheme 45	108
Scheme 46	112
Scheme 47	113
Scheme 48	114
Scheme 49	116
Scheme 50	117
Scheme 51	118
Scheme 52	120
Scheme 53	122
Scheme 54	124
Scheme 55	127
Scheme 56	129
Scheme 57	130
Scheme 58	131
Scheme 59	132
Scheme 60	134
Scheme 61	135
Scheme 62	136
Scheme 63	138

Tables

Table 1:	<i>Substrates for poly(ADP-ribose)</i>	19
Table 2:	<i>Compounds tested by Purnell and Whish²¹ for their effect on PARP activity.</i>	50
Table 3:	<i>Effect of some selected compounds on PARP, in vitro and in vivo and mono(ADP-ribosyl)transferase in vitro.</i>	52
Table 4:	<i>Some isoquinolinone and dihydroisoquinolinone inhibitors of PARP.</i>	55
Table 5:	<i>α-Hydroxy ketones synthesised by direct α-hydroxylation of the corresponding methyl ketones using [bis(trifluoroacetoxy)iodobenzene] under acidic conditions.</i>	75
Table 6:	<i>Comparison of PARP inhibitors: Percentage Inhibition Values at 2 min.</i>	150

Abbreviations

3AB	3-aminobenzamide
ara A	9- β -D-arabinofuranosyladenine
ara C	1- β -D-arabinofuranosylcytosine
ADP	adenosine diphosphate
CI	chemical-impact
COSY	correlation spectroscopy
DBD	DNA binding domain
dCTP	deoxycytidine triphosphate
ddT	dideoxythymidine
DMF	dimethylformamide
DMF DMA	dimethylformamide dimethylacetal
DMS	dimethyl sulphate
DNA	deoxyribose nucleic acid
DSB	double-strand break
e.e.	enantiomeric excess
EF2	elongation factor 2
EI	electron impact
[Eu(hfc)₃]	europium tris[3-heptafluoropropylhydroxy- methylene-(+)-camphorate
FAB	fast atom bombardment
GTP	guanosine triphosphate
HU	hydroxyurea
IR	infra-red
LG	leaving group
LMDS	locally multiply damaged sites
MMS	methylmethanesulphonate
MNNG	<i>N</i> -methyl- <i>N'</i> -nitro- <i>N</i> -nitrosoguanidine

MNU	<i>N</i> -methyl- <i>N</i> -nitrosourea
MTPA	α -methoxy- α -(trifluoromethyl)-phenylacetic acid
NAD⁺	nicotinamide adenine dinucleotide
NMR	nuclear magnetic resonance
NO	nitric oxide
NOESY	nuclear Overhauser enhancement spectroscopy
NOE	nuclear Overhauser enhancement
PARG	poly(ADP-ribose) glycohydrolase
PARP	poly(ADP-ribose) polymerase
ppm	parts per million
[Pr(hfc)₃]	praseodymium tris[3-heptafluoropropylhydroxy-methylene-(+)-camphorate]
R.T.	ambient temperature
SAR	structure-activity relationship
SCE	sister chromatid exchange
SLD	sub-lethal damage
SSB	single strand break
TG	6-thioguanine
THF	tetrahydrofuran
TLC	thin layer chromatography

Chapter One

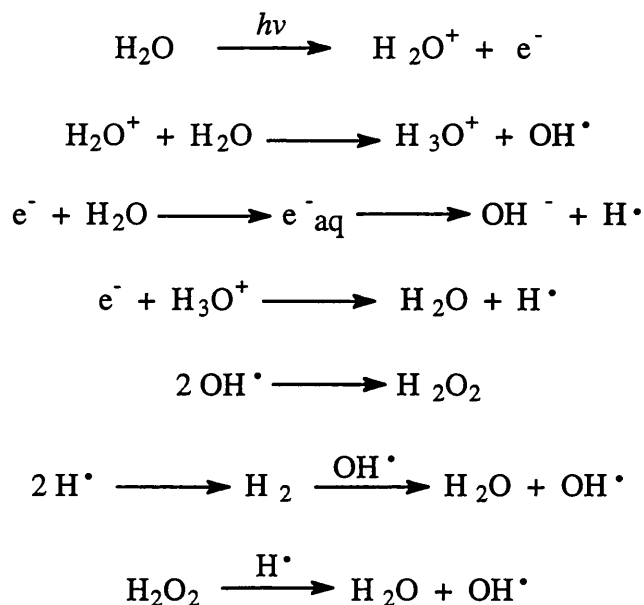
1. Radiotherapy

Radiation therapy has been used in the treatment of cancer since the late 19th century, shortly after the discovery of X-rays. Techniques have been developed and improved and radiotherapy is now widely used, alone and in combination with surgery in the treatment of many primary cancers. As with the chemotherapy of cancer, the main limitation of radiotherapy is the damage caused to normal cells. Both treatments, by the nature of their action, will damage cells which are rapidly dividing. This includes cells in the skin, gastrointestinal tract, bone marrow and blood vessels as well as the targeted tumour cells. Therefore, improvement of radiotherapy depends upon increasing the radiosensitivity and radioresponsiveness of tumour cells relative to that of the surrounding normal cells.

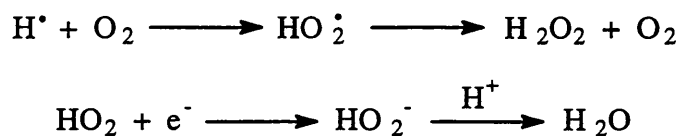
1.1 Mechanism of Action

The main types of radiation used in radiotherapy are X-rays and gamma rays. These are both types of ionising radiation, *i.e.* the radiation causes ejection of a fast electron from the target molecule and subsequent production of an ion. These species react with other molecules to form ions and free radicals.^{1,2} Direct damage due to radiation acting on macromolecules such as DNA occurs. However, since the predominant molecule present in biological systems is water, it is radicals produced from water that are the most important.¹ The excited species and radicals derived from the interaction of radiation with water are shown in Figure 1. These radicals interact with organic molecules (DNA, RNA, proteins) within the cell, represented by R in Figure 1. In the presence of oxygen a wider range of radicals is produced and more damage occurs.

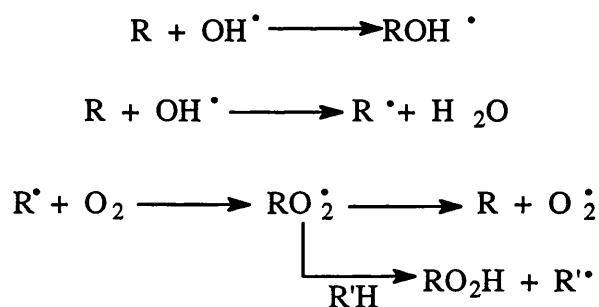
Figure 1: Radicals generated in the chain reaction following interaction of ionising radiation with water and organic molecules.



In the presence of oxygen:-



With organic molecules:-



Where the DNA has been directly damaged by the radiation, radical anionic and cationic sites are formed. In well-oxygenated cells, oxygen molecules can abstract a proton from the radical anions leaving radical cations with a long enough life to allow serious DNA damage. In the absence of oxygen the electron from the radical anion combines with the radical cation and no damage results. In

both scenarios, more damage takes place in the presence of oxygen. This is generally known as the oxygen effect and has been widely measured using the oxygen enhancement ratio (OER). This is the ratio of radiation doses given to cells hypoxically or in air to produce a given level of cell killing. The oxygen effect is significant because solid tumours are very poorly vascularised. There are, therefore, regions within the tumour where the cells are hypoxic owing to their limited blood supply and are consequently relatively radioresistant.

1.1.1 Cytotoxicity

The cytotoxicity caused by radiation has been measured in many studies and is expressed in terms of the fraction of cells surviving following a specific dose of radiation. Survival is measured by the ability of the cells to proliferate following the radiation dose. Figure 2 shows a typical survival curve. After an initial shoulder to the curve, the surviving fraction decreases exponentially with increasing dose. Therefore, in the dosage range of this linear portion, a given dose will kill a fixed fraction of the population, regardless of the initial number of cells. The shouldered portion of the graph is generally thought to be due to sub-lethal damage^{3,4} (SLD). In this dose range the cellular repair processes are able to repair the damage caused by the radiation and allow the cells to recover. However, at higher doses, cellular repair processes become saturated, are not able to repair the damage effectively and it becomes lethal.⁵ It has been shown that there is a good correlation between the steepness of the initial slope of the survival curve, measured *in vitro*, and the clinical responsiveness of human tumours.⁶

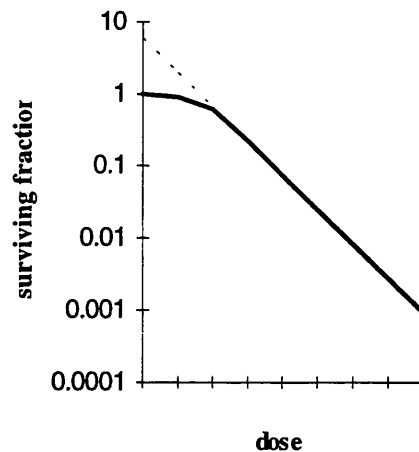


Figure 2: *Typical dose-response curve for the survival of irradiated cells*

1.1.2 DNA Damage

It is generally accepted that the lesions, produced by ionising radiation, which result in cell-death involve DNA.⁷ DNA double-strand breaks (DSB) have been particularly implicated.⁵ It is also thought that multiple lesions produced within a small region of the genome, known as "locally multiply damaged sites" (LMDS),^{5,8} may be important. Experiments have shown¹ that increasing the dose of radiation increases the proportion of lower molecular weight DNA on sucrose density-gradient analysis. This reflects an increase in the extent of strand-breakage. At lower radiation doses, the majority of lesions are rapidly repaired;⁹ this is reflected in the shouldered region of the survival curve (Figure 2). However, when the number of DSBs is increased, repair processes become less efficient and the DNA remains damaged, resulting in cell-death. Inhibition of DNA repair processes would lead to an increase in cell-kill and, consequently, improvement of radiotherapy.

1.2 Clinical Aspects of Radiotherapy

The dose of radiation used to treat a tumour is limited by the damage it will cause to the surrounding, normal tissue. The dose needs to be carefully optimised so as to produce the maximum tumour response with minimum tissue toxicity. There are three distinct types of toxicity that can occur in response to radiotherapy; transient toxicity, occurring during or shortly after therapy, early changes and late changes which may manifest themselves many years after the radiotherapy has finished. Therapy can be adjusted in response to the early injuries seen; however, the late changes are much less predictable and are therefore difficult to avoid.

The method used by radiotherapists to increase the therapeutic index of the radiotherapy of tumours, is fractionated dosage. This method has been used since the 1920s and involves giving a series of doses of radiation at daily intervals, for five days of the week, over a period of three to six weeks. The principle behind this approach depends mainly on the observation that, although the normal tissue and tumour cells suffer similar damage, the normal cells appear to be able to recover more quickly.¹⁰ Three main factors influence fractionated therapy; recovery from SLD, repopulation, and re-oxygenation. Repopulation occurs more readily in normal tissues than in tumours. There is migration of untreated cells from the surrounding tissue to the treated areas and an increase in proliferation in response to cell death. Re-oxygenation of the tumour tissue is an important factor, since the hypoxic cells are more radioresistant. This effect occurs during the course of the treatment, as the tumour cells are killed and the tumour size decreases. Tumour cells that were originally distant from capillaries are brought closer and are oxygenated. This increases their radiosensitivity.

The disadvantage of fractionated therapy is that, although the early toxicity is limited by giving smaller individual doses, the total dose of radiation given over the course of the treatment is much larger. For longer courses of treatment, the

total number of cells that must be killed increases due to the repair of SLD and recovery of the tumour cells. It seems likely that exposure to greater overall quantities of radiation will increase the amount of late injury to normal tissue. Several approaches have been made to try to increase the therapeutic index.

1.3 Modification of Radiation Effects

The relative radioresistance of hypoxic tumour cells is the major cause of failure of local control of cancer by radiotherapy. The radiation dose required to produce a given effect is about three times greater for hypoxic than aerobic cells.¹¹ Therefore, approaches to improve radiotherapy have focused on reducing the radioresistance of hypoxic cells.

1.3.1 Densely Ionising Radiation

Densely ionising radiation such as neutrons, negative π mesons and accelerated heavy ions have a much smaller oxygen effect than conventional x-rays and gamma rays.^{1,2,12} Negative π mesons also have the advantage that they penetrate the tissue and deliver the dose deeper beneath the skin therefore minimising tissue damage in the path through the skin to the tumour.

1.3.2 Radioprotectors

The oxygen effect can be minimised by protecting oxygenated tissues.¹ Radioprotectors have been developed to decrease radical production in normal tissues. Sulphydryl compounds such as cysteamine and WR-2721, shown in Figure 3, have been suggested as radioprotectors.¹

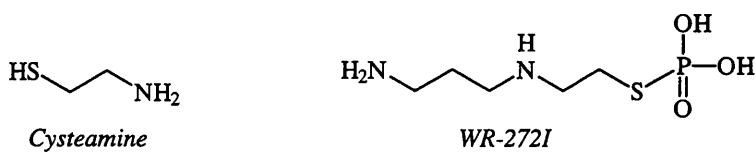


Figure 3: Radioprotectors

1.3.3 Radiosensitisers

Electron-affinic radiosensitisers have been widely studied.^{12,13,14} Also known as oxygen mimetics, these compounds can diffuse into hypoxic tumour cells and cause damage to DNA by a mechanism similar to that of oxygen. Metronidazole was first shown to sensitise hypoxic Chinese hamster cells to radiation in 1973.^{15,16} Many nitroheterocycles have since been evaluated as oxygen mimetics, the most successful being the 2-nitroimidazoles. Etanidazole and pimonidazole^{13,14,17} (Figure 4) are examples that have reached clinical evaluation.

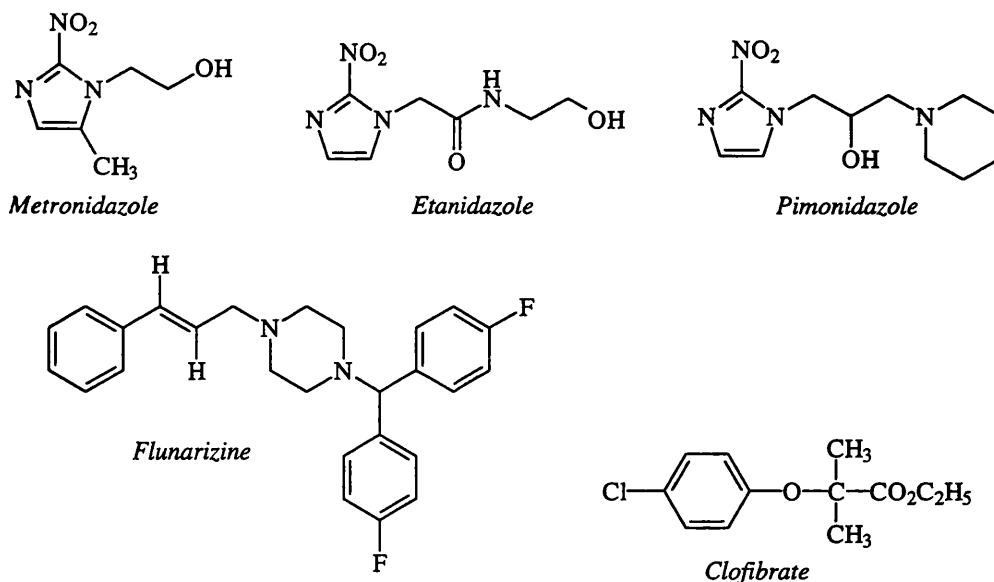


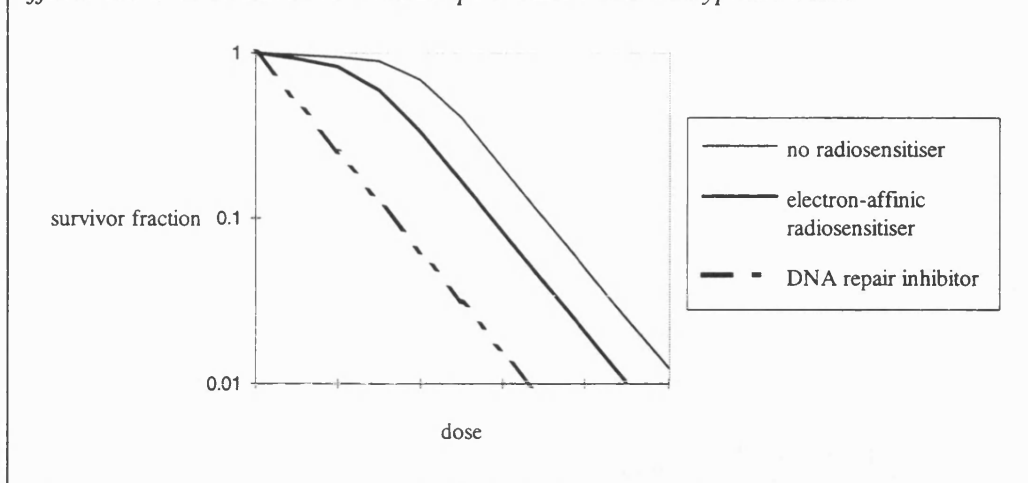
Figure 4: Radiosensitisers

Other compounds have been found to sensitise tumour cells to the effects of radiation. Calcium antagonists have been evaluated,¹⁸ the aim being to increase the blood flow in the tumour in order to reduce hypoxia and therefore increase radiosensitivity. Flunarizine (Figure 4) produced only a 20% reduction in hypoxia but produced significant sensitisation of tumours at a wide range of doses.¹⁴

Another example is clofibrate, an antilipidaemic drug.¹⁹ It was firstly thought that the radiosensitising properties of clofibrate were wholly due to its action of reducing the affinity of haemoglobin for oxygen, therefore increasing the availability of oxygen to hypoxic regions. However, when less toxic analogues of clofibrate were tested, although the effect on haemoglobin was still present, the radiosensitising properties were much less marked. It was concluded that other mechanisms must also be involved in the radiosensitisation observed with clofibrate.

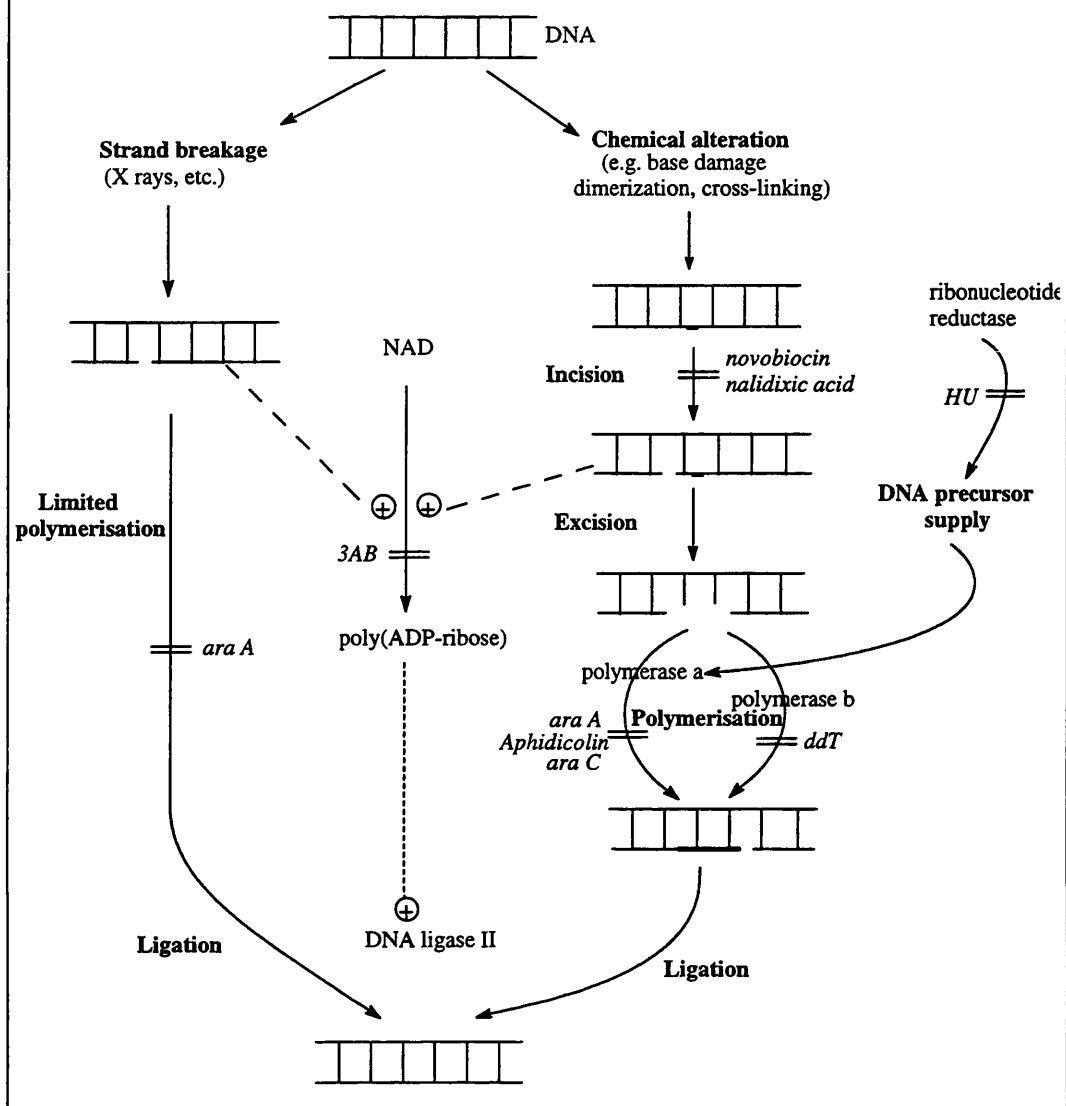
Figure 5 shows the effect that electron-affinic and the miscellaneous sensitisers discussed, have on the radiation survival curve. Since there is still repair of sub-lethal damage, there is still a shoulder to the curve and the curve is simply moved to the left. The gradient of the shouldered portion of the curve is particularly important in determining the success of the radiotherapy. Therefore an ideal sensitiser would cause increased killing in this low-dose range. By inhibiting DNA repair of sub-lethal damage and potentially lethal damage, cell-death is increased at both small and large doses. The third curve in Figure 5 shows the effect of a DNA repair inhibitor on the radiation survival curve.

Figure 5: Schematic radiation dose-response curves for the effects of electron affinic radiosensitisers and DNA repair inhibitors on hypoxic cells.



DNA repair involves a number of complex enzymatic processes and it is not yet clear which of these are important following radiation damage.⁸ Figure 6 shows several inhibitors that are known to interfere with DNA repair and their probable sites of action in DNA repair pathways. Most of the compounds shown have been evaluated as radiosensitisers. Kelland *et al*⁶ found 3-aminobenzamide (3AB), hydroxyurea (HU), and 9- β -D-arabinofuranosyladenosine (ara A) to be radiosensitisers of human carcinoma cells. Aphidicolin and novobiocin did not exhibit a significant effect. Ward and Blakely²⁰ also found HU and 1- β -D-arabinofuranosylcytosine (ara C) increased the radiosensitivity of HeLa cells. 3AB is an inhibitor of the enzyme poly(ADP-ribose) polymerase.²¹ This thesis is concerned with this enzyme, its role in DNA repair and its inhibition.

Figure 6: DNA Repair Pathways. *Inhibitors are shown in italics. Broken lines show activation interactions.*



Chapter Two

2. Poly(ADP-ribose) Polymerase

Poly(ADP-ribose) polymerase (PARP), also known as poly(ADP-ribose) synthetase and ADP-ribosyl transferase, is an abundant nuclear enzyme. It is present in almost all animal tissue, plants and lower eucaryotes, but lacking in several terminally differentiated cells and in yeasts.²² PARP is a multifunctional enzyme which requires DNA strand breaks for activity.²³⁻²⁵ The enzyme catalyses the transfer of ADP-ribose units from its substrate; nicotinamide adenine dinucleotide (NAD⁺), to a limited number of protein acceptors. These are partly nuclear proteins involved in chromatin architecture and DNA metabolism (heteromodification), but the main protein to be poly(ADP-ribosyl)ated is PARP itself (automodification).^{26,27} The exact biological role of PARP is not yet clear, despite much research over the last 30 years. In addition to the speculation that PARP may be involved in cell proliferation, differentiation and transformation, evidence shows that the enzyme plays an important part in the reaction of the cell to DNA damage. It is this involvement that has led to an interest in PARP as a target for the design of chemosensitisers and radiosensitisers.

2.1 Structural Features of Poly(ADP-ribose) Polymerase

Approximately 90% of PARP molecules are located in the cell nucleus, bound tightly to chromatin.²³ There are in the region of one million molecules per nucleus. PARP was first purified in 1977²⁸ by Okayama and co-workers from rat liver nuclei. The enzyme has since been purified to homogeneity from many tissues originating in a variety of different animals.²³ More recently, the gene encoding for human PARP, which is on chromosome 1, has been cloned. This was achieved, firstly, by Smulson and his group.²⁹ Other laboratories followed and now cDNA sequences of PARP from several species including mammals,

fish and insects, have been determined (summarised in ref. 30). The identification of the amino acid sequences of PARP from different sources has shown that the enzyme is highly conserved, particularly in the region of the protein that binds NAD^+ .

Human PARP consists of a single polypeptide chain of 1014 amino acid residues.³¹ The protein has a predicted mass of 113 kDa, but the measured mass of the purified enzyme is often 116 kDa, therefore both values are quoted in the literature. Limited proteolysis of PARP gives three functional domains:³² A 46 kDa amino-terminal fragment, containing the DNA binding domain (DBD); a central 22 kDa fragment containing the automodification sites; and a 54 kDa carboxyl terminal region containing the catalytic domain. This is shown schematically in Figure 7.

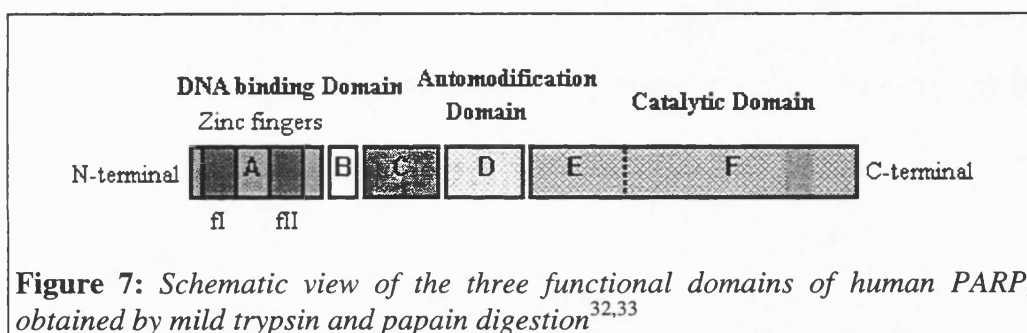


Figure 7: Schematic view of the three functional domains of human PARP, obtained by mild trypsin and papain digestion^{32,33}

2.1.1 The DNA Binding Domain

PARP is activated by binding to DNA strand breaks. Experiments have shown that PARP binds preferentially at DNA breaks, symmetrically covering seven or eight nucleotides on each side of the break.³⁴ When the DNA break is single stranded, there is a V-shaped bend in the DNA and PARP has been shown to bind at the apex.³⁵ Zahradk and Ebisuzaki³⁶ found that PARP is a metalloenzyme and requires zinc for activity. Further work has shown binding of PARP to DNA

is zinc dependent and that PARP has two zinc "fingers" in its DBD.³⁷ The zinc fingers are regions in the protein where a zinc ion binds to four amino acid residues to form a loop in the polypeptide chain. These motifs are seen in several other nucleotide binding proteins. The two zinc fingers have been named f I and f II (see Figure 7). The cDNA fragment encoding the zinc fingers was cloned and expressed in *E. coli* by Gradwohl³⁴ *et al.* Site-directed mutagenesis was used to change the structure of the zinc fingers and the effect on DNA binding was then measured. It was found that when f II was disrupted DNA binding was drastically reduced, whereas alteration of the peptide in the f I region had little effect on DNA binding. In addition to having the stronger DNA binding, f II also seems to play a role in the recognition of single-stranded DNA breaks.³⁴ It is interesting to note that it has been recently found that the human DNA ligase III enzyme has a very similar zinc finger to those found in PARP.³⁸ This may also serve for preferential binding at DNA single strand breaks.³⁹

2.1.2 The Automodification Domain

There are several glutamate residues in the PARP molecule that act as anchor points for poly(ADP-ribose) synthesis. These amino acids are mainly found in the region between the binding and the catalytic domains. Studies have suggested that two PARP molecules form a dimer at the DNA strand break and the poly(ADP-ribosyl)ation automodification is intermolecular.^{26,27}

2.1.3 The Catalytic Domain

The NAD⁺ binding site is found on the C-terminal domain of PARP. This is the most conserved region of the enzyme. The binding site also shows homology with NAD⁺ binding sites in several other enzymes.³⁹ Cloning techniques have allowed the catalytic domain of PARP to be isolated and purified.³⁷ This isolated domain contains all of the catalytic functionality of the enzyme. It can carry out

all of the enzymatic processes associated with the full length enzyme but independently of DNA strand breaks. Polymers are formed slowly (0.2% of the rate of the complete enzyme)³⁹ and automodification can occur, indicating that there are some automodification sites on this domain.³² Site-directed mutagenesis experiments were carried out to try to determine which residues in the domain are important for NAD⁺ binding and activity. Two models were proposed for the structure of the active site. Marsischky *et al*⁴⁰ suggested that the corresponding enzymatic regions of PARP and the mono(ADP-ribosyl)ating bacterial toxins (see section 2.2) have similarities. They investigated the Glu⁹⁹⁸ residue on human PARP, since the corresponding glutamic residue in several toxins is known to be important for activity. Glu⁹⁹⁸ mutations produced a reduction in catalytic activity of the enzyme, although there was no significant change in the K_m of NAD⁺. Simonin⁴¹ *et al* noted catalytic fragment sequence similarities between PARP and NAD(P)-dependent leucine and glutamate dehydrogenases. This group concluded that residues Lys⁸⁹³ and Asp⁹⁹³ are directly involved in the attachment of the first ADP-ribosyl residue from NAD⁺. The crystal structure of the catalytic fragment of PARP from chicken has recently been elucidated,⁴² although is not fully reported. The protein is composed of two structural parts; an α -helical N-terminal domain and a C-terminal domain bearing the NAD⁺ active site. It now seems clear that the PARP catalytic domain is most similar to that of the bacterial toxins, for example, diphtheria toxin and pertussis toxin. PARP has an additional α -helical domain, which, it is suggested, may relay the activation signal issued on DNA binding. The structure of the active site with a known PARP inhibitor bound was also elucidated. This is discussed later in Chapter 3. It is noteworthy that, although these structural similarities have been observed between PARP and the mono(ADP-ribose) transferases, there seem to be no structural similarities between the inhibitors of the enzymes (see Chapter 3).

2.2 Enzymatic Functions of Poly(ADP-ribose) Polymerase

2.2.1 ADP-Ribosylation Reactions

ADP-ribosylation is one of the most general ways by which living organisms modify their protein structures and functions.⁴³ A number of enzymes carry out this posttranslational modification of proteins which uses NAD⁺ as a donor of the modification group. There are two major groups of ADP-ribosylation reactions; those which result in mono(ADP-ribosyl)ation and those which result in poly(ADP-ribosyl)ation. Although this project is concerned mainly with poly(ADP-ribosyl)ation, it is important to realise the similarities and differences between these two processes.

2.2.1.1 Mono(ADP-ribosyl)ation

Mono(ADP-ribosyl)ation was first demonstrated using diphtheria toxin, an exotoxin produced by *Corynebacterium diphtheriae*.⁴⁴ The toxin is a mono(ADP-ribose) transferase enzyme which catalyses the mono(ADP-ribosyl)ation of elongation factor 2 (EF2). EF2 is involved in protein synthesis in eucaryotic cells. Its modification, by diphtheria toxin, results in the inhibition of protein synthesis, leading to the death of the host cell. There are several bacterial toxins that are mono(ADP-ribosyl) transferases. They all modify a specific amino acid acceptor site on their target proteins. There are three distinct classes:-

- a) **Diphthamide-specific ADP-ribosylation:** (Diphthamide is a hypermodified histidine residue on EF2). Diphtheria toxin and pseudomonas exotoxin A⁴⁵ are members of this group.
- b) **Arginine-specific ADP-ribosylation:** Examples are cholera toxin A and *Escherichia coli* heat-labile enterotoxin. These enzymes specifically modify an arginine residue of a GTP binding protein, Gs α .⁴⁶

c) **Cysteine-specific ADP-ribosylation:** Pertussis toxin⁴⁷ produced by *Bordetella pertussis* carries out mono(ADP-ribosyl)ation of a cysteine residue on its target membrane-bound protein resulting in the activation of adenylate cyclase.

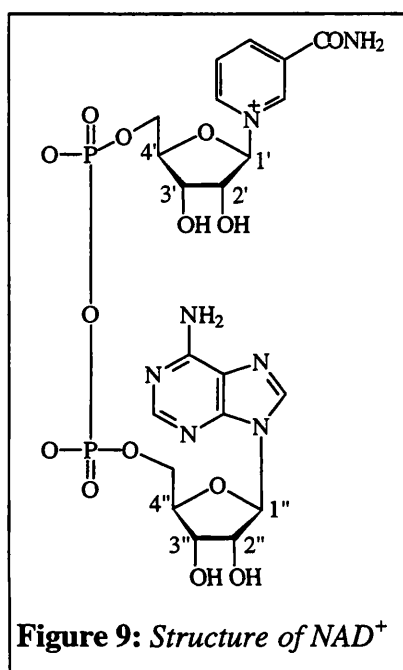
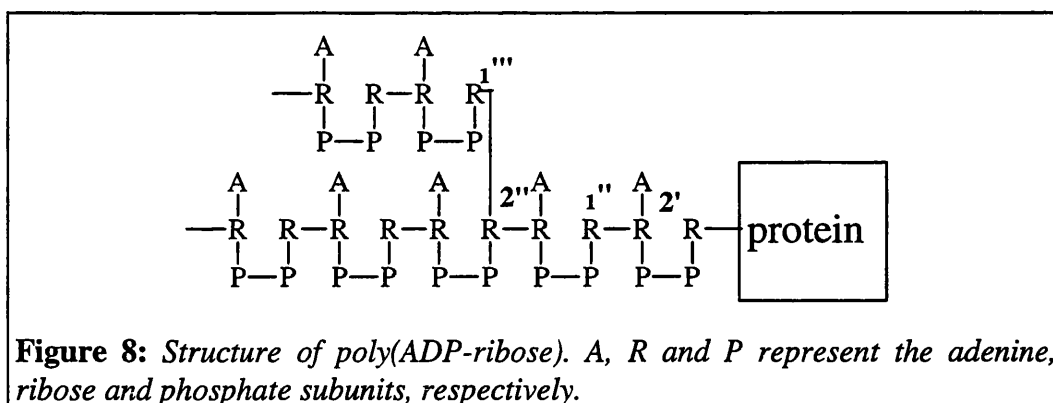
More recently mono(ADP-ribosyl) transferase enzymes have been found in animal tissues. Several enzymes have been identified and are present in most cellular compartments; cytosol, plasma membrane and cell nucleus.^{43,46} Histidine-, cysteine-, and arginine- specific mono(ADP-ribosyl) transferases have been found in mammalian cells, but those found in nuclei have all been arginine-specific. The purpose of mono(ADP-ribosyl)ation in mammalian cells is less certain than for the bacterial toxins; it is thought that it has some regulatory function within the cell.

All of these mono(ADP-ribosyl)ation reactions form N-glycosides; the enzyme interacts with a side-chain nitrogen on the amino acid acceptor site. This is in contrast to PARP which forms O-glycosides, usually interacting with a glutamic acid carboxyl group.

Crystal structures of some of the bacterial toxin mono(ADP-ribosyl)transferases have been elucidated.^{45,48,49} These have been compared with the recently elucidated crystal structure of the catalytic domain of PARP.⁴² Evidence to date suggests that the family of enzymes carrying out ADP-ribosylation reactions share a very structurally similar NAD⁺ binding site.

2.2.1.2 Poly(ADP-ribosyl)ation

Poly(ADP-ribose) was first identified in 1966⁵⁰ and its structure is well understood. The polymer is made up of ADP-ribosyl units as shown in Figure 8.



PARP uses nicotinamide adenine dinucleotide (NAD⁺) as a source of these units. The structure of NAD⁺ is shown in Figure 9. The molecule consists of a nicotinamide group linked to the 1' position of a ribose molecule, which is attached to a second ribose molecule via two phosphate groups. At the 1'' position of this ribose group is an adenine molecule. Therefore in the formation of the poly(ADP-ribose) the bond between nicotinamide and ribose must be broken. The polymer has branches at around a frequency of about one per 30-50 ADP-ribose

residues.⁴³ To produce these polymers PARP catalyses three different reactions:-²³

1) Initiation

PARP transfers the ADP-ribose portion of NAD⁺ to the protein acceptor. Nicotinamide is released.

2) Elongation

PARP transfers the ADP-ribose portion of NAD^+ to the mono(ADP-ribosyl)ated protein, linking the second ADP-ribose unit by an $\alpha(1'' \rightarrow 2')$ glycosidic bond to the adenine ribose of the preceding ADP-ribose unit.

3) Branching

In this reaction the ADP-ribose portion of NAD^+ is transferred to a ribose residue in the polymer chain which does not have an adenine molecule attached directly to it, (*i.e.* the ribose that was originally attached to nicotinamide in NAD^+). A $1''' \rightarrow 2''$ glycosidic link is formed.⁵¹

2.2.2 Protein Acceptors of Poly(ADP-ribose)

Although PARP itself is the main protein acceptor for poly(ADP-ribosyl)ation⁵² (automodification), several other enzymes have been reported to be poly(ADP-ribosyl)ated. Histone H1 is the main example, others are given in Table 1.

The effect of modification by PARP is, in general, inhibition. It is not clear what the significance of this modification is in physiological terms. The extent of poly(ADP-ribosyl)ation of other nuclear proteins is small in comparison to automodification. It has been suggested that the inhibition seen is due to steric interference and charge repulsion by polymer chains.^{39,53} Many of the experiments have been *in vitro* and there is evidence to suggest that the degree of poly(ADP-ribosyl)ation of proteins other than PARP itself is much lower *in vivo*.²² The role that histone H1 has to play in the enzymatic mechanism of PARP is still unclear.^{39,54} This is discussed later in section 2.2.3.

Table 1: Substrates for poly(ADP-ribose)

<u>Protein</u>	<u>Effect of poly(ADP- ribosyl)ation</u>	<u>Reference</u>
Poly(ADP-ribose)polymerase, PARP	INHIBITION	52
Ca ²⁺ ,Mg ²⁺ endonuclease	INHIBITION	55
DNA polymerase α	INHIBITION	56
DNA polymerase β	INHIBITION	56
Terminal deoxynucleotide transferase	INHIBITION	56
DNA ligase II	INHIBITION	56
Topoisomerase I	INHIBITION	57, 58
Topoisomerase II	INHIBITION	59
RNA polymerase II	INHIBITION	60
Ribonuclease	INHIBITION	61
Prolyl hydroxylase	INHIBITION	62
Histone H1	UNKNOWN	63, 64
Histone H2B	UNKNOWN	65
HMG proteins	UNKNOWN	63
SV40 T antigen	UNKNOWN	66
Adenoviral DNA binding protein	UNKNOWN	66

2.2.3 Regulation of Poly(ADP-ribosyl)ation

2.2.3.1 DNA Strand Breaks

Activation of PARP requires DNA strand-breaks. These may be caused directly as a consequence of DNA damage, *e.g.* ionising radiation; or indirectly following enzymatic incision. Benjamin and Gill²⁵ showed that the extent of poly(ADP-ribosyl)ation is completely dependent on the number of strand breaks and is not sequence specific. They used PARP extracted from calf thymus and measured the extent of poly(ADP-ribosyl)ation following the addition of plasmid DNA with different types of DNA damage. It was found that the DNA must be double-stranded, as single-stranded DNA does not support poly(ADP-ribose) synthesis.

The type of strand break also affects the degree of PARP activation; double-strand breaks with flush ends are the most effective, followed by double-strand breaks with unpaired nucleotides at the ends, followed by single-strand breaks.

2.2.3.2 Poly(ADP-ribose) Glycohydrolase (PARG)

Once PARP is bound to the site of DNA damage rapid polymer synthesis occurs. Several thousands of molecules of NAD^+ are converted at each strand break.²⁵ If the synthesis of these stable polymers was allowed to continue without control, the cell would soon become depleted of NAD^+ , which would lead to ATP depletion and cell death. However the polymers produced have a very short half life and are largely degraded within one or two minutes of being synthesised. The main enzyme involved in the degradation of poly(ADP-ribose) is poly(ADP-ribose) glycohydrolase (PARG). PARG, a 59 kDa protein, has been isolated and purified from several different tissues.^{43,67} Until more recently not much was known about the enzyme. There is now increased interest in its role in the regulation of poly(ADP-ribosylation). A second cytosolic form of the enzyme was recently isolated from the guinea pig liver.⁶⁸ This enzyme is structurally different and has slightly different properties to the nuclear form. The role of this second form of PARG is still to be determined.

PARG acts by breaking the ribose-ribose bonds of the poly(ADP-ribose) polymer. Until recently the enzyme was thought to have a mainly exoglycosidic action, *i.e.* cleaving one ADP-ribose unit at a time from the end of the polymer chain. Brochu and co-workers,⁶⁹ however, showed that, *in vitro*, acting on long, free polymers, PARG also exhibits endoglycosidic activity and can cleave the polymer to liberate large fragments of polymer rather than single ADP-ribose units. The final ADP-ribose unit is cleaved from the acceptor protein by a second enzyme, ADP-ribosyl protein lyase. It is also possible for phosphate-phosphate bonds to be cleaved by phosphodiesterase enzymes.⁶⁹

In experiments⁶⁷ using both bound and free poly(ADP-ribose), it was found that the degradation of large polymers by PARG is biphasic and the degradation of short polymer chains occurs at a much lower rate. A long polymer chain of twenty or more ADP-ribose units is degraded quickly until it is about half the original size. Degradation of the remaining short polymer is at about 5% of the rate of the original degradation. It was found that the K_m for the large polymers is about 100 times smaller than that for small polymers. These results suggest that PARG regulates differentially the levels of small and large polymers in the cell. Although the exact mechanism and function of PARG are not yet known it is clear that it is as equally important as PARP in the control of poly(ADP-ribosyl)ation. The accumulation of stable poly(ADP-ribose) chains would eventually cause intolerable interference with DNA replication and transcription.³⁹ Study of the actions of PARG may be facilitated by the use of specific inhibitors. Slama *et al*⁷⁰ have reported the synthesis of adenosine diphosphate (hydroxymethyl)pyrrolidinediol (Figure 10). This analogue of ADP-ribose was tested for inhibition of PARG, PARP and NAD:arginine mono(ADP-ribosyl) transferase A. The compound was found to be a specific inhibitor of PARG with an IC_{50} of 0.12 μM ; more than 10,000 times its activity for either PARP or the mono(ADP-ribose) transferase.

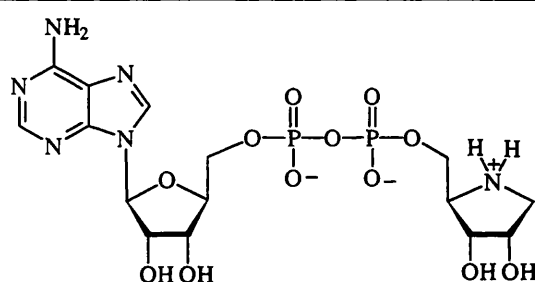


Figure 10: Structure of Adenosine Diphosphate (Hydroxymethyl)pyrrolidinediol

2.2.3.3 Automodification

It is well understood that the most significant target for poly(ADP-ribosyl)ation is PARP itself. As many as 28 polymers may be bound to a PARP molecule and each polymer chain contains up to 200 units.⁷¹ Two groups^{26,27} carried out kinetic and stoichiometric studies on the automodification reaction. Both reached the conclusion that automodification is an intermolecular reaction, with the optimal ratio of PARP to DNA being 2:1 for maximum PARP activity.²⁷ It is thought that two molecules form a dimer at the DNA binding site protecting one and a half turns of double helix. The automodification domain of *Drosophila* PARP was cloned in 1993⁷² and found to contain a leucine zipper motif. Leucine zippers consist of a repetition of leucine residues at every seventh position and are involved in protein-protein interactions. It was suggested that this region might mediate the homodimerisation. However this motif is not conserved in vertebrate PARP, making it doubtful that this is the mechanism by which the dimer forms. Experiments^{26,27} seem to favour a model of automodification that involves one PARP molecule of the dimer being activated and carrying out the poly(ADP-ribosyl)ation of the second member dimeric pair. There is, therefore a catalytic PARP molecule and an acceptor PARP molecule in each dimer.

Automodification follows a processive reaction mode. On initial activation of PARP, a distinct pattern of polymers on a small number of polymerase molecules is produced and, as the reaction proceeds, more PARP is poly(ADP-ribosyl)ated.⁵⁴

The effect of automodification on PARP is inhibition. This is thought to be due to the electrostatic repulsion between the large, charged polymer chains and the DNA, which causes PARP to leave the DNA strand-break and become inactive. In 1982 two groups^{24,73} investigated this effect. The poly(ADP-ribosyl)ation increases up to a "repulsion" point at which the negative charge of the polymer is

so high that it leaves the negatively charged DNA and activation no longer occurs. Addition of PARG restores PARP activity by removal of the charged polymer chains.⁷³ The repulsion point is also increased by addition of Mg^{2+} ions, which can neutralise the negative charges, and histones, which may shield the polymer from the DNA and/or act as acceptors of polymers.²⁴

2.2.3.4 Histones

The role of histones in poly(ADP-ribosyl)ation and the events that follow is not yet known, but some researchers in the field believe that these proteins are involved in the regulation of poly(ADP-ribosyl)ation and the repair of DNA damage that follows. Histones are fairly small, positively charged proteins. They are the principal structural proteins of eucaryotic chromosomes and are present in large numbers (about 60 million of each type per cell). The positive charges, due to a high proportion of lysine and arginine residues, help the proteins to bind tightly to DNA. Histones H2A, H2B, H3 and H4 are present in the nucleosomes. H1 molecules, larger, less well conserved proteins, hold the nucleosomes together, condensing the chromatin. It has been shown that histones can be poly(ADP-ribosyl)ated, H1 has been studied and an ADP-ribose binding site identified.⁶⁴ However, it is not clear whether direct poly(ADP-ribosyl)ation of histones takes place *in vivo*. It does not seem likely that histones bound to DNA act as polymer acceptors, *in vitro* experiments have shown that free histones are modified in favour of bound histones and high histone concentrations are required.²⁴ It is thought that fragments of poly(ADP-ribose) that have been cleaved from automodified PARP can bind non-covalently to proteins such as histones,⁶⁴ this would be facilitated by the electrostatic attraction between the oppositely charged molecules. Indeed, Althaus⁵⁴ suggests that the negatively charged polymers compete with DNA for histone binding. The experiments carried out by his research group showed that the branching points of poly(ADP-ribose) polymers have a particularly high binding affinity for histones.

Many groups have shown that histone H1 can increase the activity of PARP when added to an *in vitro* system.^{24,73,74} This was found to be due to the histone apparently increasing the affinity of PARP for DNA, probably by neutralising the electrostatic repulsion between the DNA and the polymer chain.^{24,73}

Naegeli and Althaus⁷⁴ carried out *in vitro* experiments in which they measured the effect of different histones on the number and size of poly(ADP-ribose) polymers produced by PARP. They found that the histones appeared, not only to stimulate PARP activity, but to regulate the polymer pattern and size. Each histone induced PARP to synthesise a specific polymer size pattern. There was evidence that this apparent regulatory effect of the histones was independent of their potential acceptor function. The significance of this effect *in vivo* is not known. The significance of these results is also hard to assess since the experimental system did not include PARG, which would degrade the polymers present.

2.2.3.5 Possible Mechanisms for the Role of Poly(ADP-ribose) Polymerase in DNA Strand Break Rejoining.

There are two main ideas that have been proposed to explain the events following the occurrence of DNA strand breaks. The two mechanisms are similar but differ mainly in the role that histones are given. Both are explained briefly below.

2.2.3.5.1 Histone-Shuttle Mechanism

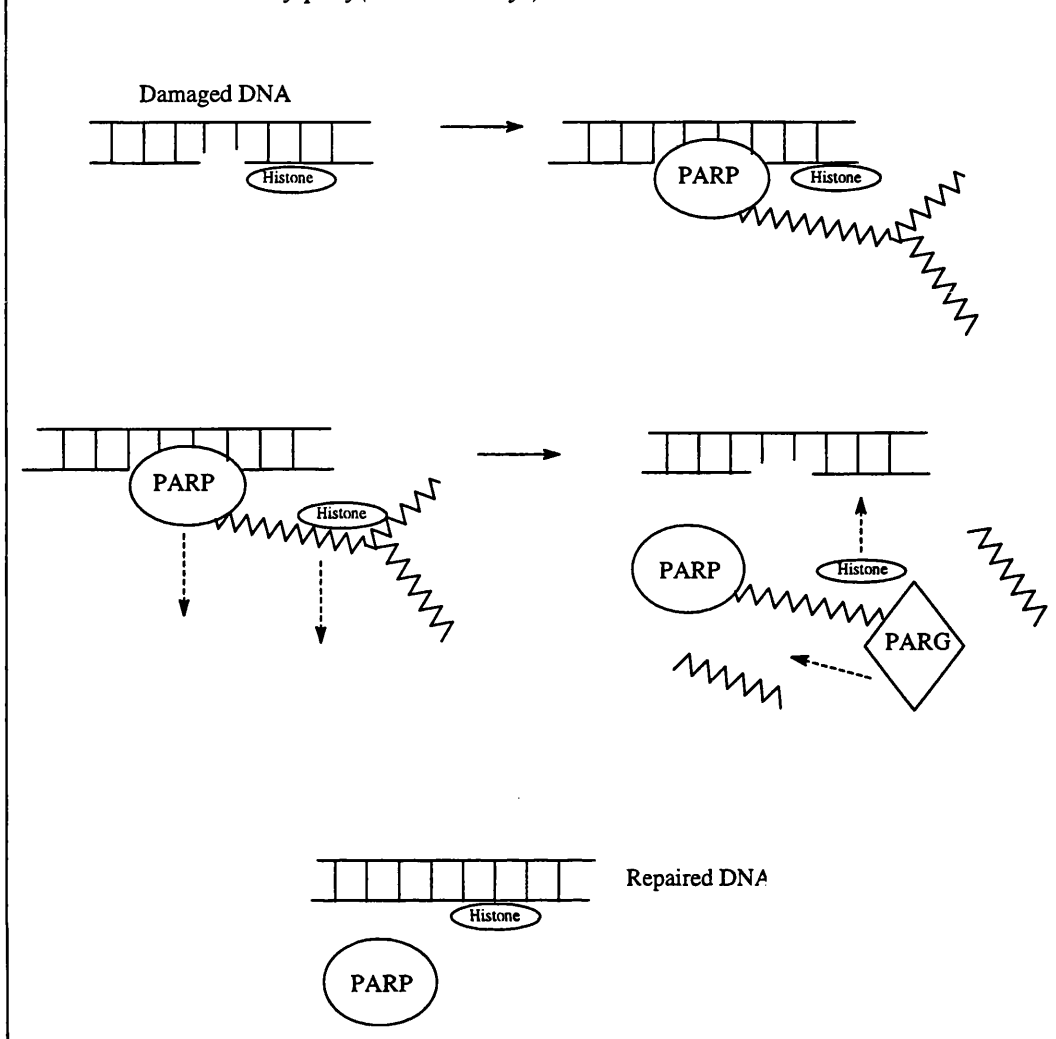
In this mechanism, the PARP automodification reaction serves to shuttle histones off and back onto DNA. Althaus⁵⁴ and his group put forward this idea and have carried out many experiments to investigate it.

Investigations of the non-covalent interaction between histones and poly(ADP-ribose) have shown that they are stronger and more specific than would be expected of purely electrostatic interactions. Of many basic proteins tested, histones were the only ones which bound to the polymer.⁷⁵ The automodified polymerase was found to compete with DNA for histone-binding, the polymers bound to PARP having greater affinity for the histones than did the free polymers.⁷⁶

PARP binds to the DNA strand break and is activated. Automodification takes place. The long polymer chains attract histones bound to nearby DNA. The histone-polymer-polymerase complex that then forms dissociates from the DNA. This leaves the damaged region of the DNA accessible to other enzymes, namely DNA-repair enzymes that carry out excision repair. PARG quickly degrades the long polymers, eliminating the histone binding sites. The histones shuttle back to the DNA and the condensed chromatin structure is resumed. The remaining short chains on PARP are slowly removed, returning the enzyme to its original form. This is pictured schematically in Figure 11.

Other groups are gradually accepting this idea and acknowledging that histones play a part in the process. Poirier, Brochu⁶⁹ and co-workers suggest a similar mechanism but conclude from previous work that, in situations of high poly(ADP-ribose) turnover, histone H1 is probably covalently poly(ADP-ribosyl)ated.^{77,78}

Figure 11: Schematic diagram to show the mechanism of histone-shuttling at DNA strand breaks by poly(ADP-ribosyl)ation



2.2.3.5.2 Non-histone Mechanism

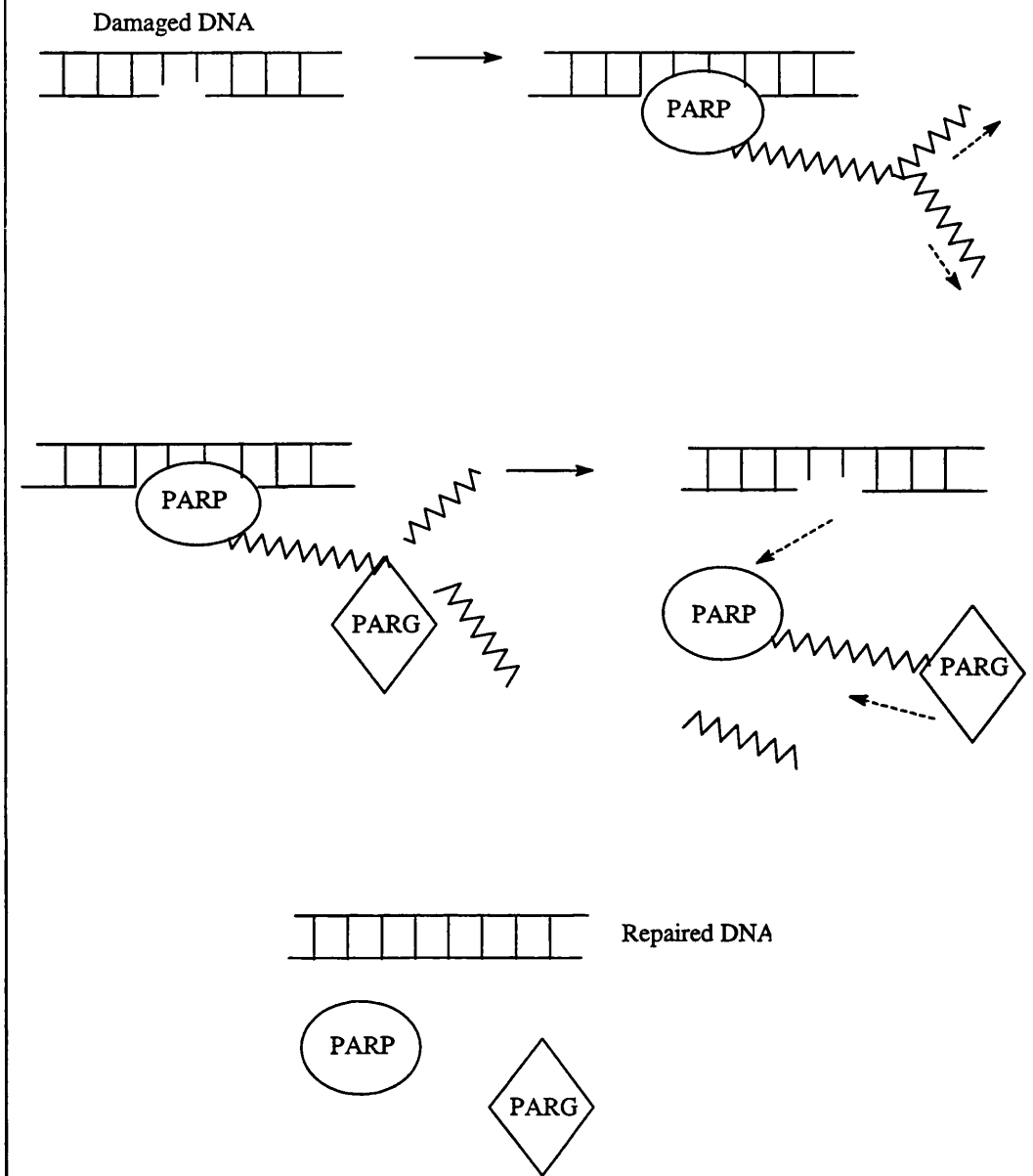
Satoh, Poirier and Lindahl⁷⁹ proposed a slightly different mechanism for poly(ADP-ribosyl)ation following the occurrence of DNA strand breaks. In this mechanism, the actions of PARP and PARG cycle PARP on and off the DNA.

In their experiments, they used a DNA-free extract from normal cells with purified PARP and PARG added. Plasmid DNA containing one γ -ray induced SSB was introduced. 3-Aminobenzamide and ADP-dihydroxypyrrrolidine⁷⁰ were

used as inhibitors of PARP and PARG respectively. They found that quite short polymers on automodified PARP were satisfactory to cause dissociation from DNA and allow DNA repair. This questions the purpose of the long polymers synthesised by PARP on activation. In their paper, these workers⁷⁹ suggest that the synthesis of long polymers might be to prevent accidental recombination events in regions of tandem repeat sequences in the DNA, by electrostatically preventing recombination with other DNA regions close to the damaged site. In their mechanism, PARP binds to the damaged DNA and is activated. Automodification takes place and these long polymer chains are quickly degraded by PARG endoglycosidically. Because there are numerous automodification sites the short polymers remaining are still enough to cause the dissociation of PARP from DNA. The DNA break is now free for DNA repair enzymes to act. The short polymers on PARP are slowly degraded by PARG and PARP is able to bind to any further DNA strand breaks. This is shown schematically in Figure 12.

When histones were introduced into this system no significant differences in the DNA repair that took place were noted.

Figure 12: Schematic diagram to show the turnover of poly(ADP-ribose) at DNA strand interruptions



2.3 Consequences of Poly(ADP-ribosyl)ation in the Cell and Possible Functions of PARP

The role that PARP plays in the cell is not yet known. In 1980, poly(ADP-ribosyl)ation was linked with DNA excision repair.⁷² Since this report, there have been several hundred papers investigating the role PARP plays in cellular recovery following DNA damage. The evidence for involvement of poly(ADP-ribosyl)ation in DNA repair is discussed in more detail in section 2.3.9.

Following activation of PARP the main measurable effect on the cell is a drop in the level of NAD^+ . Another immediate effect is a relaxation of the structure of chromatin.^{81,82} This is due to poly(ADP-ribosyl)ation of the structural proteins making up the chromosome. The large, negatively charged chains cause the structure to open out and it is likely that some of the histones are displaced from the DNA (see sections 2.2.3.4 and 2.2.3.5.1). This effect is reversed by the action of PARG. The involvement of PARP with DNA strand breaks and chromatin structure has led to investigations into the effect of PARP in DNA replication and cellular differentiation, as well as in DNA repair.

To study the effect PARP has in the cell the main approach has been to measure the effect of inhibiting PARP. Several techniques have been used to do this, the main approaches are outlined below.

2.3.1 Techniques used to study PARP actions

Chemical inhibition of PARP is the oldest and still most widely used method of studying the effects PARP might potentially have in the cell. The classical inhibitor, used in the majority of studies where PARP inhibition is required, is 3-aminobenzamide (3AB). This and other inhibitors are discussed in detail in Chapter 3.

More recently molecular biological techniques have been used to decrease PARP activity in the cell. One approach used is to cause over-expression of the cDNA encoding the DNA binding site of PARP in mammalian cells. The protein produced competes with the full enzyme for DNA binding, therefore acting as a competitive inhibitor of PARP.^{30,83} The results obtained have been similar to those obtained using 3-aminobenzamide, the classical inhibitor of PARP.

A depletion of PARP can be achieved by inducing the expression of PARP antisense RNA in cells.⁸⁴ This is done by transfecting the cDNA for human PARP in the antisense orientation, under an inducible promoter. Addition of dexamethasone to the cells induces production of the antisense RNA which binds to PARP mRNA causing the selective lowering of the production of PARP protein. These cells still contain 10^4 PARP molecules.

Complete loss of PARP activity has been engineered by inactivating the gene encoding for PARP in the mouse germline.⁸⁵ Mice are produced with no PARP and no method of synthesising poly(ADP-ribose) polymerase. This method may be a useful way of investigating the *in vivo* role of PARP.

2.3.2 Role of PARP in Carcinogenesis

Inhibition of PARP has been shown to increase and suppress carcinogenesis in various experiments. A strong link has been shown to exist between PARP and tumorigenesis *in vivo* and transformations *in vitro*. Such experiments have used various carcinogens and tumour promoters. The results have been very variable and no clear pattern has emerged as to whether inhibitors of PARP enhance or suppress the carcinogenesis. These experiments are reviewed by Boulikas.⁸⁶

2.3.3 Role of PARP in Chromosome Aberrations and Sister Chromatid Exchange

Inhibition of PARP alone was found not to induce chromosome aberrations. However, following exposure to ionising radiation or alkylating agents, inhibitors of PARP were shown to potentiate the induction of aberrations.⁵⁸

One effect of PARP inhibition that has not given conflicting results is that on sister chromatid exchange (SCE). PARP inhibitors have been shown in several different experiments to cause a dose-dependent increase in SCE.⁵⁸ SCE was also increased in cells with PARP activity inhibited by expression of DBD protein.⁸⁷ Poly(ADP-ribosyl)ation might play an important role in preventing SCE and maintaining chromosome structure. This may be achieved, as suggested by Satoh *et al*,⁷⁹ by stopping other DNA strands from approaching the damaged area, by the production of long, negatively charged poly(ADP-ribose) polymers.

2.3.4 Role of PARP in Gene Amplification

Gene amplification is the mechanism by which cells become resistant to selective agents by increasing their levels of specific proteins. PARP has been implicated in this process. An increase in gene amplification was seen in cells expressing PARP antisense RNA.⁸⁸ Other experiments using inhibitors have produced conflicting results.^{58,89}

2.3.5 Role of PARP in DNA Replication

There are several pieces of evidence linking poly(ADP-ribosyl)ation with DNA replication. There is an increase in activity of PARP and levels of poly(ADP-ribose) in the phase of the cycle when replication takes place (S phase). Activity is also higher in actively dividing cells as compared to quiescent cells.⁸⁶ Several

proteins involved in replication are acceptors for poly(ADP-ribose). These include SV40 large T antigen, topoisomerases and DNA polymerases (see Table 1). PARP is associated with DNA polymerase α and stimulates the enzyme by this physical association.⁹⁰ Activation of PARP and subsequent poly(ADP-ribosyl)ation has been shown to inhibit DNA polymerase α , δ and ϵ .⁹¹ PARP has recently been confirmed to be a component of the multiprotein DNA replication complex.⁹² It is possible that PARP functions as a molecular nick sensor associated with the replication fork. The enzyme controls the progression of the replication fork; when DNA damage is present, PARP is activated and inhibits replication, ensuring that lesions are not replicated before repair has taken place.

2.3.6 Role of PARP in Cellular Differentiation

PARP seems to be involved in terminal differentiation of cells. PARP inhibitors inhibit the differentiation of 3T3-L1 cells into adipocytes,⁹² as does the expression of antisense RNA in the preadipocyte.⁹³ There appears to be a transient increase in PARP activity that is essential for entry to the differentiation programme.⁹² This was also seen in eucaryotic differentiation demonstrated in human lymphocytes⁹⁴ and was found to coincide with a rapid rejoining of single-strand breaks present in quiescent lymphocytes. Induction of HL-60 cells with retinoic acid or dimethylsulphoxide was followed, 12-24 hours later, by an increase in PARP mRNA. A corresponding decrease occurred on terminal differentiation of the cells into granulocytes.⁹² The exact role that PARP plays in this process is as yet unknown.

2.3.7 Role of PARP in Viral Replication

Gäken and co-workers⁹⁵ found that the infection of a retrovirus into mammalian cells was blocked by inhibition of PARP activity. Inhibitors, antisense RNA and DBD techniques were used to inhibit PARP activity and all three methods gave

similar results. It was found that the inhibition occurred in the step in which the retroviral DNA is introduced into the host DNA. It appears that PARP is required to act with the virus-encoded integrase protein (IN) in order for the incorporation of the viral DNA into the host genome.

2.3.8 Role of PARP in Apoptosis

Apoptosis is an active cell death that occurs in both normal and tumour cell populations. It involves a programmed pathway that leads to removal of the apoptotic cells by phagocytosis. Apoptosis can be triggered physiologically or pathologically, following mild stress. It is distinct from the passive cell death that follows high doses of damage to the cell, *i.e.* necrosis. Apoptosis can be blocked, in mild stress conditions, by metabolic inhibitors, increasing cell survival.⁹⁶ It is thought that apoptosis might be a mechanism of eliminating potentially mutant cells that have been sub-lethally hit by a DNA-damaging agent. PARP, it has been suggested, might somehow quantify the DNA damage and translate it into a message of cell suicide.⁹⁶

The area of apoptosis, in general, has attracted a great deal of research in the last few years. There is growing evidence that dysregulation of apoptosis may lead to several human diseases, including cancer, rheumatoid arthritis and degenerative neuronal diseases such as Alzheimer's disease and Parkinson's disease.^{97,98} It is also important in the treatment of cancer, since tumour cell killing by anticancer drugs⁹⁰ and by radiotherapy¹⁰⁰ probably involves apoptosis. The exact events in apoptosis have not yet been elucidated and the role of PARP is not clear. Many experiments have been carried out in a number of different cell systems using a wide range of apoptosis-inducing agents. The main observations and theories involving PARP are described below.

Biochemically, the characteristic most commonly associated with apoptosis is internucleosomal cleavage of DNA by $\text{Ca}^{2+}/\text{Mg}^{2+}$ -dependent endonuclease. A way of measuring apoptosis is to examine cell morphology; the nuclei of apoptotic cells are fragmented and present in numerous vesicles. There is typically DNA fragmentation, such that the DNA has a ladder-like pattern on gel electrophoresis. This DNA fragmentation causes activation of PARP and synthesis of poly(ADP-ribose) polymers, resulting in a lowering of concentrations of NAD^+ in the cell. This activation of PARP occurs whatever type of stress has caused the apoptosis. Inhibition of this activation of PARP will prevent the depletion in NAD^+ but will not prevent apoptosis.⁹⁶ Therefore, apoptosis induced in human myeloid leukaemia cells, by cycloheximide or cell ageing, stress which does not cause immediate DNA damage, is not prevented by incubation with PARP inhibitors.⁹⁶ However, when apoptosis is induced by an agent that does cause DNA damage, such as mild doses of hydrogen peroxide or hyperthermia, the drop in cellular NAD^+ levels is biphasic. The first sharp drop in the NAD^+ level is due to the activation of PARP as a result of DNA damage caused directly by the stress. The levels then recover, just as apoptosis begins to be detectable, indicating that the DNA strand breaks have been rejoined. The apoptotic fragmentation of the DNA causes a second drop in NAD^+ . When the PARP inhibitor 3AB is present, the NAD^+ levels are preserved, the extent of apoptosis is reduced and cell survival is considerably increased. These results seem to suggest that the initial poly(ADP-ribosyl)ation activated by mild DNA damage is required for the induction of apoptosis. There are, however, other pathways to apoptosis for which poly(ADP-ribosyl)ation is not required. The activation of PARP by the fragmented DNA appears to be circumstantial and not critical in the apoptotic process.

It was originally proposed that a mechanism of cell suicide might be through NAD^+ depletion caused by PARP activated by extensive cell damage. Since ATP is required to convert nicotinamide back to NAD^+ and NAD^+ is required in the

production of ATP, this would lead to a depletion of ATP and cell death.¹⁰¹ This is more likely to be a passive death caused by less mild stress conditions. It has also been shown that, in thymocytes undergoing irradiation-induced apoptosis, there was a decrease in PARP enzyme activity.¹⁰² This is due to a cleavage of PARP that takes place in the early stages of apoptosis. Experiments on HL60 human leukaemia cells, with apoptosis induced by the anticancer drug etoposide,¹⁰² showed that there is an initial activation of PARP and a fall in NAD⁺ levels just before PARP cleavage takes place, but by the time the DNA fragments start to appear, a large number of PARP molecules have already been cleaved.

The cleavage of PARP is now recognised as being one of the early signs of apoptosis. The 116 kDa PARP protein is specifically cleaved into two fragments of about 85 and 25 kDa.¹⁰² The large fragment contains the automodification domain and the catalytic domain. It retains the ability to synthesise poly(ADP-ribose), although at a much lower rate and not through activation by DNA damage. The small amino-terminal fragment contains the DNA-binding domain. It has been suggested that this fragment may act as a competitive inhibitor of any intact PARP that might be present, enhancing DNA fragmentation.³⁹ Recently the protease, prICE (also known as Yama, CPP32 β or apoptosis, that carries out this cleavage of PARP has been identified.^{103,104} prICE is one of the family of interleukin 1- β -converting (ICE) / *ced-3* enzymes. These proteases are thought to be involved in the initiation of the active phase of apoptosis;¹⁰³ indeed inhibition of prICE has been shown to abolish all manifestations of apoptosis, including PARP cleavage and DNA fragmentation.¹⁰³ It is not certain whether PARP is part of a signalling system for apoptosis or whether the cleavage of PARP is just part of a general protein cleavage that occurs at the beginning of apoptosis. Other proteins have been shown to be cleaved during apoptosis by similar proteases.^{105,106}

A possible consequence of the cleavage of PARP might be the derepression of the $\text{Ca}^{2+}/\text{Mg}^{2+}$ -dependent endonuclease that causes the DNA fragmentation seen in apoptosis. Poly(ADP-ribosyl)ation of the endonuclease inhibits the enzyme; it has been suggested that when PARP is cleaved the inhibition is removed and allows the enzyme to attack the DNA.¹⁰⁷ Rice *et al*¹⁰⁸ found that apoptosis could be induced in human leukaemia cells, by the addition of C-nitroso-ligands of PARP. This was explained as follows: The C-nitroso compounds bind to one of the zinc fingers on PARP's DBD so inactivating it. The $\text{Ca}^{2+}/\text{Mg}^{2+}$ -dependent endonuclease, normally kept in a latent state by poly(ADP-ribosyl)ation, is derepressed, DNA degradation takes place and cell death follows.

The most recent work has focused on the regulation of pRICE. It has been shown that granzyme B, a protein produced by cytotoxic T-cells, activates pRICE, through the cleavage of its precursor.^{109,110} Another group of proteins, the Bcl-2 family, have also been shown to regulate apoptosis induced by a number of agents including nitric oxide (NO), ara C, etoposide and mitoxantrone.^{99,111} Overexpression of Bcl-2 blocks the cleavage of PARP and apoptosis.^{99,111}

Experiments involving PARP inhibitors have given conflicting results. 3AB has been shown to increase,¹¹² reduce,^{96,113} or not to alter¹¹⁴ the extent of apoptosis. Variations in experimental conditions, cell type and apoptosis inducers may be the cause of these discrepancies. In dominant negative mutant cells, in which the DBD of PARP is overexpressed, there were found to be increased levels of apoptosis.⁸⁷ Experiments using cells from mice lacking the PARP gene¹¹⁵ showed decreased apoptosis at low concentrations. At low concentrations of NO, apoptosis was induced in normal cells and was reduced by the presence of 3AB. The cells lacking PARP did not show signs of apoptosis at this concentration. However at higher concentrations, NO induced apoptosis in the PARP-deficient cells, and in the normal cells, 3AB was not successful in preventing apoptosis. It appears in this system NO induces apoptosis through PARP-dependent pathways

at low concentrations, but at higher concentrations an alternative pathway takes over.

It is clear from the experimental data gathered so far that PARP plays some part in apoptosis. However the complexity of the process has not allowed any firm conclusions to be drawn.

2.3.9 Role of PARP in DNA repair

It has been known since the 1950s that alkylating agents and radiation lower cellular NAD^+ levels.²² In 1975,^{116,117} this depletion of NAD^+ was shown to be due to the activation of PARP by DNA damage caused by agents such as streptozotocin.

It was soon found that agents causing DNA damage in general; alkylating chemicals, X-rays and DNA hydrolysing enzymes all increase the activity of PARP.^{22,118} It was deduced that PARP might play an important role in DNA repair. In 1980, Benjamin and Gill²⁴ found that PARP is completely dependent on strand breaks for activity and the initial rate of synthesis of poly(ADP-ribose) increases linearly with X-ray dose given or dose of endonuclease added. In the same year, Durkacz *et al*⁸⁰ concluded that poly(ADP-ribose) participates in DNA excision repair, when they found that PARP inhibitors prevented the rejoining of DNA strand breaks caused by dimethyl sulphate (DMS). The same effect was achieved by depleting NAD^+ levels, showing that the process is dependent on polymer formation. The PARP inhibitors consequently potentiated the cytotoxicity of DMS.

Excision repair can be divided into two types:- nucleotide-excision repair and base-excision repair. Nucleotide-excision repair is carried out following damage by UV light and chemicals producing relatively bulky lesions in the DNA helix.

The lesion is excised with a number of undamaged nucleotides to give a repair patch of 25-40 nucleotides. Base-excision repair follows damage to DNA by ionising radiation or methylating/ethylating compounds. Here the repair patch is much shorter. Ahnström and Ljungman¹¹⁹ found that 3AB increased the number of transient DNA strand breaks in cells treated with methylating and ethylating agents, but had little effect on UV light or chemicals triggering nucleotide-excision repair, *e.g.* 7-bromomethylbenzanthracene. Other groups also concluded that PARP seems to be involved in base-excision and not nucleotide-excision repair.^{58,120,121} These studies have shown that PARP inhibitors have little effect on UV-induced cytotoxicity and it is generally accepted that repair of UV damage is not regulated by poly(ADP-ribosyl)ation.

Excision repair of DNA damage can be summarised into three basic steps: The damaged region is firstly excised by nuclease enzymes. DNA polymerase then binds to the 3'-OH terminal of the cut strand and synthesises DNA to fill the gap. DNA ligase enzymes then seal the nick in the damaged strand. Experiments have shown that poly(ADP-ribose) synthesis is involved in the ligation step.^{80,120} Following doses of DMS, assays of repair synthesis showed that the PARP inhibitor, 3AB, had no effect at low doses and caused stimulation of repair synthesis at high doses of DMS.¹²⁰ Poly(ADP-ribosyl)ation, therefore, is not required for the polymerisation step in excision repair. 3AB was, however, found to cause a delay in strand-break rejoining^{80,120} (the ligation stage). This persistence of strand-breaks may allow nick-translation, giving larger repair patches under certain conditions. This may explain the increase in DNA repair synthesis seen at higher DMS doses in the presence of 3AB. Similar results have been seen with other alkylating agents.²²

Following the conclusion that PARP has a role in the ligation step of excision repair following DNA damage by alkylating agents, the effect of poly(ADP-ribose) on ligase enzymes was investigated. Creissen and Shall¹²² investigated

the effect of DMS on ligase activity. They found that treatment of cells with DMS increased ligase II activity and this increase was blocked by PARP inhibitors. They concluded that following DNA damage and activation of PARP, either ligase II or a closely related protein is poly(ADP-ribosyl)ated and this causes activation of the ligase enzyme. Other experiments have since shown that the direct poly(ADP-ribosyl)ation of ligase II results in its inhibition⁵⁶ (see Table 1), therefore disagreeing with this hypothesis. Ohashi *et al*¹²³ proposed that histones were also involved in the mechanism. They showed that in the resting state histones inhibit ligase activity. This inhibition is reversed by the automodification of PARP. They suggested that when DNA damage occurs PARP is activated, automodification takes place, this somehow reverses the histone inhibition of ligase and results in ligase activation and repair of the DNA. The activation of the ligase enzyme may be as a result of the dissociation of the histones from the DNA, due to the neutralisation of their charges by the polymer chains, making the DNA more accessible to ligase. Ligase has also been shown to have an affinity for poly(ADP-ribose) and this may facilitate its positioning near the site of damage. This fits in with the histone-shuttle mechanism for PARP discussed in section 2.2.3.5.1.

The evidence for a role for poly(ADP-ribose) in the repair of DNA damage following ionising radiation is less clear. There is certainly an increase in PARP activity following the treatment of cells with gamma or X-ray radiation. However, a clear demonstration of inhibition of strand-break rejoining by PARP inhibitors has not been given. This may be due to the low net level of SSB's after irradiation and difficulty in following the repair. DMS treatment results in many more strand breaks and less sensitive methods of analysis can be used. Reports of experiments using 3AB have given conflicting results. The inhibitor has been shown to inhibit repair following gamma irradiation,²² have no reproducible effect¹²⁰ on DNA strand-breaks following gamma irradiation and also to increase strand rejoining following gamma irradiation.¹²⁴ Further evidence is required to

show whether or not the synthesis of poly(ADP-ribose) following DNA damage by ionising radiation has a role in repair of the damage. Cell killing by x-rays and gamma radiation has been shown, by several groups, to be enhanced by the inhibition of PARP in a dose dependent way.¹²⁵⁻¹³⁰ In most cases this has been attributed to an inhibition of DNA repair and cellular recovery but by what mechanism is not clear.

Stevnsner *et al*¹³¹ carried out studies using human HeLa cells with dexamethasone-inducible PARP antisense transcripts, in which the cellular PARP content is reduced by 90% on induction. They found that, in agreement with studies using inhibitors, repair of UV damage was not altered from that in control cells. However, the PARP deficient cells were deficient in gene-specific repair of alkylation damage and showed an increased susceptibility to nitrogen mustard agents. Here, the repair of specific, essential genes was measured rather than the genome as a whole. This work indicates that PARP activity is required for cellular recovery from alkylating agents.

Trans-dominant inhibition of poly(ADP-ribosyl)ation by overexpression of the PARP DBD resulted in sensitisation to gamma radiation and the alkylating agent N-methyl-N'-nitro-N-nitrosoguanidine (MNNG).³⁰ This was shown to be due to a disturbance in the cellular recovery from the damage. Again damage by UV radiation was not affected.

PARP deficient "knock-out" mice, which have no PARP and cannot produce poly(ADP-ribose), are otherwise healthy and fertile.⁸⁵ This indicates that PARP does not play an essential role in cellular proliferation, differentiation or development. Cells from the mice show normal DNA repair after UV irradiation and, more surprisingly, after treatment with an alkylating agent.⁸⁵ However, proliferation of primary fibroblasts and thymocytes following gamma irradiation was impaired. The mutant mice are susceptible to spontaneous development of

skin diseases and the investigators conclude that, although PARP does not seem to be essential for normal chromatin function, it might play a part in response to environmental stress.⁸⁵ These results seem to disagree with the many studies carried out using inhibitors and other techniques which lower PARP levels but do not completely abolish PARP content.

Satoh *et al*^{132,133} have also recently reported that their findings have brought them to the conclusion that PARP has an incidental and negative role in DNA excision repair. In an *in vitro* system using cell extracts, they found that complete removal of PARP improved DNA-repair of gamma radiation lesions. This is explained by the fact that PARP interferes with base-excision repair by binding to the damaged site. Release of PARP facilitates DNA repair (see non-histone mechanism for PARP in section 2.2.3.5.2). 3AB inhibits DNA repair by inhibiting the automodification of PARP and therefore its release from the DNA strand-break.

Despite the confusing evidence, it seems that likely that PARP plays a role, however subtle, in the reaction of the cell to DNA damage. Discrepancies between results may be due to the very wide range of experimental techniques, cell systems, and DNA damaging agents. Recently, Mizumoto and Farber pointed out that "cytotoxicity" in replicating cells commonly refers to an inhibition of cell growth, rather than to cell killing.¹³⁴ In their study they found that at lower levels of DNA damage [2.5 mM *N*-methyl-*N*-nitrosourea (MNU)], 3AB potentiated cell growth inhibition, supposedly by limiting DNA repair mechanisms. However, when more extensive damage was present (> 5 mM MNU), cell kill was achieved by depletion of ATP, due to excessive poly(ADP-ribosyl)ation, rather than by DNA strand-breaks. In this case, 3AB prevents cell death by preventing the depletion of ATP. These observations further confuse the issue, as does the suspected involvement of PARP in apoptotic pathways.

The fact remains that PARP inhibitors, in the vast majority of studies, have brought about sensitisation of cells to radiation and alkylating agents. The recent studies in "knock out" mice make PARP inhibitors more desirable as radiosensitisers and chemosensitisers. The study indicates that PARP plays a non-essential role in normal chromatin function, therefore a specific PARP inhibitor should not have any intrinsic cytotoxic effects. In the next chapter, PARP inhibitors, their actions, and their potential role as radiosensitisers and chemosensitisers are discussed.

Chapter Three

3. Inhibitors of Poly(ADP-ribose) Polymerase

3.1 Poly (ADP-ribose) Polymerase Inhibitors as Chemosensitisers and Radiosensitisers

With the discovery that poly(ADP-ribose) polymerase seems to be involved in DNA excision repair,⁸⁰ came the revelation that PARP inhibitors can potentiate the cytotoxicity of DNA-damaging agents.^{80,120,121} Such inhibitors are, therefore, prime targets for the design of radiosensitisers and chemosensitisers for the treatment of cancer. Experiments so far have been largely *in vitro* and the inhibitors used have often lacked specificity and/or potency. However, results suggest that a specific, potent inhibitor of PARP might be useful in the potentiation of radiotherapy and chemotherapy.³⁹

3.1.1 Chemosensitisation

Durkacz *et al*⁸⁰ first reported that 3AB increased the cytotoxicity of the alkylating agent DMS in L1210 mouse leukaemia lymphoblast cells. The cells were treated with increasing doses of DMS either alone or in the continuous presence of 3AB or its analogue 3-aminobenzoic acid which is not an inhibitor of PARP. A concentration of 90 μM DMS was needed to reduce survival to 10% in the absence of 3AB, whereas in the presence of 3AB, 22 μM was found to be sufficient. 3-Aminobenzoic acid did not have any effect on the cytotoxicity of DMS. Several other *in vitro* studies on different cell lines using alkylating agents, such as DMS,²² MNNG,^{22,135,136} MNU,²² methyl methanesulphonate (MMS)^{135,136} and temozolomide,^{137,138} have provided similar results. The effect of PARP inhibition on the cytotoxicity of bifunctional alkylating agents, however is much smaller.^{135,137} 3AB was found to potentiate 1-(2-chloroethyl)-1-

nitrosourea or busulfan cell killing by only 0.9 to 1.5-fold.¹³⁵ The benzamides have also been found to potentiate the cytotoxicity of the S-phase acting drug 6-thioguanine (TG).^{139,140} However, TG does not produce a decrease in NAD⁺ levels in the cell, indicating that PARP is not activated. This potentiation of cytotoxicity is not thought to be through the inhibition of DNA repair. In addition, higher doses of 3AB can protect the cell against TG toxicity.¹³⁹

Reports of demonstration of chemosensitisation by PARP inhibitors *in vivo* are much less abundant. Although the most successful potentiation of cytotoxicity has been seen with mono-functional alkylating agents *in vitro*, equivalent experiments *in vivo* have not been reported. Experiments demonstrating potentiation, by 3AB, of the cytotoxicity of agents such as bleomycin¹²⁵ and cisplatin¹⁴¹ on the Ehrlich ascites tumour have been carried out. However, at the doses generally used, 3AB is known to cause a marked hypothermia;¹⁴² this may affect the results seen. This highlights the main problem with these experiments; especially those carried out using early non-specific inhibitors of PARP such as thymidine and pyrazinamide (these agents will be discussed later in the chapter).

The lack of specificity and potency of the early PARP inhibitors means that it is difficult to assess whether any chemosensitisation seen is the result of PARP inhibition. The concentrations of the benzamides used in these studies are often in the millimolar range, whereas the PARP inhibitory IC₅₀ values are in the micromolar range. At these higher concentrations, these inhibitors have been shown to cause inhibition of cell growth¹⁴³ and interference with metabolic processes such as glucose metabolism and purine biosynthesis.¹⁴³ Certainly, in the case of the potentiation of TG cytotoxicity by 3AB, inhibition of *de novo* purine biosynthesis has been implicated as the mechanism rather than PARP inhibition.^{139,140}

The lack of specificity of chemotherapeutic agents also implies that any therapeutically useful chemosensitiser has to be specific for tumour cells and must not cause potentiation of damage to normal cells.

More recently, Boulton *et al*¹³⁸ carried out experiments *in vitro* measuring the potentiation of temozolomide cytotoxicity by various PARP inhibitors. Two of the compounds tested were about 50-fold more potent PARP inhibitors than was 3AB. The study showed that the sensitisation of the cells to the temozolomide toxicity was dependent on the potency of the sensitiser as a PARP inhibitor. Therefore, much lower concentrations of these newer generation inhibitors can be used, with less risk of other non-specific effects occurring in the cell.

3.1.2 Radiosensitisation

Many studies *in vitro* have shown that inhibitors of PARP can increase the sensitivity of cells to X-ray and gamma radiation.^{22,125-128} Earlier studies,¹²⁰ however, only reported a marginal enhancement of killing or no effect at all. This is attributed to the fact that there was not sufficient time allowed for the inhibitor to be taken up by the cells or that the concentration of inhibitor was too low.¹²⁵ The effect of the inhibitor also has to be measured within the two hours following irradiation since this is when PARP is active and repair is taking place. Therefore, studies using higher concentrations of inhibitors for shorter times were more successful.¹²⁵ The radiosensitisation seen is dependent on the potency of the PARP inhibitor. Ben-Hur¹²⁹ showed that, although the benzamides do inhibit glucose metabolism, he found no correlation between effectiveness in inhibiting PARP and effectiveness in inhibiting glucose metabolism, despite a correlation between the inhibitory potential of PARP and the enhancement of radiation response. This indicates that it is the inhibition of PARP that is causing the radiosensitisation and not any other effect of the inhibitors. Even higher concentrations of PARP inhibitors seem to be needed for radiosensitisation than

for chemosensitisation. It is thought that a higher level of inhibition of PARP may be required since even a low level of PARP activity is sufficient for recovery to take place.¹⁴⁵

The effect of 3AB on the survival curve of cell populations, following treatment with ionising irradiation, is to reduce the shoulder of the curve and decrease the gradient (as shown in Figure 5). This would be therapeutically desirable if achieved *in vivo*.

Nicotinamide and pyrazinamide are both weak inhibitors of PARP and have been shown to produce potentiation of radiation effects *in vivo*.^{14,146,147} However, this is thought to be largely due to their ability to alter tumour blood flow and decrease hypoxia. Nicotinamide, in combination with carbogen breathing therapy and radiotherapy, is now in Phase II trials for the treatment of tumours.^{147,148} A recent study suggests that, although reduction in hypoxia is the main mechanism of action, inhibition of DNA repair is responsible for part of the effect seen.¹⁴⁸

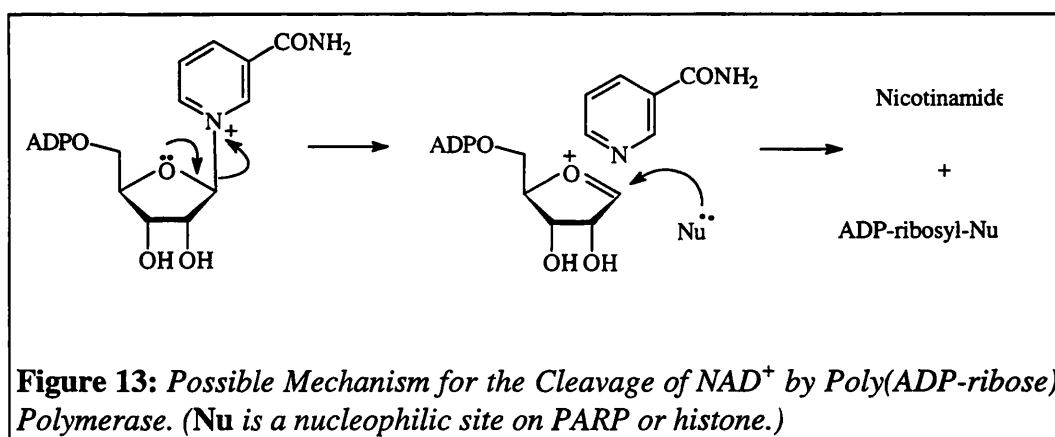
Experiments with benzamides have been carried out *in vivo*. 3AB and several other benzamide derivatives were shown to potentiate the effects of X-rays in the EMT-6 tumour system. 3AB was also shown to cause an increase in tumour growth delay in the Greene melanoma in hamsters.¹⁴⁵ One of the newer PARP inhibitors, 3,4-dihydro-5-methylisoquinolin-1-one (PD128763) has been shown to be active *in vivo* as a radiosensitiser.¹⁴ It produced a 1.4-1.6 fold increase in cell kill in various murine tumours and increased growth delay by 10-15 days, compared to radiotherapy alone. It also brought about tumour regression which was not seen with radiation alone.¹⁴⁵

These results, especially those in which newer PARP inhibitors have been used suggest that selective, potent PARP inhibitors are ideal candidates for development as radiosensitisers and chemosensitisers in the treatment of cancer.

3.2 The Development of Inhibitors of Poly(ADP-ribose) Polymerase

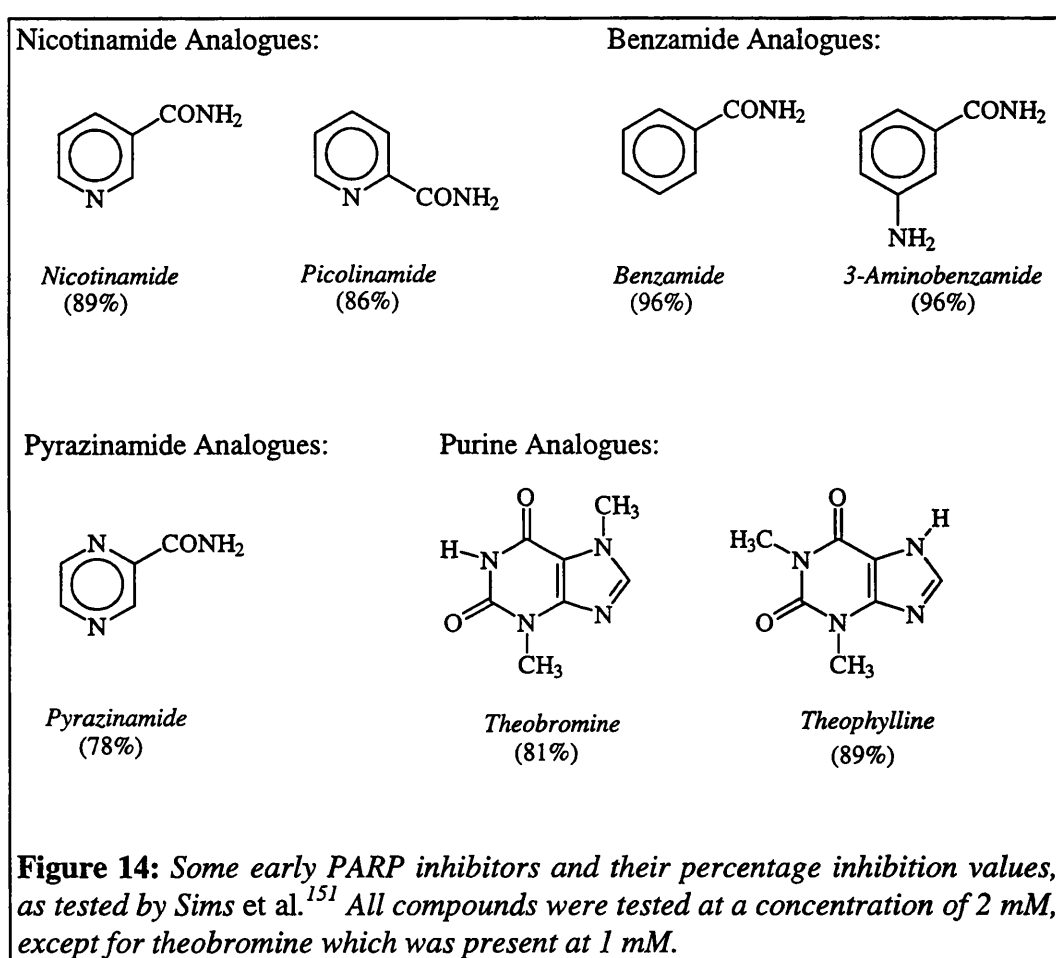
Many compounds have been tested for their ability to inhibit PARP. It is difficult to compare individual studies since a great variety of assay methods and conditions, cell lines and inhibitor and NAD^+ concentrations have been used. These factors must be taken into consideration when comparing inhibitors.

Most of the inhibitors of PARP tested so far are competitive, reversible inhibitors that bind to the NAD^+ binding site of the enzyme. As explained in Chapter Two, PARP binds the NAD^+ molecule and catalyses its cleavage; adding the ADP-ribose portion to the poly(ADP-ribose) chain and releasing the nicotinamide portion. This is shown in Figure 13; there is nucleophilic attack of the anomeric carbon by a site on the acceptor protein and cleavage of the carbon-nitrogen bond. The mechanism probably proceeds *via* the oxonium ion shown.



It is therefore no surprise that the first compounds found to inhibit PARP were nicotinamides.¹⁴⁹ Thymidine, which has some structural similarities to NAD^+ , was also found to inhibit PARP.¹⁵⁰ Theophylline and other xanthines were also among some of the inhibitors first discovered and used. These compounds and their analogues were among the thirty three compounds tested by Sims *et al*¹⁵¹ In

this study, the effect on PARP activity, as indicated by incorporation of radioactivity from [^3H]NAD $^+$ into acid insoluble material, was measured. The effect of the inhibitors on lowering of NAD $^+$ levels following treatment of lymphocytes with MNNG was also measured. The inhibitors were all present at a concentration of 2 mM, except for theobromine at 1 mM. This was a useful study in that several compounds were compared in the same system at equivalent concentrations. Certain structure activity relationships can be concluded from the study.



Some examples of the compounds tested are shown in Figure 14 along with their percentage inhibition values. Nicotinamide itself was the most potent of the nicotinamide analogues tested (89% inhibition). In this series, it was found that an unsubstituted amide group was required for activity but its position in the

pyridine ring did not seem to be crucial; 86% inhibition was achieved with picolinamide. The aromaticity of the ring was also essential for activity and substitution of the ring nitrogen resulted in a loss of activity.

Pyrazinamide, which has a similar structure to nicotinamide but with two heterocyclic nitrogen atoms, was a reasonably good inhibitor (78%). Other analogues in this series were not active. The extra ring nitrogen is tolerated but the amide group, again, was found to be essential for activity, with a second amide group *ortho* to the first resulting in a loss of activity.

Purine analogues theophylline and theobromine were found to be good inhibitors of PARP (89% and 81% inhibition respectively) although caffeine only inhibited PARP activity by 35%.

Although these compounds are reasonable inhibitors of PARP, they lack specificity and have been shown to affect other cellular processes: Nicotinamides affect the synthesis of NAD^+ and may deplete cellular phosphoribosyl diphosphate pools. Thymidine inhibits DNA synthesis by depleting dCTP concentrations in the cell. Methylated xanthines are known to affect cyclic diphosphodiesterase²¹ Therefore, more specific inhibitors had to be found. Benzamide is a close analogue of nicotinamide but does not have the ring nitrogen and so cannot be metabolised by NAD-biosynthetic enzymes. In the study by Sims and his co-workers,¹⁵¹ benzamide inhibited PARP activity by 96%, as did the 3-amino analogue, 3AB. In the series of analogues tested here the carbamoyl group was found to be essential for activity; 3-aminobenzoic acid was devoid of activity. Activity was also decreased when there was substitution in either the 2- or the 4- position of benzamide. These results agreed with those of Purnell and Whish who earlier investigated a series of benzamides.²¹

Benzamide was first shown to be an inhibitor of PARP by Shall in 1975.¹⁵² Although this compound is a good, specific inhibitor of PARP, it is a hydrophobic molecule. The poor solubility of benzamide in aqueous solutions made physiological studies difficult; this led Purnell and Whish to examine the activity of less hydrophobic analogues of benzamide.²¹ Their results are shown in Table 2 below. PARP activity was measured by the incorporation of radioactivity from [³H]NAD⁺ into acid insoluble material and the inhibition was expressed as a percentage of total inhibition. Much lower concentrations of inhibitor were used in this study than that of Sims;¹⁵¹ concentrations of 50 μ M of inhibitor were used, which was equimolar with the substrate NAD⁺. All the 3-substituted benzamides, with the exception of 3-nitrobenzamide, were found to be potent, with over 90% inhibition achieved at 50 μ M. These benzamides have their substituent in the position corresponding to the ring-nitrogen in nicotinamide.

Table 2: *Compounds tested by Purnell and Whish²¹ for their effect on PARP activity. Inhibition was measured at a concentration of 50 mM and expressed as a percentage of total inhibition.*

<u>Compound</u>	<u>Inhibition (%)</u>
Nicotinamide	63
Benzamide	96
3-Aminobenzamide	90
3-Bromobenzamide	95
3-Hydroxybenzamide	96
3-Methoxybenzamide	98
3-Nitrobenzamide	71
Nicotinic acid	0
3-Aminobenzoic acid	10
3-Hydroxybenzoic acid	0
3-Nitrobenzoic acid	0
2-Aminobenzoic acid	0
4-Aminobenzoic acid	0
3-Aminoacetophenone	31
3-Acetylpyridine	0
Acetophenone	36
3-Amino-N-methylbenzamide	0
3-Acetamidobenzamide	98

This study also confirmed the theory that a free carbamoyl group is required for activity. The benzoic acid derivatives showed no activity, although the acetophenones showed some activity. Another study by the same group¹⁵³ found that 56% inhibition of PARP was achieved by 3-methoxyacetophenone at 50 μ M. This indicates that the carbonyl group conjugated to the aromatic ring is important for activity. In agreement with the study by Sims and co-workers,¹⁵¹ substitution of the nicotinamide ring nitrogen results in a loss of activity. Acylation of the amino group of 3-aminobenzamide (3AB), however, seems to give an increase in potency; 3-acetoamidobenzamide exhibited 98% inhibition of PARP.

3AB and 3-methoxybenzamide were highlighted as potentially useful PARP inhibitors for *in vitro* and *in vivo* studies. K_i values of $1.8 \pm 0.2 \mu\text{M}$ and $1.5 \pm 0.3 \mu\text{M}$ were calculated for 3AB and 3-methoxybenzamide, respectively. These compounds were found by this group to be physiologically specific. More recent reports have shown that 3AB can interfere with cell growth¹⁴³ and with metabolic processes such as glucose metabolism and purine biosynthesis.¹⁴⁴ However, these studies used very high concentrations of 3AB; in the millimolar, rather than the micromolar, range. In fact, 3AB has since become the standard and most widely used PARP inhibitor. It should be pointed out that weaker, less specific inhibitors, such as nicotinamide, have been used in PARP investigations and care must be taken when drawing conclusions from such studies.

The specificity of the benzamides and some of the earlier inhibitors was investigated by Rankin *et al.*¹⁵⁴ This group measured inhibition of the two other classes of enzyme that consume NAD^+ ; mono(ADP-ribosyl)transferases and NAD^+ glycohydrolases. IC_{50} values (the concentration of inhibitor required to inhibit the enzyme activity by 50%) were measured for 20 compounds, for PARP, mono(ADP-ribosyl)transferase A, and NAD^+ glycohydrolase. Some

examples of the results are shown in Table 3. The benzamides were fairly specific inhibitors of PARP with 500 to 1000-fold more activity for PARP than for the mono(ADP-ribosyl)transferase. The IC₅₀ value for benzamide for the inhibition of NAD⁺ glycohydrolase was 40 mM. There would, therefore, be no inhibition of this enzyme at the concentrations used to inhibit PARP. In the cases of nicotinamide, thymidine and theophylline, the IC₅₀ values for the two ADP-ribosylating enzymes are much closer.

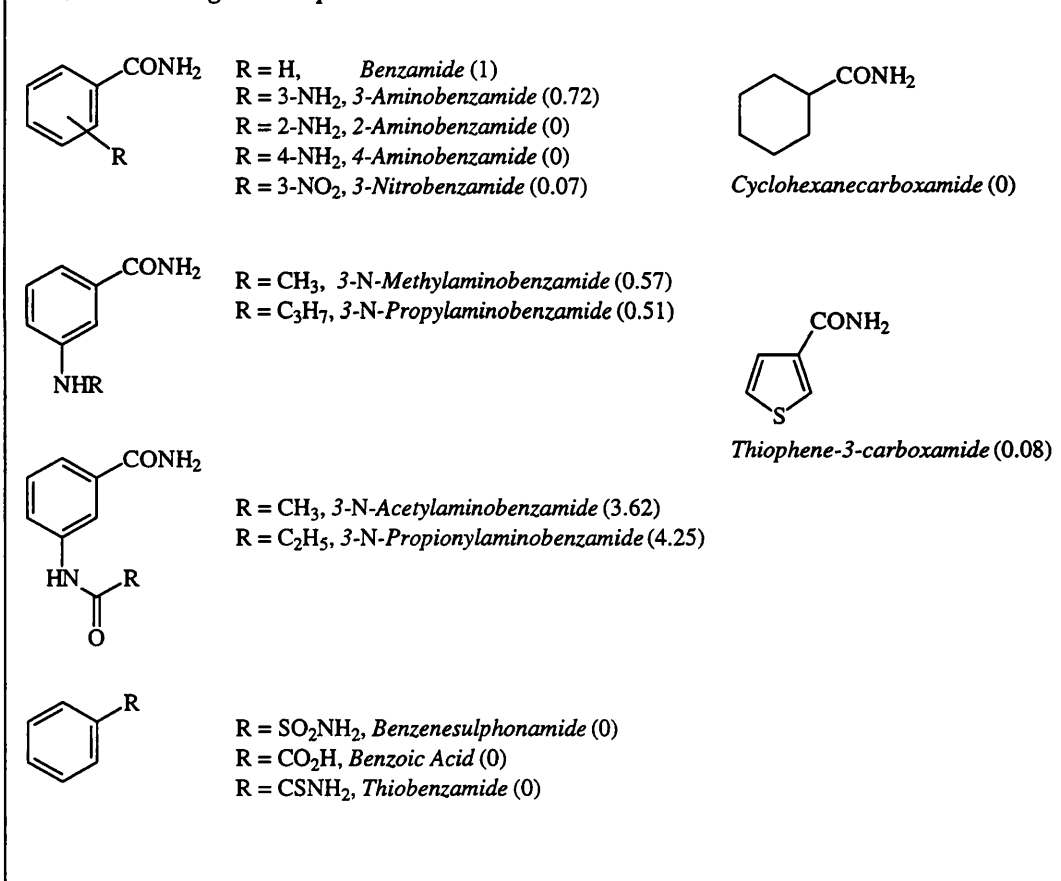
Table 3: *Effect of some selected compounds on PARP, in vitro and in vivo and mono(ADP-ribosyl)transferase in vitro. Results from Rankin et al.¹⁵⁴*

<u>Compound</u>	<u>IC₅₀ (μM)</u>		
	PARP <i>(in vitro)</i>	mono(ADP- ribosyl)transferase	PARP <i>(in vivo)</i>
Benzamide	3.3	4.1×10 ³	3.5
3AB	5.4	3.0×10 ³	3.0
Nicotinamide	31	3.4×10 ³	100
Thymidine	43	1.9×10 ³	-
Theophylline	46	2.8×10 ³	230

A second useful observation was made in this study: The IC₅₀ values for the benzamide PARP inhibitors *in vitro* were very similar to values obtained in intact cells. However, for the other inhibitors tested, such as nicotinamide and 5-bromodeoxyuridine, 3 to 5-fold higher concentrations were required *in vivo* to achieve the equivalent inhibition as in the *in vitro* system. This suggests that it should be possible to achieve PARP inhibition in intact cells using micromolar concentrations of benzamide inhibitors in the culture medium.

Sestili *et al*¹⁵⁵ carried out further investigations into the structure activity relationships (SAR) for the benzamides. In this study, however, PARP activity was not measured directly. Activity was assessed by measuring the effect of the inhibitor, present at 5 mM concentrations, on the rejoining of DNA SSB, following treatment with MMS. The effect was expressed by comparison with benzamide itself. This method of assessment should give similar results to those obtained by the direct measurement of PARP inhibition. However, it should be remembered that the exact role of PARP in DNA repair is not yet known and the two methods should be treated separately.

Figure 15: Benzamide analogues and their effect on the rejoining of DNA SSB produced by MMS as tested by Sestili *et al*.¹⁵⁵ Relative potencies with respect to benzamide are given in parentheses.



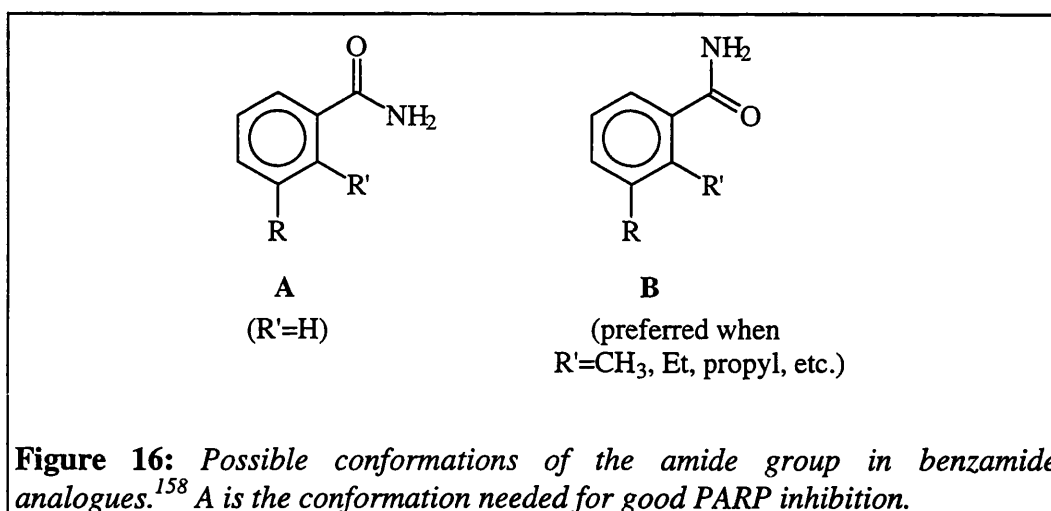
This investigation confirmed results seen before and added to SAR information.

- ◆ For benzamides substitution must be in the 3- position to retain activity.

- ◆ Substitution with a nitro group resulted in a significant loss of activity, implying that electron-withdrawing groups decrease activity
- ◆ Alkylation of the amino group of 3AB results in a loss of activity but acetylation significantly enhances activity.
- ◆ The aromatic ring is essential for activity; the saturated analogue of benzamide, cyclohexane, is devoid of activity.
- ◆ The unsubstituted carbonyl group is essential for activity; replacement of the amide oxygen or carbon atom with sulphur resulted in a loss of activity.

This group reported that thiophene-3-carboxamide was only weakly active in this assay. In a further study, in which sulphur containing benzamides were tested for their effect on NAD^+ depletion following treatment of cells with H_2O_2 , thiophene-3-carboxamide was again found to be much less active than the parent benzamide.¹⁵⁶ This is surprising, since thiophene-3-carboxamide is regarded as a close isostere of benzamide. Work being carried out in our laboratories suggests that the thiophene-carboxamides are good PARP inhibitors; 80% inhibition of PARP was achieved using 5-aminothiophene-2-carboxamide at a concentration of 10 μM .¹⁵⁷

The investigations of nicotinamide and benzamide analogues as PARP inhibitors show that the carbamoyl group is essential for activity. Suto *et al*¹⁵⁸ designed compounds in which the conformation of this amide group is restricted, with a view to determining the preferred binding conformation. Figure 16 shows two possible conformations of the amide group in relation to the aromatic ring and its substituents.



The conformation pictured in structure A can be fixed by joining the nitrogen to the benzene ring via an ethane or an ethene bridge, to give a 3,4-dihydroisoquinolin-1-one or and isoquinolin-1-one. Suto and his colleagues tested several 5-, 6- 7- and 8-substituted 3,4-dihydroisoquinolin-1-ones and 5-substituted isoquinolin-1-ones. The 5-substituted compounds in each series showed very high activity as PARP inhibitors, with IC₅₀ values less than 1 μM in most cases. These results are shown in Table 4.

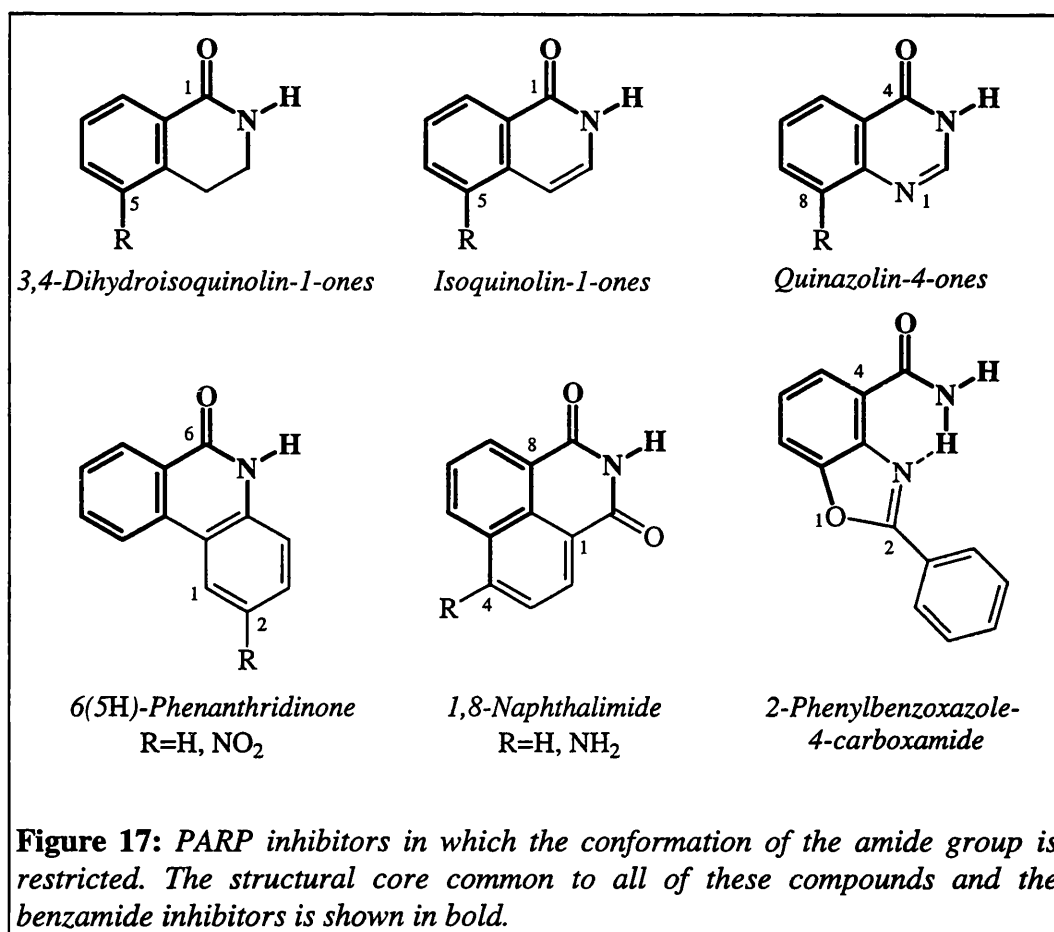
Table 4: Some isoquinolinone and dihydroisoquinolinone inhibitors of PARP. As tested by Suto et al.¹⁵⁸

<u>Compound</u>	<u>IC₅₀ (μM)</u>
Isoquinolin-1-ones	
5-OMe	0.58
5-OH	0.14
5-NO ₂	3.2
5-NH ₂	0.24
5-H	6.2
3,4-Dihydroisoquinolin-1-ones	
5-OMe	0.42
5-OH	0.1
5-NO ₂	3.2
5-NH ₂	0.41
5-H	1.5
3-Aminobenzamide	9.0

3,4-Dihydro-5-hydroxyisoquinolin-1-one was the most active compound tested with an IC_{50} of 0.1 μM . Some 90-fold more active than 3AB as tested in the same assay. As in the benzamide series, the nitro-substituted analogues were significantly weaker inhibitors.

This dramatic increase in activity indicated that this conformation is preferred for binding. This was further confirmed by the second part of the study in which 2,3-disubstituted benzamides were synthesised and tested. Compounds had either a methoxy or hydroxyl group in the 3-position and various alkyl groups in the 2-position. All of the compounds tested were devoid of activity except for 3-Hydroxy-2-methylbenzamide which was a very weak inhibitor with an IC_{50} of 590 μM . This is compared to an IC_{50} value of 2.0 μM measured for the unsubstituted 3-hydroxybenzamide. The larger substituents in the 2-position force the amide into the conformation shown in B (Figure 16) which is not favoured for binding to the enzyme.

The 3,4-dihydroisoquinolin-1-ones were also tested for their effect on the cell survival curve, following treatment with X-ray irradiation. These compounds were found to reduce significantly the shoulder and the gradient of the curve and act as radiosensitisers *in vitro*. As mentioned earlier, 3,4-dihydro-5-methylisoquinolin-1-one (PD128763) has also been found to be a radiosensitiser *in vivo*.¹⁴⁵



Other compounds in which the 3-substituted benzamide core is present, with the conformation of the amide group fixed covalently, are shown in Figure 17. All of these groups of compounds are very potent PARP inhibitors.

2-Methyl-4[3H]-quinazolinone was extracted from a culture of *Bacillus cereus* by Yoshida *et al.*¹⁵⁹ This compound was tested and found to produce a 50% reduction in PARP activity at 1.1 μ M. Kinetic studies showed that this compound is a competitive inhibitor of PARP, with a K_i value of 1.1 μ M. Two further quinazolinones have been tested by Griffin *et al.*¹⁶⁰ 8-Hydroxy-2-methylquinazolin-4-one was synthesised and tested and found to give 92% inhibition of PARP at a concentration of 10 μ M; the IC_{50} value measured was 0.44 ± 0.13 . This is one of the best known inhibitors of PARP, with activity in the same range as the isoquinolinones. 8-Hydroxy-2,3-dimethylquinazolin-4-one

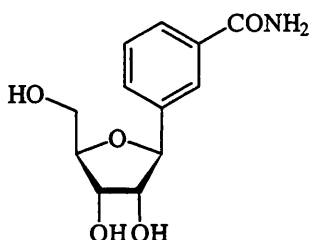
was also tested, but as would be expected, the substitution of the "amide" nitrogen brings about a loss of activity (11% inhibition was observed at 10 μM). 8-Hydroxy-2-methylquinazolin-4-one has also been shown to enhance strand breaks produced by temozolomide (a monofunctional alkylating agent) and to increase its toxicity *in vitro*.¹³⁸

2-Methylquinazolin-4-one was also included in a comprehensive study carried out by Banasik and his colleagues in 1992.¹⁶¹ In this study, in the region of 150 compounds were tested, firstly for activity as PARP inhibitors and secondly, for inhibition of an arginine-specific mono(ADP-ribosyl) transferase from hen heterophils. A wide range of compounds were tested including nicotinamide, several benzamides and some of the heterocycles pictured in Figure 17. IC_{50} values were measured. For 2-methylquinazolin-4-one, the IC_{50} value measured was 5.6 μM ; significantly greater than the value obtained in the earlier study.¹⁵⁹ This was also the case for many of the benzamides; e.g. 3AB had an IC_{50} of 22 μM in this system, compared to 9.0 μM ¹⁵⁸ and 5.4 μM ¹⁵⁴ measured in other assays. This illustrates the variation in results that can be seen for different assay conditions and substrate concentrations. In this study, benzamide was found to be 205-fold more active as a PARP inhibitor than as an inhibitor of mono(ADP-ribosyl)transferase, whereas 3-hydroxybenzamide was more specific with 989-fold more activity against PARP. 5-Hydroxyisoquinolinone was also found to be extremely specific for PARP, the IC_{50} value measured for PARP was 0.39 μM , compared to a value of 890 μM for the mono(ADP-ribosyl)transferase. Another important outcome of this screening for PARP activity was the discovery of four potent inhibitors. These are 1,8-naphthalimide [IC_{50} 1.4 μM]; 4-amino-1,8-naphthalimide [IC_{50} 0.18 mM]; 6(5*H*)-phenanthridinone [IC_{50} 0.30 μM]; and 2-nitro-6(5*H*)-phenanthridinone [0.35 μM]. These compounds are large planar structures based on the isoquinolinone structure with fused substituents (see Figure 17). They contain the amide group in its fixed, active conformation. 6(5*H*)-Phenanthridinone was around 3000 times more specific for PARP. The

best inhibitor of mono(ADP-ribosyl)transferase in this study was vitamin K₁ (IC₅₀ 1.9 μ M).

The final compound shown in Figure 17 is 2-phenylbenzoxazole-4-carboxamide.¹⁶⁰ This compound is slightly different to the others in that the amide group conformation is fixed by hydrogen-bonding interactions rather than a covalent bridge. The IC₅₀ value measured for this compound was 2.1 μ M. Again the benzamide activity has been improved upon by fixing the conformation of the amide.

Figure 18: Structure of Benzamide riboside

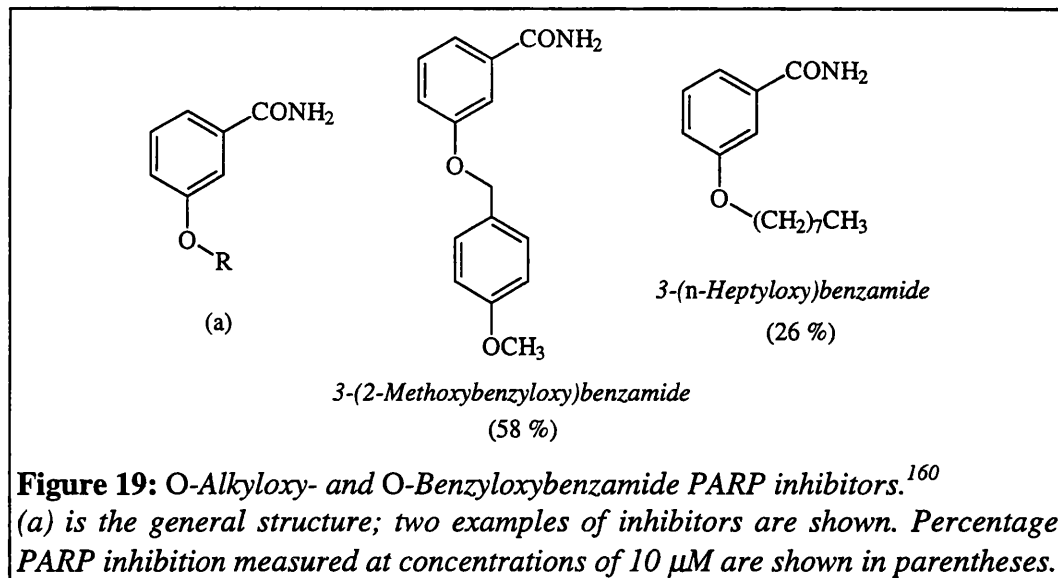


Studies on benzamide PARP inhibitors have shown that relatively bulky groups can be substituted in the 3-position without loss of activity. Indeed, NAD⁺ itself has an ADP-ribose group in the equivalent position.

The ribose-nucleoside binding domain requirements have been considered. Figure 18 shows the structure of benzamide riboside. This compound is a C-glycoside analogue of the nicotinamide ribonucleotide of NAD⁺. This compound was synthesised and tested for PARP inhibition.¹⁶² However, PARP inhibition could not be evaluated due to the cytotoxic effect of the compound at nanomolar concentrations. It is thought that the analogue might be taken up into the NAD⁺ biosynthetic cycle and interferes with NAD⁺ dependent processes, enzymes using NAD⁺ as a cofactor and possibly energy metabolism. Benzamide riboside may be of use as a cytotoxic drug for cancer chemotherapy.

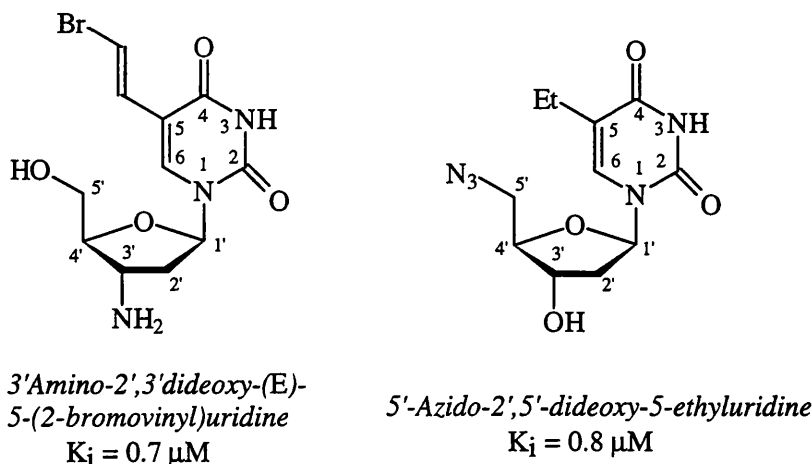
Griffin *et al*¹⁶⁰ synthesised and tested several compounds of the form shown in Figure 19. These O-alkyloxybenzamides and benzyloxybenzamides were generally of around the same PARP inhibitory activity as the parent compound 3-hydroxybenzamide. The results confirmed that a bulky group at the 3- position of

benzamide does not affect activity but none of the side chains tested gave a significant increase in activity.



A final group of compounds that should be mentioned is that of thymidine analogues. Thymidine was one of the first PARP inhibitors discovered but, due to its weak and non-specific action, is not of much practical use. However, in 1992, a large number of nucleoside analogues of deoxythymidine and deoxyuridine were screened.¹⁶³ It was found that compounds with a combination of substituents at the 5-position of the pyrimidine ring and the 3'- or 5'-position of the deoxyribose, were generally the most potent inhibitors. 3'-Amino-2',3'-dideoxy-(*E*)-5-(2-bromovinyl)uridine and 5'-azido-2',5'-dideoxy-5-ethyluridine were among the most potent PARP inhibitors with K_i values of 0.7 μM and 0.8 μM , respectively (Figure 20). Most of the analogues tested also have antiviral and/or anticancer activities which may suggest they are non-specific and have multiple effects in the cell; or may imply as the authors suggest, that PARP is involved in viral reproduction (see section 2.3.7). Further work needs to be done to see if any of the other potent PARP inhibitors have antiviral activity.

Figure 20: Nucleoside analogues of thymidine. Two of the most potent PARP inhibitors as tested by Pivazyan et al.¹⁶³

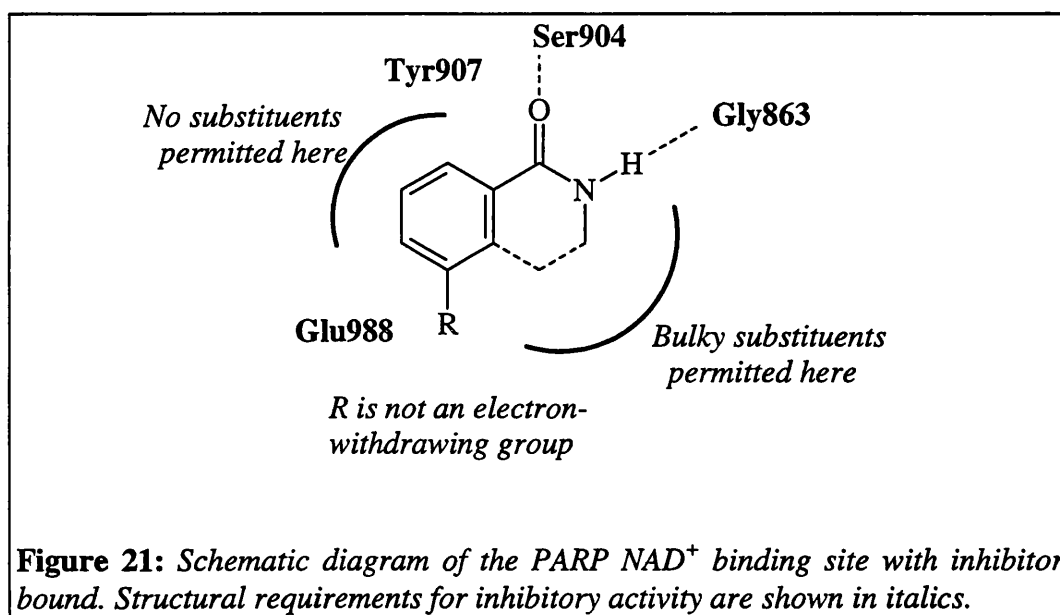


3.3 Summary of Structure-Activity Relationships and Binding Predictions

The characteristics which SAR studies have shown are required to give good PARP inhibition are summarised in Figure 21. The recent elucidation of the crystal structure of the catalytic fragment of chicken PARP⁴² has provided more information about inhibitor binding to PARP. The crystal structure of PARP with the inhibitor PD128763 (3,4-dihydro-5-methylisoquinolin-1-one) bound was also claimed. This is one of the most potent inhibitors known indicating a strong interaction with the binding site on the enzyme.

The crystal structure showed that two hydrogen bonds form from the carbamoyl group to the peptide backbone of residue Gly⁸⁶³ of PARP and from the oxygen atom to the side chain of Ser⁹⁰⁴. The conformation of the amide group is important for these interactions with the active site. This agrees with the SAR established and the fact that compounds in which the amide group is fixed in this conformation, are significantly more potent inhibitors than those with a free amide group. Results have shown that the nitrogen of the amide must be unsubstituted for activity:- this is because the group is required to make a hydrogen bond in the active site. It has been shown, using molecular orbital

calculations, that, in the benzamide series, the ability of the carbonyl oxygen to donate π electrons correlates well with inhibitory activity.¹⁴⁵ This has been shown, in the crystal structure study to be an important binding interaction. This interaction is improved by an electron-rich benzene ring in conjugation with the carbonyl group. This is evident in the weak activity of 3-nitrobenzamide and other derivatives with electron-withdrawing groups.



As well as these hydrogen bonding interactions the crystal structure indicates a non-polar interaction between Tyr⁹⁰⁷ and the aromatic ring(s). This interaction might contribute to the increased activity of the larger, planar, fused ring molecules.

The carboxylate group of Glu⁹⁸⁸ has been known to be important for PARP catalytic activity for some time⁴⁰ (see also section 2.1.3). The crystal structure showed that the distance from this group to the methyl group of PD128763 is 4Å. This position in the inhibitor molecule is equivalent to the anomeric carbon attached to the nicotinamide ring of NAD⁺. The authors conclude that at this location the Glu⁹⁸⁸ residue could function either as a general base facilitating nucleophilic attack of the anomeric carbon of NAD⁺ and cleavage of the C-N

bond. This was the mechanism put forward by Marsischky *et al.*⁴⁰ Alternatively, the Glu⁹⁸⁸ could function to stabilise an intermediate oxocarbenium ion at the anomeric position of NAD⁺ (shown in Figure 13). This mechanism was proposed for ADP-ribosylation by diphtheria toxin.¹⁶⁴ Experimental evidence for the second possibility is provided by Slama and Simmons^{165,166} who synthesised an analogue of NAD⁺ with a 2,3-dihydroxycyclopentane ring in place of the ribose ring. In this analogue there is no oxygen atom adjacent to the anomeric carbon and the oxocarbenium ion cannot form. It was found that this analogue was an inhibitor of NAD⁺ glycohydrolase and ADP-ribosyl transferase enzymes, attributed to the fact that the C-N bond could not be cleaved. The first mechanism, in which there is direct nucleophilic attack of the anomeric carbon, does not require the participation of the ribose oxygen. These results therefore favour the formation of the oxocarbenium ion.

This information on structure activity relationships of PARP inhibitors and the crystal structure of the NAD⁺ binding site of the enzyme should enable further potential inhibitors to be designed. One reservation which must be expressed about the utility of the crystal structure is the claim that the NAD⁺ binding site is very similar to that of diphtheria toxin, a mono(ADP-ribosyl)ating enzyme. This contrasts with the widely differing structure-activity requirements for inhibition of the two enzymes. There is, indeed, a need for more specific, potent, soluble PARP inhibitors both as biochemical tools for the determination of PARP functions in the cell and as potential radiosensitisers and chemosensitisers for the treatment of cancer.

Chapter Four

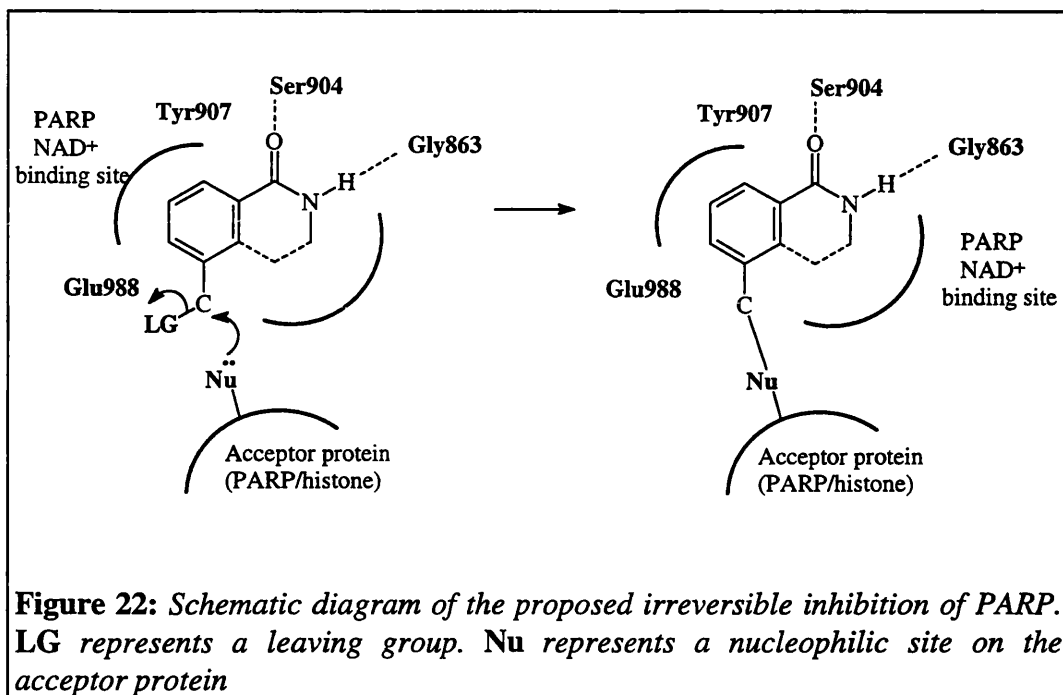
4. Aims of the Study

The PARP inhibitors that have been tested so far have been competitive and reversible inhibitors. They compete with NAD^+ for its binding site on the PARP catalytic domain. Once bound, the inhibitor does not contain the C-N bond present in NAD^+ and cannot be cleaved and therefore inhibits the enzyme. However this inhibition can be overcome by the addition of more NAD^+ , which displaces the inhibitor. The aim of this study was to synthesise irreversible inhibitors of PARP as well as improving potency and specificity.

In designing potential irreversible inhibitors, the mechanism of ADP-ribosylation was examined. This is shown in Figure 13. When NAD^+ is bound the oxocarbenium ion is thought to form, stabilised by Glu⁹⁸⁸. A nucleophilic site on the acceptor protein or on the growing poly(ADP-ribose)chain then attacks the ribose C1 carbon and the ADP-ribose unit is bound. In the majority of cases, the nucleophile will be on the automodification domain of a second PARP molecule, in other cases on a histone. An NAD^+ analogue with an electrophile in the same spatial location as the ribose anomeric carbon (C1) should act as a potential inhibitor of PARP. The analogue would be recognised by PARP and would bind to the NAD^+ binding site. The nucleophile on the acceptor protein would then attack the electrophile in the ribose C1 position. The acceptor protein is then covalently bound to the inhibitor and the active site is blocked. This is shown in Figure 22. The electrophilic group is shown as a leaving group attached to the benzylic carbon in order to demonstrate the mechanism.

Using the SAR information that has accumulated from studies of PARP inhibitors, molecules were chosen which consisted of the 3-substituted

benzamide core. This analogue of nicotinamide is known to fit well into the binding site.



The aim was to make both 3-substituted benzamides and 5-substituted isoquinolin-1-ones with electrophilic substituents of the general form shown in Figure 23.

Studies have shown that fairly bulky groups are tolerated in this position. The aim was to create analogues with larger substituents; possibly with hydroxyl groups present or cyclic groups, to imitate the ribose portion of NAD^+ . Increased interaction with the ADP-ribose-binding region of the active site might create a more potent inhibitor. Strongly electron-withdrawing substituents were to be avoided, since studies have shown that this may result in a loss of activity.

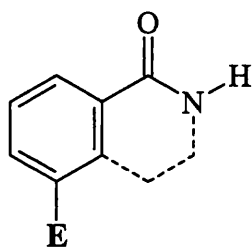


Figure 23: *General structure of potential irreversible PARP inhibitors synthesised, where E is an electrophile.*

Ideally an inhibitor should be water soluble at micromolar and preferably millimolar concentrations. This was also taken into consideration.

For asymmetric molecules the aim was to synthesise, stereoselectively, both enantiomers, and compare their relative activities as PARP inhibitors. It was predicted that the form which corresponds better to the stereochemistry of NAD^+ will be the active enantiomer.

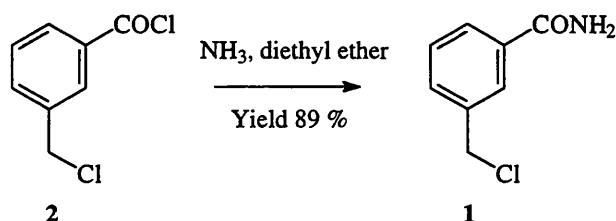
Potential inhibitors were synthesised and then tested *in vitro* for inhibition of PARP. For successful candidates IC_{50} values were estimated and for potential irreversible inhibitors time dependent assays were carried out.

Chapter Five

5. Benzamides

As explained in Chapter Four, the original aim of the project was to synthesise analogues of NAD^+ with an electrophilic substituent, of the form shown in Figure 23. The compounds synthesised can be divided into two groups; benzamides, which are discussed in this chapter, and isoquinolinones, which are discussed in Chapter Six. In the first instance, a benzamide with a simple electrophilic side chain is discussed. This potential inhibitor is of the type shown in the proposed mechanism for irreversible inhibition in Figure 22. The next group of targets are single enantiomers of analogues of NAD^+ . These have a heterocyclic group to correspond to the ribose portion of the NAD^+ molecule. Finally, the approaches taken towards an aziridine target compound are discussed.

The first target compound was 3-chloromethylbenzamide **1**. This is a benzamide with an electrophilic group in the 3-position; the benzylic carbon is susceptible to nucleophilic attack and the chloride ion is a good leaving group. Therefore **1** is a potential irreversible inhibitor. The benzamide **1** was synthesised in one step from the corresponding acid chloride **2** as shown in Scheme 1.



Scheme 1

The acid chloride **2** was treated with ammonia; a standard method for preparing amides from acyl halides. The reaction was carried out under mild, dilute

conditions. This was necessary because there are two positions which can undergo nucleophilic attack by ammonia. Substitution occurs readily at the carbonyl carbon of the acyl chloride group and in less mild conditions nucleophilic attack at the chloromethyl carbon is also possible. The reaction was followed carefully to ensure that only the acyl halide group was converted.

The next group of benzamides that were investigated were those with a chiral centre at the benzylic carbon. It was our hypothesis that the stereochemistry at this position might be important for PARP inhibitory activity, since at the equivalent position in NAD^+ (the anomeric carbon) there is also a chiral centre (Figure 24). For a good binding interaction with the PARP NAD^+ binding domain, the inhibitor should have stereochemistry corresponding to that in NAD^+ and present an oxygen atom in a region of space corresponding to the oxygen of ribose. The opposite enantiomer would be expected to be relatively inactive.

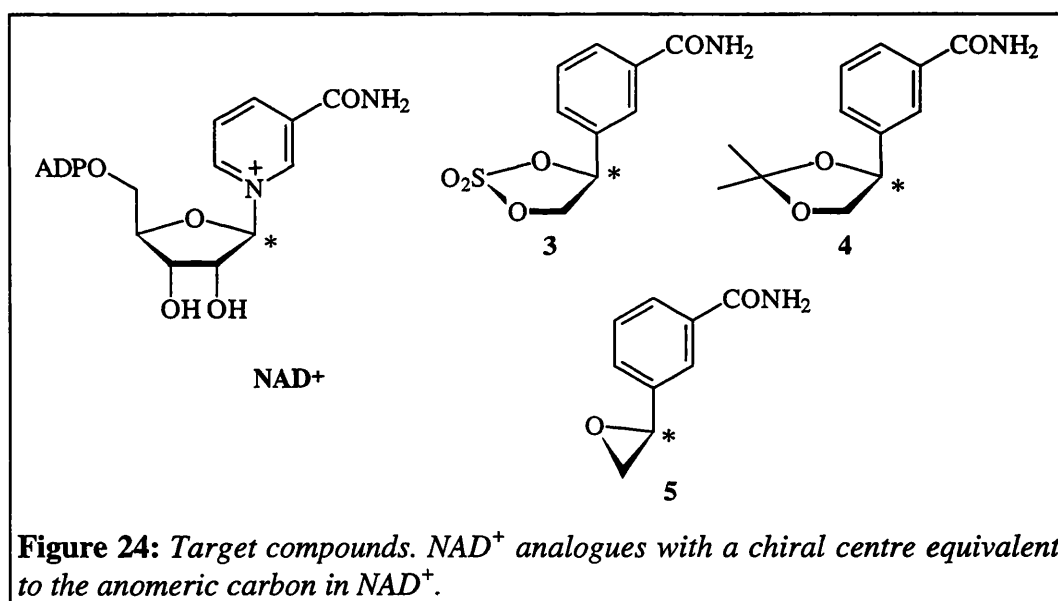
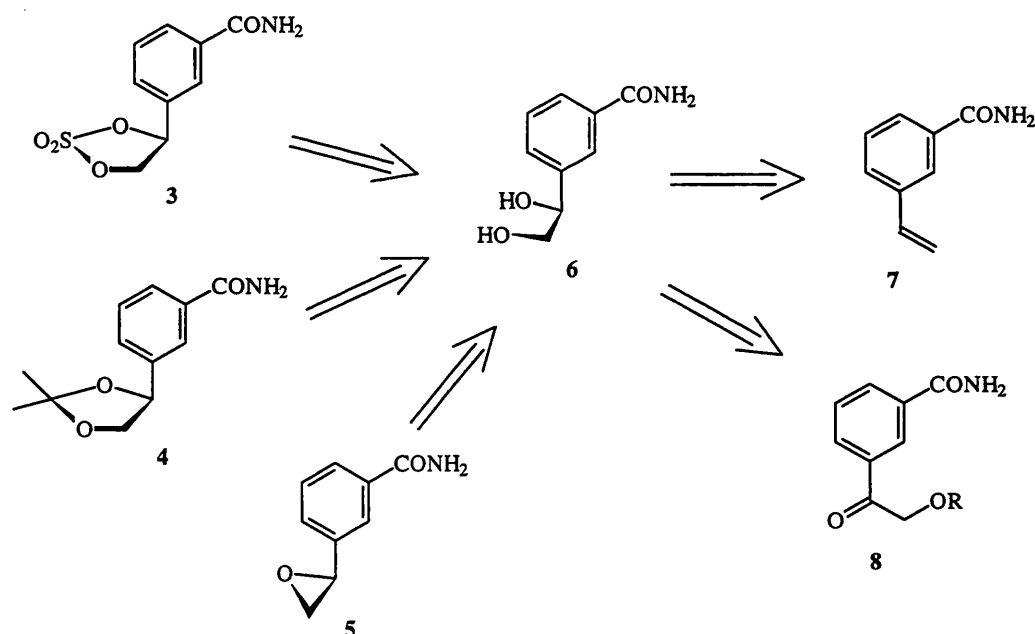


Figure 24 shows two target compounds of this series; a cyclic sulphate 3, a 1,3-dioxolane 4 and an epoxide 5. The arrangement of atoms around the benzylic carbon in these NAD^+ analogues is analogous to the arrangement of groups around the anomeric carbon in NAD^+ . They also have a cyclic structure in the

space occupied by ribose in NAD⁺. The cyclic sulphate **3** and epoxide **5** are electrophilic and should act as irreversible inhibitors, as explained in Chapter Four.

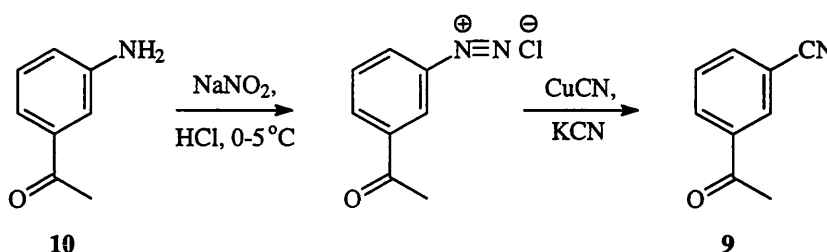
The retrosynthetic analysis in Scheme 2 shows that all of these compounds, **3**, **4** and **5** can be synthesised from the corresponding diol **6**. Two approaches for the stereocontrolled synthesis of the diol **6** were considered. The first method investigated was to make the diol from the alkene **7** using Sharpless asymmetric dihydroxylation methodology.¹⁶⁸⁻¹⁷⁰ The second approach was to obtain the diol **6** by the asymmetric reduction of the protected hydroxyketone **8**. The amide group does not necessarily have to be present in the intermediate structures. A cyano group was used as a synthon for the amide group and the nitrile analogues were often converted to amides towards the end of the synthesis.



Scheme 2

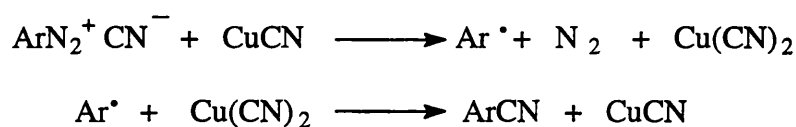
In the case of both approaches, 3-acetylbenzonitrile **9** was chosen as the starting material for this set of compounds. The nitrile group is easily converted to the required amide group, the acetyl group provides a two carbon chain and has an

oxygen atom adjacent to the benzylic carbon. This nitrile **9** was prepared by diazotisation of 3-aminoacetophenone **10** and treatment of the diazonium salt with a mixture of copper (I) cyanide and potassium cyanide (Scheme 3).



Scheme 3

This is a variation on the Sandmeyer Reaction, in which the substitution of the diazo group with a cyano group is catalysed by a copper (I) salt. The mechanism for the reaction is thought to be as shown in Scheme 4 below.¹⁶⁷



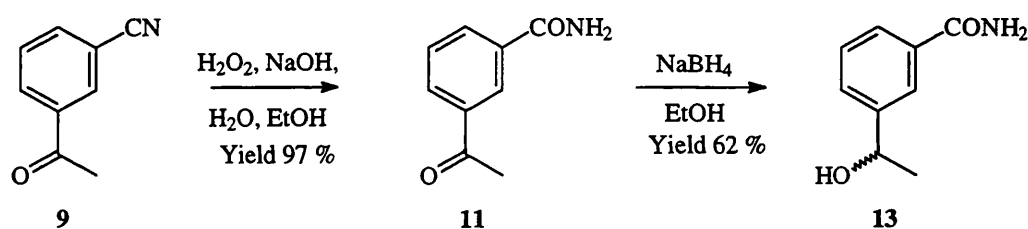
Scheme 4

In the first step, the diazonium ion is reduced by the cuprous ion resulting in the formation of an aryl radical. This requires an excess of cyanide ions; these are provided by the potassium cyanide. In the second step, the aryl radical abstracts a cyanide radical from the copper (II) salt, reducing it to the original copper (I) cyanide.

A fair yield of the nitrile **9** was obtained, although the process was not very clean and difficulty in separation of the product from the highly coloured by-products may have led to a loss of yield.

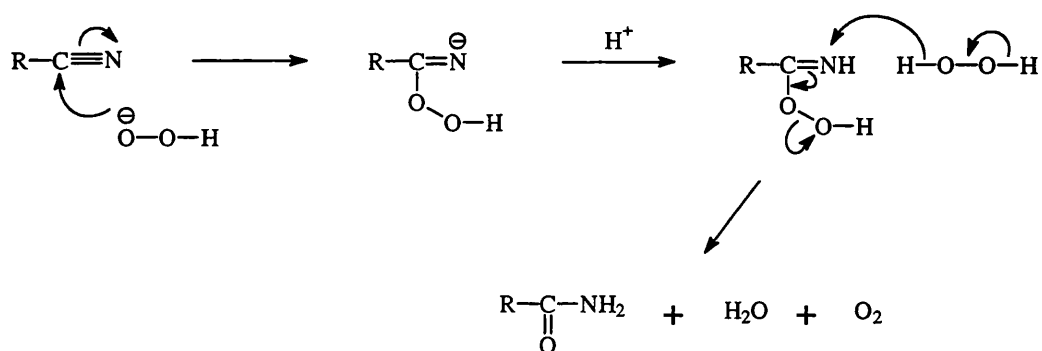
A suitable procedure was required to convert the cyano group into the desired carbamoyl group. Nitriles can be hydrolysed partially to amides or completely to carboxylic acids. There are a number of procedures for stopping the hydrolysis at the amide stage. These include using concentrated sulphuric acid; hydrochloric acid;¹⁷¹ acetic acid and boron fluoride;¹⁷² sodium hydroxide in dimethyl sulphoxide;¹⁷³ hydrogen peroxide and sodium hydroxide¹⁷⁴ and manganese dioxide in dichloromethane. After examination of the literature, the sodium hydroxide and hydrogen peroxide method was chosen. This a reasonably mild and straightforward method and has been employed in a standard synthesis of toluamide.¹⁷⁴

Indeed, this method proved effective for the partial hydrolysis of benzonitrile **9**, giving the corresponding amide **11** in almost quantitative yield. (Scheme 5). This method was therefore employed throughout the series of compounds.



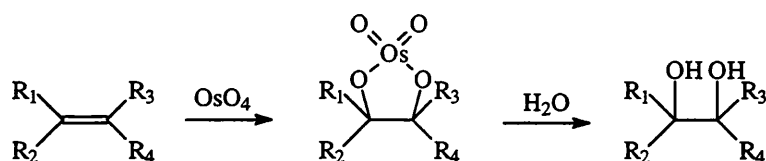
Scheme 5

A mechanism proposed by Beckwith¹⁷⁵ for this reaction is shown in Scheme 6 below. There is firstly nucleophilic addition of a peroxide ion to the C≡N group. This is followed by the transfer of a hydride ion from a second hydrogen peroxide molecule to the intermediate peroxyimine, resulting in the formation of the amide, molecular oxygen and water.



Scheme 6

The first approach to form the enantiomerically pure diol **6** involved the synthesis of the styrene derivative **7** which was then to be asymmetrically dihydroxylated using the method of Sharpless.¹⁶⁸⁻¹⁷⁰ This method was developed from the reaction shown in Scheme 7.



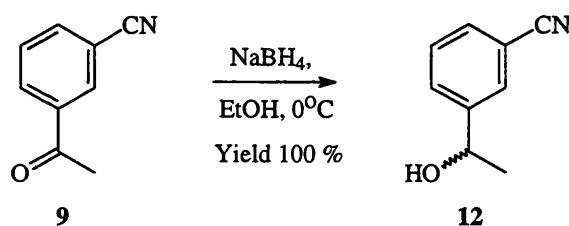
Scheme 7

Here osmium tetroxide is used to carry out the dihydroxylation of an alkene, by forming a cyclic osmate with the alkene which is then hydrolysed to give the diol. The use of chiral ligand catalysts allows the stereochemistry of the reaction to be controlled and only catalytic amounts of osmium tetroxide are required. The chiral ligands are mostly derivatives of quinidine and quinine which bind to the osmium tetroxide and control the direction from which the oxygens approach the double bond of the alkene. Therefore, whether the quinine ligand or the quinidine ligand is used, determines the enantiomer obtained. Enantiomeric excesses are dependent on the ligand used and the substrate and can vary from 20% to 99%.^{168,169} More recently, new classes of ligands have improved enantioselectivity; recently both (*R*)- and (*S*)-phenylethane-1,2-diol were

synthesised by asymmetric dihydroxylations of styrene, both with an enantiomeric excess of 97%.¹⁷⁰

To synthesise the alkene **7**, the route taken was to reduce the acetophenone **9** to give the alcohol **12**; this could then be dehydrated to give 3-cyanostyrene. An analogous route for 4-cyanostyrene is described by Marvel and Overberger.¹⁷⁶ Alternatively, reduction of the ketone of **11** would give the alcohol **13** (Scheme 5), which could be dehydrated to give **7**.

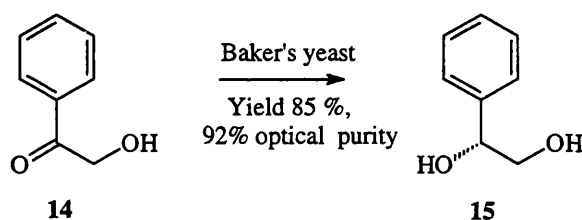
The reduction of **9** was carried out using sodium borohydride in ethanol to give (±)-3-(1-hydroxyethyl)benzonitrile **12** (Scheme 8). Sodium borohydride is a relatively selective reducing agent; it reduces aldehydes and ketones to alcohols without affecting halogeno, cyano, nitro, amido and alkoxycarbonyl groups. Initially this reaction was carried out at room temperature, although these attempts were successful, the apparent degradation of the product on the chromatography column led to very low yields. Later it was found that addition of the sodium borohydride at 0°C was preferable, giving quantitative yield and no need for chromatography.



Scheme 8

3-Acetylbenzamide **11** was also reduced using this method to give **13** (shown in Scheme 5). Benzamides **11** and **13** were both tested for activity as PARP inhibitors; although they were not intended target compounds, their activities have not yet been reported in the literature.

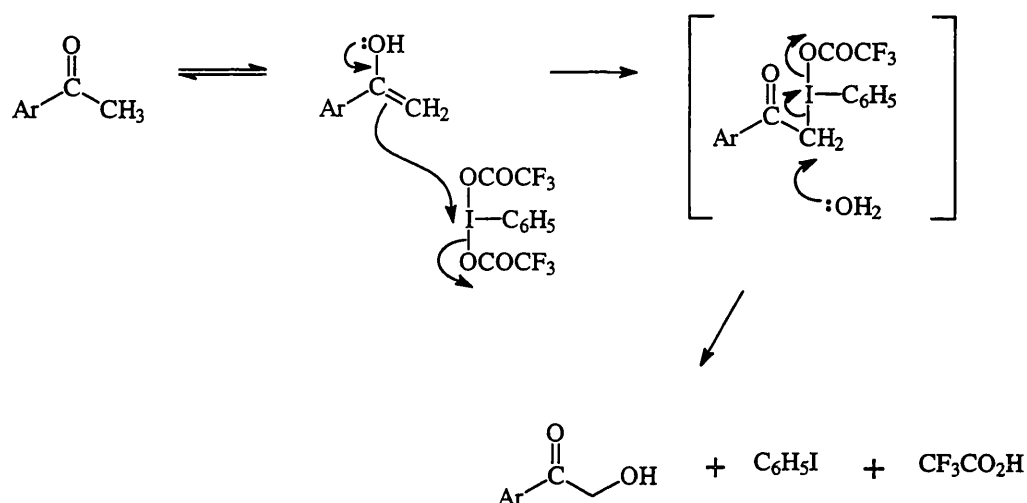
When problems were encountered with the purification of **12**, another route to the enantiomeric diols was considered and work continued in this direction. This approach involved using biotransformations to carry out the asymmetric synthesis. Biotransformations are often very effective and cheap methods of carrying out enantioselective syntheses. The reduction of carbonyl compounds by baker's yeast (*Saccharomyces cerevisiae*) is one of the most widely used biotransformations for the preparation of enantiomerically pure alcohols.¹⁷⁷ Aromatic α -hydroxyketones have been reported to be asymmetrically reduced to diols by baker's yeast.¹⁷⁸⁻¹⁸⁰ For example 2-hydroxyacetophenone **14** is reduced to (*R*)-phenylethane-1,2-diol **15** in high yield and high optical purity^{178,179} (Scheme 9).



Scheme 9¹⁷⁹

It was proposed that this method should produce the corresponding (*R*)-diol **16** from the α -hydroxyketone **17** in the benzonitrile series. In fact, for the target compounds shown in Figure 24 we require the (*S*) enantiomer of the diol; however, it was also desirable to have the potentially inactive opposite enantiomer.

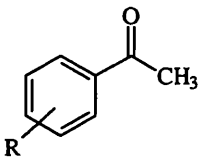
As part of their work on hypervalent iodine, Moriarty *et al*¹⁸¹ reported a "one-pot" method for the preparation of α -hydroxyketones. Various aromatic, heteroaromatic and aliphatic ketones, mainly of the form $R-COCH_3$, were treated with [bis(trifluoroacetoxy)]iodobenzene under acidic conditions to give the corresponding α -hydroxyketones. A possible mechanism is shown in Scheme 10.



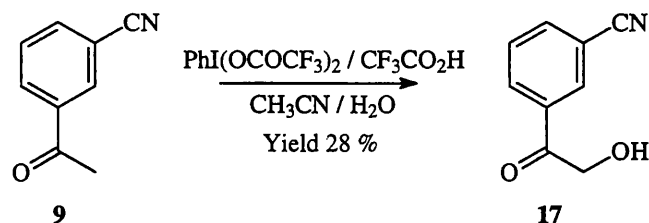
Scheme 10

The enol form of the ketone reacts with the [bis(trifluoroacetoxy)iodobenzene] displacing one of the trifluoroacetoxy ligands. This intermediate is then attacked by water and the hypervalent iodine moiety is displaced to give the α -hydroxyketone. The yields obtained by Moriarty were quite variable, ranging from 21% to 94%. The results for the substituted aromatic ketones investigated are shown in Table 5.

Table 5: α -Hydroxy ketones synthesised by direct α -hydroxylation of the corresponding methyl ketones using bis(trifluoroacetoxy)iodobenzene under acidic conditions. Results from Moriarty et al.¹⁸¹

	Aromatic ketone R group	Yield of Hydroxy ketone (%)
	H	69
	4-Me	72
	4-OMe	58
	4-F	67
	4-NO ₂	29
	2-Me	70

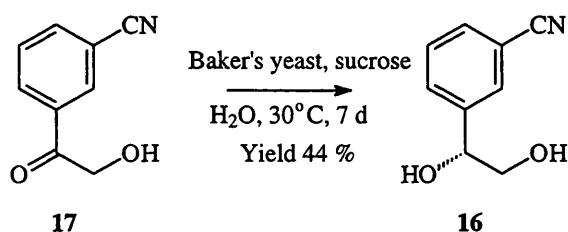
Since this method appeared to work reasonably well for aromatic ketones, the α -hydroxyketone, 3-(2-hydroxyacetyl)benzonitrile **17** was prepared in a similar way (Scheme 11).



Scheme 11

Unfortunately, the yields obtained in several attempts were fairly low (25-28%). By comparison with Table 5, this may be the case for aromatic compounds with electron-withdrawing groups on the ring in that 4-nitroacetophenone also gave a fairly poor yield (29%). Moriarty reported that 4-nitrobenzoic acid (29%) was also produced in the reaction as a result of over-oxidation. In the case of the 3-cyano-derivative Scheme 11, a carboxylic acid was detected (^1H NMR) as a by-product but was not isolated. Despite the fairly low yield, this method is a convenient route to the desired α -hydroxyketone **17**.

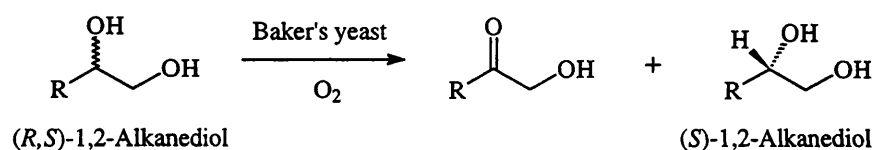
As shown in Scheme 12, the α -hydroxyketone **17** was then treated with baker's yeast using a similar method to that of Manzocchi *et al*¹⁷⁹ who synthesised the Ar-unsubstituted (-)-*R*-diol **15**.



Scheme 12

The mixture of fermenting yeast and the ketone **17** was stirred at about 30°C for seven days. The low concentration of substrate meant that it was not possible to follow the reaction by TLC. Extraction of the product may have also been inefficient, since the diol **16** is relatively polar and some may have been left behind in the large volume aqueous phase. These factors may have contributed to fairly low yield obtained. The optical rotation of the product was -46.6° (c , 1.0, dichloromethane). This is a novel compound and therefore the absolute stereochemistry cannot be known from this measurement. However by comparison with several compounds in this series,¹⁸⁰ it is highly likely that the (-) enantiomer is the *R*-enantiomer.

A method was also needed to prepare the other enantiomer, the (*S*)-diol **18**. Kometani¹⁸² reported a method by which the (*S*)-diol is obtained, from the corresponding racemic diol, using baker's yeast. (Scheme 13).

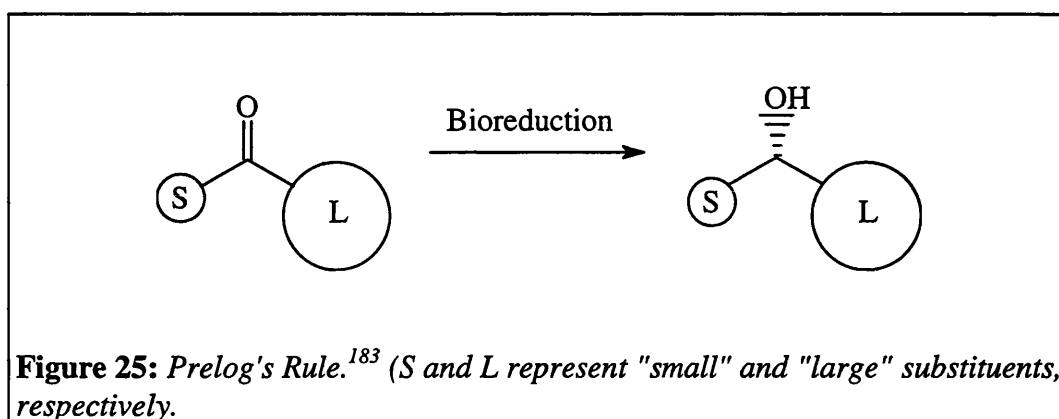


Scheme 13¹⁸²

It is proposed that the (*R*)-diol, is selectively oxidised by an oxidoreductase with an accompanying reduction of NAD⁺ to NADH. The NADH is then reconverted to NAD⁺ in the respiratory chain within the cells. The (*S*)-diol remains and is easily separated from the ketone. Unfortunately this method only appears to work for alkyl diols and not aromatic compounds.

The baker's yeast-mediated reduction of **14** and **17** follows Prelog's rule for the stereochemical outcome for bioreductions.¹⁸³ Prelog noted that the stereochemistry of the products of many bioreductions followed a pattern and

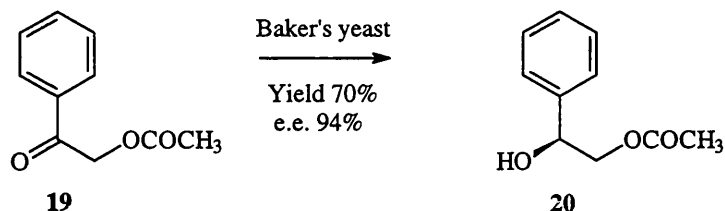
could be predicted according to the scheme shown in Figure 24. The substituents on the carbonyl carbon are designated large (L) and small (S) and the rule describes the arrangement of these groups and the hydroxyl group formed around the chiral centre.



Most bioreductions with alcohol dehydrogenases follow Prelog's rule but there are some exceptions that are anti-Prelog in their specificity. These can be partly explained by the ambiguities involved in determining which groups are "large" and "small" in a molecule. Also, in the case of baker's yeast, it is now recognised that several oxidoreductases are present in *Saccharomyces cerevisiae*; Prelog's rule is based on one enzyme carrying out the reduction. The enzymes present might reduce the same substrate with opposite stereochemistry. Some substrates have been reported to be reduced by baker's yeast giving the opposite product to that predicted by the rule. These include a few aliphatic ketones, an example being 1-hydroxyacetone, which gave the (–)-*R*-diol, 1,2-propanediol.¹⁸⁴

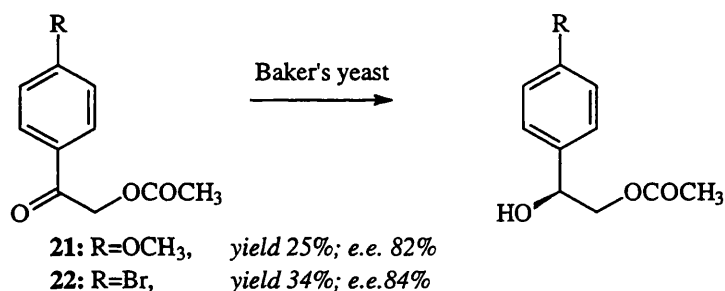
It has also been found that protection of the hydroxyl group of aromatic α -hydroxyketones can, in some cases, result in anti-Prelog bioreduction.^{179,180} Manzocchi *et al*¹⁷⁹ carried out baker's yeast reductions on various analogues of 2-hydroxyacetophenone **14** in which the hydroxy group was protected by esters. The best protecting group was found to be acetyl (**19**); larger groups led to a loss of yield and enantiomeric selectivity. The formate ester was too vulnerable to

hydrolysis. The reduction of **19** was reported to give the acetoxy-protected (+)-(*S*)-diol **20** in good yield and high enantiomeric excess (Scheme 14).



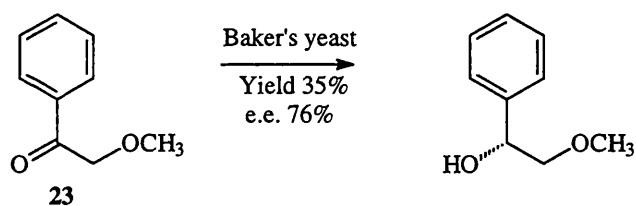
Scheme 14¹⁷⁹

Another study found that the enantiomeric excesses were reduced when the aromatic ring was substituted. The *para*-methoxy derivative **21** and *para*-bromo derivative **22** gave lower yields and enantiomeric excesses.^{180,185} (Scheme 15)



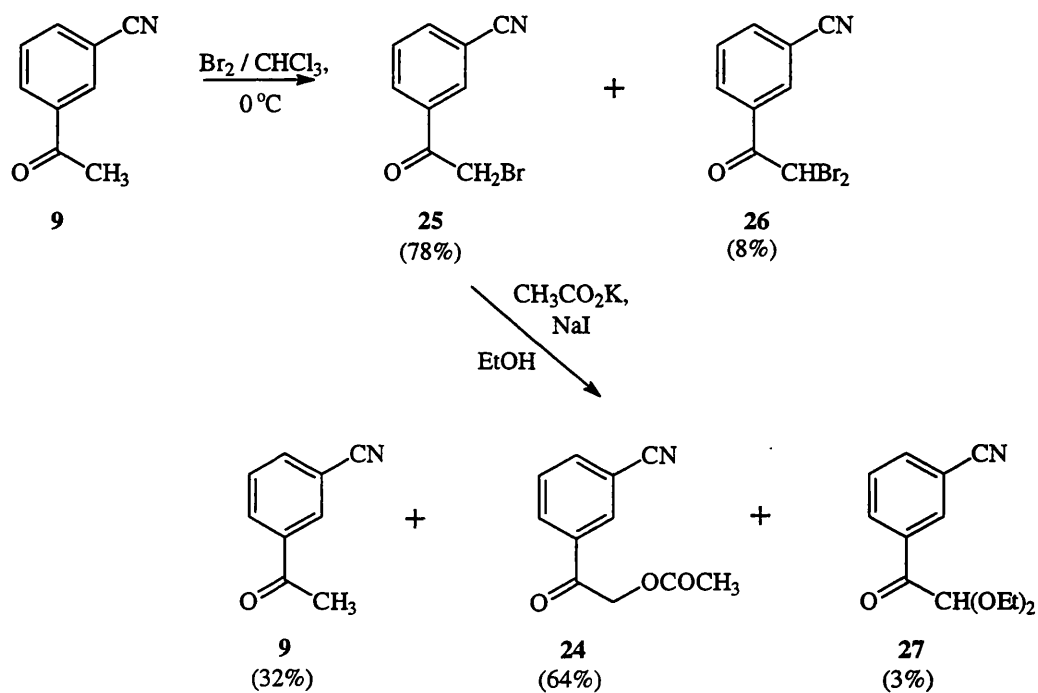
Scheme 15^{180,185}

It is interesting to note that when a methyl ether is used to protect the hydroxy group as in **23**, the same enantiomer is produced as in reduction of the unprotected hydroxyketone **14**.¹⁸⁰ This system, unlike the acetoxy-protected system, follows Prelog's rule (Scheme 16).



Scheme 16¹⁸⁰

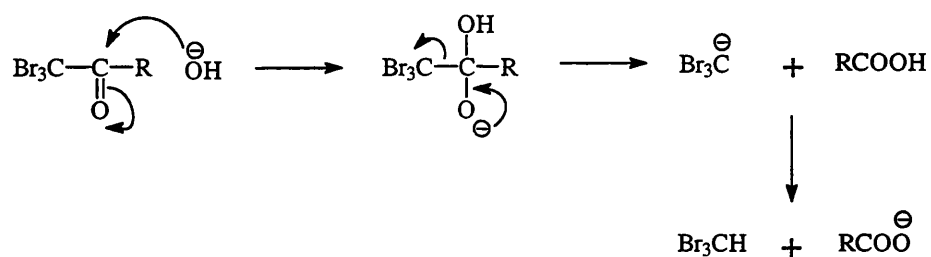
For the purposes of this project, synthesis of the acetoxy-protected analogue of α -hydroxyketone **17** and its bioreduction provided a convenient route to the (*S*)-diol **18**. Scheme 17 shows the synthesis of the protected α -hydroxyketone **24**. Introduction of the acetoxy group into the acetophenone **9** was carried out in a two step process *via* the α -bromoketone **25**.



Scheme 17

Ketones can be α -brominated in the presence of either acid or base. The purpose of the acid/base catalyst is to catalyse the formation of either the enol, in the case of an acid, or the enolate ion, in the case of the base. For monobromination,

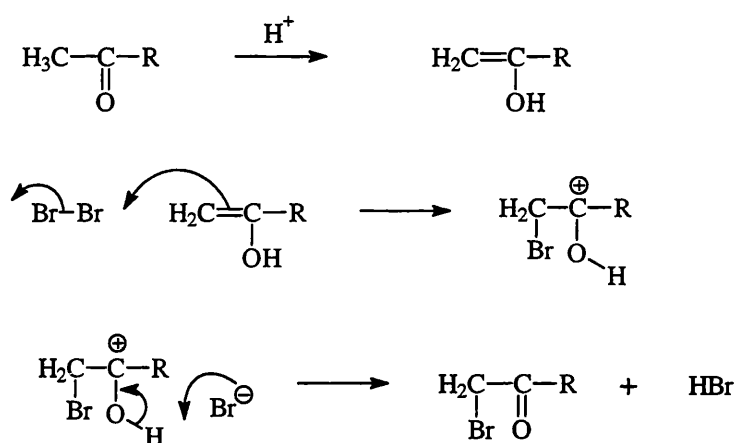
acidic conditions are required. In basic conditions it is not possible to isolate the monobrominated product because the electronegativity of the first halogen increases the acidity of the remaining hydrogens and the enolate ion forms even more readily. In the case of methyl ketones, the haloform reaction takes place in basic conditions. In this reaction methyl ketones are cleaved by treatment with halogen and a base. Two reactions take place: The methyl group is firstly trihalogenated. The intermediate trihalo ketone is attacked by the hydroxide ion, as shown in Scheme 18, and the trihalomethyl group leaves to give the carboxylic acid.



Scheme 18

Acidic conditions should limit the substitution to monobromination; there is slow formation of the enol form of the ketone, followed by electrophilic attack by bromine and substitution of one of the methyl protons with a bromine atom (Scheme 19). The dibrominated ketone can be produced if there is an excess of bromine present.

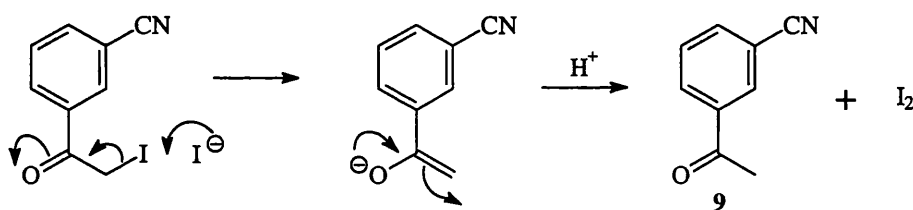
Electrophilic substitution by bromine can also take place on aromatic rings. However, in the case of compound **9**, this is not a problem since the ring is deactivated by the electron-withdrawing substituents present.



Scheme 19

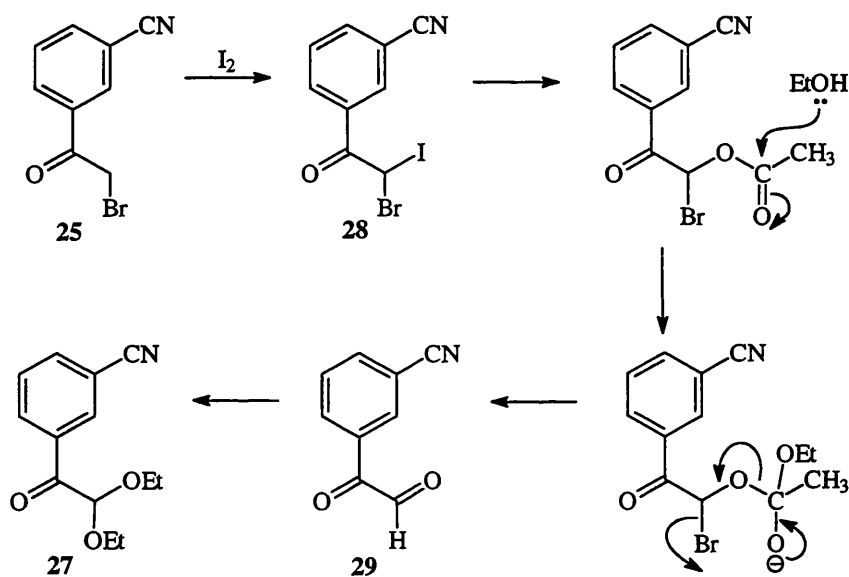
When acetic acid was used as the solvent at room temperature, the reaction gave a low yield (32%) of the monobromoketone **25** and a 6% yield of the dibromo product **26**. The yield of the desired product **25** was greatly improved (78%) by carrying out the addition of bromine at 0°C and using chloroform as the solvent.¹⁸⁶ The yield of dibrominated product, **26**, was only increased by 2%. The solvent in this case is only very slightly acidic but there are enough H⁺ ions present to catalyse the formation of the enol.

3-(Bromoacetyl)benzonitrile **25** was treated with potassium acetate and a catalytic amount of sodium iodide, according to the general method of Kaufmann and Müller,¹⁸⁷ to give the acetoxy-protected hydroxyketone **24** in good yield (64%). Two other products were recovered and characterised; the methyl ketone **9** and a third minor but unexpected product, 3-(diethoxyacetyl)benzonitrile **27**. The sodium iodide is present as a nucleophilic catalyst and in the main reaction there is firstly a nucleophilic substitution to form the iodoketone. The iodide is a better leaving group than the bromide ion and therefore catalyses the nucleophilic substitution by the acetate group. The sodium iodide can also act as a reducing agent and this leads to the formation of the methyl ketone, as shown in Scheme 20.



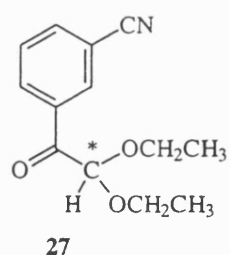
Scheme 20

A possible mechanism for the formation of the acetal **27** relies on the formation of an α -disubstituted ketone species as shown in structure **28** (Scheme 21). There is substitution of one iodo group by an acetoxy group. This group is then attacked by the solvent ethanol to give the aldehyde **29**. Ethanol will then attack the more electrophilic aldehyde carbon and an acetal formation takes place to give **27**.



Scheme 21

The ^1H NMR spectrum for this compound is interesting because the methylene groups in the two ethoxy moieties act like pro-chiral methylenes. There is not a true chiral centre but each methylene group "sees" the centre marked by * below as an asymmetric centre.

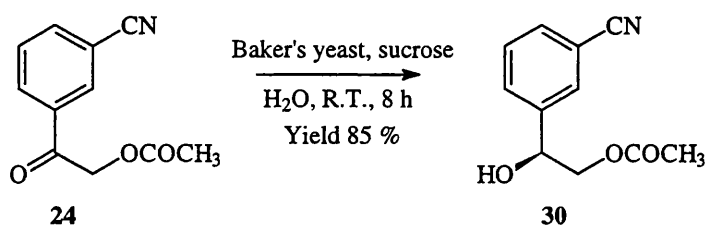


The protons within each methylene group are not magnetically equivalent, there is, therefore, geminal as well as vicinal coupling. The ethoxy groups are however equivalent to each other and their signals coincide. This results in the methylene signals appearing in the spectrum as two double quartets. (Figure 26)

Figure 26: The methylene region of the ^1H NMR spectrum of **27** (270.05 MHz, CDCl_3).



The protected α -hydroxyketone **24** was reduced to (+)-3-(2-acetoxy-1-hydroxyethyl)benzonitrile (**30**) using baker's yeast (Scheme 22).



Scheme 22

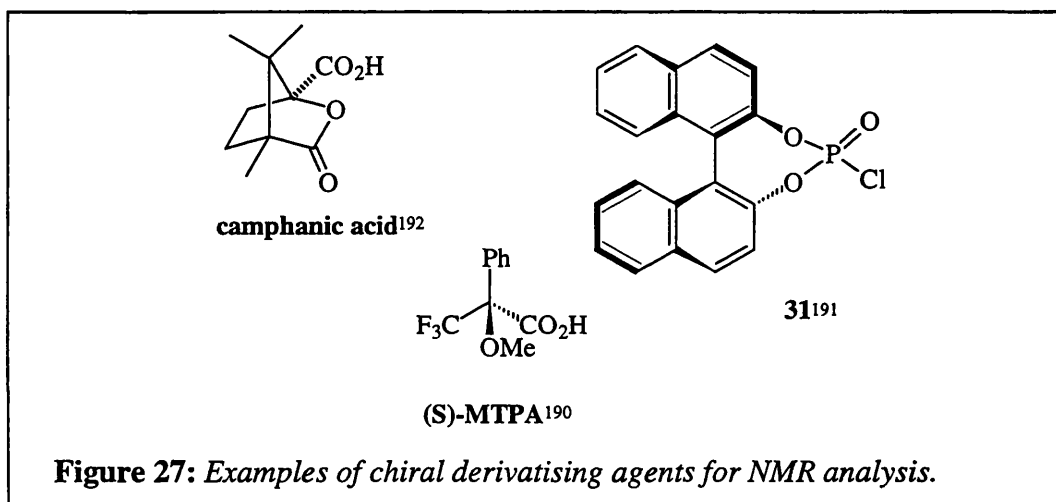
A method similar to that used by Manzocchi *et al*¹⁷⁹ was used. The conditions differ from those used for the reduction of the α -hydroxyketone in that; more concentrated solutions were used; the reaction vessel was kept at room temperature and the reaction was complete within eight hours. A small amount of the diol 3-(1,2-dihydroxyethyl)benzonitrile was also present in the crude product. This could have been formed in two ways; either by the reduction of hydrolysed starting material, i.e. unprotected α -hydroxyketone [(-)-(*R*)-diol]; or by the hydrolysis of the product [(+)-(*S*)-diol]. Unfortunately the sample was too small to get an optical activity measurement.

The optical activity of **30** was found to be +34.9° (*c*, 2.9, dichloromethane). By comparison with similar compounds,¹⁷⁹ the (+) isomer is likely to be the (*S*) isomer. The optical rotation measurements for both the products of the yeast reductions did not provide any information as to the absolute stereochemistry or the proportion of enantiomers present, as these are novel compounds and there are no reference values. The optical purity of both of the products **16** and **30** had to be determined by some other method.

There are a number of ways to determine optical purity of a chiral compound.

a) Chiral Derivatising Agents:^{188,189} The mixture of enantiomers to be determined is derivatised with an optically pure compound. The diastereomers produced will often have non-equivalent chemical shifts in their NMR spectra. The ratio of the integrations of a pair of inequivalent diastereomeric signals

gives a measure of the optical purity. Several chiral compounds have been used as chiral derivatising agents, some examples are shown in Figure 27. These compounds will often have a fluorine group, *e.g.* Mosher's acid (MPTA),¹⁹⁰ or a phosphorus group, *e.g.* 1,1'-binaphthyl-2,2-diyl phosphoryl chloride **31**.¹⁹¹ This allows ¹⁹F and ³¹P NMR analysis as well as ¹H NMR to be used. For this method to be accurate: the derivatising agent must be enantiomerically pure; the derivatisation reaction must occur under conditions which exclude the possibility of racemisation or of kinetic resolution due to the enantiomers reacting at different rates with the agent and any purification of the diastereomers must not allow enrichment of one diastereomer.



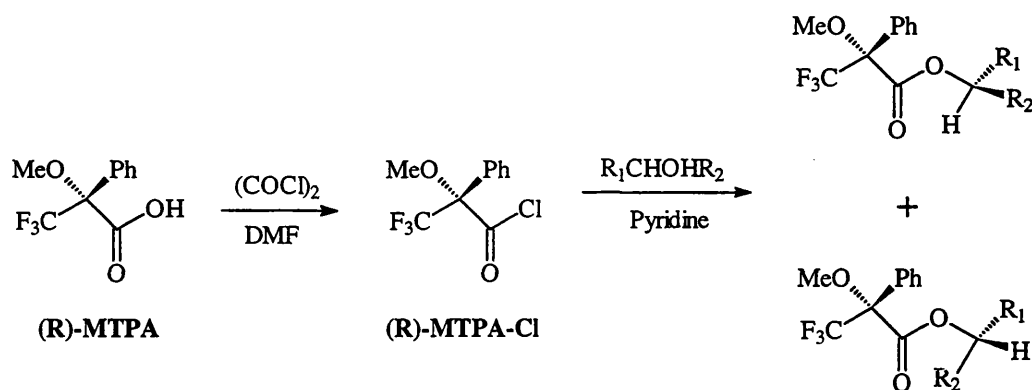
b) Chiral Lanthanide Shift Reagents:^{189,193} Lanthanide shift reagents can form weak addition complexes with a wide range of organic compounds. This causes a change in the magnetic field around nuclei in the compound and this in turn causes a shift of signals in the NMR spectra to a higher or lower frequency. When the shift reagent contains a chiral group, such as a camphor derivative in its optically pure form, it can form diastereomeric complexes with a mixture of enantiomers. These diastereomeric complexes may have non-equivalent NMR spectra allowing determination of optical purity. Europium shift reagents cause a downfield shift, whereas praseodymium shift reagents cause an upfield shift. Examples of chiral shift reagents are

europium tris[3-heptafluoropropylhydroxymethylene-(+)-camphorate], [Eu(hfc)₃] and praseodymium tris[3-heptafluoropropylhydroxymethylene-(+)-camphorate], [Pr(hfc)₃].¹⁹⁴

c) **Cyclodextrins:** Cyclodextrins¹⁹⁵ have a central cavity into which (usually aromatic) organic molecules can enter to form inclusion complexes. This can alter the chemical shift of the protons located in the cavity.¹⁹⁶ Since cyclodextrins are chiral molecules, enantiomeric mixtures can form diastereomeric inclusion complexes which may in some cases have different NMR spectra, allowing determination of optical purity. This has been demonstrated very successfully with the drug propranolol hydrochloride.¹⁹⁷

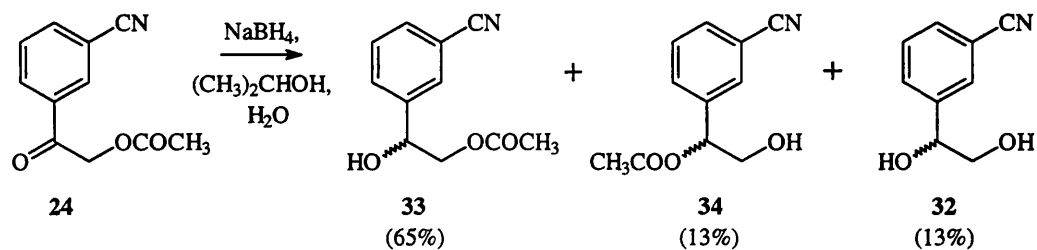
d) **Chiral HPLC:**¹⁹⁸ HPLC can be manipulated to allow the separation of enantiomers. This can be done indirectly by making diastereomeric derivatives using an enantiomerically pure chiral reagent and then separating the diastereomers by HPLC. Alternatively diastereomeric complexes can be formed either by having a chiral stationary phase or a chiral mobile phase, with the aim of altering the retention time of each enantiomer in the system and allowing their separation.

One of the mostly widely used methods for determining the optical purity of alcohols, such as **16** and **30**, is to use the chiral derivatising agent α -methoxy- α -(trifluoromethyl)phenylacetic acid (MTPA). MTPA was introduced by Mosher¹⁹⁰ in 1969 and both enantiomers of the acid are commercially available. The optically pure MTPA is converted to the corresponding acid chloride and then treated with the chiral alcohol to give diastereomeric esters (Scheme 23).



Scheme 23

This method was used to determine the optical purity of **30**. As a comparison, a racemic sample of the alcohol was also needed, so that it could be derivatised and both diastereomeric sets of signals could be identified. The protected α -hydroxyketone **24** was reduced using sodium borohydride in propan-2-ol with only a trace amount of water to minimise hydrolysis of the acetoxy group to the diol **32**. As shown in Scheme 24, the product consisted mainly of the desired protected diol **33**. However 13% yields of the racemic diol **32** and 3-(1-acetoxy-2-hydroxyethyl)benzonitrile **34** were obtained. This second by-product is formed by the migration of the acetoxy group to the benzylic hydroxy group formed in the reduction. The reaction therefore has to be followed carefully and stopped as soon as the reduction is complete.



Scheme 24

It was not possible to isolate the desired product by chromatography; attempts to do so resulted in the product being lost. However in the NMR spectrum of the

mixture the signals for the aliphatic protons were distinct and easily distinguishable, therefore the mixture was treated with MTPA-Cl without further purification. Alternatively, using racemic MTPA-Cl with the asymmetrically prepared alcohol gives the same result since the diastereomers produced here will be the enantiomers of those produced by using the racemic alcohol.

The asymmetrically prepared acetoxy-protected diol **30** and the racemic analogue **33** were treated with (*R*)-MTPA-Cl, as in Scheme 23. Unfortunately the MTPA derivatisation reactions did not go to completion and about 40% of underivatised alcohols **30/33** remained. This may be because the hydroxyl group is a secondary alcohol with bulky groups on either side and is hindered. For a completely accurate determination of enantiomeric excess, the reaction should go to completion in quantitative yield to show that, in the racemic sample, equal amounts of each diastereomer are formed. This shows that there is no kinetic enhancement. However, the use of MTPA as a chiral derivative is very well known, with very few reports of any kinetic resolution.¹⁸⁹ Therefore calculation of enantiomeric purity from the results obtained are likely to be a good estimate of the true picture.

In the ¹H NMR spectrum of the sample derived from the racemic alcohol there are two sets of signals of approximately equal integral. The CH₃ protons of the acetoxy group gave clearly separated signals. The starting material CH₃ group protons resonate at δ 2.11, whereas in the two diastereomeric esters the signals are at δ 2.00 and δ 2.07. (Figure 28). An enantiomeric excess of 96% was calculated using the integrations of these two signals for the asymmetrically prepared sample.

On a second occasion when the experiment was carried out using racemic MTPA as the control rather than racemic alcohol, the same value of 96% was calculated

using the CF_3 signal in the ^{19}F NMR spectra. The diastereomers gave signals at δ -71.5 and δ -71.9 ppm (Figure 29).

Figure 28: ^1H NMR (CDCl_3 , 270 MHz) of the products of the MTPA derivatisation of (i) (+)-2-acetoxy-1-(hydroxyethyl)benzonitrile **30** and (ii) (\pm)-2-acetoxy-1-(hydroxyethyl)benzonitrile **33**.

Key to Assignments:

U : unreacted **30/33** CH_3 protons

I : diastereomer I CH_3 protons

II : diastereomer II CH_3 protons

A : 1-acetoxy-2-(hydroxyethyl)benzonitrile **34**

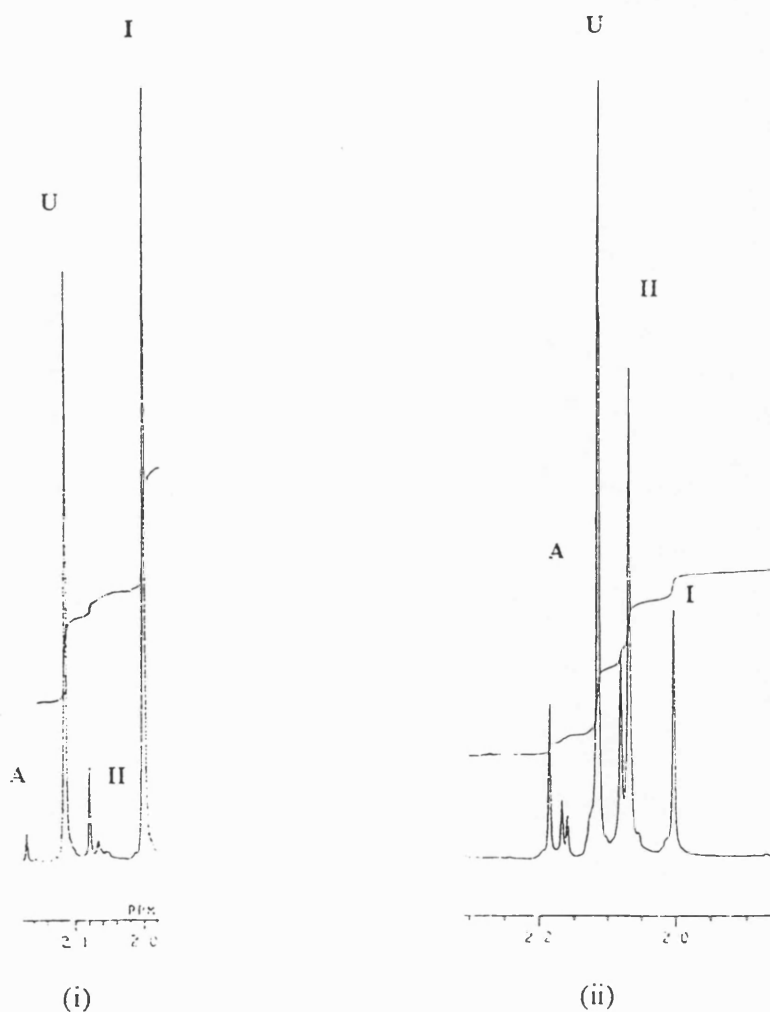
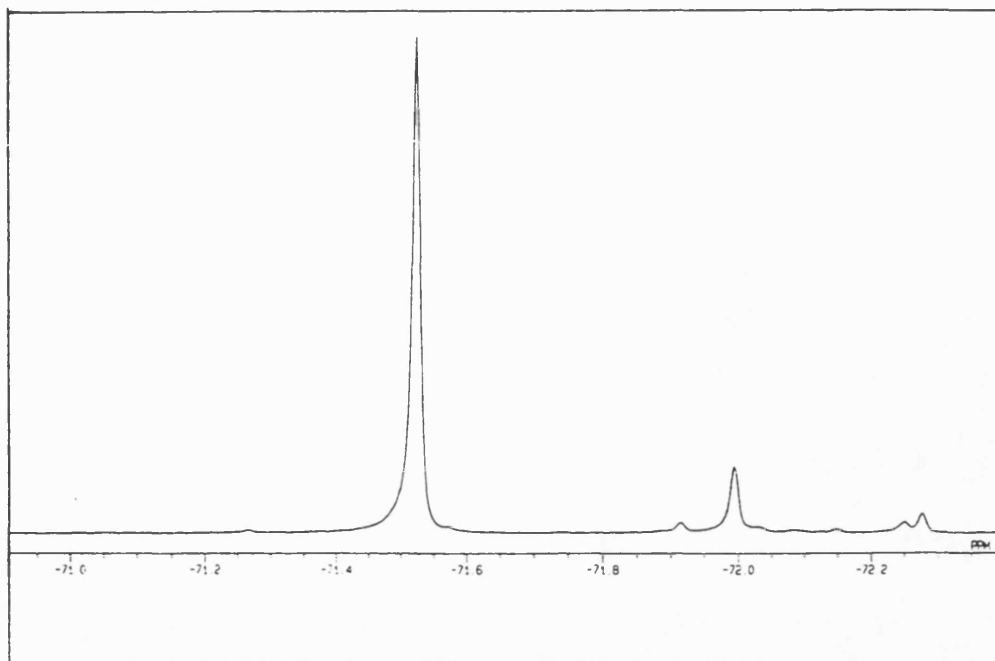
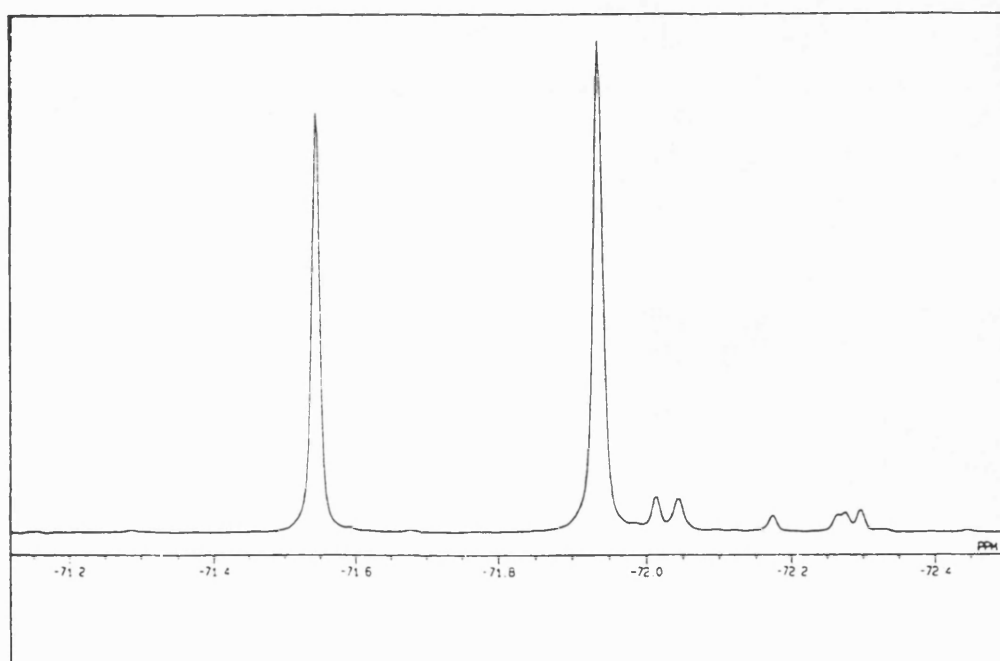


Figure 29: ^{19}F NMR spectra for the products of MTPA derivatisation of (+)-2-acetoxy-1-(hydroxyethyl)benzonitrile **30** (a) Using (R)-MTPA. (b) Using racemic MTPA. (CDCl_3 , 376.05 MHz).

(a)

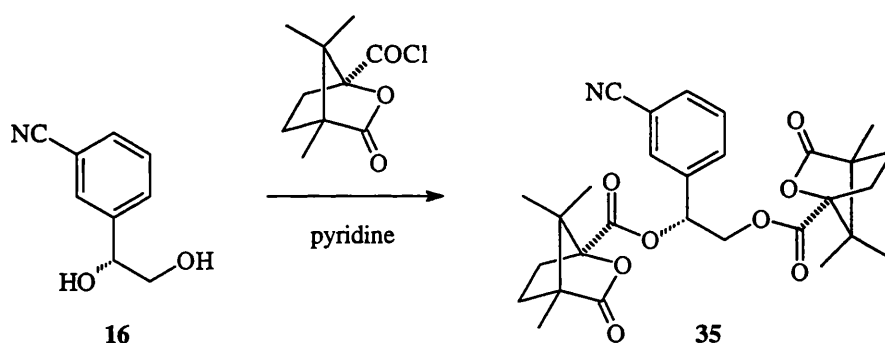


(b)



Determination of the optical purity of the (–)-diol **16** was less straightforward. The racemic diol **32**, was obtained by treating the α -hydroxyketone **17** with sodium borohydride in ethanol. The mono-MTPA esters of both the racemic and asymmetrically prepared diols **32** and **16** were synthesised and their ^1H and ^{19}F NMR spectra examined. Unfortunately the signals for the two diastereomers were too similar for any calculation of enantiomeric excess to be made. The diesters were also prepared using a method described by Dale and Mosher.¹⁹⁹ The reaction mixture was heated to 45°C to encourage derivatisation of both hydroxyl groups. However, there was not sufficient separation of the diastereomeric signals to allow calculation of the enantiomeric excess.

A second chiral derivatising agent was then tried. The synthesis of the biscamphanate of the diol **35** was attempted as shown in Scheme 25. Unfortunately, this was not helpful as even after several days stirring the starting diol **16** remained and the main product was the mono-camphanate with a much smaller amount of the bis-camphanate **35** present. There was no sign of separation of the diastereomers of the monocamphanate in the NMR spectrum.

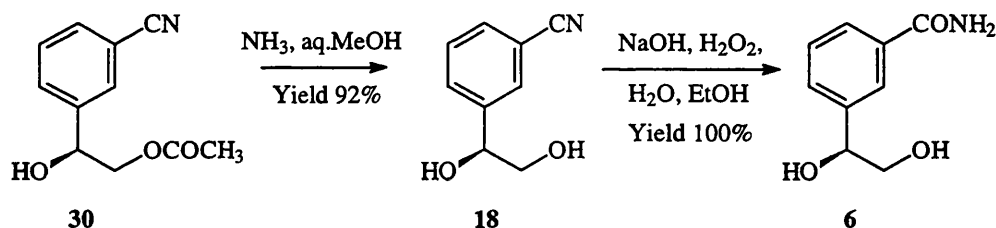


Scheme 25

Another approach taken towards determining the enantiomeric purity of the diol **15** was to use lanthanide chiral shift agents. Both $[\text{Eu}(\text{hfc})_3]$ and $[\text{Pr}(\text{hfc})_3]$ were added to NMR samples of the racemic diol to see if there was any separation of

the enantiomers. The only effect seen was a general line broadening of the NMR spectra in both cases.

Finally an estimate of optical purity was made from the optical rotation readings of the (–)-diol **16** and the (+)-diol **18**. (+)-3-(1,2-Dihydroxyethyl)benzonitrile **18** was synthesised by hydrolysis of the asymmetrically prepared acetoxy-protected diol **30**. The enantiomeric purity of **30** had already been determined and the hydrolysis using ammonia in aqueous methanol (Scheme 26) should not have affected this. The optical rotation of the (+)-diol **18** obtained was $+46.6^\circ$ (c 2.0, dichloromethane). Since the (–)-diol **16** was found to have an optical rotation of -46.6° (c 1.0, dichloromethane); this would suggest strongly that the enantiomeric excess of the (–)-diol synthesised is approximately 96%. Subsequent preparations of both enantiomers gave similar results.



Scheme 26

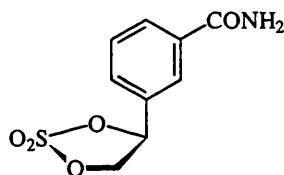
Therefore, both baker's yeast reductions of the protected and unprotected α -hydroxyketones proceeded well in terms of enantiomeric excess. This indicates that substitution by a cyano group in the 3-position of the aromatic ring does not affect the efficiency or selectivity of the reactions. This is in contrast to the *para*-disubstituted derivatives in the acetoxy-protected series mentioned earlier (Scheme 15).^{180,185}

As shown in Scheme 26, the acetoxy-protected diol **30** was deprotected to give the (+)-diol **6**. This procedure was also carried out on the racemic compound **33**

to give **32**. Initially, potassium methoxide was used as the nucleophile to carry out this transesterification reaction. This resulted in a mixture of compounds that were difficult to separate by chromatography. Use of ammonia in methanol proved to be a much more clean, efficient procedure, not requiring chromatography.

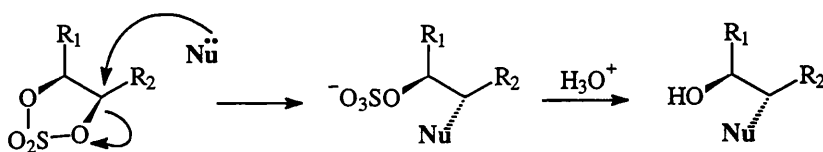
The nitriles **16**, **18** and **32** were treated with hydrogen peroxide and sodium hydroxide to give the corresponding amides (-)-3-(1,2-dihydroxyethyl)benzamide **36**, (+)-3-(1,2-dihydroxyethyl)benzamide **6** and (±)-3-(1,2-dihydroxyethyl)benzamide **37**. Scheme 26 shows this step for the (+) isomer. The amides are very hygroscopic gums and are not soluble in most organic solvents. They could not be extracted using organic solvents in the usual way and were freeze-dried immediately prior to use in subsequent steps.

The properties of cyclic sulphates made benzamide **3** an ideal target compound for the synthesis of irreversible inhibitors of PARP.



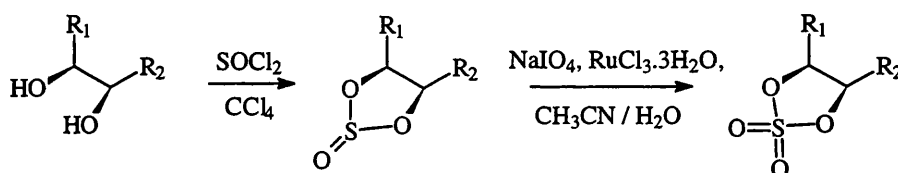
3

Cyclic sulphates are very good electrophiles and have a high reactivity towards various nucleophiles.²⁰⁰ Nucleophiles generally attack the less hindered carbon in the ring and the β-sulphate is formed. The SO₃⁻ group is then removed by hydrolysis (Scheme 27). However, the mechanism of PARP may favour attack of the nucleophile at the benzylic position.



Scheme 27

Optically active cyclic sulphates are prepared from the corresponding enantiomerically pure diol *via* the cyclic sulphite. Cyclic sulphites are usually synthesised by the treatment of the diol with thionyl chloride or sulphur tetrafluoride.²⁰⁰ The reaction is carried out in anhydrous conditions to prevent hydrolysis of the reagent or the sulphite product. If the substrate diol contains acid-labile groups, pyridine or triethylamine is added to scavenge the hydrogen chloride which is produced in the reaction.

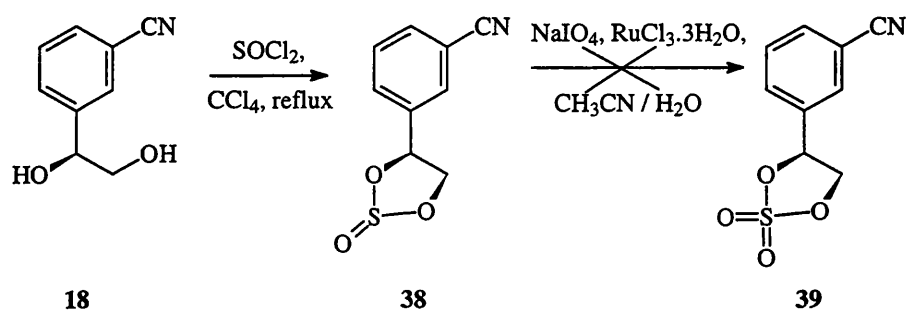


Scheme 28

The oxidation of the sulphite to the sulphate has been carried out in the past using potassium permanganate²⁰¹ which tends to give fairly low yields, or stoichiometric amounts of ruthenium tetroxide which is expensive.²⁰² More recently, however, a system was described by Gao and Sharpless,²⁰³ in which ruthenium tetroxide is present in catalytic amounts. Ruthenium trichloride and sodium periodate are used to create the ruthenium tetroxide *in situ*. This method has since proved to be the most general method for the synthesis of cyclic sulphates in good yields. The reaction is fairly versatile and can be carried out in the presence of acid or base labile groups but does not work in the presence of groups that can bind the ruthenium tetroxide and stop catalytic turnover. Some cyclic sulphites with amide functionalities have presented this problem; here the

amide functionality was adjacent to the sulphite group,²⁰⁴ other sulphites with amides elsewhere in the molecule were oxidised using this system.²⁰⁰

This method of synthesising the cyclic sulphite and sulphate was firstly tried on the nitrile **18** rather than the amide (Scheme 29). The formation of the cyclic sulphate, however has to be carried out on the benzamide rather than the benzonitrile because of the instability of the cyclic sulphate to nucleophiles. The cyclic sulphite was formed and used immediately as it is likely to be unstable to storage.



Scheme 29

NMR analysis of the intermediate showed that the cyclic sulphite **38** was formed and that two geometrical isomers were present in approximately equal proportions. These occur because the sulphur has a lone pair of electrons that can be either *cis* or *trans* to the aromatic substituent with respect to the cyclic sulphite ring.

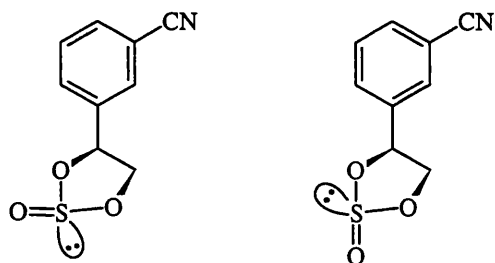
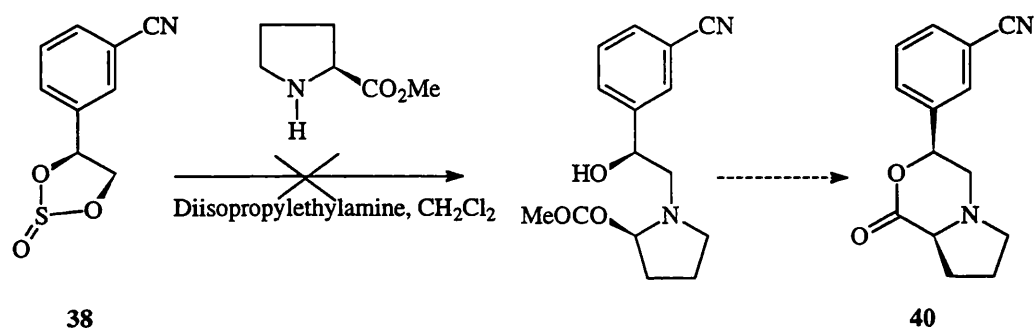


Figure 30: Geometrical isomers of the cyclic sulphite 4(S)-4-(3-cyanophenyl)-1,3,2-dioxathiolane-2-oxide (**38**).

Attempted oxidation of the cyclic sulphite **38** to sulphate **39** gave only the diol **18**, indicating that cleavage of the cyclic sulphite/sulphate had occurred.

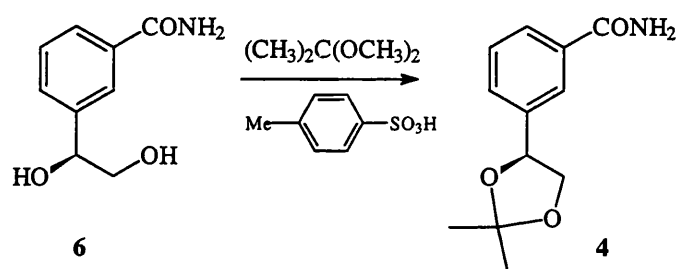
The amide **6** is not soluble in organic solvents such as carbon tetrachloride and is very hygroscopic. These properties would not favour the synthesis of the cyclic sulphate **3**. Therefore this was not considered as a feasible substrate.

In an attempt to confirm the absolute stereochemistry of the series of diols, the reaction of the methyl ester of (*S*)-proline with the cyclic sulphite was studied, as shown in Scheme 30. In the cyclic product **40**, the positions of the two chiral centres are fixed in relation to each other. Although the cyclic sulphite is a mixture of epimers, this is irrelevant since the sulphur is discarded in the reaction. The stereochemistry of the proline centre is known; comparison of the positions of the groups around the second chiral centre in relation to the proline can be used to determine whether the benzylic centre is *R* or *S*. This could be done using NMR analysis and NOE (nuclear Overhauser effect) experiments to determine which protons are close in space. Alternatively a crystalline sample would enable X-ray crystallography to be carried out and the stereochemical arrangement determined in this way. Unfortunately, the reaction did not proceed. Cyclic sulphites are generally less susceptible to nucleophilic attack than are the cyclic sulphates.²⁰⁰



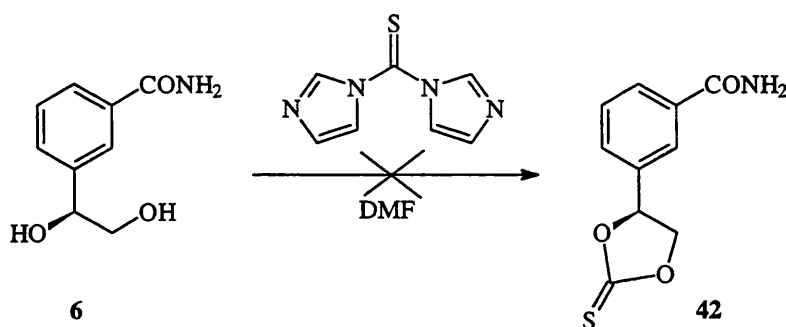
Scheme 30

The second target compound shown in Figure 24, (+)-3-(2,2-dimethyl-1,3-dioxolan-4-yl)benzamide **4**, was synthesised from **6** in a transketalisation as shown in Scheme 31. The diol **6** was treated with 2,2-dimethoxypropane in acidic conditions to give the dioxolane **4** in good yield. The enantiomer **36** is treated in the same way to give (–)-3-(2,2-dimethyl-1,3-dioxolan-4-yl)benzamide **41**.



Scheme 31

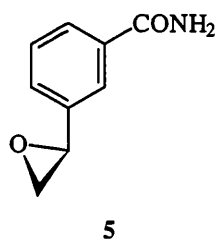
Following on from the successful synthesis of **4**, the synthesis of the thiocarbonate **42** was attempted. The thiocarbonate group is electrophilic unlike the dioxolane group in **4**, and **42** would be a potential irreversible inhibitor. Thiophosgene (CSCl_2) is the obvious reagent to use for this nucleophilic substitution reaction, but since it is very toxic, a safer alternative, 1,1'-thiocarbonyldiimidazole, was used (Scheme 32).



Scheme 32

The product from the reaction was a mixture of compounds and could not be separated due to lack of solubility in almost all solvents. There were no signals in the region of the ^1H NMR spectrum corresponding to the predicted shifts of the methylene protons in the desired product. These protons would be expected to resonate in the same region as the methylene protons in the acetoxy-protected diol **30**. This work was taken no further.

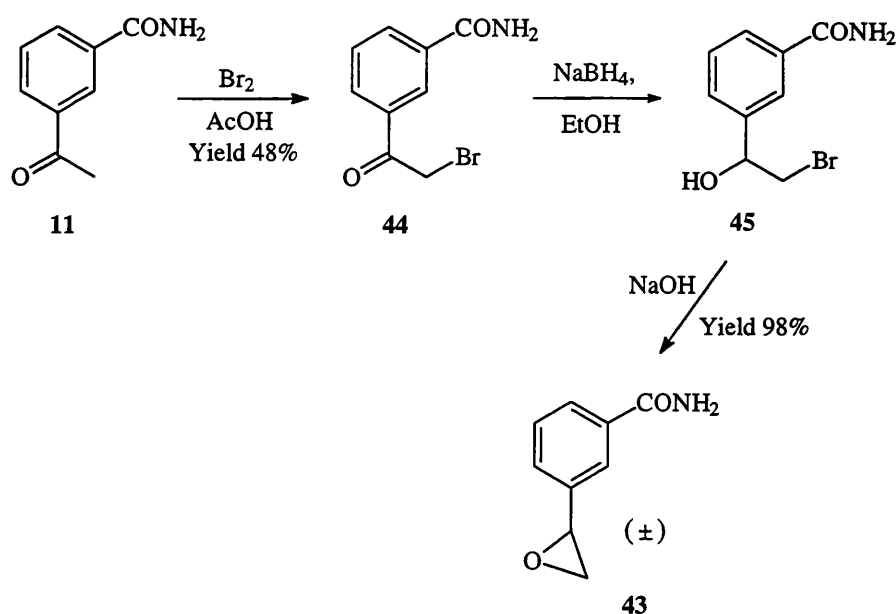
Another desirable target compound was the epoxide **5**. This has the characteristics required for potential irreversible inhibition of PARP. Like the cyclic sulphate, the epoxide is susceptible to nucleophilic attack and has the potential to become irreversibly bound to the nucleophilic site on the acceptor protein.



Three main methods used to synthesise epoxides are:-

- a) Epoxidation of alkenes; Sharpless asymmetric epoxidation methodology can be used to produce epoxides with high enantioselectivity.²⁰⁵
- b) Intramolecular cyclisation of alcohols bearing a leaving group on the adjacent carbon.
- c) Nucleophilic alkylation of carbonyl compounds, *e.g.* Darzens condensation²⁰⁶

The racemic epoxide **43** was prepared in the first instance using a method of the type (b) above. Scheme 33 shows the steps involved in the synthesis. The α -bromoketone **44** was prepared by bromination of the methylketone **11**. This method was used earlier for the preparation of the benzonitrile analogue **25**. The reduction of **44** with sodium borohydride gave the bromohydrin **45** (not isolated) which then undergoes an intramolecular $\text{S}_{\text{N}}2$ reaction to form the epoxide **43**.



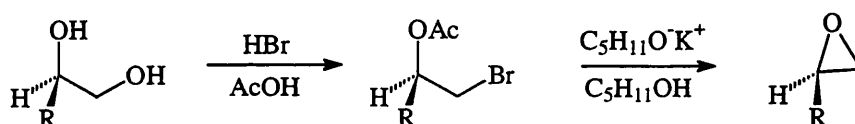
Scheme 33

Both the bromoketone **44** and the epoxide **43** were evaluated as PARP inhibitors.

The enantiomerically pure epoxide **5** would be obtained if the reduction of the bromoketone to the bromohydrin is carried out asymmetrically. As a continuation of the work on baker's yeast, the reduction of **44** and subsequent cyclisation by treatment with sodium hydroxide was attempted. The baker's yeast seemed to be unable to reduce this substrate. It may be that this analogue of NAD^+ binds irreversibly to the NAD^+ site of the alcohol dehydrogenase inhibiting the enzyme.

Another approach to the preparation of the enantiomerically pure epoxide **5** is to use the asymmetrically prepared diol **6** and derivatise the primary alcohol to give a good leaving group while not affecting the chiral centre. For example, the 2,4,6-trimethylbenzenesulphonate ester could be made. Cyclisation would then follow, by treatment with base, as for the bromohydrin above. For the stereochemistry to be retained, activation must take place exclusively at the primary hydroxyl group.

An example of a method of a similar type is to form the bromoalkyl acetate from the diol as shown in Scheme 34. This method²⁰⁷ is reported to be superior to methods in which the 1-O-sulphonate ester is made in terms of retention of optical purity.²⁰⁸ When this method was used for the preparation of (*R*)- and (*S*)-methyloxirane the optical purity of the starting materials was retained through the synthesis to the epoxides.²⁰⁹ However in the case of (–)-(*R*)-phenylethane-1,2-diol **15** when this method was used to form the corresponding epoxide, the optical purity was reduced to 88% (*i.e.* 76%).²⁰⁷ An aromatic group as a substituent on the secondary alcohol leads to the bromine attacking the carbon here rather than at the primary position, as in Scheme 34. This is due to the stabilisation of a carbocation at the benzylic position. This makes this method unsuitable for the preparation of **5**.



Scheme 34²⁰⁷

Diaryldialkoxysulphuranes (Figure 31) can also be used to make epoxides from diols. Martin *et al*²¹⁰ described the formation of epoxides from the corresponding diols in excellent yields, in mild conditions using this reagent. However this reagent also reacts with amides and so is not suitable for the preparation of **5**.²¹¹

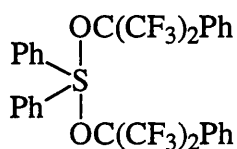
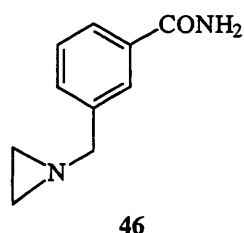


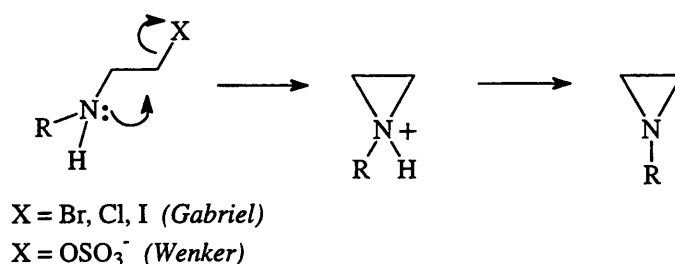
Figure 31: Structure of a diaryldialkoxysulphurane²¹⁰

The preparation of further analogues from the amide **6** was fraught with difficulties due to its hygroscopic nature and insolubility in any solvents other than water and ethanol.

The final compound to be discussed in the benzamide series is the aziridine **46**. In common with the other cyclic derivatives mentioned above, aziridines undergo ring opening reactions with nucleophiles. However, in the case of aziridines this only occurs in acidic conditions. It is likely that a residue in the enzyme active site would provide an H^+ . It is also likely that the active site would provide an environment in which cations are stable in this region of space, since the likely mechanism for the cleavage of NAD^+ by PARP involves the formation of an oxonium ion. The site for nucleophilic attack is fairly close in space to the equivalent position in NAD^+ . The aziridine should therefore bind covalently to and irreversibly inhibit PARP.

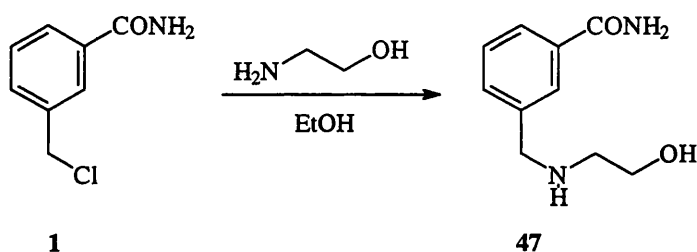


Many of the preparative routes to aziridines involve the internal cyclisation of an amino group in an intramolecular displacement reaction. The best known and oldest of these procedures are the Gabriel^{212,213} and Wenker²¹²⁻²¹⁴ syntheses of aziridines. (Scheme 35).



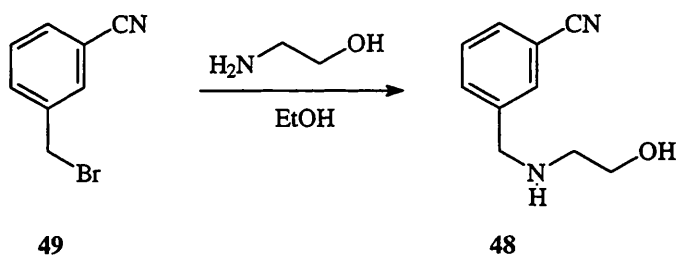
Scheme 35

The Wenker synthesis involves the conversion of an amino alcohol to an aziridine whereas the Gabriel synthesis uses an β -haloamine. Many methods developed since involve the treatment of an amino alcohol to convert the OH to a good leaving group and subsequent cyclisation. A useful starting material for the synthesis of the aziridine **46** might be the amino alcohol **47** or its nitrile analogue **48** (Schemes 36 and 37). Both of these amino alcohols were made by treating either the chloromethyl (**1**) or the bromomethyl (**49**) derivative with ethanolamine in ethanol.



Scheme 36

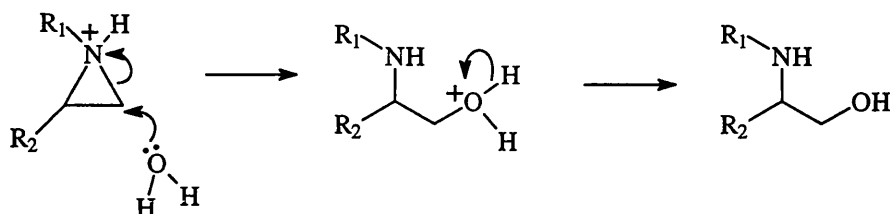
The amide **47** was, in common with other compounds in this series, insoluble in many solvents and difficult to manipulate. Therefore the nitrile **48** was the amino alcohol used to attempt aziridine preparation.



Scheme 37

Aziridines are unstable to acids because protonation at nitrogen increases the susceptibility to ring opening. In acidic conditions hydrolysis occurs rapidly, as shown in Scheme 38. However, unlike epoxides and cyclic sulphates, aziridines are much more stable in alkaline conditions. Therefore, partial hydrolysis of the

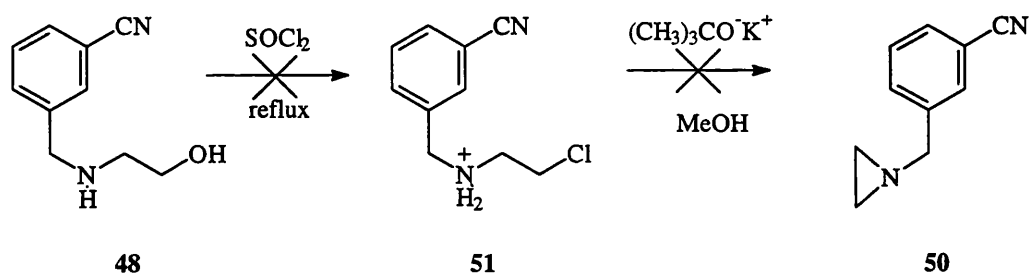
cyano group to the amide using hydrogen peroxide and sodium hydroxide, should be possible without affecting the aziridine.



Scheme 38

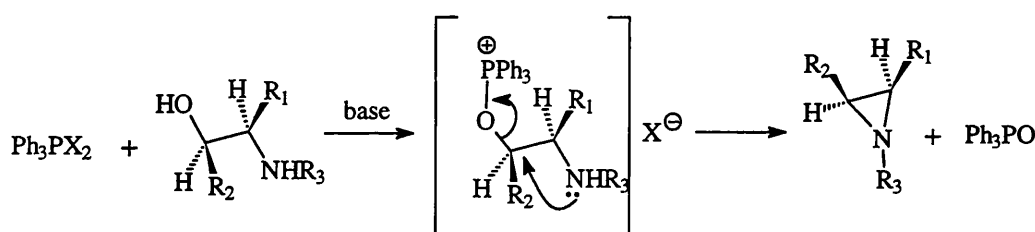
The Wenker procedure for the conversion of amino alcohols to aziridines originally involved boiling the amino alcohol with concentrated sulphuric acid to produce the hydrogen sulphate ester.²¹⁴ A variation which has been used in more sensitive systems is the use of chlorosulphonic acid at room temperature.²¹⁵ This method requires addition to hot concentrated sodium/potassium hydroxide to effect the cyclisation, which tends to occur with yields less than 40%. These low yields and harsh conditions make these methods undesirable.

The first method tried in the attempted preparation of the aziridine **50** was of the Gabriel type (Scheme 35). The amino alcohol **48** was boiled with thionyl chloride in an attempt to form the 2-chloroethylamine intermediate, **51**, which would then undergo cyclisation by treatment with potassium *tert*-butoxide (Scheme 39). A complex mixture of products was obtained which, by NMR analysis did not contain the aziridine.



Scheme 39

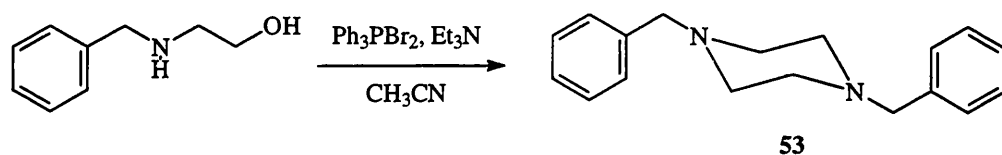
More recently there have been several reports of the one-step preparation of aziridines from β -amino alcohols.²¹⁶⁻²¹⁹ These have largely utilised reagents formed from triphenylphosphine (Ph_3P) and chlorine, bromine or carbon tetrachloride, in basic conditions. It is suggested that the triphenylphosphine forms a complex with the halogen which then undergoes nucleophilic attack by the OH group of the amino alcohol. the OPPh_3^+ group formed is a good leaving group and drives the intramolecular cyclisation. This general mechanism is depicted in Scheme 40.



Scheme 40

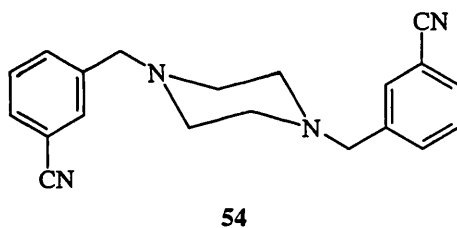
Three methods of this type were used in the attempted preparation of the aziridine **50**. The first of these was based on a method reported by Okada *et al*²¹⁷ for the preparation of aziridines and by Freeman and Mondron²¹⁶ for the preparation of azetidines. In this procedure, the reagent is triphenylphosphine dibromide with triethylamine as the base. Okada *et al*²¹⁰ made several different substituted aziridines in reasonable yields. However, in the case of 1-substituted aziridines the only product isolated was the corresponding piperazine. The piperazine is formed by a bimolecular reaction, rather than an intramolecular reaction, occurring at the intermediate stage shown in Scheme 40. A nitrogen from a second molecule attacks the carbon of the C-O bond to join the two molecules. An equivalent reaction occurs to complete the piperazine ring. This intermolecular reaction occurs more readily in the amino alcohols that have no substituents on the carbon adjacent to the hydroxyl group, *i.e.* in Scheme 40, R_2

is H. This is because it is easier for the second molecule to approach and react before the intramolecular cyclisation has taken place. When there is a substituent at this position, there is more steric hindrance to prevent the intermolecular reaction. In the attempted synthesis of the analogue of **49**; 1-phenylmethylaziridine **52**, the only product reported to be isolated was the piperazine **53** (Scheme 41).

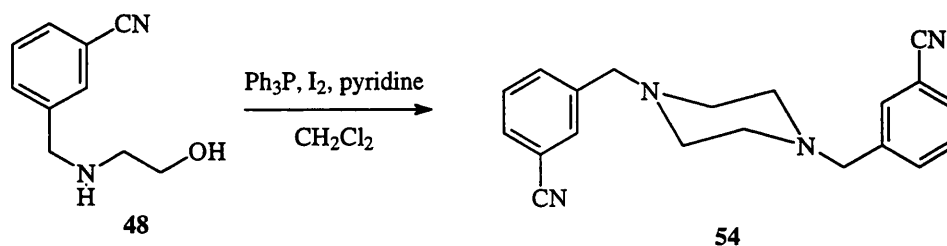


Scheme 41²¹⁷

The amino alcohol **48** was treated with triphenylphosphine dibromide in basic conditions. In agreement with the results of Okada *et al.*,²¹⁷ the only product isolated was the piperazine **54**.

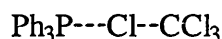


Similarly, treatment of **48** with the analogous triphenylphosphine diiodide (formed *in situ*) gave only the piperazine **54** (Scheme 42).



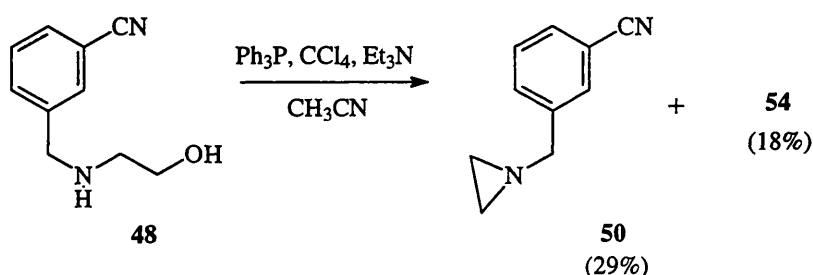
Scheme 42

The most successful method of this type was one in which the amino alcohol **48** was treated with carbon tetrachloride and triphenylphosphine in basic conditions. This procedure was first reported by Appel and Kleinstück.²¹⁸ Among other examples, these workers reported a yield of 66% of 1-phenylmethylaziridine (**52**) and only 12% of the corresponding piperazine **53**. In this system the carbon tetrachloride is thought to form a complex, **55**, with the triphenylphosphine.



55

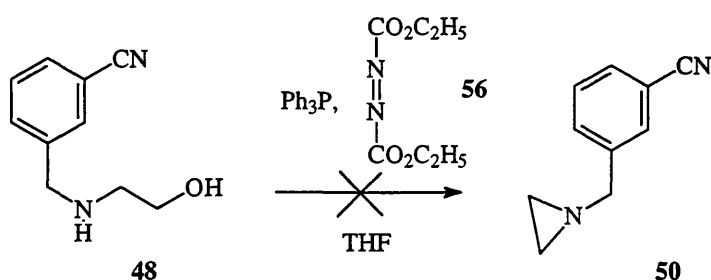
As shown in Scheme 43, a mixture of the aziridine **50** and the piperazine **54** was obtained; some starting material was also present in the mixture. This was determined by NMR analysis. The aziridine ring protons resonate upfield of the other signals in the spectrum at 1.30 ppm and 1.69 ppm. These two signals correspond to the *trans* and *cis* protons, respectively. Those protons on the same side of the ring as the aromatic substituent (*cis*) are magnetically equivalent so resonate at the same chemical shift. The *trans* protons on the opposite side of the ring to the aziridine are also equivalent to each other and give the second signal. These signals were similar to those reported for 1-phenylmethylaziridine (**52**).²²⁰



Scheme 43

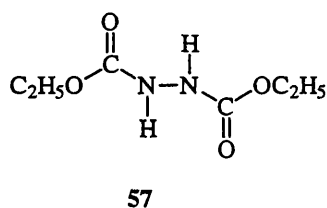
More recently Pfister²¹⁹ reported a procedure for the "one-pot" synthesis of aziridines from amino alcohols. Again triphenylphosphine was used as the reagent, but in this case diethyl azodicarboxylate **56** forms a complex with the triphenylphosphine, rather than a halogen. As with other triphenylphosphine methods, although yields for other more substituted examples were high, 1-

phenylmethylaziridine **52** was obtained in a yield of only 18%. Nevertheless this method was used in an attempt to form the aziridine **50** as shown in Scheme 44.

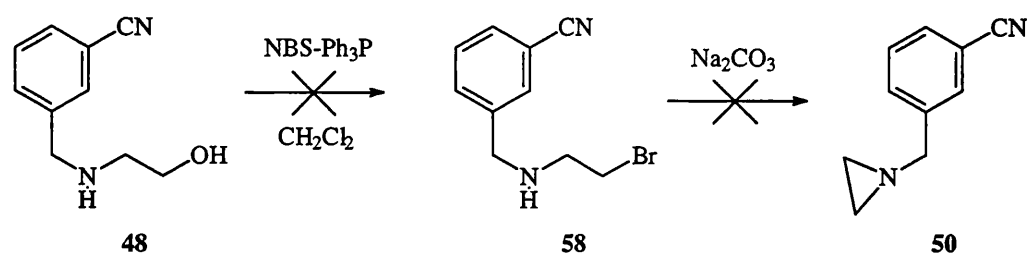


Scheme 44

In this case only a trace amount of the piperazine **54** and no aziridine **50** was recovered. The main product recovered following chromatography was a mixture consisting of triphenylphosphine oxide and dicarbethoxyhydrazine, **57**. This was confirmed by NMR and mass spectroscopy.



Finally the amino alcohol was treated with *N*-bromosuccinimide and triphenylphosphine. This method was used by Ponpipom and Hanessian to brominate primary alcohols selectively.²²¹ It was the intention that treatment of the resulting reaction mixture with base would cause the cyclisation of the bromoamine **58** to the required aziridine **50** (Scheme 45). Once again the only product detected was the piperazine **54**.



Scheme 45

A suitable method for the preparation of the aziridine **50** has yet to be found. In the one case where the compound was shown to be present in the crude product, it was not recovered on purification. The majority of the methods tried involved the use of triphenylphosphine as a reagent. This gives rise to the problem of having to separate the aziridine product from the triphenylphosphine oxide produced. The formation of piperazine **54**, in these conditions at least, seems to be more favourable than the formation of the aziridine **50**. This seems to be the major reason for failure of these methods.

The crude mixture produced by the reaction shown in Scheme 43 was treated with hydrogen peroxide and sodium hydroxide solution to convert the cyano groups present to the corresponding amide groups. It was hoped that 3-(aziridin-1-ylmethyl)benzamide **47** might be easier to separate from the mixture than **50**. However this was not the case. This target compound remains to be prepared and tested.

Chapter Six

6. Isoquinolinones

In this series of compounds, the initial aim was to synthesise isoquinolin-1-one analogues of NAD^+ with electrophilic groups at the 5-position (corresponding to the 3-position in benzamides, Figure 23). The isoquinolin-1-ones have the benzamide core in their structure, but with the amide group as part of a heterocyclic fused ring. By conformationally restricting the amide group in this way, the activity of these compounds as inhibitors of PARP is greatly increased.

An early target was 5-cyanoisoquinolin-1-one **59**. From this analogue, it was intended that several electrophilic-side chains could be developed. For example, the Pinner reaction could be used to furnish the methyl ester **60**, which in turn could be used to prepare the chloromethyl analogue **61** (Figure 32).

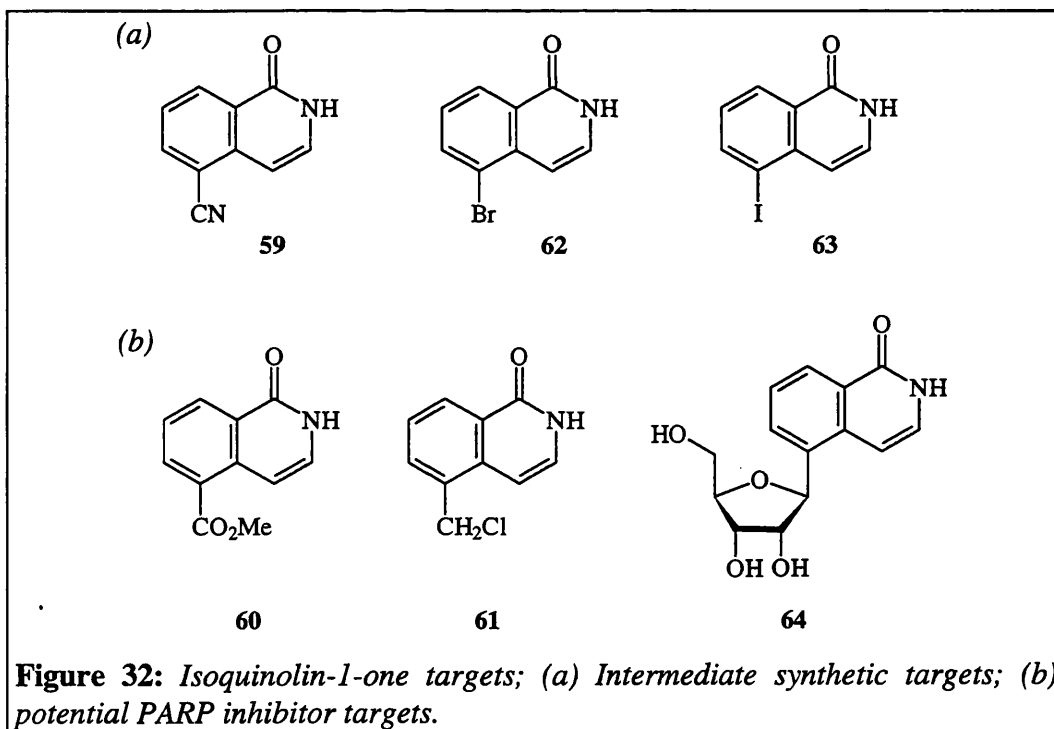


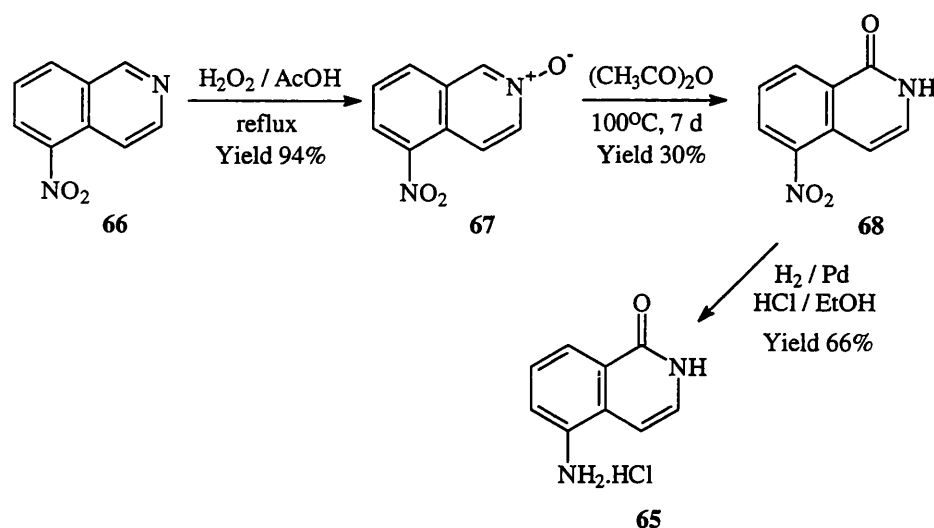
Figure 32: Isoquinolin-1-one targets; (a) Intermediate synthetic targets; (b) potential PARP inhibitor targets.

Following several approaches to the synthesis of **59**, it was found that, due to lack of solubility and reactivity, this compound was not a suitable intermediate in the synthesis of a series of isoquinolinones. Efforts were then directed towards derivatising isoquinolinones *via* the C-metallated isoquinolinones. This approach involved the preparation of halogenated isoquinolin-1-ones **62** and **63**.

In addition to electrophilic side-chains, groups mimicking the ribose moiety in NAD⁺ were also considered. Steps towards the synthesis of the isoquinolinone riboside **64** were also taken.

The first target compound was 5-aminoisoquinolin-1-one **65**. This compound is known to be a potent PARP inhibitor.¹⁵⁸ A method of extracting PARP from nuclear extracts using magnetic beads has been under development.²²² The principle behind this method is that the magnetic beads, when added to the nuclear extract, bind PARP and are then separated magnetically. The enzyme is then eluted from the beads. Various methods of binding PARP to the surface of the beads are under investigation. One method of binding PARP to the beads would be to attach a PARP inhibitor *via* a "spacer" or "linker" to the surface of the beads. Isoquinolinones are potent inhibitors and should provide a strong binding interaction with PARP. 5-Aminoisoquinolinone **65** has an amino group which can be easily linked to a "spacer" group. Therefore, a protected "spacer" with the isoquinolinone moiety attached was synthesised for this purpose.

5-Aminoisoquinolin-1-one, **65**, was prepared by a method similar to that described by Wenkert *et al*,²²³ shown in Scheme 46. 5-Nitroisoquinoline **66** was treated with hydrogen peroxide and acetic acid to give the *N*-oxide **67**. Rearrangement of the *N*-oxide **67** by heating with acetic anhydride gave 5-nitroisoquinolin-1-one **68**. The amine **65** was obtained by the catalytic hydrogenation of **68**.



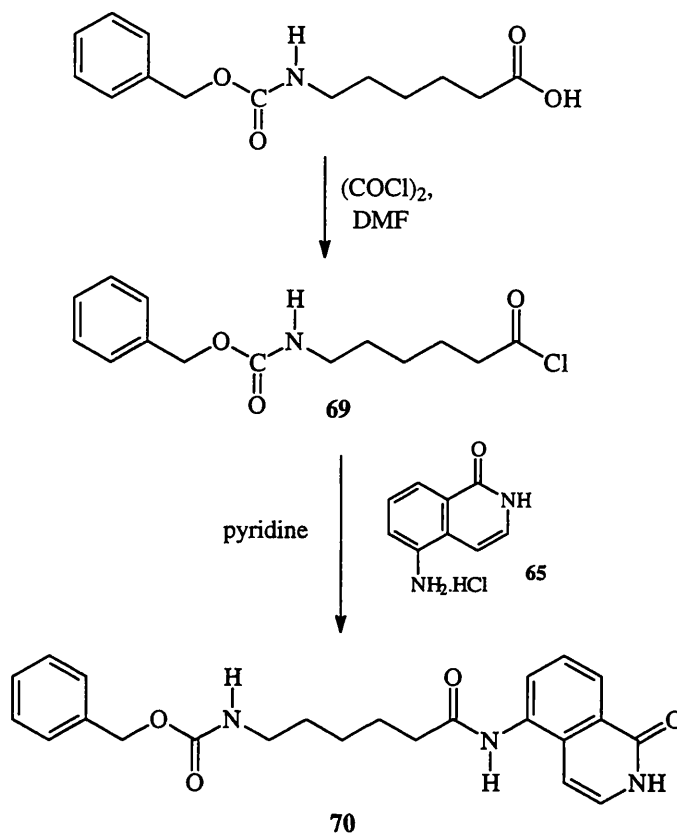
Scheme 46

The rearrangement of the *N*-oxide **67** was a fairly low yielding step, largely because of the lengthy and inefficient extraction and purification processes involved (the yields in Scheme 46 are the best yields obtained in a number of runs). Attempts to carry through the crude product, which consisted, nevertheless, mainly of **68**, resulted in a large reduction in the yield of hydrogenation product **65**.

5-Aminoisoquinolinone **65** was coupled to Cbz-protected 6-aminohexanoyl chloride **69** to form the amide **70**, as shown in Scheme 47. The derivatised inhibitor **70** can be deprotected and coupled to biotin, for example, *via* an amide linkage.²²⁴ In this example, the biotinylated linker would bind strongly to streptavidin-coated beads.

A possible method of preparation of 5-cyanoisoquinolinone **59**, is to diazotise the amine **65** and treat the diazonium salt with copper (I) cyanide (the Sandmeyer reaction, discussed in Chapter 5). However, large quantities of 5-cyanoisoquinolinone **59** were required, as this was to be a starting material for the preparation of several target compounds. The diazotisation step is likely to be

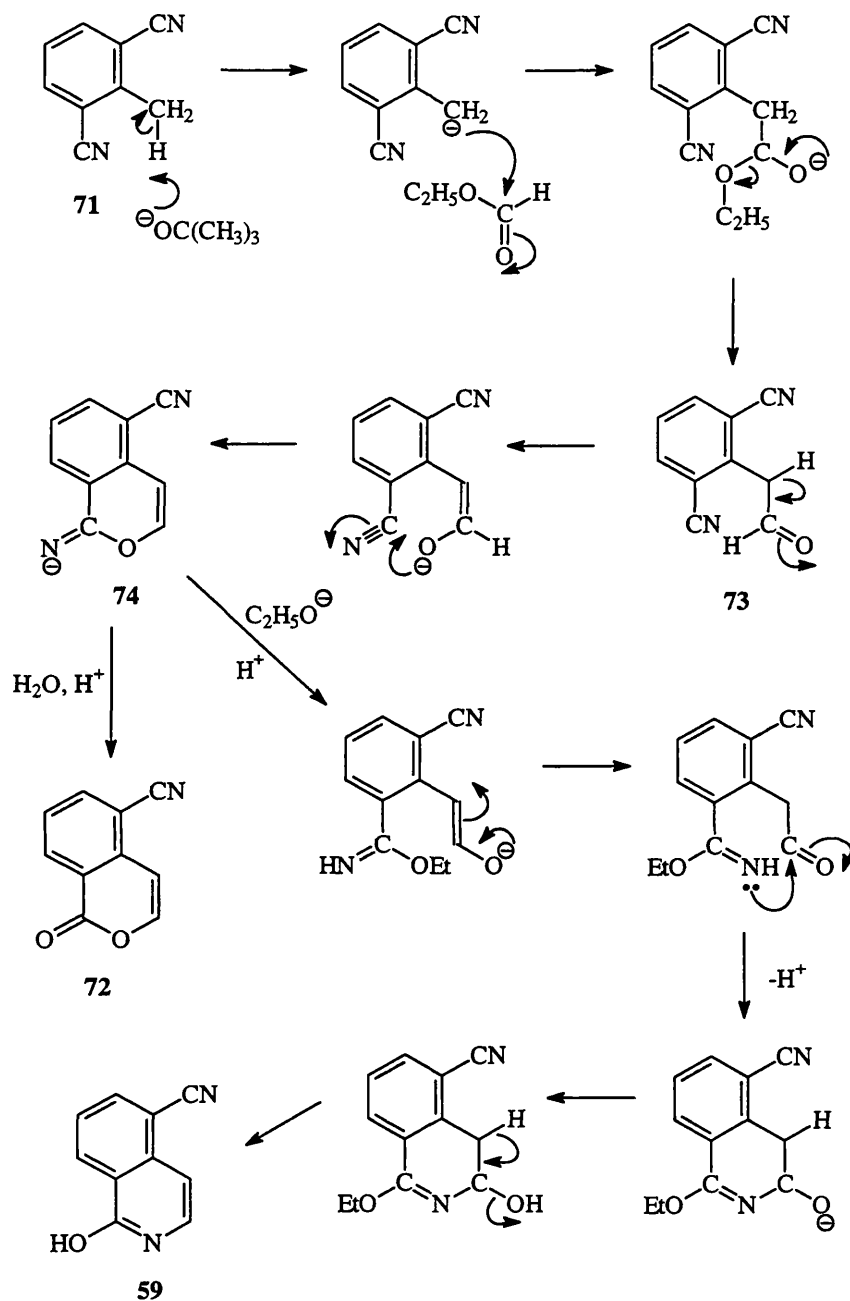
fairly low yielding; it was therefore decided to use a less lengthy and higher yielding route to **59**.



Scheme 47

One method for the preparation of 5-cyanoisoquinolin-1-one **59**, is reported in the literature by Wenkert *et al.*²²³ 2,6-Dicyanotoluene **71** was treated with ethyl formate under basic conditions, followed by acid hydrolysis. The reported yield of **59** was 20%.²²³ This procedure was repeated and both the isoquinolinone **59**, and 5-cyanoisocoumarin, **72**, were isolated from the complex mixture of products (Scheme 49). These two products have similar structures and similar ^1H NMR spectra. However, on closer inspection, a clear distinguishing feature is the coupling constant of the protons at positions 3 and 4. In the isoquinolinone, with

nitrogen in the ring, $J_{3,4}$ is 7.0 Hz; whereas in the oxygen heterocycle $J_{3,4}$ is 5.7 Hz. These assignments were confirmed by mass spectrometry.

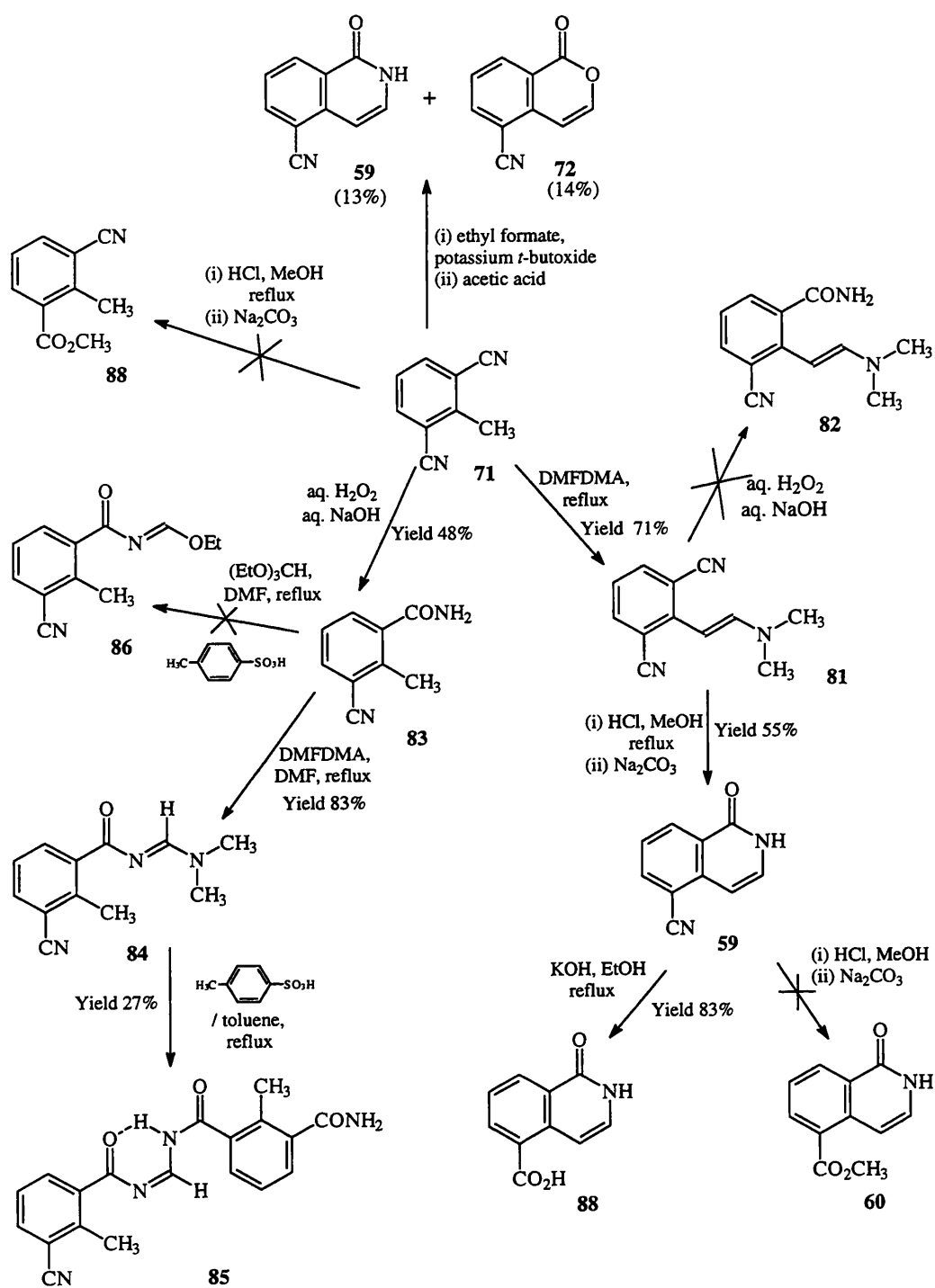


Scheme 48

Mechanisms for the formation of these products are proposed in Scheme 48. The base abstracts a proton from the methyl group and the carbanion formed attacks

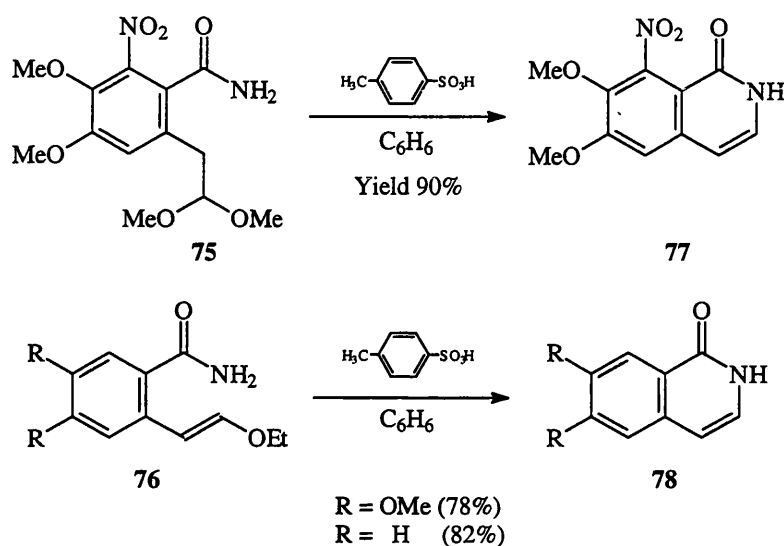
the ethyl formate. This leads to the formation of the intermediate aldehyde **73**. Cyclisation occurs and the imino lactone (imidate) **74** is formed. From this intermediate **74**, the isocoumarin **72** can be formed by hydrolysis. The isoquinolinone is formed possibly as a result of the attack of **74** by an ethoxide ion and ring opening. Rearrangement, cyclisation and, finally, hydrolysis follow to give **59**.

The yield of **59** was low using this method. The isocoumarin **72** could be manipulated to give further amounts of **59**; syntheses of some isoquinolinones from the corresponding isocoumarins, by treatment with ammonia in ethanol at increased pressure, have been described.²²⁵ However, the yield of **72** was also low. Therefore, other methods of synthesis of 5-cyanoisoquinolinone and its analogues were investigated. These approaches are summarised in Scheme 49.



Scheme 49

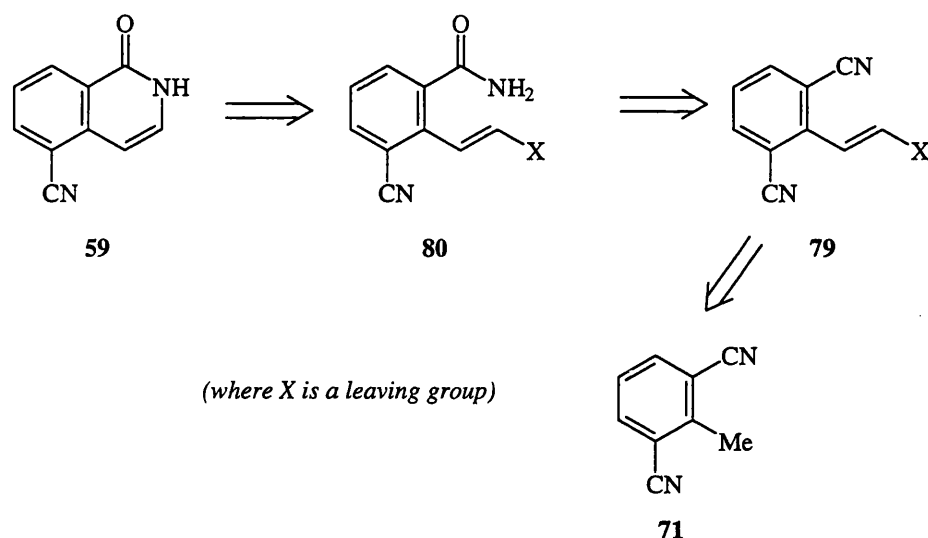
Sakamoto *et al*^{226,227} reported the synthesis of various unsubstituted, 6,7-disubstituted and 6,7,8-trisubstituted isoquinolin-1-ones. These procedures involve the cyclisation of substituted benzamides of the type shown in **75** and **76** (Scheme 50).



Scheme 50^{226,227}

In the position *ortho* to the amide group is a substituent with two-carbon chain and with a potential leaving group attached. On heating in the presence of acid, these benzamides **75** and **76** cyclise to form the isoquinolin-1-ones **77** and **78**.^{226,227}

A similar strategy was investigated for the synthesis of the 5-cyano derivative. The intended pathway is shown retrosynthetically in Scheme 51. The aim was to derivatise the methyl group of 2,6-dicyanotoluene **71** with an ethenyl group with a leaving group attached (**79**). One of the cyano groups is hydrolysed to an amide and the product **80** is cyclised under acidic conditions to give **59**.



Scheme 51

The dimethylamino group ($X = \text{NMe}_2$) was one of the leaving groups employed. Treatment of substituted toluenes, such as **71**, with dimethylformamide dimethyl acetal (DMFDMA) gives the corresponding enamine.²²⁸ As in 2,6-dicyanotoluene **71**, the other substituents on the ring should be electron-withdrawing so as to encourage the loss of a proton from the methyl group to form the CH_2^- anion. This method was used to prepare the enamine **81** in good yield (Scheme 49). Attempts to convert one of the cyano groups to give the corresponding amide **82** were not successful. Therefore, selective hydrolysis of the cyano group was carried out on the toluene derivative **71**. This step was successful; the only product isolated was that in which only one of the cyano groups had been converted (**83**). This can be seen clearly in the infra-red spectrum, a band at $\nu_{\text{max}} 2218 \text{ cm}^{-1}$, corresponding to the cyano group and the characteristic amide bands at $\nu_{\text{max}} 1625$ and 1680 cm^{-1} are present.

Treatment of **83** with DMFDMA did not result in enamine formation at the methyl group. In this case the amide nitrogen, rather than the methyl carbanion attacked the acetal and the formamidine **84** was formed. Attempts to cyclise the

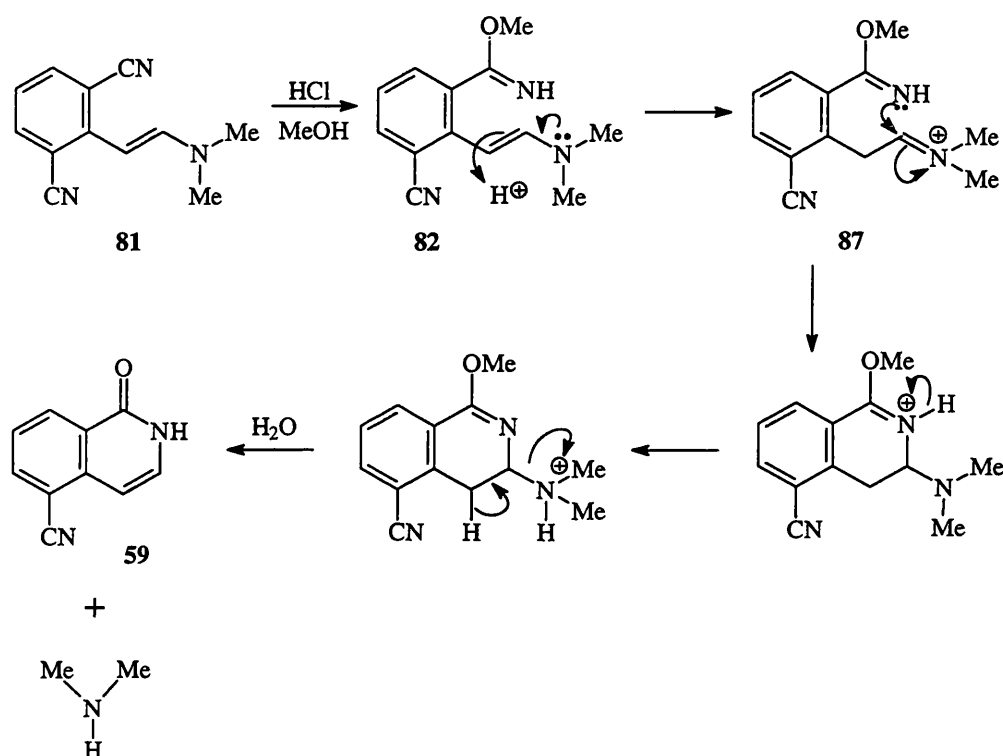
product **84** by heating in acidic conditions resulted in the formation of the "dimer" diacyl formamidine **85** rather than the required isoquinolinone **59**.

A slightly different approach was then studied. The amide **83** was heated with triethyl orthoformate in an attempt to form **86**, where an ethoxymethylene group is condensed onto the amide group. The ethoxy group acts as a leaving group in this case. This product did not form and, when DMF was added as a co-solvent, only the dimethylformamidine derivative **84** was obtained.

The next approach was to take the enamine **81** and convert one or both of the cyano groups to methyl esters using the Pinner reaction.²²⁹ Cyclisation of this product would give the isocoumarin, which could then be converted to the corresponding isoquinolinone by treatment with ammonia at reduced pressure.²²⁵ Theoretically, two products are possible from the two-step process; 5-cyanoisoquinolinone **59** formed if only one of the cyano groups is converted to the methyl ester; and **60**, if the diester is formed. However, when the enamine **81** was treated with dry HCl and methanol, the product isolated was found to be 5-cyanoisoquinolinone, **59**. A possible mechanism for the formation of **59** is shown in Scheme 52. In the first step one of the cyano groups of the enamine **81** is converted to the corresponding imino ester (**82**). Protonation occurs followed by rearrangement to form the dimethyliminium ion **87**. Cyclisation followed by hydrolysis gives **59**. Evidence that the methyl ester did not form as was intended, was seen when the Pinner synthesis of ester **88**, from 2,6-dicyanotoluene **71**, was unsuccessfully attempted.

This method of cyclisation of the enamine **81** produced a 55% yield of isoquinolinone **59**, with an overall yield of 39% for the two steps from 2,6-dicyanotoluene. This procedure is more than adequate for the preparation of large quantities of 5-cyanoisoquinolinone **59**. However this compound proved to be insoluble in most solvents and very difficult to handle. Attempts to make the

methyl ester by treatment with HCl and methanol were unsuccessful. The compound could not be assessed as a PARP inhibitor due to lack of solubility in the aqueous buffer used. It was possible to hydrolyse the cyano group to give the corresponding carboxylic acid **89**. This compound was assessed for PARP inhibition.



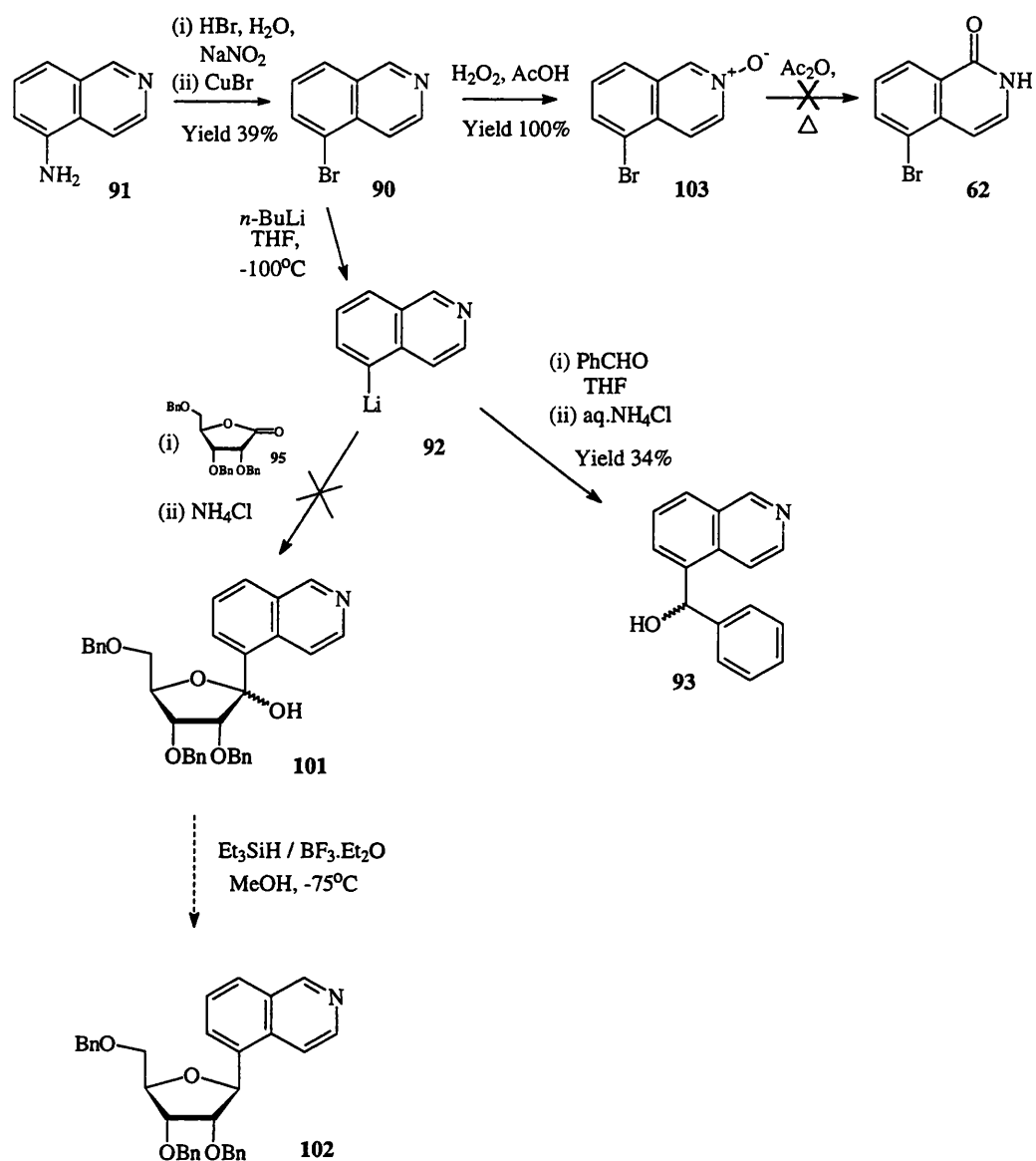
Scheme 52

Following the difficulties with **59**, a new strategy was required. It was proposed that, rather than introduce the benzylic carbon using the cyano group, the carbon-carbon bond could be introduced through the formation of a C-metallated isoquinolinone. The reaction of C-metallated isoquinolinones with electrophiles should afford C-substituted products. Organolithium compounds can be prepared from the corresponding halide using butyllithium. In the isoquinoline series, various haloisoquinolines have also been coupled to form C-substituted products

using palladium^{230,231} and nickel^{232,233} reagents. Two of these three examples of C-metallation were investigated.

There are a few reports of the preparation of 1- and 4-lithioisoquinolines by halogen-lithium exchange from 1-bromo²³⁴ and 4-bromoisquinolines.²³⁴⁻²³⁶ These lithioisoquinolinones undergo subsequent reactions with electrophiles to generate C-substituted products. The lithiation of 5-bromoisquinoline **90** was therefore investigated, with a view to converting the derivatised isoquinoline product to the required isoquinolinone *via* the rearrangement of the *N*-oxide as was carried out in the synthesis of the nitro derivative **68**.

5-Bromoisquinoline **90** was prepared from 5-aminoisoquinoline **91** by forming the diazonium salt and treating it with cuprous bromide. This is the Sandmeyer reaction; a variation of this reaction was also used in the preparation of 3-acetylbenzonitrile **9**, in the benzamide series. The lithiation of **90** was carried out at -100°C using 1.1 equivalents of butyllithium. These conditions are analogous to those used in the lithiation of 3-bromopyridine.²³⁷ In this initial experiment, the lithioisoquinoline **92** was treated with benzaldehyde as the electrophile. The desired product **93** was formed in modest yield (Scheme 53). The other products isolated from the reaction were the starting material **90** (13%) and isoquinoline **94** which is formed when the lithioisoquinoline **92** is quenched with water before reacting with the benzaldehyde. It was confirmed, using NMR techniques, that the 1-phenyl-1-hydroxymethyl group was attached to the ring at position 5. A NOESY spectrum (NOE correlation spectroscopy) of **93** was obtained and the cross peaks for the benzylic proton were studied. The benzylic proton showed cross peaks with the protons at positions 4 and 6 of the isoquinolinone ring; a cross peak indicates that the two protons are close in space. This model experiment demonstrates, for the first time, successful lithiation of isoquinoline at the 5'-position and reaction with a carbonyl electrophile.



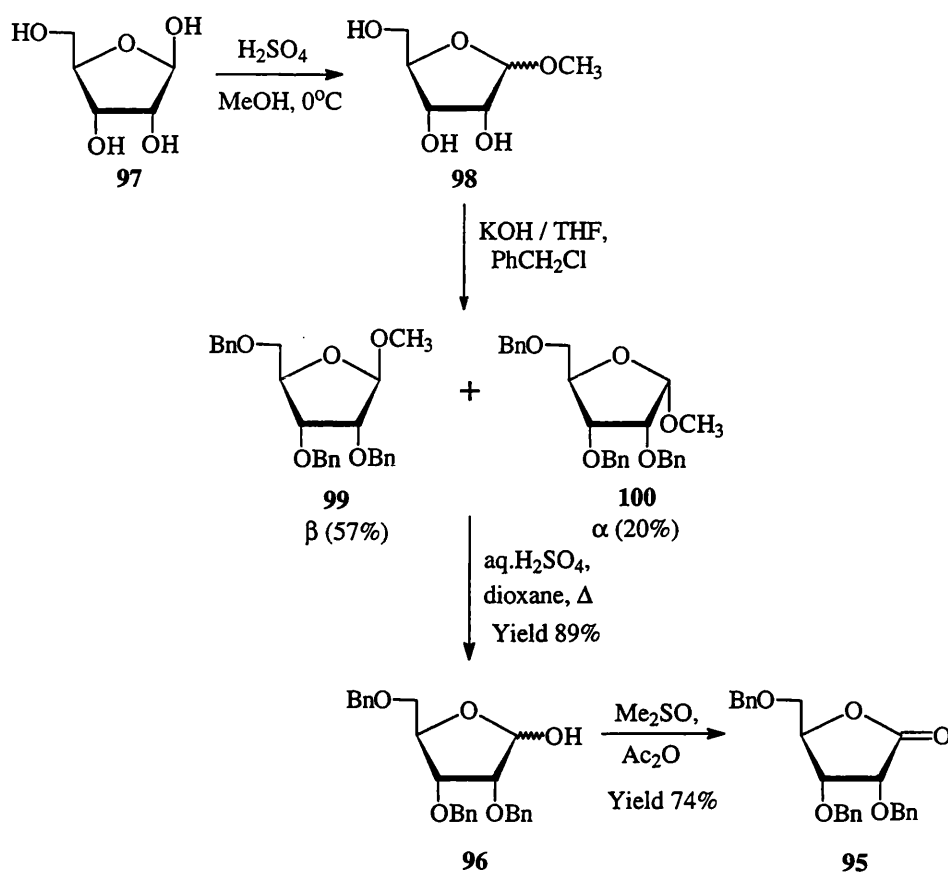
Scheme 53

The successful lithiation of **90** would allow the synthesis of several isoquinolinone derivatives, including the isoquinolinone riboside **64**. The riboside **64** would be an interesting compound to test for activity as a PARP inhibitor. An analogue of this compound **64**, benzamide- β -D-ribose was found to be very toxic to cells¹⁶² (see Chapter Three). This toxicity prevented evaluation of PARP inhibition and is probably due to interference with NAD⁺-dependent cellular processes. The majority of compounds tested for PARP

activity have mimicked the nicotinamide moiety of NAD⁺. More information about the binding interactions in the ribose region of the NAD⁺ site might be gained from compounds with a ribose-like group in the equivalent position.

The reported synthesis of benzamide- β -*D*-riboside involved lithiation of carboxamide-protected bromobenzamide and treatment of the lithiobenzamide with the ribonolactone **95** to form the *C*-riboside.¹⁶² A similar strategy was used here in the attempted preparation of the isoquinoline riboside **64** (Scheme 53).

The ribonolactone **95** was prepared as shown in Scheme 54. The synthesis of the 2,3,5-benzylated ribose **96** was reported in the literature by Barker and Fletcher.²³⁸ Treatment of β -*D*-ribose **97** with methanolic sulphuric acid gave a mixture of α and β methyl-*D*-ribofuranosides **98**. The free OH groups were then protected in one step, using benzyl chloride and powdered potassium hydroxide in tetrahydrofuran. At this stage the α and β anomers, **99** and **100**, were separated by chromatography. The signal corresponding to the anomeric proton in the ¹H NMR spectrum is a doublet, due to coupling with the proton at C-2. The coupling constant for this doublet is different in **99** and **100**, due to the different angles between the anomeric protons and the adjacent proton as explained by the Karplus equation. The coupling constant for the α anomer **99** is very small (<1 Hz) and the signal appears as a broad singlet, whereas the β anomer **100** gives a doublet with coupling constant of *ca* 4 Hz.²³⁹ Although these diastereomers were separated in the course of the synthesis, this was not necessary to the overall preparation since the key intermediate **95** is trigonal at C-1. The next step involved the hydrolysis of the acetal group by boiling with dilute acid, which resulted in a mixture of both α and β 2,3,5-tri-*O*-benzyl-*D*-ribose **96**. The protected ribose **96** was oxidised using acetic anhydride in dry methyl sulphoxide under Moffatt-like conditions.²⁴⁰



Scheme 54

All attempts to couple the ribonolactone **95** to the lithioisoquinoline **92** were unsuccessful. A complex mixture was obtained in each case. Extensive chromatography failed to furnish the desired product **101** (Scheme 53). 5-Bromoisoquinoline **90** was isolated, as was 5-H isoquinoline. The ribonolactone **95** was not recovered indicating that maybe this reagent was degraded before electrophilic reaction with the lithiated isoquinoline could occur. It might be that the anion is too basic and facilitated the removal of the lactone 2'-H (there is no equivalent α -proton in benzaldehyde). In one case, no attempt was made to isolate the alcohol **101** and the crude product was treated with boron trifluoride etherate and triethylsilane which would reduce the alcohol to give **102**. No such product was isolated. This method was not suitable for the preparation of the isoquinolinone riboside **64**.

The preparation of 5-substituted isoquinolinones *via* the lithioisoquinoline **92** requires the conversion of the derivatised isoquinoline to the corresponding isoquinolinone. The intention was that this conversion would be carried out, as in the synthesis of 5-nitroisoquinolinone **68** (Scheme 46); *via* the *N*-oxide **67**. The preparation of 5-bromoisquinolinone **62** was attempted using this method. The *N*-oxide **103** was formed in quantitative yield, although the reaction was slow. The rearrangement to form **62** was not successful, however, with a complex mixture of products being produced. It was decided that this route would not be convenient for the production of 5-substituted isoquinolinones. The last steps to convert the isoquinoline into the isoquinolinone are likely to be low yielding and involve harsh conditions which might interfere with the substituent which has been introduced.

An alternative pathway was considered in which a protected form of the isoquinolinone is lithiated. It is not possible to lithiate the unprotected isoquinolinone at carbon. The acidic NH proton and electrophilic carbonyl group present lead to the butyllithium reacting at these positions in the molecule rather than carrying out the halogen-lithium exchange. A possible pathway to substituted isoquinolinones *via* halogen-lithium exchange might be to prepare the halo-isoquinolinone protected at preferably the 1-, or alternatively, the 2-position.

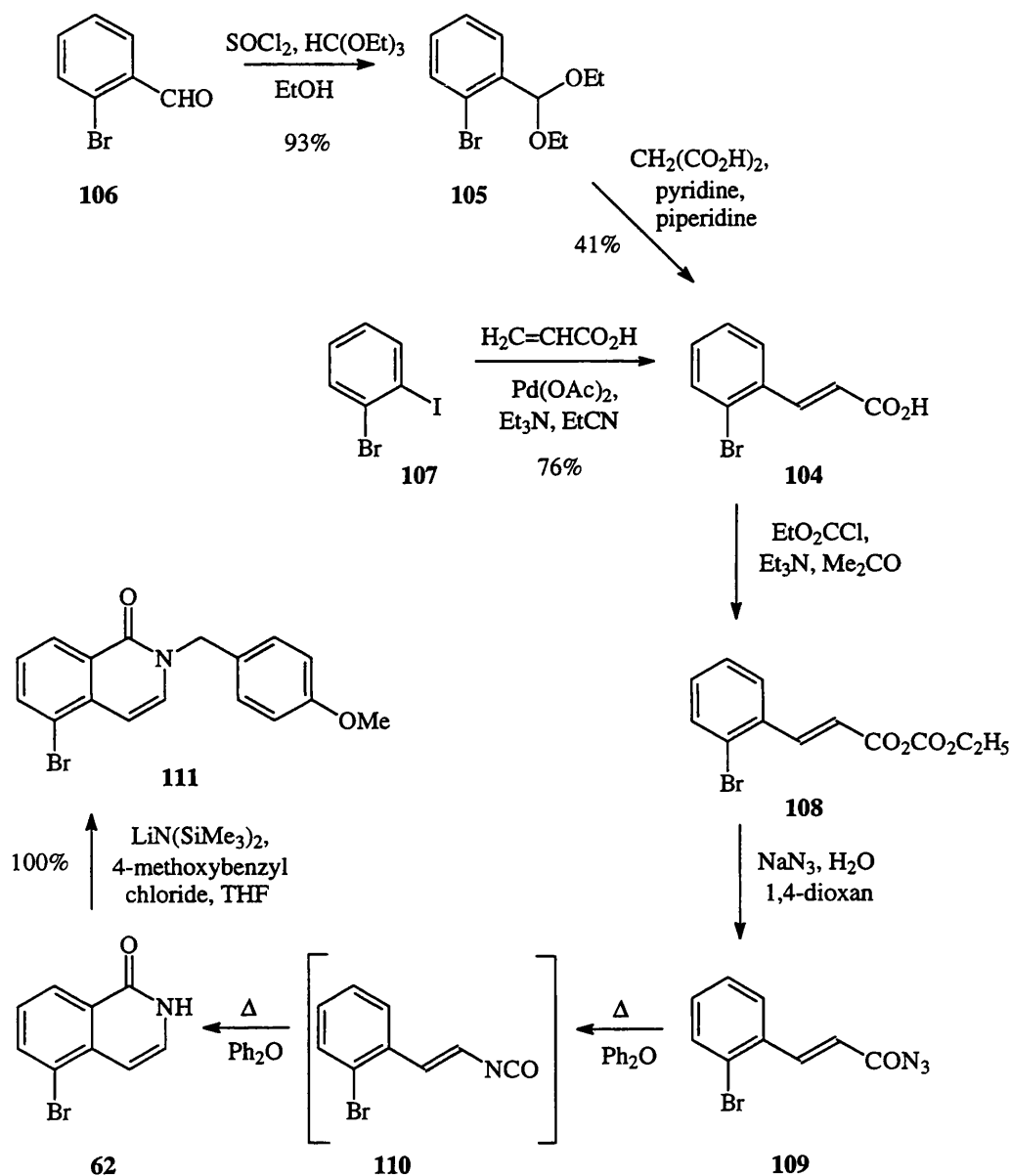
Only a few simple examples of 1-alkoxyisoquinolines have been reported. The method used to prepare these compounds, which include 1-methoxy and 1-ethoxy isoquinolinones, is treatment of the corresponding 1-chloroisoquinoline with sodium alkoxides under vigorous conditions.²⁴¹⁻²⁴⁴ For our purposes, protection of the isoquinolinone with a benzyl group was desirable. Such a protecting group is removed using hydrogenolysis or with hydrogen bromide. Given the vigorous conditions required for the substitution of 1-

chloroisoquinolinones and the lack of examples using larger alkoxy groups, the direct alkylation of 5-bromoisoquinolinone **62** was carried out.

The synthesis of 5-bromoisoquinoline **62** has not been reported in the literature. A preparation of the 5-chloro derivative is, however, described by Eloy and Deryckere.²⁴⁵ This group synthesised several substituted isoquinolin-1-ones using a "one-pot" process which involves Curtius rearrangement of cinnamyl azides and subsequent thermal cyclisation. The method is only suitable for the preparation of isoquinolinones which do not have electron-withdrawing substituents. The 5-bromo derivative **62** was prepared using this general method (Scheme 55). The bromocinnamic acid **104** was prepared by two methods. The first required the formation of the diethyl acetal **105** from the corresponding aldehyde **106**. The acetal **105** was then condensed with malonic acid under Knoevenagel-Doebner conditions.²⁴⁶ A more convenient method is described by Plevyak *et al.*²⁴⁷ 2-Bromoiodobenzene **107** is converted, in one step to the desired cinnamic acid **104** using an iodine-selective Heck reaction. The Heck reaction involves the palladium-catalysed vinylation of organic halides.^{248,249} The catalyst required depends upon the halide present; aryl iodides require only palladium acetate, whereas aryl bromides also require triphenylphosphine to be present as a ligand for palladium. Therefore, only the iodo group in **107** reacts with the acrylic acid to form **104**. The method of Plevyak *et al.*²⁴⁷ was adapted in that a different solvent was used. It was found that the use of boiling propionitrile was a good alternative to acetonitrile in conducting the reaction at 100°C; the latter necessitated heating the reaction mixture in a sealed tube. This method was successfully used in the preparation of large quantities of **104** (Scheme 55).

The cinnamic acid **104** was firstly converted to the mixed anhydride **108** by treatment with ethyl chloroformate. Subsequent addition of sodium azide furnished the acyl azide **109**. This was confirmed by analysing a small sample using infra-red spectroscopy. A characteristic azide band, a strong band at ν_{\max}

2150 cm^{-1} , was detected. The acid azide was cyclised by addition to boiling diphenyl ether. There is initially thermal rearrangement of the azide **109** to the isocyanate **110**, believed to occur at around 60-80°C.²⁴⁵ This is followed by cyclisation at approximately 240°C²⁴⁵ (Scheme 55)



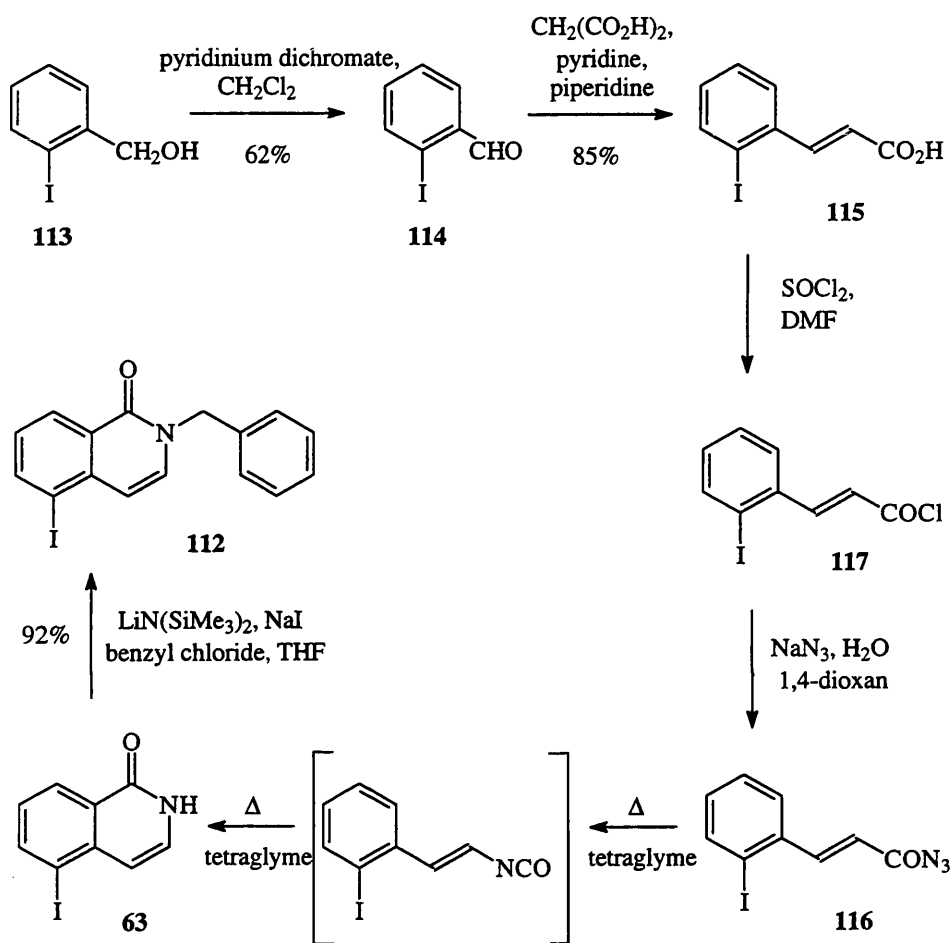
Scheme 55

The yield of **62** was moderate; several compounds were present in the crude product and recovery of the desired isoquinolinone **62** was difficult. However, following several stages of chromatography and recrystallisation, pure **62** was obtained and a sample was evaluated for PARP inhibition.

Alkylation of 5-bromoisoquinolin-1-one **62** was carried out by deprotonation with the non-nucleophilic base lithium bis(trimethylsilyl)amide followed by 4-methoxybenzyl chloride. The alkylation was found to occur exclusively at the nitrogen, rather than the oxygen, to give **111** in excellent yield. Assignment of the structure of **111** as being the *N*-(arylmethyl)isoquinolin-1-one rather than the 1-(arylmethoxy)isoquinoline was carried out by analogy with the protected iodoisoquinolinone **112** (Scheme 56), which is described below. Examination of the literature for reports of alkylation of other isoquinolinones revealed that, in the relatively few examples described, alkylation occurs predominately at nitrogen of the conjugate anion, under various conditions using simple haloalkanes.²⁵⁰⁻²⁵² Although protection at the 1-position would have been preferable, the *N*-alkylated isoquinolinone **111** should undergo lithium-halogen exchange by butyllithium.

5-Iodoisoquinolinone **64** was prepared in a similar way to the bromo derivative **62**, but was obtained in much better yields. It was consequently a more convenient aryl halide for metal-halogen exchange. As shown in Scheme 56, 2-iodobenzyl alcohol **113** was oxidised to the corresponding aldehyde **114** with pyridinium dichromate^{253,254} and a direct Doebner-Knoevenagel condensation with malonic acid afforded the cinnamic acid **115**. In this case, the corresponding acyl azide **116** was prepared by the treatment of the acid chloride **117**, rather than the mixed anhydride, with sodium azide. A further modification of the process was to use boiling tetraglyme as the solvent for the Curtius rearrangement and cyclisation of **116** to give **63**. This allowed the isolation of the isoquinolinone product **63** by precipitation with water. In general, recovery of the

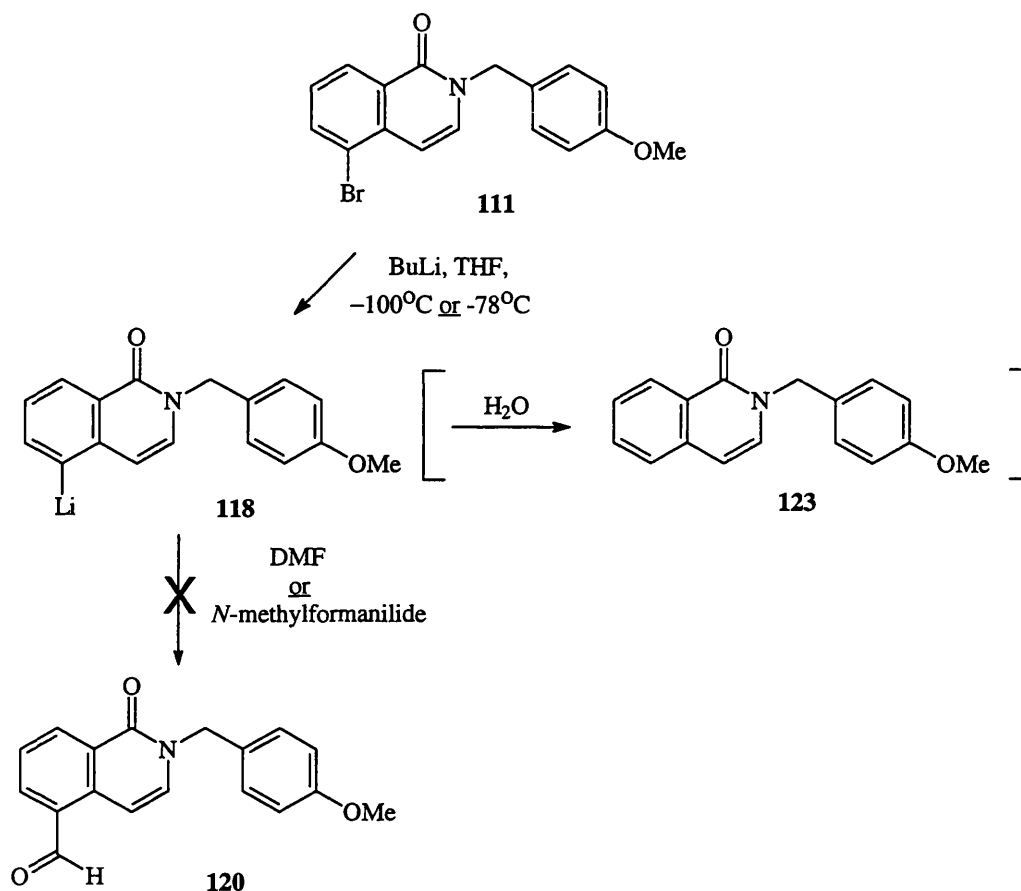
isoquinolinones prepared was poor. This is largely due to very poor solubility in the non-polar organic solvents which are used in normal phase chromatography. Using tetraglyme as opposed to diphenyl ether apparently increased the yield of **63**; yields ranged from 28 to 42% when tetraglyme was used, compared to 11 to 14% when diphenyl ether was used.



Scheme 56

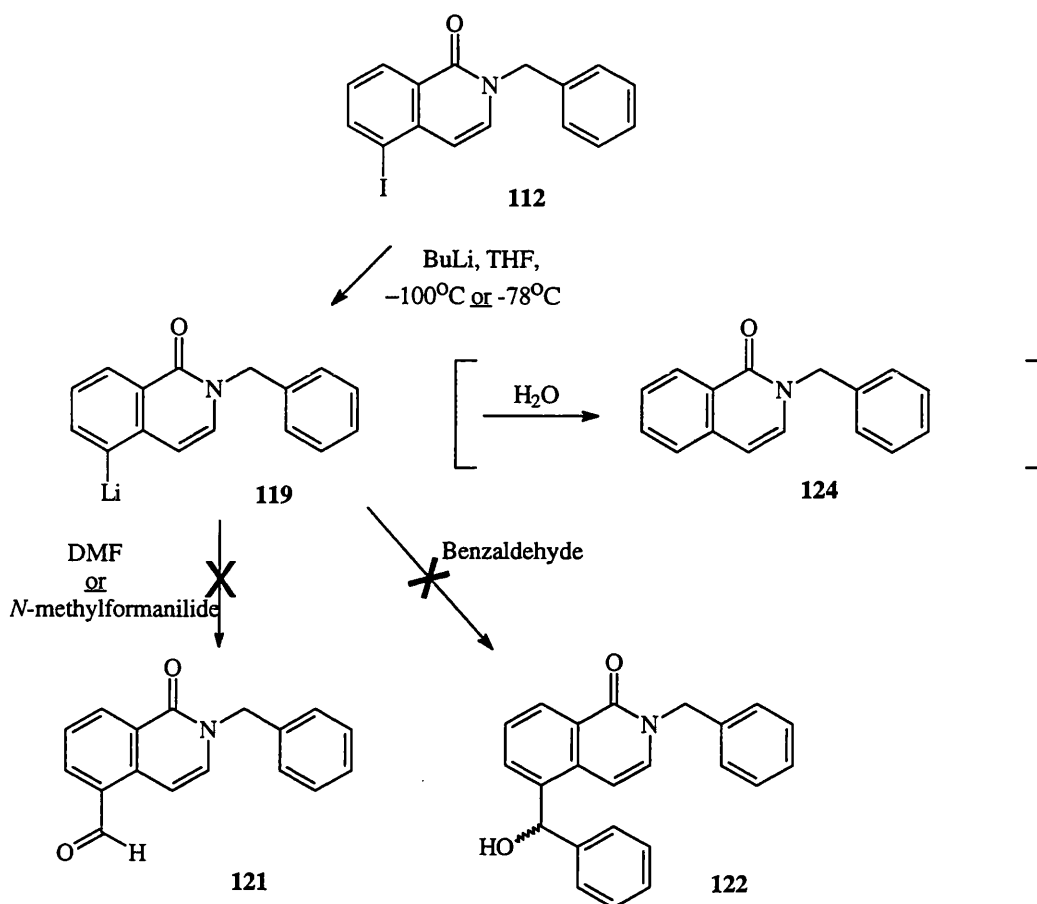
The anion of 5-iodoisoquinolinone **63** was formed and benzylated in high yield, using lithium bis(trimethylsilyl)amide followed by benzyl chloride, to give **112**. Assignment of the structure of **112** as being the N-(arylmethyl)isoquinolinone rather than the 1-(arylmethoxy)isoquinoline was made by both ^{13}C NMR and IR. The benzyl CH_2 carbon resonates at δ 51.9 ppm. Using published tables to

calculate predicted shifts for this carbon when the 1-position of the isoquinolinone is alkylated (giving PhCH₂O), the predicted shift is δ 69 ppm, compared to δ 48 ppm when the 2-position is alkylated (giving PhCH₂N). This confirms structure **112**. This was further substantiated by the IR spectrum which contains a band at ν 1650 cm⁻¹, confirming the presence of a carbonyl group.



Scheme 57

Both protected isoquinolinones **111** and **112** were treated with butyl lithium, to form lithio derivatives **118** and **119**, followed by one of three simple electrophiles, as shown in Schemes 57 and 58.

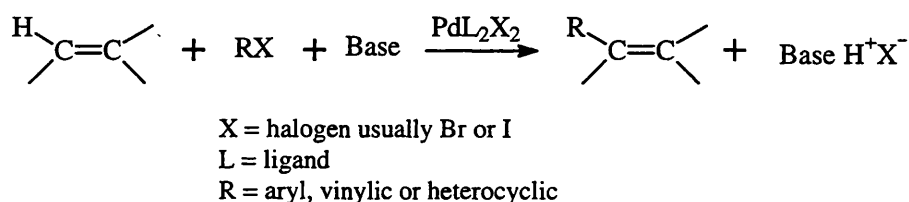


Scheme 58

DMF was chosen as an electrophilic formylating agent in these preliminary experiments as it has been used to prepare the corresponding aldehydes of various lithioisoquinolines.^{235,236} Preparation of the aldehydes **120** and **121** would allow further extension of the side-chain and development of additional isoquinolinone derivatives. *N*-Methylformanilide was used as an alternative to DMF. This reagent has a chromophore and it was hoped that this would allow improved monitoring of the reaction by TLC. Benzaldehyde was also used as a model in these investigations. This electrophile was successfully coupled to 5-lithioisoquinoline **92** to give **93**, as described earlier. The 1-methoxybenzyl derivative **122** was not formed. Several experiments with various reaction conditions were carried out; temperatures of -100°C and -78°C were investigated. The outcome was similar in all cases (a typical example is given in

the experimental section). In addition to unreacted starting material, the main products of these reactions were the protected isoquinolinones **123** and **124**, recovered in *ca.* 20% yields. These results indicate that a proportion of the aryl halide was lithiated but then reacted with water rather than the intended electrophile. In all cases none of the expected derivatives were isolated.

The second method of coupling haloisoquinolinones investigated was using a palladium reagent as the catalyst. This type of reaction was first described, and has been extensively investigated, by Heck and his colleagues.^{248,249} As described previously in the preparation of 2-bromocinnamic acid **104**, the Heck reaction involves the palladium-catalysed vinylation of organic halides. It is a convenient method of forming carbon-carbon bonds at unsubstituted vinylic positions, the general reaction is shown in Scheme 59.



Scheme 59

A limited number of examples of reactions of this type have been reported for the isoquinolines. 4-Bromoisoquinoline,^{230,231} 3-bromoisoquinoline²³¹ 1-chloroisoquinoline²³¹ and 1-iodoisoquinoline²³¹ have been used as substrates for this method. However, no isoquinolinones have been prepared. In this case, the C-metallation should not be affected by the isoquinolinone amide group. Therefore, the unprotected haloisoquinolinone should undergo halogen-vinylic substitution.

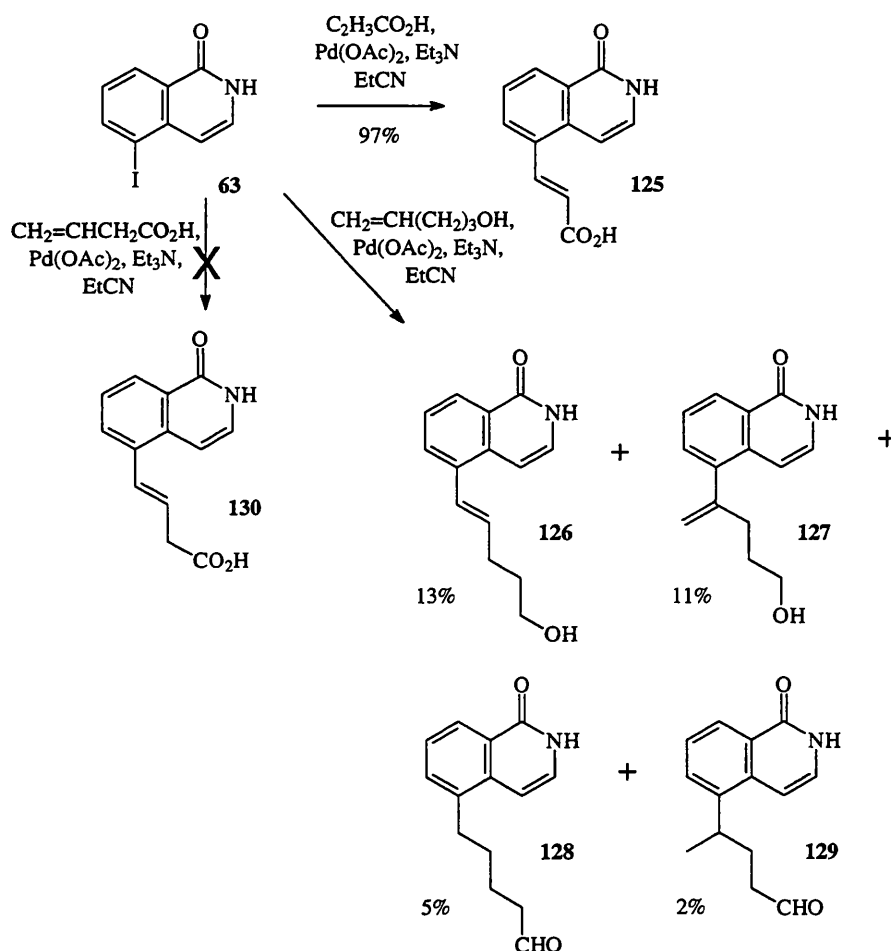
These reactions, as shown in Scheme 60 and 62 were carried out using 5-iodoisoquinolinone **63**. Heck reactions using aryl iodides are more

straightforward in that triphenylphosphine is not required as a ligand, unlike when aryl bromides are used.

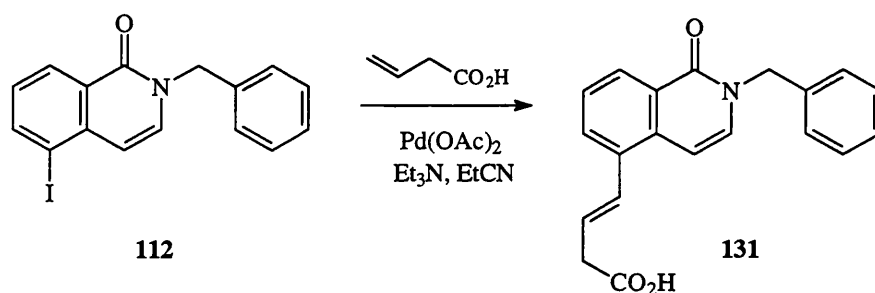
In the first example of Heck coupling carried out, acrylic acid was coupled to the aryl iodide **63**, in the preparation of the α,β -unsaturated carboxylic acid **125** (Scheme 60), in almost quantitative yield. This target compound is a Michael acceptor and will undergo nucleophilic attack at the benzylic position. It is therefore a potential irreversible inhibitor of PARP. This compound was evaluated for PARP inhibition but was found to be less active than the other isoquinolinones that have been tested, with activity corresponding more with the benzamides. This may be due to the electron-withdrawing properties of the side chain, which, it has been noted (see Chapter 3), can result in a diminution in activity.

The successful coupling of acrylic acid to the isoquinolinone **63** led to other larger alkenes being investigated, also shown in Scheme 60. 4-Pentenol gave a mixture of four main products; two alcohols **126** and **127**, and two aldehydes **128** and **129**. Complete separation was not possible, the two alcohols **126**, **127** had identical R_f values in all of the mobile phases examined, as did the aldehydes **128**, **129**. The two isomeric alcohols are produced because there are two possible directions for the addition of the organopalladium intermediate to the unsymmetrically substituted double bond. This is, in most cases, largely sterically controlled. The presence of an electron-withdrawing group at one of the carbons of the double bond also directs addition to the other carbon. When allylic alcohols are used as the olefinic moiety in Heck reactions, carbonyl compounds are usually obtained as significant or exclusive products.^{255,256} This is due to the migration of the double bond along the carbon chain until captured by the alcohol to give a carbonyl product. In this example the yield of the two aldehydes **128**, **129** is fairly small.

4-Butenoic acid was also investigated as a substrate. This example was less successful as none of the desired product **130** or any related product could be isolated. The crude product was insoluble in all suitable organic solvents. This problem led to investigation of the replacement of **63** with its benzyl-protected analogue **112** in the reaction, as shown in Scheme 61. The increased solubility of the reagent and products allowed a much greater recovery of products from the reaction mixture. However, a mixture of isomers was produced and complete isolation of the major product was not possible even following several stages of chromatography. From ^1H NMR analysis, the main constituent appeared to be **131**, however further NMR experiments on a pure sample would be necessary to confirm this.

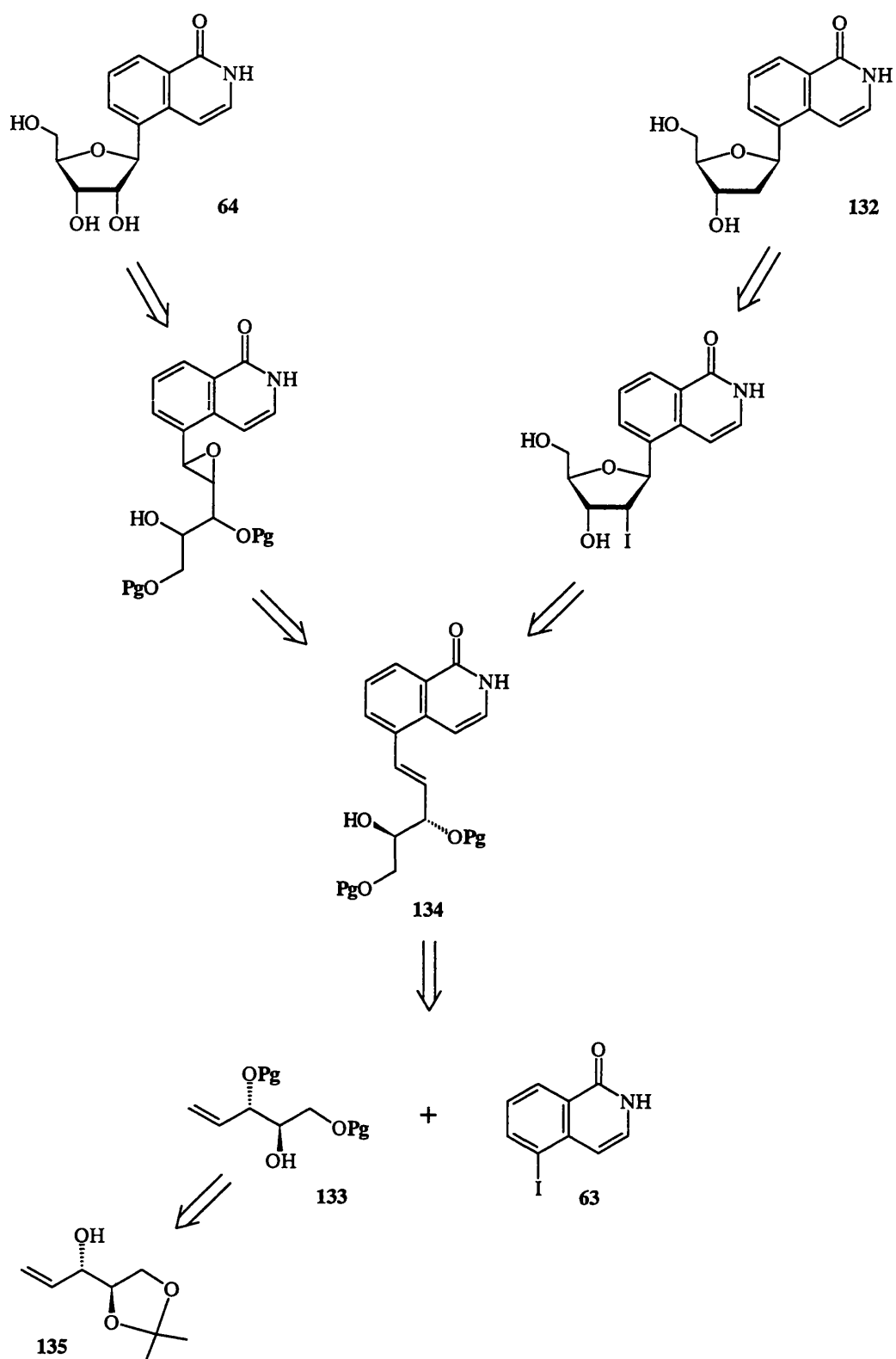


Scheme 60



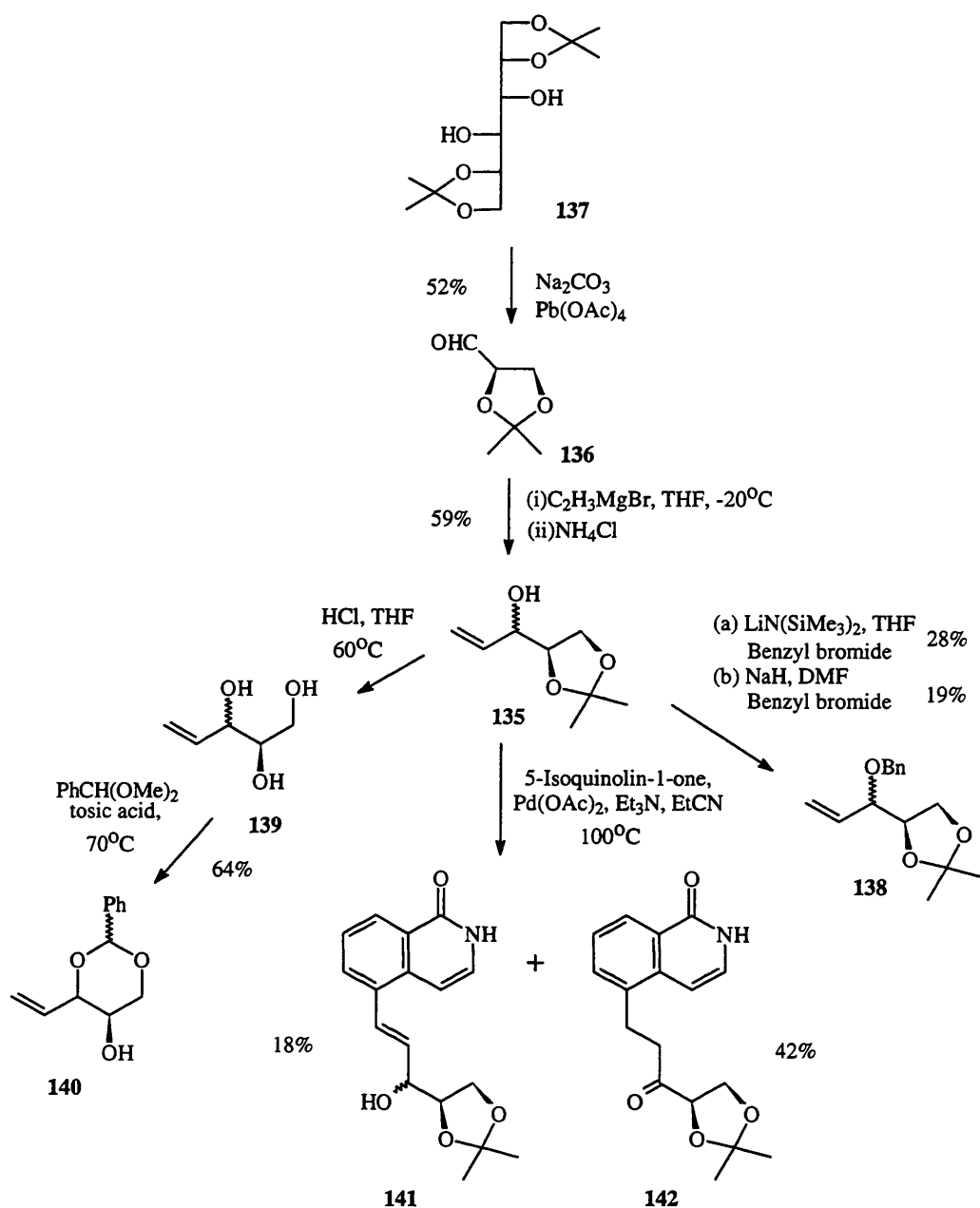
Scheme 61

Further investigations towards the synthesis of the riboside **64** were carried out using the Heck reaction to form the required C-glycosidic bond. Scheme 62 shows a suggested retrosynthetic pathway that was considered for the synthesis of **64** and also for its deoxyribose analogue **132**. This involves the synthesis of the pentene derivative **133** with the appropriate stereochemistry at each of the chiral centres and the hydroxyl groups at positions 3 and 5 protected. This fragment is then coupled to the isoquinolinone **63** to give **134** and cyclised to give either **62** or **132** as shown in Scheme 62. A pentenetriol derivative of the form of **133** could be prepared from the acetonide protected precursor **135**. Protection, for example benzylation, of **135** allows selective protection of the hydroxyl group at the 3 position. The removal of the acetonide protecting group by mild acid treatment followed by selective protection of the primary alcohol, for example by benzylation, affords the 3,5-protected pententriol derivative **133**.²⁵⁷ Approaches towards these pathways were taken, as shown in Scheme 63.



Scheme 62

The aldehyde **136** was prepared by the cleavage of the acetonide-protected mannitol derivative **137** according to the method of Dumont and Pfander.²⁵⁸ Addition of vinylmagnesium bromide in a Grignard reaction afforded the protected pententriol **135**.²⁵⁹ This product **135** is a mixture of diastereomers as the centre at C-3 is racemic. This was confirmed by NMR spectroscopy. ¹H NMR correlation spectroscopy aided the assignment of most of the signals in the complicated ¹H NMR spectrum, the COSY spectrum for **135** is included in Appendix A. Some separation of the signals produced by the two diastereomers is seen: The protons at C-1 and C-3 resonate at δ 3.78 and 4.27 ppm, respectively, in the major isomer, but, in the minor isomer, these protons resonate at *ca.* δ 4.05 ppm - a region of overlapping multiplets. The molar ratio of the two isomers is approximately 10:7, although it not possible to assign relative stereochemistry from these spectra. The ¹³C NMR spectrum shows clear evidence of two isomers, with most signals present in duplicate. It was hoped that benzylation of the free hydroxyl group, to give **138**, would allow separation of the diastereomers by chromatographic methods. However this was not the case. The yield of the protected triol **138** was also fairly low, the method in which lithium bis(trimethyl)amide was used as the base was slightly better than when sodium hydride was used. NMR analysis of **138**, following chromatography, showed that two diastereomers were present. A second attempt to separate the diastereomers was to deprotect **135** to give **139** and then carry out a benzylidene protection to form the 1,3-dioxane derivative **140**. This diastereomeric mixture was successfully formed but it was not possible to separate the components of the mixture. Clearly, further work needs to be done to afford the pure diastereomers in order that, once coupled to the isoquinolinone ring, the correct sugar will be formed on cyclisation.



Scheme 63

The Heck coupling of the alkene fragment to the isoquinolinone ring was tested on the protected triol **135**. This reaction afforded a mixture of the desired allylic alcohol **141** in poor yield and a significantly greater amount of the ketone **142**. The assignment of the structure of the ketone **142** was made by ^1H NMR

analysis. The two aliphatic methylene groups resonate at δ 3.00 and 3.20 ppm and there are no signals in the alkenic region of the spectrum. The structure was also confirmed by a band at ν 1715 cm^{-1} in the infra-red spectrum corresponding to the ketone C=O vibration. The allylic alcohol **141** is a mixture of diastereomers. This is evident from the ^1H NMR spectrum. 2-Dimensional correlation NMR spectroscopy, which identifies signals directly coupled to each other, allowed assignment of the spectrum and confirmation of the structure. The COSY spectrum is given in Appendix A. The ketone **142** is formed by the migration of the double bond in the presence of palladium. When the double bond reaches the alcohol the enol that is formed tautomerises to give the ketone **142**.

The yield of the desired allylic alcohol in this case was quite low in comparison to the ketone. This indicates that this pathway will be fairly low yielding, however further work and development of this synthetic pathway might furnish the deoxyriboside **132** and possibly the riboside **65**. These two targets would be very interesting biological as well as synthetic targets for continued investigations.

Chapter Seven

7. Biological Results

7.1 Introduction

The inhibitory effects of several benzamides and isoquinolinones on PARP activity were examined using an assay system *in vitro*. The enzyme was extracted from nuclei isolated from L929 cells (mouse areolar and adipose tissue cells). PARP activity was estimated by the rate of incorporation of radioactivity from adenosine [³H]NAD into acid-insoluble material.

The effect on PARP activity was measured in the presence of the potential inhibitors at concentrations *ca.* 10 μ M over a time-course of 4 minutes. These initial assays were used to compare the test compounds in terms of their activity as PARP inhibitors at a particular concentration. The results were also used as a feedback into the design of new compounds. Some of the most active compounds of those assessed earlier in the project were tested at a range of concentrations. This allowed an approximate estimate to be made of the IC₅₀ values for these compounds. Finally, for three potentially irreversible inhibitors, the effect of pre-incubating the inhibitor with the enzyme for one of three time intervals before the addition of the radiolabelled NAD was measured.

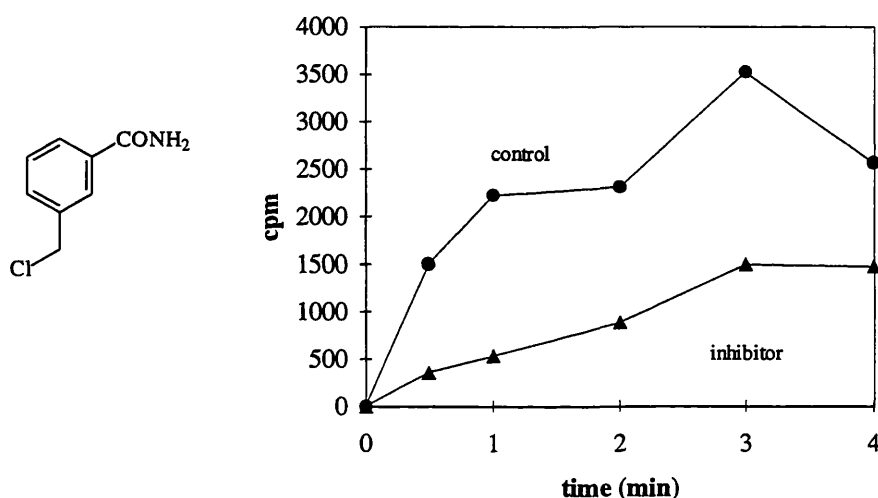
7.2 Initial PARP Activity Assays

PARP activity was measured over a 4 minute time-course in the presence of approximately 10 μ M test compound. A summary of the percentage inhibition values calculated from the results is given in Table 6, later in the chapter.

7.2.1 Benzamides

3-Chloromethylbenzamide **2** was one of the first compounds tested for its effect on PARP activity. This target compound was synthesised as a potentially irreversible inhibitor of PARP with an electrophilic group in the 3-position. Figure 33 shows a graph of PARP activity, estimated as the rate of incorporation of radioactivity from adenosine [^3H] NAD into acid-insoluble material, against time, for the 4 minute time-course. Data are plotted for the control system, with no inhibitor present, and for the system with the addition of 10.5 μM benzamide **2**.

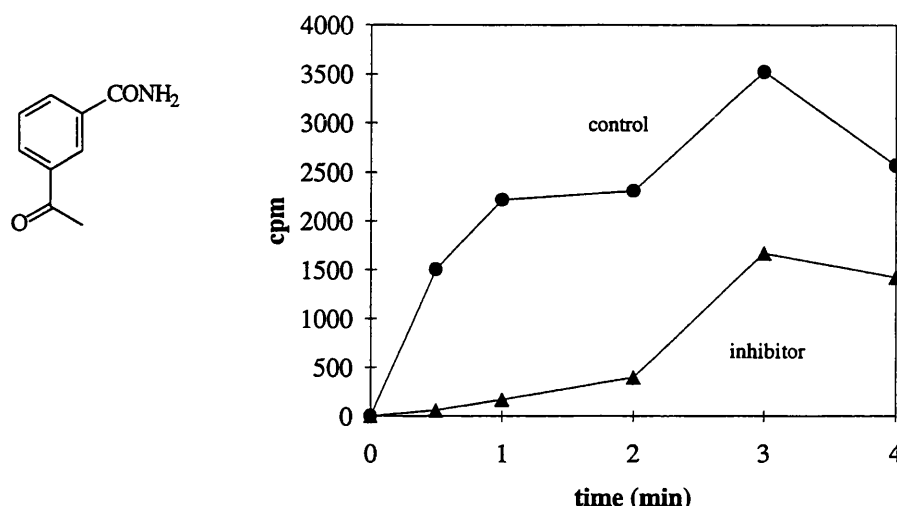
Figure 33: PARP activity in the presence of 3-chloromethylbenzamide **2** at 10.5 μM



The percentage inhibition is calculated by comparison of PARP activity with and without the inhibitor present. At the 2 minute time-point, the value calculated for this benzamide **2** is 62 %. This value is in the same order as other benzamides that have been assessed. An IC_{50} value of 9.0 μM for 3AB was reported by Suto *et al.*,¹⁵⁸ Pemberton *et al.*²⁶⁰ reported 36% and 37 % inhibition at 10 μM for 3AB and 3-hydroxybenzamide, respectively. This compound is therefore of potency similar to that of 3AB.

3-Acetylbenzamide **9** was not a specific target compound but was synthesised as an intermediate as part of the synthetic investigations into other inhibitors. However, this compound proved to be a good inhibitor as is shown in Figure 34.

Figure 34: *PARP activity in the presence of 3-acetylbenzamide **9** 11.0 μM*



The inhibition calculated for this compound **9** was 83% at 11.0 μM ; showing it to be a highly potent benzamide inhibitor. This result led to the investigation of the analogous bromomethylketone **44** (Figure 35). This compound is similar in that it has a carbonyl group adjacent to the benzene ring. This compound had very similar activity; 84% inhibition of PARP activity was achieved at 10.7 μM . These values are more in line with the inhibition seen for the isoquinolinones (see Table 6).

The epoxide **43** was designed as a potentially irreversible inhibitor of PARP. In the *S*-enantiomer, the location of the oxiranyl oxygen, relative to the aromatic ring, is approximately equivalent to that of the ribose oxygen in NAD⁺. As explained in Chapter 5, the epoxide **43** will undergo nucleophilic attack and may become covalently bound to the active site, thus irreversibly inhibiting the enzyme. Racemic compound **43** proved to be the most potent PARP inhibitor of the

benzamides tested, with an inhibition of 88% at 9.2 μM . The time course is shown in Figure 36.

Figure 35: *PARP activity in the presence of 3-(2-bromoacetyl)benzamide 44 at 10.7 μM .*

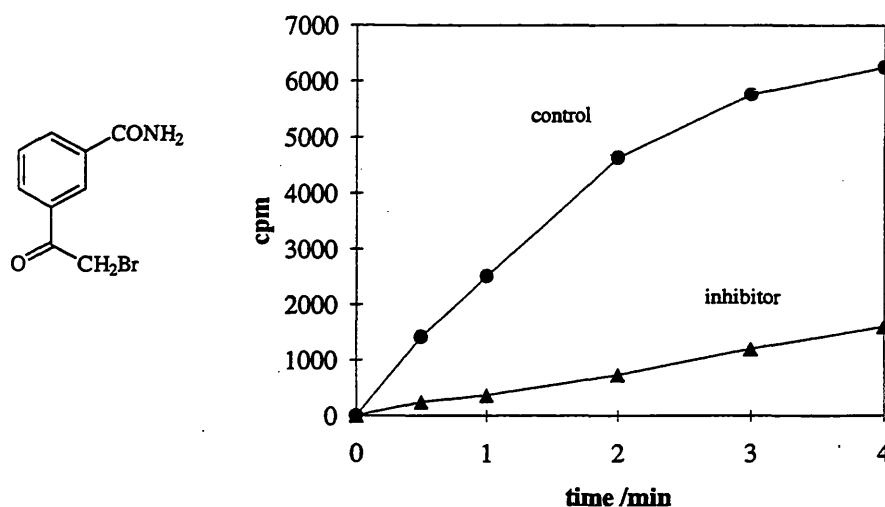
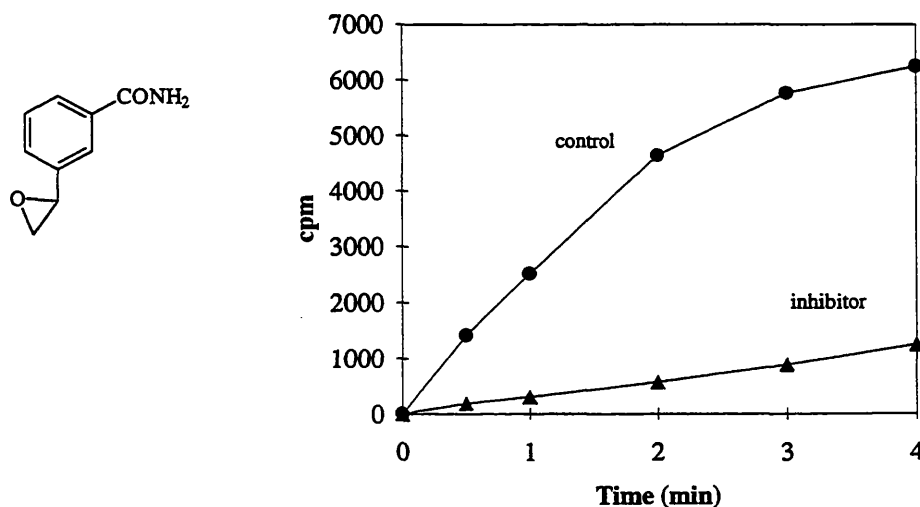


Figure 36: *PARP activity in the presence of (\pm)-3-(oxiran-2-yl)benzamide 43 at 9.2 μM .*



This is more potent than any of the benzamides reported in the literature. It is also freely soluble in the aqueous buffer in which the assay is carried out, at the concentrations required. This is a desirable property for a good inhibitor; poor

solubility is a problem with many of the isoquinolinones. The epoxide **43** tested is racemic, it would therefore be interesting to investigate the relative potencies of the two pure enantiomers. These results might give important information about the interactions that take place with the residues of the PARP active site in this region of the inhibitor molecule. It may be that the enantiomer with an equivalent spatial arrangement of groups around its chiral centre as in NAD^+ , is more active. Alternatively, the interaction of the epoxide group may be non-specific.

Two further compounds tested also have an oxygen atom bonded to the benzylic carbon. These are the (+) and (-) diols **6** and **36**. The PARP assay results for these compounds are shown in Figures 37 and 38. These compounds are intermediates in the synthesis of asymmetric benzamides. Both enantiomers were tested to investigate whether one enantiomer binds preferentially and so is a more potent PARP inhibitor. The (+)-(S)-isomer **6** represents the same arrangement of groups at the chiral centre as in the equivalent position in NAD^+ . Neither of these benzamides **6** and **36** were very potent inhibitors, with inhibitions of 44% and 32% at 9.4 μM and 9.3 μM , respectively. These are less potent PARP inhibitors than 3AB. The (+)-diol **6** is slightly more potent than the opposite enantiomer **36**, although this difference may not be significant. These compounds might have been expected to have been better inhibitors than was apparent from these experiments. One problem with these compounds is that they are hygroscopic gums and, consequently, accurate measurement of dry mass is very difficult. The samples used in the PARP assays were prepared by freeze-drying. The actual concentration of test compound in the assay mixture may have been less than calculated due to the presence of residual water.

Figure 37: PARP activity in the presence of (+)-S-3-(1,2-dihydroxyethyl)-benzamide **6** at 9.4 μM .

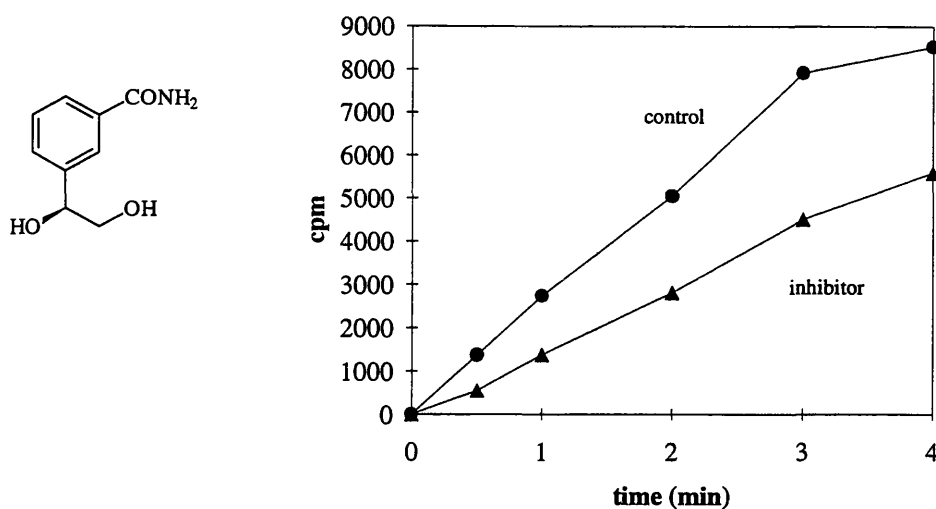
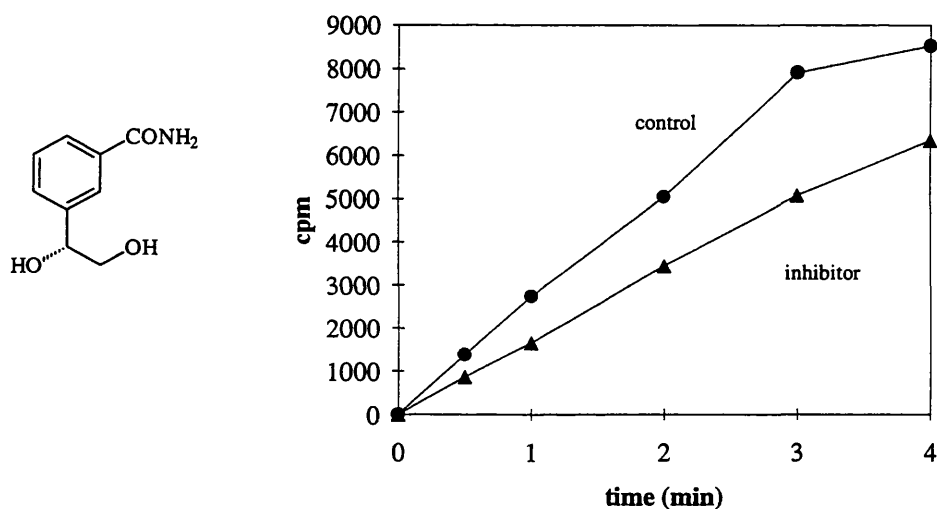


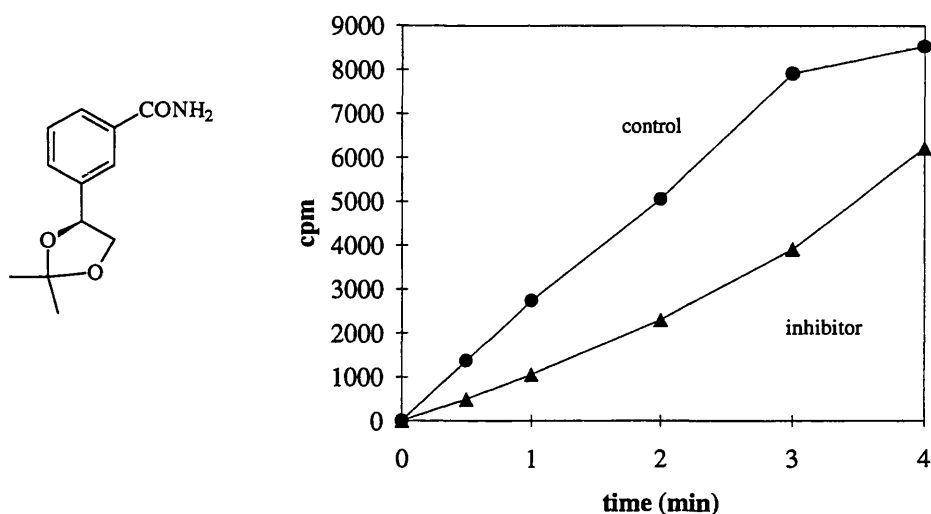
Figure 38: PARP activity in the presence of (-)-R-3-(1,2-dihydroxyethyl)-benzamide **36** at 9.3 μM .



The final benzamide tested was the dioxolane derivative **4**. This has an oxygen containing cyclic group, in common with the epoxide **43**, but does not undergo nucleophilic attack in the same way and was not, therefore, designed as a potentially irreversible inhibitor. This compound was asymmetrically prepared and this enantiomeric form resembles the arrangement of groups at the anomeric carbon in NAD^+ . This compound was found to be a moderate PARP inhibitor,

slightly less potent than 3AB. A 54% inhibition of PARP activity was achieved at a concentration of 10.0 μM (Figure 39).

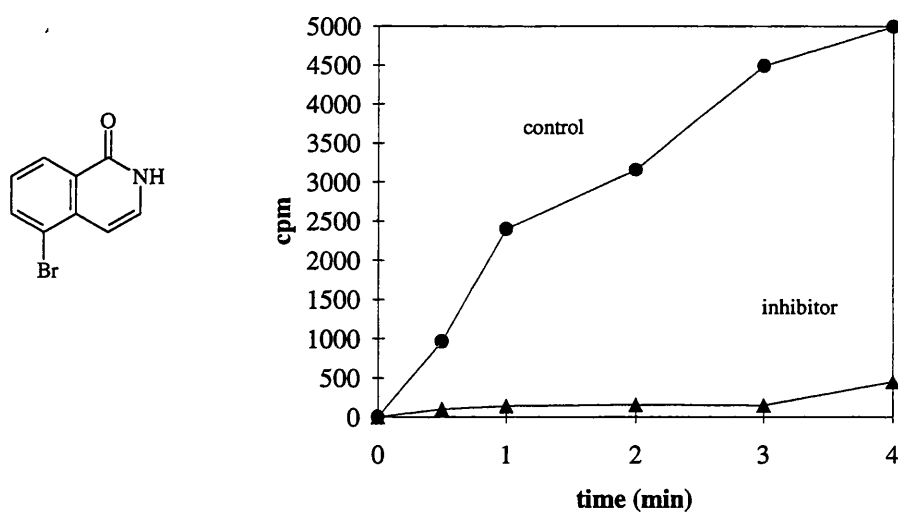
Figure 39: PARP activity in the presence of (+)-S-3-(2,2-dimethyl-1,3-dioxolan-4-yl)benzamide **4** at 10.0 μM .



7.2.2 Isoquinolinones

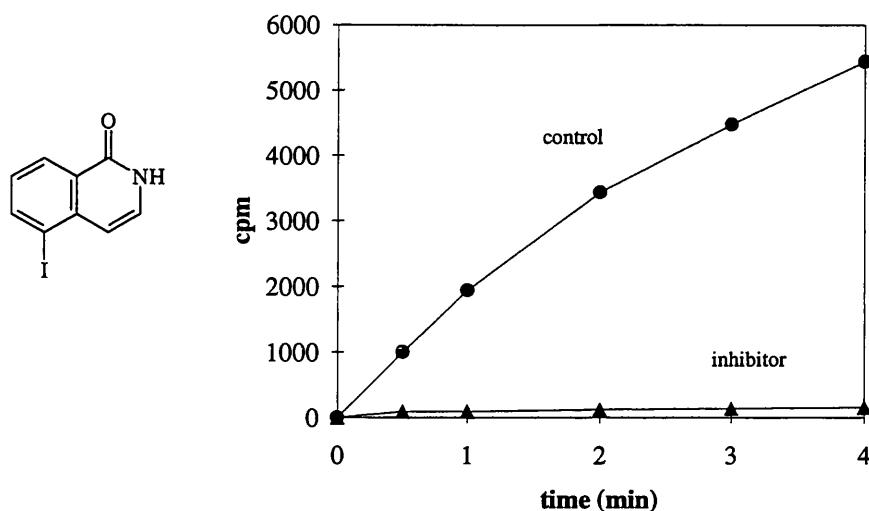
5-Bromoisoquinolinone **62** was one of the first compounds tested. Although not designed as a potential irreversible PARP inhibitor, this compound is a novel isoquinolinone derivative, and as a member of the series of compounds in which the amide group is conformationally restricted (see Figure 17), should be a potent PARP inhibitor. Indeed, the assay results shown in Figure 40 below confirm this prediction. At 11.2 μM , PARP activity was virtually abolished with an inhibition of 95% calculated at the 2 minute time-point. The lack of solubility of the isoquinolinones is a problem that restricts their use as PARP inhibitors. The bromo derivative **62** is slightly more soluble than some of the other isoquinolinone derivatives handled in this work; 5-cyanoisoquinolinone **59**, for example, would not dissolve to any extent and could not, therefore, be tested.

Figure 40: *PARP activity in the presence of 5-bromoisoquinolinone 62 at 11.2.μM.*



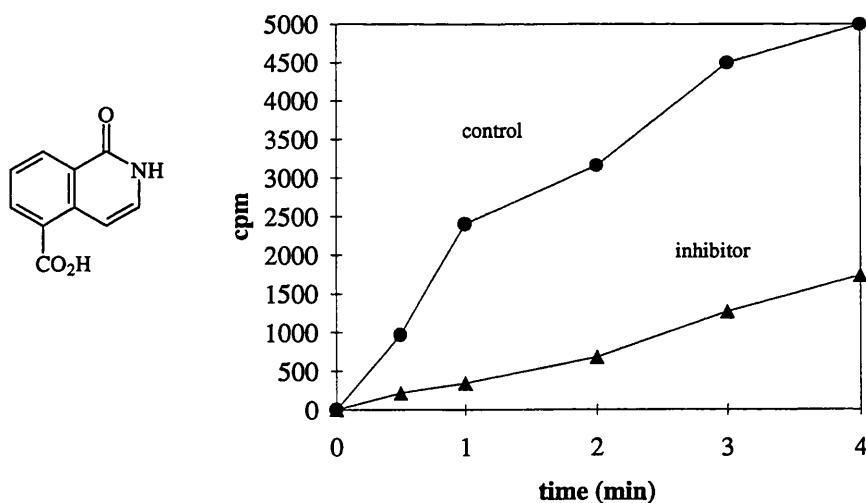
5-Iodoisoquinolinone **63** is a synthetically useful intermediate and a very potent PARP inhibitor as is shown in Figure 41. This isoquinolinone has a similar effect on PARP activity as has the bromo derivative **62**, in that 96% inhibition is achieved at a concentration of 8.0 μM. These results indicate that a moderately bulky substituent at the 5-position in the isoquinolinone series is tolerated in the active site of the enzyme and halides appear to be effective inhibitors.

Figure 41: PARP activity in the presence of 5-iodoisoquinolinone **63** at a concentration of 8.0 μM .



The isoquinolinone-5-carboxylic acid **89** was also tested. This compound has the advantage that it is soluble in the assay reaction mixture, since it is buffered to pH 8. This isoquinolinone was a potent inhibitor, although not as potent as some of the other isoquinolinones (Figure 42). This is to be expected as the carboxylic acid is an electron withdrawing group; a structural feature that tends to result in lower activity in both the benzamide and isoquinolinone series.

Figure 42: PARP activity in the presence of 1-oxoisoquinoline-5-carboxylic acid **89** at 13.2 μM .



The final isoquinolinone tested was the α,β -unsaturated carboxylic acid **125**. This isoquinolinone has a soft electrophilic group in the 5-position and may, therefore, be an irreversible inhibitor. Initial studies show that, in common with the isoquinolinone carboxylic acid **89**, this isoquinolinone is not as potent as the bromo- and iodo- derivatives **62** and **63**, in terms of PARP inhibition. This is probably due to the electron-withdrawing nature of the side-chain. Nevertheless, at 11.6 μM , compound **125** inhibited PARP activity by 81% in comparison to the control system (Figure 43). This inhibition is greater than that measured for the majority of benzamides at similar concentrations.

Figure 43: PARP activity in the presence of 3-(1-oxoisoquinolin-5-yl)propenoic acid **125** at 11.6 μM .

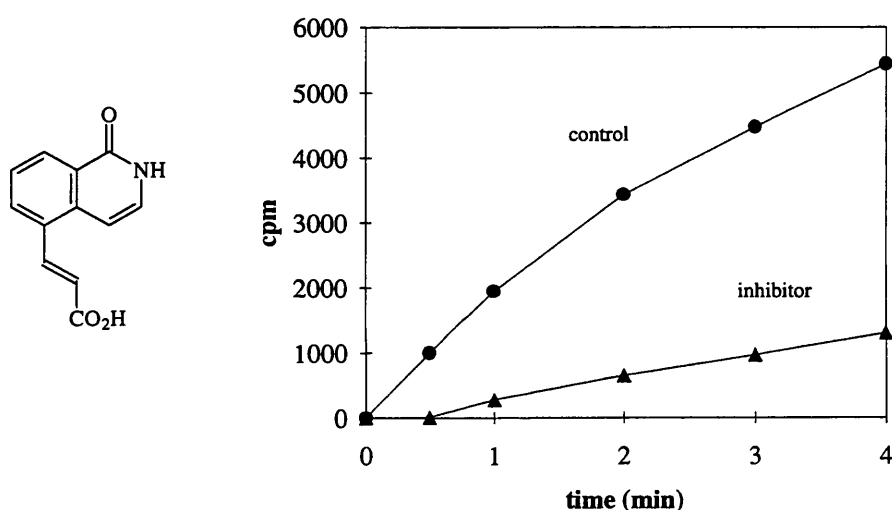
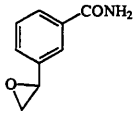
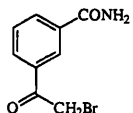
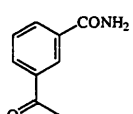
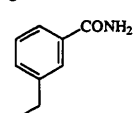
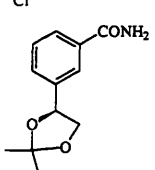
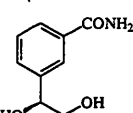
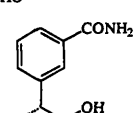
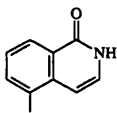
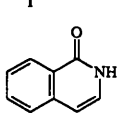
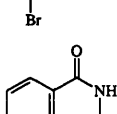
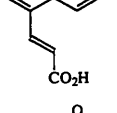


Table 6 gives a summary of the results of the PARP activity assays with inhibitors at concentrations *ca.* 10 μM . All the compounds tested were good inhibitors of PARP. Particularly promising results were obtained from the epoxide **43** and the acetyl and bromoacetyl derivatives of benzamide, **9** and **44**. These results suggest that a side chain containing an oxygen bonded to the benzylic carbon, which is not part of a hydroxyl group, might be favoured for activity. Compounds of this type are closer analogues of NAD^+ .

Table 6: Comparison of PARP Inhibitors: Percentage inhibition values at 2 min.

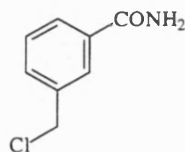
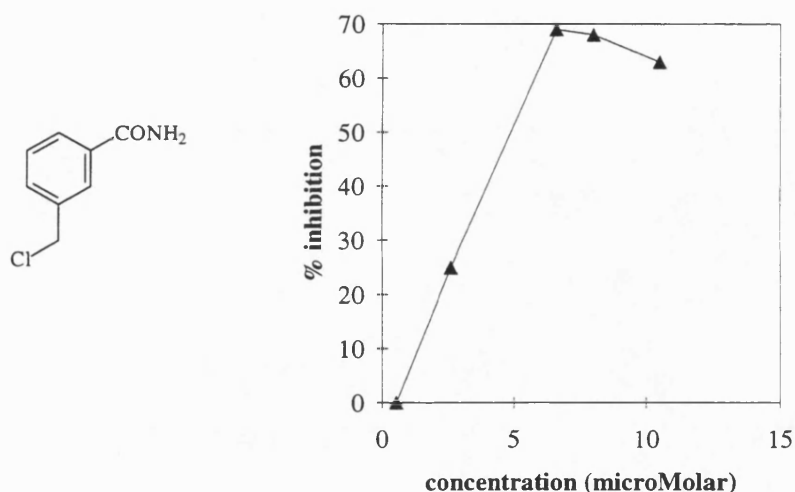
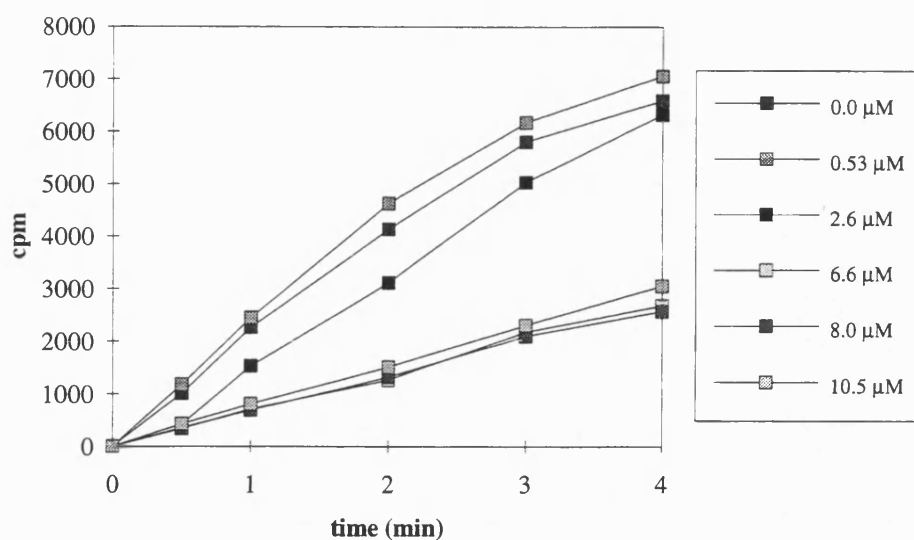
Compound Number	Structure	Concentration (μM)	% Inhibition
<i>Benzamides</i>			
43		9.2	88
44		10.7	84
9		11	83
2		10.5	62
4		10	54
6		9.4	44
36		9.3	32
<i>Isoquinolinones</i>			
63		8	96
62		11.2	95
125		11.6	81
89		13.2	79

7.3 PARP Assays at Various Inhibitor Concentrations

For some of the earlier, most active, PARP inhibitors tested, experiments were carried out in which a range of five different concentrations of inhibitor were used. These concentrations were estimated so that 50% inhibition would be achieved at, or in the region of, one of the values in the range. The purpose of these studies was to estimate an IC_{50} value for the inhibitor, *i.e.* the concentration at which 50% inhibition is achieved. The IC_{50} value is the most suitable value by which to compare inhibitors, as most reported inhibitor potencies are expressed in this way.

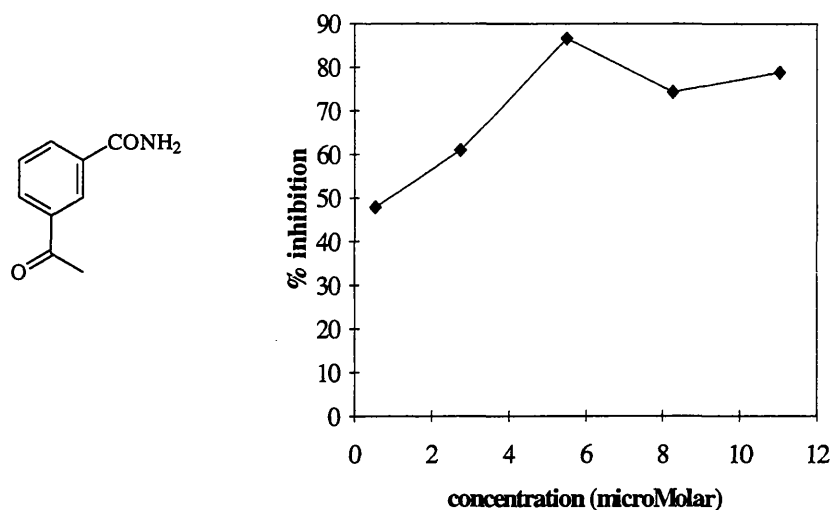
The results for the five assays carried out using varying concentrations of chloromethylbenzamide **2** are shown in Figure 44. For this compound, the time-course graphs for all five concentrations are shown in the first part of the figure. In the second part of the figure the percentage inhibition achieved at the 2 minute time point in each assay is plotted against the concentration to show how concentration affects the inhibition achieved. From this graph, the concentration that would give 50% inhibition can be estimated as 5 μ M.

Figure 44: PARP activity in the presence of various concentrations of 3-chloromethylbenzamide **2**



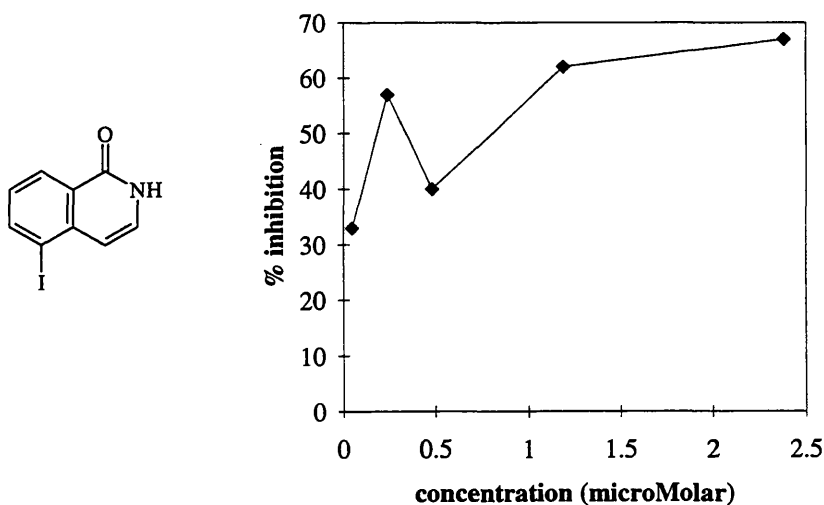
These assays were also carried out for 3-acetylbenzamide **9**, one of the more potent benzamides. Figure 45 shows inhibition *versus* concentration of inhibitor. As the graph shows, the concentration range was not well chosen in this case. Assays with lower inhibitor concentrations need to be carried out. These results tend to suggest an IC_{50} in the region of between 0.6 and 1.0 μM , demonstrating that this is a particularly potent benzamide inhibitor.

Figure 45: PARP inhibition in the presence of 3-acetylbenzamide **9** as a function of concentration.



Of the isoquinolinone inhibitors, three have been assessed at different concentrations. Figure 46 shows the results for 5-iodoisoquinolinone **63**.

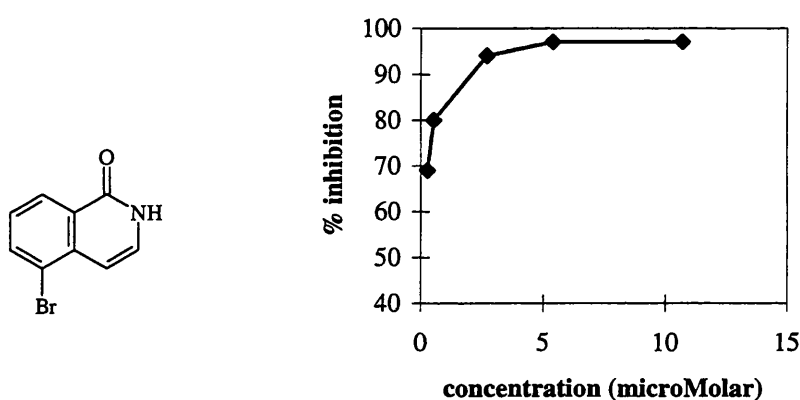
Figure 46: PARP inhibition in the presence of 5-Iodoisoquinolinone **63** as a function of concentration.



This graph does not easily allow an estimate of the concentration that would give 50% inhibition as the second two points of the series are do not follow the general trend. Further data points would confirm the shape of the curve. The

results suggest that the IC_{50} value is below 1 μM , which is in line with other isoquinolinones. The results obtained for the bromo derivative **62** are out of the required range of inhibition. The inhibition obtained for the lowest concentration tested (0.27 μM) was 69 %. This implies that the IC_{50} value is less than 0.27 μM , making one of the most potent PARP inhibitors known. The results are shown in Figure 47.

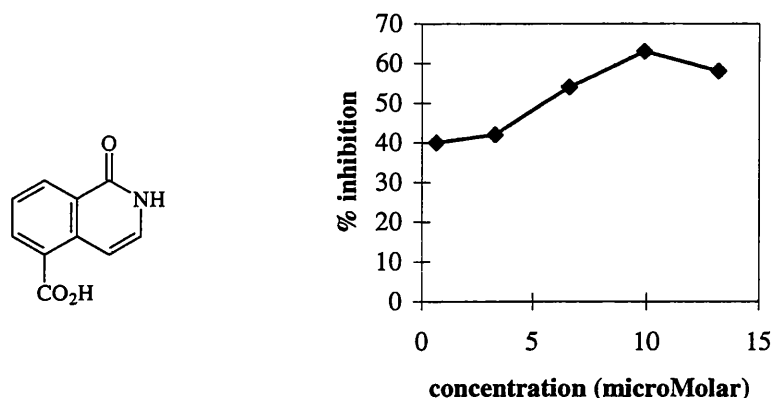
Figure 47: PARP inhibition in the presence of 5-bromoisoquinolinone **62** as a function of concentration.



The final isoquinolinone tested in this way was the carboxylic acid derivative **89**. This was a less potent isoquinolinone PARP inhibitor. This is reflected in the assay results shown in Figure 48. The estimated concentration of **89** that would give 50% inhibition of PARP is approximately 5 μM .

These assays require further development to be very useful. For our initial purpose of assessing whether or not a compound is a good PARP inhibitor, the PARP assays in the presence of a 10 μM concentration of the test compound are sufficient. Determination of accurate IC_{50} values require several more experiments.

Figure 48: *PARP inhibition in the presence of 1-oxoisoquinoline-5-carboxylic acid 89 as a function of concentration.*



7.4 Assays involving pre-incubation of the inhibitor with the enzyme

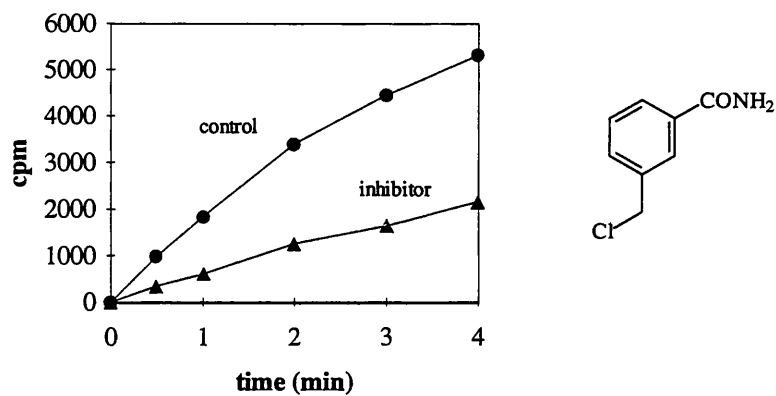
Three of the inhibitors tested were designed to be irreversible inhibitors of PARP. To fully determine the kinetic properties of an enzyme inhibitor, experiments need to be carried out in which the concentration of substrate, in this case NAD^+ , is varied. The effect of a reversible inhibitor is reversed by addition of further amounts of substrate, this would not be the case for an irreversible inhibitor. These assays are expensive to carry out due to the cost of the radiolabelled NAD^+ . Therefore the properties of these potentially irreversible inhibitors were examined by pre-incubating the inhibitor with the enzyme before adding the radiolabelled NAD^+ and starting the assay. The effect of pre-incubating the inhibitors with the enzyme for 1 minute, 15 minutes and 30 minutes was measured. A control system was incubated for the same time interval but with no inhibitor in order that any change in enzyme activity over the pre-incubation time period was taken into account. The rationale behind this study was that an irreversible inhibitor when incubated with the enzyme undergoes nucleophilic attack and becomes covalently bound to the PARP active site. If this is the case, the inhibition seen when the radiolabelled NAD^+ is added should be greater than when the inhibitor is not allowed pre-incubation with the

enzyme, since the NAD^+ cannot displace the already covalently bound inhibitor from its binding site. Results are shown below for 3-chloromethylbenzamide **2**, the epoxide **43** and for the α,β -unsaturated carboxylic acid **125**. Graphs of time-courses following pre-incubation times of 1 minute, 15 minutes and 30 minutes are shown for each compound. Graphs comparing PARP inhibition for each of the three assays through the time course are also given.

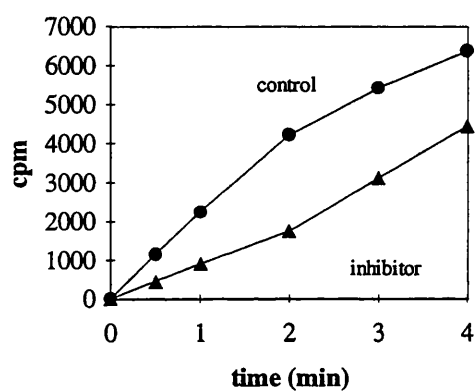
The results for 3-chloromethylbenzamide **2** are shown in Figure 49. The effect of increasing the length of time that the inhibitor is in contact with the enzyme before the substrate is added, in this case, seems to cause a general decrease in the amount of PARP inhibition seen. This is shown in graph (d) in which PARP inhibition is plotted for each assay as a function of time. The experiment involving 1 minute pre-incubation gave the highest PARP inhibition. Following 15 and 30 minutes pre-incubation the inhibition falls markedly after the two minutes point in the time-course. There is only a slight decrease, with time, for the 1 minute pre-incubation assay.

Figure 49: PARP activity in the presence of 3.9 μM 3-chloromethylbenzamide 2.

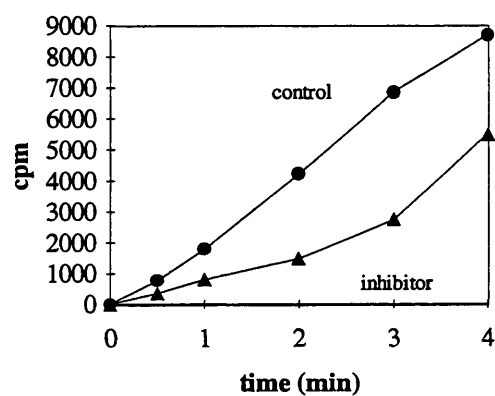
(a) 1 minute pre-incubation



(b) 15 minutes pre-incubation



(c) 30 minutes pre-incubation



(d) PARP inhibition for each time course

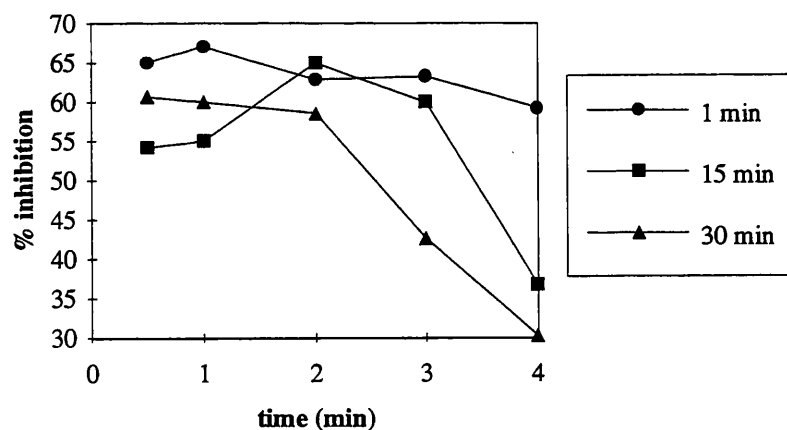
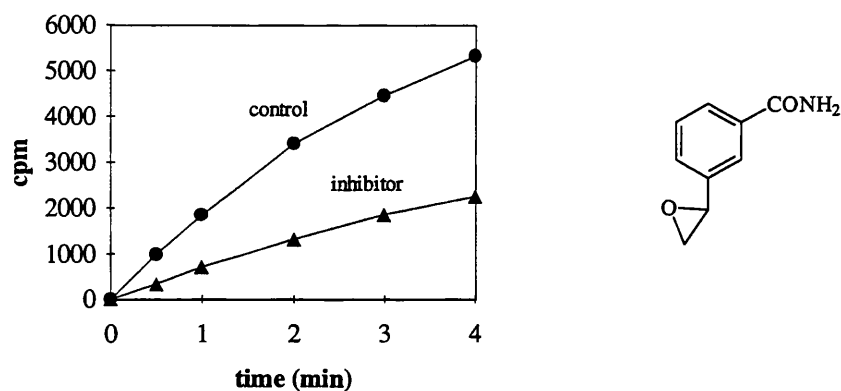
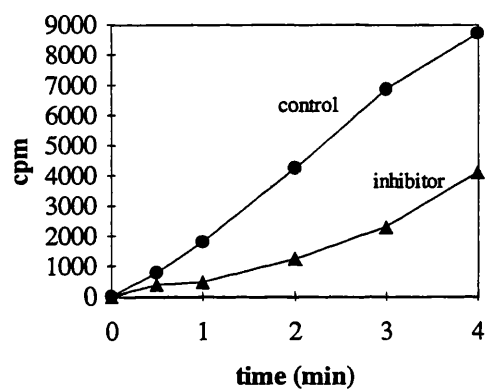


Figure 50: PARP activity in the presence of 2.8 μM (\pm)-3-(oxiran-2-yl)benzamide **43**.

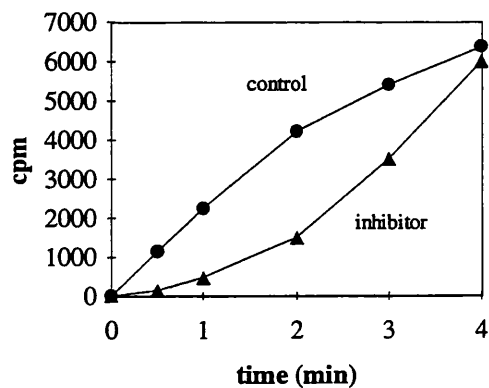
(a) 1 minute pre-incubation



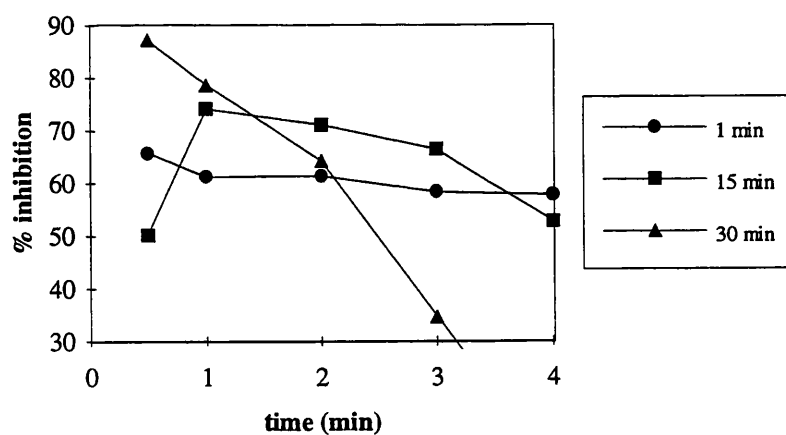
(b) 15 minute pre-incubation



(c) 30 minute pre-incubation



(d) PARP inhibition for each time course



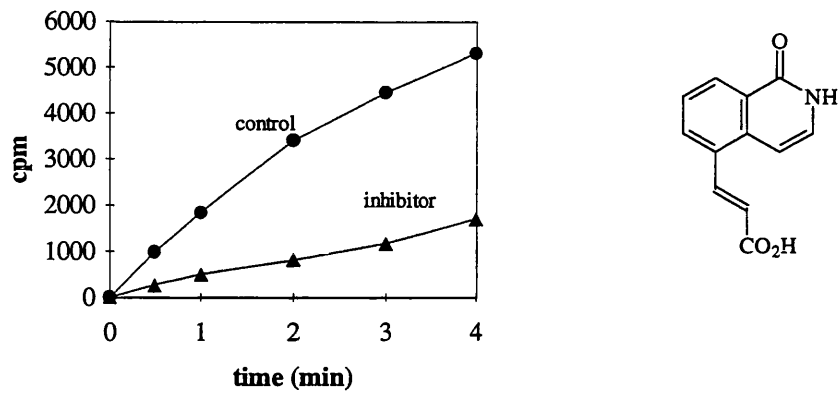
The results for the assays carried out using the epoxide inhibitor **43** are shown in Figure 50. Inhibition of PARP, measured in the presence of this compound, was greater following pre-incubation of the inhibitor and the enzyme, at least for the first part of the time course. The results for the samples taken at 1 minute, show that pre-incubation for 15 and 30 minutes gave inhibition values of 74% and 79% in comparison with the 61% inhibition seen following only 1 minute pre-incubation. The inhibition decreases markedly for the second half of the time course. The final 4 minute sample for the 30 minute pre-incubation assay shows that PARP activity appears to have recovered to control levels. This apparent decrease in inhibition seen with both benzamides **2** and **43** may be due to a number of factors. One possibility is that PARG, the enzyme that breaks down the poly(ADP-ribose) polymers, is inhibited by the benzamides. Further experiments would be required to investigate this phenomenon.

Finally, the results for the isoquinolinone **125** are shown in Figure 51. These graphs show that the inhibition was more constant throughout the time course. On average 10% more inhibition was achieved following 30 minutes pre-incubation as compared to the assay in which only 1 minute pre-incubation was allowed.

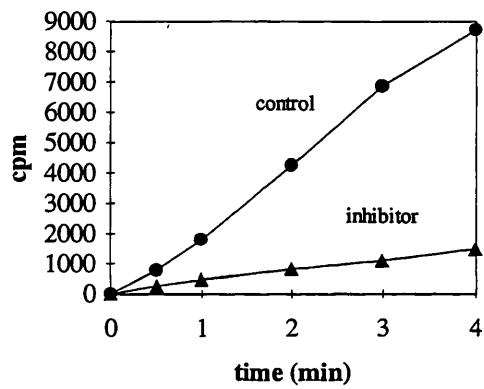
Clearly these are only preliminary studies and many more experiments need to be carried out to investigate these inhibitors fully. The pre-incubation time is one variable which should be investigated. Sufficient time must be allowed for the chemical reaction to take place, in which the inhibitor becomes covalently bound to the enzyme. However, other components of the nuclear extract may be affected by the pre-incubation. It would also be useful to ascertain whether the inhibitors have any effect on the glycohydrolase enzyme PARG.

Figure 51: PARP activity in the presence of 5.1 μM 3-(1-oxoisoquinolin-5-yl)propenoic acid **125**

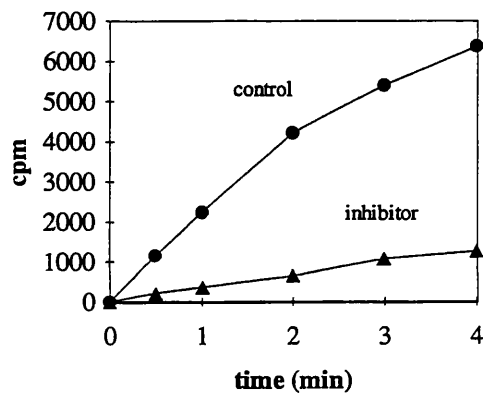
(a) 1 minute pre-incubation



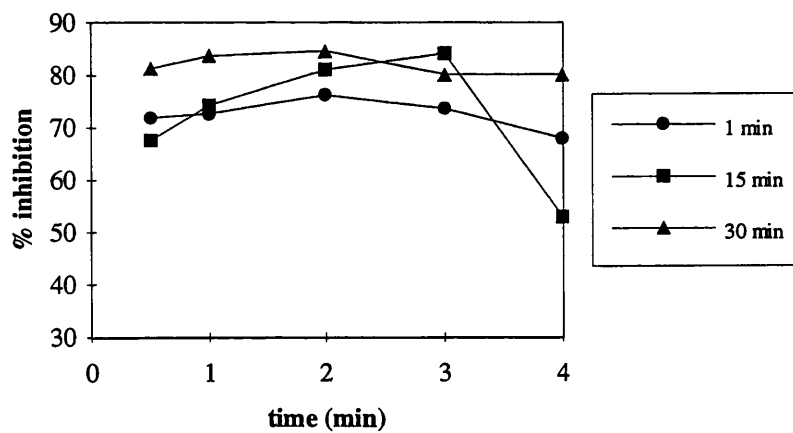
(b) 15 minutes pre-incubation



(c) 30 minutes pre-incubation



(d) PARP inhibition for each time course



These preliminary studies into the effect of the potential inhibitors of PARP on enzyme activity gave very promising results. All the compounds tested showed inhibition with potencies ranging from moderate to possibly some of the most potent PARP inhibitors tested so far. The few studies carried out suggest the epoxide **43** and the propenoic acid derivative **125** are possibly irreversible inhibitors but more extensive investigation into this concept is required.

Conclusions

Several novel benzamide derivatives have been synthesised and evaluated for their effect on PARP activity. Two benzamides with electrophilic side chains have been prepared. The first, 3-chloromethylbenzamide, was at least as potent as 3-aminobenzamide as a PARP inhibitor. The second, 3-(oxiran-2-yl)benzamide, was a very potent PARP inhibitor; one of the most potent of its benzamide class. This compound was also more freely soluble in the aqueous buffer used in the assay than were most of the other compounds tested. Approaches were made towards the asymmetric synthesis of benzamides with chiral substituents. The preparation of chiral alcohols of >95% enantiomeric purity was carried out using baker's yeast reduction of the corresponding ketones. Several investigations into the synthesis of benzamides with cyclic side chains were also carried out.

Various methods of synthesis of isoquinolinones have been investigated and several novel isoquinolin-1-one derivatives have been prepared. The successful preparation of 5-bromoisquinolinone and 5-iodoisquinolinone, by the "one-pot" Curtius rearrangement of the corresponding substituted 3-phenylpropenoyl azides followed by cyclisation, allowed investigations into the *C*-metallation of isoquinolinones. 5-Bromoisquinoline was successfully lithiated and treated with benzaldehyde to give 5-(α -hydroxyphenylmethyl)isoquinoline. However, an *N*-protected form of the equivalent isoquinolinone was not successfully coupled to a selection of electrophiles. 5-Iodoisoquinolinone was coupled to several alkenes using the palladium-catalysed Heck reaction. One product of these reactions was 3-(1-oxoisquinolin-5-yl)propenoic acid. This has an electrophilic side chain and was designed as an irreversible inhibitor. However, it was not as potent as might be expected for an isoquinolinone, possibly owing to the electron-withdrawing nature of the side chain. The Heck reaction with 5-iodoisquinolinone should prove a very useful method of synthesising many complex isoquinolinone

derivatives. Several approaches towards the synthesis of 1-(1-oxoisoquinolin-5-yl)ribose have been made. Development of these ideas and synthesis of this compound will be both synthetically challenging and biologically interesting.

Some preliminary studies have been carried out to investigate the effect of pre-incubating the inhibitors with PARP before adding the substrate. The initial results suggest that the inhibition is increased in two cases, these compounds may possibly be irreversible inhibitors and further work on their full evaluation is certainly warranted.

EXPERIMENTAL

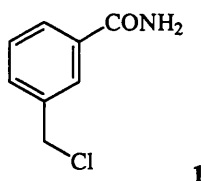
General procedures.

All melting points were determined on a Reichert-Jung Thermo Galen Kofler Block and are uncorrected. Kugelrohr distillations were carried out using Büchi GKR51 apparatus; the boiling points given correspond to the Kugelrohr oven temperature. Optical rotations were determined in an Optical Activity Ltd polarimeter type AA-10 in dichloromethane solution at ambient temperature. NMR spectra were recorded on a Jeol GX270 spectrometer (270.05 MHz ^1H ; 67.8 MHz ^{13}C) and a Jeol EX 400 (399.65 MHz ^1H ; 100.4 MHz ^{13}C , 376.05 MHz ^{19}F). Tetramethylsilane was used as an internal standard for samples dissolved in CDCl_3 , $(\text{CD}_3)_2\text{SO}$, CD_3OD or $\text{CD}_3\text{CO}_2\text{D}$. 3-(Trimethylsilyl)propanoic-2,2,3,3- d_4 acid sodium salt was used for samples dissolved in D_2O . Multiplicities are indicated as follows; s (singlet), bs (broad singlet), d (doublet), dd (doublet of doublets), t (triplet), q (quartet), qu (quintet) and m (multiplet). IR spectra were recorded on a Perkin-Elmer 782 IR spectrometer, either as a liquid film (film) or as a KBr disc (KBr); ν_{max} values are given in cm^{-1} . Mass spectra were obtained by electron impact (EI), chemical impact (CI), or fast atom bombardment (FAB) using a VG7070E spectrometer. Data are reported in the form m/z (intensity relative to base = 100) for selected ions. Analytical thin layer chromatography (TLC) was carried out using Merck Kieselgel 60F plates or Polygram Alox N plates (aluminium oxide on polyester), visualisation was achieved by UV light, iodine or phosphomolybdic acid. Flash chromatography was performed using Merck Silica Gel 60 (0.040-0.063mm) flash silica.

Where repetitive experimental procedures were employed, only one description is provided. All solutions were aqueous unless otherwise stated. Solvents were evaporated under reduced pressure. Solutions in organic solvents were dried using anhydrous MgSO_4 , unless otherwise noted. Solvents were distilled from

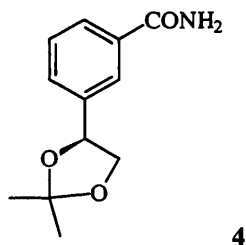
the indicated drying agents according to standard procedures: Carbon tetrachloride, acetonitrile (phosphorus (V) oxide); tetrahydrofuran (sodium/benzophenone); triethylamine (potassium hydroxide).

The baker's yeast used in the asymmetric reductions was obtained from Phipps Bakery, George Street, Bath.



3-Chloromethylbenzamide **1**

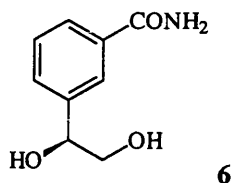
3-Chloromethylbenzoyl chloride **2** (2.85 g, 15.1 mmol) was dissolved in diethyl ether (25 ml) and a dried solution of ammonia in diethyl ether (4% w/v, 200 ml) was added in small portions. A white precipitate formed. The mixture was stirred for 30 min then washed with water. The organic layer was washed twice with 10% w/v sulphuric acid, with water, then dried and concentrated to give **1** (2.27 g, 89%) as colourless needles; $R_f = 0.38$ (ethyl acetate / hexane, 1:1); mp 118-120°C (from ethyl acetate / hexane (lit.,²⁶¹ 119-120°C); IR (KBr) 3360, 3190 (N-H), 1655 (amide I), 1625 (amide II), 705 (C-Cl); ^1H NMR (CDCl_3 , $(\text{CD}_3)_2\text{SO}$) δ 4.64 (2 H, s, CH_2Cl), 6.34 (1 H, bs, NH), 7.30 (1 H, bs, NH), 7.44 (1 H, t, $J = 7.7$ Hz, 5-H), 7.54 (1 H, d, $J = 7.7$ Hz, 4-H), 7.84 (1 H, d, $J = 7.7$ Hz, 6-H), 7.94 (1 H, s, 2-H); MS (EI) 169 ($\text{M}^+[\text{}^{35}\text{Cl}]$, 58), 171 ($\text{M}^+[\text{}^{37}\text{Cl}]$, 18).



(+)-3-(2,2-Dimethyl-1,3-dioxolan-4-yl)benzamide **4**

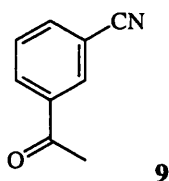
Freeze-dried (+)-3-(1,2-dihydroxyethyl)benzamide **6** (62 mg, 0.34 mmol), 2,2-dimethoxypropane (1 ml) and 4-methylbenzenesulphonic acid (1 mg) were stirred at room temperature for 3 d. Ethyl acetate (50ml) was added to dissolve the white precipitate that had formed and the solution was then washed with 10% w/v sodium carbonate solution and saturated sodium chloride solution, dried and concentrated to give **4** (55 mg, 82%) as a white solid; $R_f = 0.52$ (methanol / ethyl acetate, 1:19); mp 128-130°C; $[\alpha]_D^{20} = +39.2$ (c 2.5, dichloromethane); ^1H NMR (CDCl_3) δ 1.50 (3 H, s, CH_3), 1.57 (3 H, s, CH_3), 3.70 (1 H, t, $J = 8.0$ Hz,

$\text{CH}_\text{A}\text{H}_\text{B}$), 4.35 (1 H, dd, $J = 8.0, 6.2$ Hz, $\text{CH}_\text{A}\text{H}_\text{B}$), 5.13 (1 H, dd, $J = 8.0, 6.2$ Hz, $\text{CH}_\text{C}\text{O}$), 5.71 (1 H, bs, NH), 6.11 (1 H, bs, NH), 7.57 (1 H, t, $J = 7.6$ Hz, 5-H), 7.55 (1 H, dt, $J = 7.6, 1.5$ Hz, 4-H), 7.73 (1 H, dt, $J = 7.6, 1.5$ Hz, 6-H), 7.82 (1 H, t, $J = 1.5$ Hz, 2-H); MS (FAB⁺) 222.1153 (MH⁺, 100) $\text{C}_{12}\text{H}_{15}\text{NO}_3$ requires 222.1130, 164 (34).



(+)-3-(1,2-Dihydroxyethyl)benzamide 6

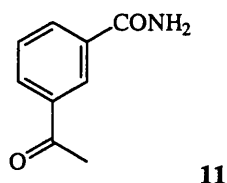
(+)-3-(1,2-Dihydroxyethyl)benzonitrile **18** (330 mg, 2.2 mmol) in ethanol (6.5 ml), was treated with 0.5 M sodium hydroxide (1.0 ml, 0.52 mmol) and 27.5 % w/v hydrogen peroxide solution (0.85 ml, 6.8 mmol). The reaction mixture was heated to 50°C for 1 h, allowed to cool and was neutralised with 2 M hydrochloric acid solution. The solvent was removed and the residue dried to give **6** (366 mg, 2.2 mmol) as a colourless gum; $R_f = 0.1$ (methanol / chloroform, 1:9); ¹H NMR ((CD₃)₂SO) 3.45 (2 H, d, $J = 6.4$ Hz, CH₂), 4.0 (2 H, bs, OH), 4.57 (1 H, t, $J = 6.4$ Hz, CH), 7.32 (1 H, bs, NH), 7.37 (1 H, t, $J = 7.7$ Hz, 5-H), 7.48 (1 H, d, $J = 7.7$ Hz, 4-H), 7.74 (1 H, d, $J = 7.7$ Hz, 6-H), 7.85 (1 H, s, 2-H), 7.96 (1 H, bs, NH); MS (FAB⁺) 182.0822 (MH⁺, 100) ($\text{C}_9\text{H}_{11}\text{NO}_3$ requires 182.0817).



3-Acetylbenzonitrile 9

3-Aminoacetophenone **10** (15.0 g, 0.111 mol) in a mixture of iced water (28 ml) and concentrated hydrochloric acid (28 ml) was diazotized by slow addition of sodium nitrite (8.0 g, 0.115 mol) in iced water (36 ml). Following neutralisation

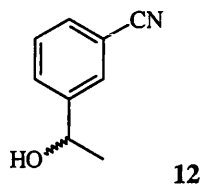
with sodium carbonate, the diazonium salt was added to a solution of copper cyanide (12.0 g, 0.134 mol) and potassium cyanide (17.0 g, 0.262 mol) in water (45 ml) heated to 60-70°C. The resulting mixture was stirred at 100°C for 15-20 min. The cooled mixture was extracted twice with ethyl acetate washed twice with water, with 10% w/v sulphuric acid and with water. The organic phase was dried and concentrated to give an orange-brown solid. Recrystallization from hexane provided 3- acetylbenzonitrile **9** (7.54 g, 47%) as pale orange crystals; R_f = 0.77, (ethyl acetate / hexane, 1:1); mp 93-94°C (lit.,²⁶² 98-100°C); IR (KBr) 2240 (C≡N), 1695 (C=O); ¹H NMR (CDCl₃) δ 2.64 (3 H, s, COCH₃), 7.62 (1 H, t, J = 7.7 Hz, 5-H), 7.85 (1 H, dt, J = 7.7, 1.7 Hz, 6-H), 8.18 (1 H, dt, J = 7.7, 1.7 Hz, 4-H), 8.24 (1 H, t, J = 1.7 Hz, 2-H).



3-Acetylbenzamide **11**

3-Acetylbenzonitrile **9** (5.0 g, 34.4 mmol) was suspended in ethanol (50 ml) and 0.5 M sodium hydroxide solution (17 ml, 8.5 mmol) was added. To the stirred mixture, 27.5% w/v hydrogen peroxide solution (15 ml, 121 mmol) was added dropwise, whilst the temperature of the reaction mixture was not allowed to exceed 50°C. On completion of the exothermic reaction, in which oxygen was evolved, the reaction mixture was stirred at 50°C for 1 h. Following neutralisation with 10 % w/v sulphuric acid, the volume of ethanol was reduced *in vacuo* and the residue taken up into dichloromethane. The organic extract was washed with water and brine, then dried and concentrated to give **11** (5.48 g, 97%) as a white crystalline solid; R_f = 0.17 (ethyl acetate / hexane, 1:1); mp 125.5-126.5°C; IR (KBr) 3380, 3185 (N-H), 1680 (C=O acetyl), 1655, 1630 (C=O, amide); ¹H NMR (CDCl₃) δ 2.67 (3 H, s, COCH₃), 5.93 (1 H, bs, NH), 6.30 (1 H, bs, NH), 7.58 (1 H, t, J = 7.8 Hz, 5-H), 8.06 (1 H, dt, J = 7.8, 1.5 Hz,

4-H), 8.12 (1 H, dt, $J = 7.8, 1.5$ Hz, 6-H), 8.40 (1 H, t, $J = 1.5$ Hz, 2-H); MS (EI) 164.0671 (M^+ , 7) ($^{13}C^{12}C_9H_9NO_2$ requires 164.0667), 163.0636 (M^+ , 75) ($C_9H_8NO_2$ requires 163.0633), 148 (100); Anal. Calcd. for $C_9H_9NO_2$: C, 66.25; H, 5.56; N, 8.58. Found C, 66.1; H, 5.55; N, 8.20. [11 is reported in the literature²⁶³ but not characterised]

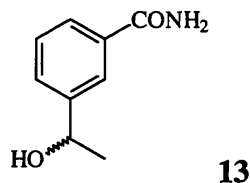


(±)-3-(1-Hydroxyethyl)benzonitrile 12

Method A: 3-Acetylbenzonitrile **9** (1.0 g, 6.9 mmol) was dissolved in ethanol (30 ml) and a suspension of sodium borohydride (0.8 g, 21.1 mmol) in ethanol (10 ml) was added slowly. The mixture was stirred for 1 h. 2 M hydrochloric acid was then added dropwise until effervescence ceased. Following concentration, ethyl acetate was added and the organic extract was washed twice with water, dried and the solvent was removed to give an orange oil, which was crude **12** (0.96 g, 95%); $R_f = 0.4$ (methanol / chloroform, 1:19); IR (film) 3400 (O-H), 2210 ($C\equiv N$), 1070 (C-O); 1H NMR ($CDCl_3$) δ 1.49 (3 H, d, $J = 6.6$ Hz, CH_3), 2.3 (1 H, bs, OH), 4.94 (1 H, q, $J = 6.6$ Hz, CH), 7.45 (1 H, t, $J = 7.7$ Hz, 5-H), 7.55 (1 H, dt, $J = 7.7, 1.5$ Hz, 4-H), 7.62 (1 H, dt, $J = 7.7, 1.5$ Hz, 6-H), 7.68 (1 H, t, $J = 1.5$ Hz, 2-H); MS (CI, iso-butane) 148 (MH^+ , 100). (Although NMR showed that the crude product was mainly (±)-3-(1-hydroxyethyl)benzonitrile, TLC showed other spots, however an attempt to purify the product by flash chromatography (methanol / chloroform, 1:19) gave only a small percentage of the product and it was concluded that degradation occurs on silica.)

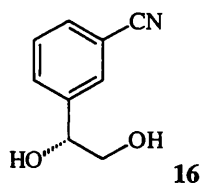
Method B: 3-Acetylbenzonitrile **9** (1.0 g, 6.89 mmol) was suspended in ethanol (12 ml) at 0°C. Sodium borohydride (156 mg, 4.1 mmol) was added and the mixture was stirred at 0°C for 30 min, followed by 1 hour at RT. Procedure

continued as for Method A, above, to give **12** (1.01 g, 100%) an orange oil, pure by NMR analysis; data identical to those above.



(±)-3-(1-Hydroxyethyl)benzamide 13

3-Acetylbenzamide **11** (500 mg, 3.1 mmol) was treated with sodium borohydride at 0°C as described in Method B for the corresponding benzonitrile **12** above. This yielded **13** (311 mg, 62%) as a white crystalline solid; R_f = 0.57 (acetone / hexane, 2:1); mp 127-129°C; IR (KBr) 3360, 3190 (N-H), 1670 (amide I), 1620 (amide II); ^1H NMR ($(\text{CD}_3)_2\text{SO}$) δ 1.33 (3 H, d, J = 6.6 Hz, CH_3), 4.76 (1 H, *ca.* qu, CH), 5.24 (1 H, d, J = 4.0 Hz, OH), 7.32 (1 H, bs, NH), 7.38 (1 H, t, J = 7.7 Hz, 5-H), 7.49 (1 H, d, J = 7.7 Hz, 4-H), 7.72 (1 H, d, J = 7.7 Hz, 6-H), 7.86 (1 H, s, 2-H), 7.95 (1 H, bs, NH); MS (EI) 166.0867 (M^+ , 100) ($\text{C}_9\text{H}_{11}\text{NO}_2$ requires 166.0868).

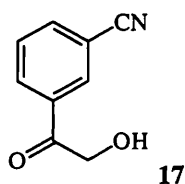


(-)-3-(1,2-Dihydroxyethyl)benzonitrile 16

To a fermenting slurry of bakers' yeast (88 g), water (880 ml) and sucrose (88 g) was added 3-(2-hydroxyacetyl)benzonitrile **17** (600 mg, 3.7 mmol). The mixture was stirred at 30°C for 7 days. Diethyl ether (100 ml) and Celite® (100 g) were added to the mixture and stirring continued for a further 15 min. The slurry was then filtered through a sintered funnel and the residue was washed with diethyl ether (2 × 50 ml). The aqueous filtrate was extracted with diethyl ether (5 × 100ml) and the combined organic extracts were dried and concentrated. Flash chromatography (ethyl acetate / hexane, 1:1 → 3:2) gave **16** (268 mg, 44%) as a

white solid; $R_f = 0.13$ (ethyl acetate / hexane, 1:1); mp 64-66°C; $[\alpha]_D^{20} = -46.6^\circ$ (c 1.0, DCM); ^1H NMR (CDCl_3) δ 2.33 (2 H, bs, OH), 3.62 (1 H, dd, $J = 11.4$, 7.7 Hz, $\text{CH}_A\text{H}_B\text{OH}$), 3.81 (1 H, dd, $J = 11.4$, 3.6 Hz, $\text{CH}_A\text{H}_B\text{OH}$), 4.87 (1 H, dd, $J = 7.7$, 3.6 Hz, CH_COH), 7.48 (1 H, t, $J = 7.7$ Hz, 5-H), 7.6 (2 H, m, 4,6- H_2), 7.71 (1 H, s, 2-H); MS (CI) 164 (MH^+ , 100), 146 (32).

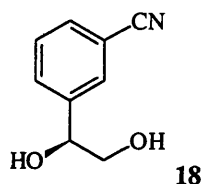
The MTPA esters of (+) and (–) 3-(1,2-dihydroxyethyl)benzonitrile gave signals in their NMR spectra which were too similar to resolve and no enantiomeric excess calculations were possible. Attempts to separate the signals from enantiomers using praesodimium $[\text{Pr}(\text{hfc})_3]$ and europium $[\text{Eu}(\text{hfc})_3]$ chiral shift reagents were unsuccessful. However comparison of optical rotations of **18** and **16** would suggest an enantiomeric excess of $\geq 95\%$ for **16**.



3-(2-Hydroxyacetyl)benzonitrile **17**

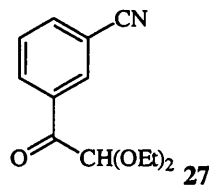
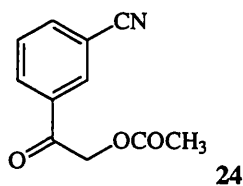
3-(2-Hydroxyacetyl)benzonitrile **17** was prepared by the general method described by Moriarty *et al.*¹⁸¹ 3-Acetylbenzonitrile **9** (1.0 g, 6.9 mmol) was added to a stirred solution of trifluoroacetic acid (1.06 ml, 13.8 mmol), water (8 ml) and acetonitrile (40 ml). [Bis(trifluoroacetoxy)iodo]-benzene (5.9 g, 13.8 mmol) was added and the solution heated to reflux for 8 hours. The reaction was monitored by TLC. The acetonitrile was removed and the residue was partitioned between ethyl acetate and water. The aqueous phase was extracted three times with ethyl acetate. The combined organic extracts were washed with saturated sodium hydrogen carbonate solution, and were dried and concentrated. Flash chromatography (ethyl acetate / hexane, 1:1) gave the starting material **9** (0.05 g, 5%); mp 93-94°C (lit.²⁶² 98-100°C); IR spectrum matched that of an authentic sample; and 3-(2-hydroxyacetyl)benzonitrile **17** (0.31 g, 28%) as white crystals;

$R_f = 0.37$ (ethyl acetate / hexane, 1:1); mp 102-105°C; IR (KBr) 3400-3600 (O-H), 2200 (C≡N), 1650-1700 (C=O); ^1H NMR ($(\text{CD}_3)_2\text{SO}$) δ 3.37 (1 H, bs, OH), 4.91 (2 H, s, CH_2), 7.68 (1 H, t, $J = 7.7$ Hz, 5-H), 7.92 (1 H, d, $J = 7.7$ Hz, 4-H), 8.15 (1 H, d, $J = 7.7$ Hz, 6-H), 8.22 (1 H, s, 2-H); MS (CI, iso-butane) 162 (MH^+ 100); MS (EI) 161.0471 (M^+ , 5) ($\text{C}_9\text{H}_7\text{NO}_2$ requires 161.0432) 130 (100), 102 (42). [17 is reported in the literature²⁶⁴ but no data are given.]



(+)-3-(1,2-Dihydroxyethyl)benzonitrile 18

(+)-3-(2-Acetoxy-1-hydroxyethyl)benzonitrile **30** (0.50 g, 2.4 mmol) was treated with ammonia in methanol as described for the synthesis of **32**, Method C. This gave **18** (0.36 g, 92%) as a white crystals; $R_f = 0.3$ (methanol / chloroform, 1:9); $[\alpha]_D^{20} +46.6^\circ$ (c 2.0, dichloromethane); ^1H NMR (CDCl_3) δ 2.86 (2 H, bs, OH), 3.60 (1 H, dd, $J = 11.4, 7.9$ Hz, $\text{CH}_\text{A}\text{H}_\text{B}\text{OH}$), 3.78 (1 H, dd, $J = 11.4, 3.3$ Hz, $\text{CH}_\text{A}\text{H}_\text{B}\text{OH}$), 4.84 (1 H, dd, $J = 7.9, 3.3$ Hz, $\text{CH}_\text{C}\text{OH}$), 7.46 (1 H, t, $J = 7.7$ Hz, 5-H), 7.60 (2 H, m, 4,6- H_2), 7.71 (1 H, s, 2-H); MS (FAB^+) 164.0657 (MH^+ , 100 %) ($\text{C}_9\text{H}_9\text{NO}_2$ requires 164.0712).



3-(2-Acetoxyacetyl)benzonitrile 24

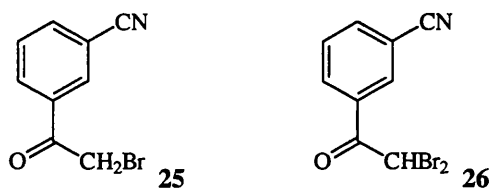
3-(Bromoacetyl)benzonitrile **25** (5.50 g, 24.6 mmol) and potassium acetate (2.40 g, 24.5 mmol) were dissolved in ethanol (100 ml). To the stirred solution, sodium iodide (0.36 g, 2.4 mmol) was added and the solution was refluxed for 6 h. After removal of ethanol, the residue was extracted with ethyl acetate, washed

three times with water and dried. Concentration, followed by flash chromatography (hexane / ethyl acetate, 4:1) gave the following products:

3-(Diethoxyacetyl)benzonitrile 27 (160 mg, 3%); a yellow oil; R_f = 0.45 (hexane / ethyl acetate, 4:1); IR (KBr) 2240 (C≡N), 1705 (C=O); ^1H NMR (CDCl_3) δ 1.26 (6 H, t, J = 7.2 Hz, $2 \times \text{CH}_3$), 3.65 (2 H, dq, J_{gem} = 9.5 Hz, J_{vic} = 7.2 Hz, $2 \times \text{OCH}_A\text{H}_B\text{CH}_3$), 3.81 (2 H, dq, J_{gem} = 9.5 Hz, J_{vic} = 7.2 Hz, $2 \times \text{OCH}_A\text{H}_B\text{CH}_3$), 7.59 (1 H, t, J = 7.7 Hz, 5-H), 7.83 (1 H, dt, J = 7.7, 1.5 Hz, 6-H), 8.39 (1 H, dt, J = 7.7, 1.5 Hz, 4-H), 8.51 (1 H, t, J = 1.1 Hz, 2-H); ^{13}C NMR (CDCl_3) δ 15.00 ($2 \times \text{CH}_3$), 64.01 ($2 \times \text{CH}_2$), 103.68 ($\underline{\text{CHCO}}$), 112.58 (C_q), 117.92 (C_q), 129.14 (5-C), 133.71 (2-C), 133.78 (4-C), 134.07 (C≡N), 135.97 (6-C), 192.03 (C=O); MS (FAB^+) 234.1137 (MH^+ , 100) ($\text{C}_{13}\text{H}_{16}\text{NO}_3$ requires 234.1130).

3-Acetylbenzonitrile 9 (1.15 g, 32%); this fraction was not pure and did contain a small amount of **27**; R_f = 0.31 (hexane / ethyl acetate, 4:1); mp 83-87°C (lit.²⁶² 98-100°C); ^1H NMR (CDCl_3) δ 2.65 (3 H, s, CH_3), 7.65 (1 H, t, J = 7.7 Hz, 5-H), 7.86 (1 H, dt, J = 7.7, 1.5 Hz, 6-H), 8.18 (1 H, dt, J = 7.7, 1.5 Hz, 4-H), 8.24 (1 H, t, J = 1.5 Hz, 2-H).

3-(2-Acetoxyacetyl)benzonitrile 24 (3.20 g, 64%); white crystals; R_f = 0.21 (hexane / ethyl acetate, 4:1); mp 70-72°C; IR (KBr) 2240 (C≡N), 1755, 1710 (C=O); ^1H NMR (CDCl_3) δ 2.24 (3 H, s, CH_3), 5.31 (2 H, s, CH_2), 7.66 (1 H, t, J = 7.8 Hz, 5-H), 7.90 (1 H, dt, J = 7.8, 1.3 Hz, 6-H), 8.14 (1H, dt, J = 7.8, 1.3 Hz, 4-H), 8.20 (1 H, t, J = 1.3 Hz, 2-H); MS (CI, iso-butane) 204 (MH^+ , 100); Anal. Calcd. for $\text{C}_{11}\text{H}_9\text{NO}_3$: C, 65.02; H, 4.46; N, 6.89. Found: C, 64.9; H, 4.42; N, 6.76.



3-(Bromoacetyl)benzonitrile **25**

Method A: To a solution of **9** (0.80 g, 5.5 mmol) in glacial acetic acid (3 ml), bromine (0.3 ml, 5.5 mmol) was added slowly. The orange solution was stirred for 3 h. The dichloromethane extract was washed three times with sodium carbonate solution (10%w/v), with water and dried. Concentration and flash chromatography (hexane / ethyl acetate, 9:1), gave two products:

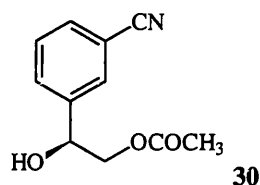
3-(Dibromoacetyl)benzonitrile **26** (0.10 g, 6%); a white solid; $R_f = 0.89$ (ethyl acetate - hexane, 1:1); mp 84.5-86°C; IR (KBr) 2240 (C≡N), 1705 (C=O); ^1H NMR (CDCl_3) δ 6.56 (1 H, s, CHBr_2), 7.68 (1 H, t, $J = 7.9$ Hz, 5-H), 7.92 (1 H, dt, $J = 7.9, 1.5$ Hz, 6-H), 8.37 (1 H, dt, $J = 7.9, 1.5$ Hz, 4-H), 8.42 (1 H, t, $J = 1.5$ Hz, 2-H); MS (CI, iso-butane) 306 ($\text{M}[^{81}\text{Br}, ^{81}\text{Br}]\text{H}^+$, 40), 304 ($\text{M}[^{79}\text{Br}, ^{81}\text{Br}]\text{H}^+$, 82), 302 ($\text{M}[^{79}\text{Br}, ^{79}\text{Br}]\text{H}^+$, 42); Anal. Calcd. for $\text{C}_9\text{H}_5\text{Br}_2\text{NO}$: C, 35.68; H, 1.66; N, 4.62. Found: C, 35.65; H, 1.62; N, 4.58.

3-(Bromoacetyl)benzonitrile **25** (0.40 g, 32%); white crystalline solid; $R_f = 0.82$ (ethyl acetate / hexane, 1:1); mp 65-67°C (lit.²⁶⁵ 65.5-66.5°C); IR(KBr) 2240 (C≡N), 1710 (C=O); ^1H NMR (CDCl_3) δ 4.43 (2 H, s, CH_2Br), 7.67 (1 H, t, $J = 7.9$ Hz, 5-H), 7.90 (1 H, dt, $J = 7.9, 1.5$ Hz, 6-H), 8.22 (1 H, dt, $J = 7.9, 1.5$ Hz, 4-H), 8.28 (1 H, t, $J = 1.5$ Hz, 2-H); MS (CI, iso-butane) 224 ($\text{M}[^{79}\text{Br}]\text{H}^+$, 100), 226 ($\text{M}[^{81}\text{Br}]\text{H}^+$, 98).

Method B: 3-Acetylbenzonitrile **9** (3.0 g, 20.7 mmol) was dissolved in chloroform (15 ml) and the solution cooled to 0°C. Bromine (1.1 ml, 21.3 mmol) was added dropwise to the stirred solution over the course of 30 min. The solution was stirred at ambient temperature for 2 h. The solvent was evaporated, leaving an orange solid which consisted of two products; these were separated by flash chromatography (hexane / ethyl acetate, 9:1) to give:

3-(Dibromoacetyl)benzonitrile 26 (0.50 g, 8%); a white crystalline solid; mp 84.5-86°C; ^1H NMR data were identical to those above.

3-(Bromoacetyl)benzonitrile 25 (3.60 g, 78%); white needles; mp 70-71°C (lit.²⁶⁵ 65.5-66.5°C); ^1H NMR data were identical to those above.



(+)-3-(2-Acetoxy-1-hydroxyethyl)benzonitrile 30

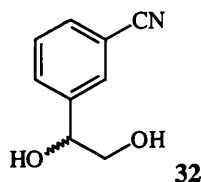
Bakers' yeast (7.5 g) was suspended in lukewarm tap water (56 ml) and sucrose (11.2 g) was added gradually. To this fermenting slurry, powdered 3-(2-acetoxyacetyl)benzonitrile **24** (0.76 g, 3.7 mmol) was added. The mixture was stirred at ambient temperature, in a conical flask closed with a cotton wool plug for 8 h. The slurry was then filtered through a Celite[®] pad and was extracted with diethyl ether (4 x 30 ml). The extracts were dried and concentrated to give a pale yellow oil. Flash chromatography (ethyl acetate / hexane, 2:3) gave two colourless oils:

(±)-3-(1,2-Dihydroxyethyl)benzonitrile 32 (14 mg, 2%), R_f = 0.21 (ethyl acetate / hexane, 1:1); ^1H NMR (CDCl_3) δ 2.5 (2 H, bs, OH), 3.62 (1 H, dd, J = 11, 8 Hz, $\text{CH}_\text{A}\text{H}_\text{B}\text{OH}$), 3.80 (1 H, dd, J = 11 Hz, 3.5 Hz, $\text{CH}_\text{A}\text{H}_\text{B}\text{OH}$), 4.87 (1 H, dd, J = 8, 3.5 Hz, $\text{CH}_\text{C}\text{OH}$), 7.48 (1 H, t, J = 7.7 Hz, 5-H), 7.6 (2 H, m, 4,6- H_2), 7.71 (1 H, s, 2-H).

3-(2-Acetoxy-1-hydroxyethyl)benzonitrile 30 (0.65 g, 85%); R_f = 0.49 (ethyl acetate / hexane, 1:1); $[\alpha]_\text{D}^{20}$ +34.9° (c 2.9, dichloromethane); IR (film) 3400-3500 (OH), 2240 ($\text{C}\equiv\text{N}$), 1740 ($\text{C}=\text{O}$); ^1H NMR (CDCl_3) δ 2.11 (3 H, s, CH_3), 3.04 (1 H, bs, OH), 4.12 (1 H, dd, J = 11.6, 7.9 Hz, $\text{CH}_\text{A}\text{H}_\text{B}\text{OAc}$), 4.30 (1 H, dd, J = 11.6, 3.5 Hz, $\text{CH}_\text{A}\text{H}_\text{B}\text{OAc}$), 5.01 (1 H, dd, J = 7.9, 3.5 Hz, $\text{CH}_\text{C}\text{OH}$), 7.49 (1 H, t, J = 7.7 Hz, 5-H), 7.62 (2 H, m, 4,6- H_2), 7.73 (1 H, t, J = 1.6 Hz, 2-H); MS (FAB^+) 206.0869 (MH^+ , 74) ($\text{C}_{11}\text{H}_{11}\text{NO}_3$ requires 206.0817), 188 (100).

A sample of **30** was transformed into the (R)-(+)- α -methoxy- α -(trifluoromethyl)-phenylacetic acid (MTPA) ester (see procedure below). An enantiomeric excess of 96% was calculated using the integration of the signal of the acetoxy group in the 270.05 Mz ^1H NMR spectrum. The methyl group showed singlets centred at 2.00 and 2.07 ppm (ratio 1:1 and 98:2 for the derivatives from racemic **33** and optically active **30** 3-(2-acetoxy-1-hydroxyethyl)benzonitrile).

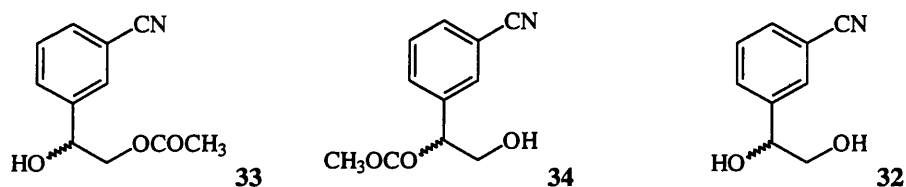
Similarly in the ^{19}F NMR spectrum, the CF_3 group showed signals at -71.5 and -71.9 ppm. Integration ratios were 1:1 and 98:2 corresponding to the esters of the racemic and asymmetrically prepared alcohols, respectively. Again 96% ee was calculated.



3-(1,2-Dihydroxyethyl)benzonitrile **32**

Method A: 3-(2-Hydroxyacetyl)benzonitrile **17** (80 mg, 0.50 mmol) was dissolved in ethanol (3 ml) and sodium borohydride (9.5 mg, 0.25 mmol) was added. The solution was stirred and the reaction followed by TLC (methanol / chloroform, 1:9). After a period of 30 min a further portion (10 mg) of sodium borohydride was added, and this was repeated for a total of 3 h. The ethanol was removed and the residue was extracted with ethyl acetate, the extracts were washed with water, dried and concentrated to give **32** (70 mg, 86%), as a pale yellow viscous liquid; R_f = 0.3 (methanol / chloroform, 1:9); IR (film) 3340-3410 (O-H), 2220 ($\text{C}\equiv\text{N}$); ^1H NMR (CDCl_3) δ 2.9 (1 H, bs, OH), 3.5 (1 H, bs, OH), 3.60 (1 H, dd, J = 11.3, 3.2 Hz, $\text{CH}_\text{A}\text{H}_\text{B}\text{OH}$), 3.78 (1 H, dd, J = 11.3, 8.1 Hz, $\text{CH}_\text{A}\text{H}_\text{B}\text{OH}$), 4.85 (1 H, dd, J = 3.2, 8.1 Hz, $\text{CH}_\text{C}\text{OH}$), 7.47 (1 H, t, J = 7.7 Hz, 5-H) 7.6 (2 H, m, 4,6- H_2), 7.72 (1 H, s, 2-H).

Method B: A solution of the mixture containing (\pm)-3-(2-acetoxy-1-hydroxy)benzonitrile **30** (250 mg, 1.2 mmol) (see method above) and concentrated aqueous ammonia solution (2.5 ml) in methanol (7.5 ml) was stirred for 45 min. The solvent was removed and the residue was taken up in anhydrous tetrahydrofuran and again concentrated. This was repeated twice and finally the residue was taken up in dichloromethane the solvent was evaporated to give **32** (183 mg) as a slightly yellow viscous oil; R_f = 0.3 (methanol / chloroform, 1:9); IR (film) 3340-3410 (O-H), 2220 (C \equiv N); ^1H NMR (CDCl_3) δ 2.25 (1 H, bs, OH), 2.9 (1 H, bs, OH), 3.62 (1 H, dd, J = 11.3, 7.5 Hz, $\text{CH}_\text{A}\text{H}_\text{B}\text{OH}$), 3.80 (1 H, dd, J = 11.3, 3.4 Hz, $\text{CH}_\text{A}\text{H}_\text{B}$), 4.86 (1 H, dd, J = 7.5, 3.4 Hz, $\text{CH}_\text{C}\text{OH}$), 7.48 (1 H, t, J = 7.7 Hz, 5-H), 7.6 (1 H, m, 4,6-H), 7.7 (1 H, s, 2-H).



(\pm)-3-(2-Acetoxy-1-hydroxyethyl)benzonitrile **33**

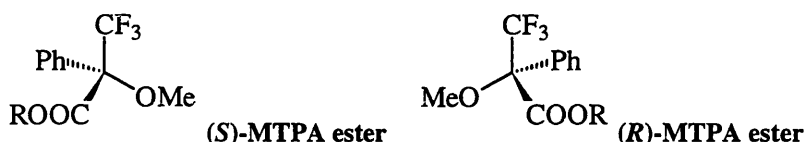
To 3-(2-acetoxyacetyl)benzonitrile **24** (300 mg, 1.5 mmol) in propan-2-ol (7 ml), was added sodium borohydride (95 mg, 2.5 mmol), dissolved in a minimum amount of propan-2-ol / water (5:1). The solution immediately became orange in colour. After 10 min, sufficient 2 M hydrochloric acid was added to dissipate the orange colour. The product was extracted with dichloromethane, washed twice with water, dried and concentrated to give a yellow oil (0.27 g). ^1H NMR analysis showed three products to be present:

3-(1,2-Dihydroxyethyl)benzonitrile **32** (32 mg, 13%); ^1H NMR (CDCl_3) δ 2.9 (2 H, bs, OH), 3.62 (1 H, m, CH_2) 3.80 (1 H, m, CH_2), 4.85 (1 H, m, CH), 7.48 (1 H, t, J = 7.7 Hz, 5-H), 7.6 (2 H, m, 4,6- H_2), 7.7 (1 H, s, 2-H).

3-(1-Acetoxy-2-hydroxyethyl)benzonitrile **34** (40 mg, 13%); ^1H NMR (CDCl_3) δ 2.17 (3 H, s, CH_3), 2.9 (1 H, bs, OH), 3.8 (2 H, m, CH_2), 5.85 (1 H, m, CH), 7.5 (1 H, t, J = 7.7 Hz, 5-H), 7.64 (2 H, m, 4,6-H), 7.7 (1 H, s, 2-H).

3-(2-Acetoxy-1-hydroxyethyl)benzonitrile 33 (198 mg, 65%); ^1H NMR (CDCl_3) δ 2.11 (3 H, s, COCH_3), 3.1 (1 H, bs, OH), 4.12 (1 H, dd, $J = 11.5, 3.5$ Hz $\text{CH}_\text{A}\text{H}_\text{B}\text{O}$), 4.29 (d, 1H, $J = 11.5, 8.5$ Hz $\text{CH}_\text{A}\text{H}_\text{B}\text{O}$), 5.03 (dd, 1H, $J = 8.5, 3.5$ Hz $\text{CH}_\text{C}\text{OH}$), 7.5 (t, 1H, 5-H), 7.6 (m, 2H, 4,6- H_2), 7.7 (s, 1H, 2-H).

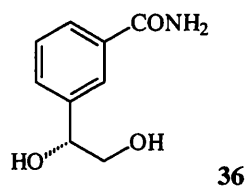
Attempts to separate these components were unsuccessful.



General method for the formation of α -Methoxy- α -(trifluoromethyl)-phenylacetic acid (MTPA) esters from racemic alcohols.

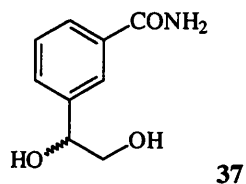
MTPA chloride: Oxalyl chloride in dichloromethane (2.0 M, 0.15 ml, 0.3 mmol) was added to either enantiomerically pure or racemic MTPA (234 mg, 0.1 mmol) in dichloromethane (0.85 ml) and dimethylformamide (10 μl) was added. The mixture was stirred overnight. The solution was then concentrated and the residue taken up into dichloromethane. The solvent was evaporated. This was repeated three times with dichloromethane and then once with hexane.

MTPA esters: A solution of racemic alcohol (0.1 mmol), pyridine (0.01 ml) and 4-(dimethylamino)pyridine (1 mg) in dichloromethane (1 ml) was added to the freshly prepared MTPA chloride. The mixture was stirred overnight and then partitioned between dichloromethane ($3 \times 15\text{ml}$) and potassium carbonate solution (10% w/v, 15ml). The organics were washed with copper sulphate solution (5% w/v) dried, concentrated and analysed by ^1H and ^{19}F NMR.



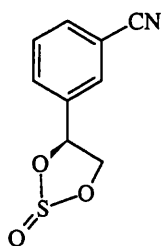
(-)-3-(1,2-Dihydroxyethyl)benzamide 36

(-)-3-(2-Acetoxy-1-hydroxyethyl)benzonitrile **16** (125 mg, 0.77 mmol) in ethanol (2.5 ml) was treated with 0.5 M sodium hydroxide solution (0.35 ml, 0.18 mmol) and 27.5% w/v hydrogen peroxide solution (0.3 ml, 2.4 mmol) as described for the synthesis of **6** above, to give a white glue, **36** (139 mg, 100%); $R_f = 0.1$ (chloroform / methanol, 9:1); ^1H NMR ($(\text{CD}_3)_2\text{SO}$) δ identical to that of the opposite enantiomer **6**; MS (FAB $^+$) 182.0816 (MH^+ , 100) ($\text{C}_9\text{H}_{11}\text{NO}_3$ requires 182.0817).



(±)-3-(1,2-Dihydroxyethyl)benzamide 37

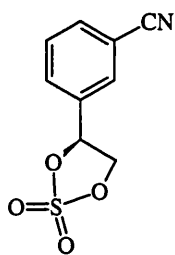
(±)-3-(1,2-Dihydroxyethyl)benzonitrile **32** (170 mg, 1.0 mmol) in ethanol (5 ml), was treated with 0.5 M sodium hydroxide solution (0.5 ml, 3.6 mmol) and 27.5% w/v hydrogen peroxide solution as described for the synthesis of **6** above to give **37** (188 mg, 99%) as a white gum; $R_f = 0.08$ (methanol / chloroform, 1:9); IR (KBr) 3360, 3200 (N-H), 3200-3500 (O-H), 1670 (amide I), 1615 (amide II); ^1H NMR ($(\text{CD}_3)_2\text{SO}$) δ 3.44 (2 H, d, $J = 5.8$ Hz, CH_2), 3.5 (2 H, bs, OH), 4.57 (1 H, t, $J = 5.8$ Hz, CH), 7.33 (1 H, bs, NH), 7.37 (1 H, t, $J = 7.7$ Hz, 5-H), 7.48 (1 H, d, $J = 7.7$ Hz, 4-H), 7.73 (1 H, d, $J = 7.7$ Hz, 6-H), 7.85 (1 H, s, 2-H), 7.96 (1 H, bs, NH); MS (CI) 182 (MH^+ , 35), 164 (100).



38

4(S)-4-(3-Cyanophenyl)-1,3,2-dioxathiolane-2-oxide 38

To a solution of (+)-3-(1,2-dihydroxyethyl)benzonitrile **18** (65 mg, 0.40 mmol) in dry carbon tetrachloride (1.4 ml), thionyl chloride (0.035 ml, 0.48 mmol) in dry carbon tetrachloride (0.4 ml) was added. The mixture was heated to reflux for 30 min, then allowed to cool. The solvent was evaporated to give a brown oil (85 mg) which was carried through to the next stage without further purification. The crude product was the cyclic sulphite, **38** (85 mg, *ca.* 100%); $R_f = 0.6$ (methanol / chloroform, 1:19); $^1\text{H NMR}$ ($(\text{CD}_3)_2\text{SO}$) δ 4.26 (1 H, dd, $J = 8.8, 6.5$ Hz, $\text{CH}_\text{A}\text{H}_\text{B}$ [diastereomer I]), 4.45 (1 H, dd, $J = 9.2, 10.3$ Hz, $\text{CH}_\text{A}\text{H}_\text{B}$ [diastereomer II]), 4.9 (1 H, dd, $J = 9.2, 6.6$ Hz, $\text{CH}_\text{A}\text{CH}_\text{B}$ [II]), 5.05 (1 H, dd, $J = 8.8, 6.5$ Hz, $\text{CH}_\text{A}\text{H}_\text{B}$ [I]), 5.51 (1 H, dd, $J = 10.3, 6.6$ Hz, $\text{CH}_\text{C}\text{O}$ [II]), 6.0 (1 H, t, $J = 6.5$ Hz, $\text{CH}_\text{C}\text{O}$ [I]), 7.5-7.8 (2×4 H, m, Ar- H_4 [I, II]).

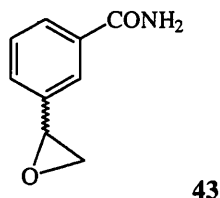


39

4-(3-Cyanophenyl)-1,3,2-dioxathiolane-2,2-dioxide 39

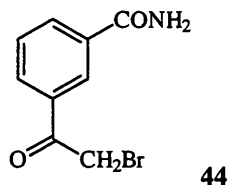
Attempted synthesis: To an ice-cold solution of the cyclic sulphite **38** (85mg, 0.41 mmol) in acetonitrile (0.4 ml) and carbon tetrachloride (0.4 ml), sodium iodate (0.128 g, 0.60 mmol) was added, followed by ruthenium (III) chloride (1 mg) and water (0.6 ml). The resulting mixture was stirred for 60 min at ambient temperature. After dilution with diethyl ether (4 ml), the organic extract was washed successively with water, saturated sodium hydrogen carbonate solution

and saturated sodium chloride solution was dried and concentrated. This gave a brown oil which ^1H NMR analysis showed was mainly the diol **18**.



(±)-3-(Oxiran-2-yl)benzamide **43**

3-(2-Bromoacetyl)benzamide **43** (0.50 g, 2.1 mmol) was suspended in ethanol (6 ml) and cooled to 0°C . Sodium borohydride (47 mg, 1.2 mmol) was added and the mixture was stirred at 0°C for 30 min, then at ambient temperature for 2 h. Following the addition of sodium hydroxide solution (1 M 1.5 ml, 1.5 mmol) the solution was stirred for 20 min at ambient temperature and then for 10 min at 50°C . Water was added and the resulting mixture was extracted three times with dichloromethane. The organic extract was washed with brine, dried and concentrated to give **43** (331 mg, 98%) as colourless crystals; $R_f = 0.38$ (hexane / acetone, 1:2); mp $95.5\text{--}97^\circ\text{C}$; ^1H NMR ($(\text{CD}_3)_2\text{SO}$) δ 2.89 (1 H, m, oxirane 3-H), 3.15 (1 H, t, $J = 4.8$ Hz, oxirane 3-H), 3.99 (1 H, m, oxirane 2-H), 7.40 (1 H, bs, NH), 7.44 (2 H, m, 4,5- H_2), 7.79 (2 H, m, 2,6- H_2), 8.01 (1 H, bs, NH); MS (FAB^+) 164.0736 (MH^+ , 100) ($\text{C}_9\text{H}_9\text{NO}_2$ requires 164.0712); Anal Calcd for $\text{C}_9\text{H}_9\text{NO}_2$: C, 66.25; H, 5.56; N, 8.58. Found: C, 66.0; H, 5.67; N, 8.38.

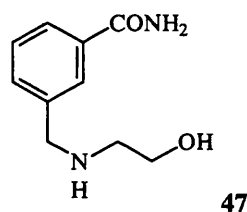


3-(2-Bromoacetyl)benzamide **44**

Method A: 3-Acetylbenzamide **11** (2.0 g, 12 mmol) was suspended in chloroform (10 ml) and the mixture was cooled to 0°C . Bromine (0.64 ml, 2.0 g, 12 mmol) in chloroform (5 ml) was added dropwise to the cooled suspension.

After 2 d, the reaction mixture was heated to 50°C for 1 h. The solvent was evaporated. Flash chromatography (methanol /ethyl acetate 1:49) of the solid remaining was unsuccessful in separating its components, however, recrystallisation of one of the fractions yielded **44** (486 mg, 16%) as colourless crystals; $R_f = 0.45$ (hexane / acetone 1:2); mp 133-135°C (from acetonitrile); ^1H NMR ($(\text{CD}_3)_2\text{SO}$) δ 4.67 (2 H, s, CH_2), 6.82 (1 H, bs, NH), 7.59 (1 H, t, $J = 7.8$ Hz, 5-H), 8.01 (1 H, bs, NH), 8.12 (1 H, dt, $J = 7.8, 1.5$ Hz) and 8.21 (1 H, dt, $J = 7.8, 1.5$ Hz) (4,6- H_2), 8.57 (1 H, t, $J = 1.5$ Hz, 2-H); MS (FAB^+) 243.9796 ($([\text{}^{81}\text{Br}]\text{M}+\text{H})^+$, 100) ($\text{C}_9\text{H}_8\text{}^{81}\text{BrNO}_2$ requires 243.9796), 241.9810 ($([\text{}^{79}\text{Br}]\text{M}+\text{H})^+$, 100) ($\text{C}_9\text{H}_8\text{}^{79}\text{BrNO}_2$ requires 241.9817); Anal. Calcd. for $\text{C}_9\text{H}_8\text{BrNO}_2$: C, 44.66; H, 3.33; N, 5.79. Found: C, 44.8; H, 3.33; N, 5.78.

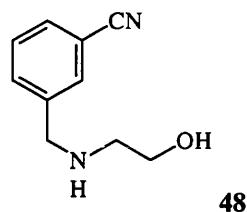
Method B: 3-Acetylbenzamide **11** (2.0 g, 12 mmol) was added to glacial acetic acid (180 ml) warmed to 60°C. Bromine (0.634 ml, 1.966 g, 12 mmol) was added to the stirred solution and stirring was continued at ambient temperature for 2.5 h. The acetic acid was evaporated. Recrystallisation of the residue from acetonitrile gave **44** (1.74 g, 48 %) as colourless crystals; data identical to those given above. **44** is reported in the literature²⁶⁶ but was not isolated or characterised).



3-[N-(2-hydroxyethyl)methylamino]benzamide **47**

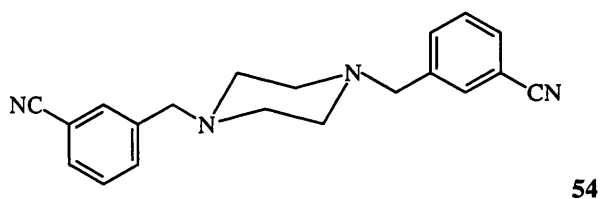
3-Chloromethylbenzamide **1** (0.5 g, 2.9 mmol) in ethanol (1 ml) was added to a solution of ethanolamine (0.5 ml, 0.51 g, 8.4 mmol) in ethanol (5 ml) over the course of 2 h. The solution was stirred at ambient temperature for 7 d. The ethanol was evaporated and the ethanolamine removed on the Kugelrohr apparatus to give **47** as a colourless gum; ^1H NMR ($(\text{CD}_3)_2\text{SO}$) δ 2.83 (2 H, t, $J = 5.5$ Hz, $\text{CH}_2\text{CH}_2\text{OH}$), 3.58 (2 H, t, $J = 5.5$ Hz, CH_2OH), 3.83 (2 H, s, PhCH_2),

5.5 (2 H, bs, NH, OH), 7.38 (1 H, bs, NH), 7.41 (1 H, t, $J = 8.0$ Hz, 5-H), 7.55 (1 H, d, $J = 8.0$ Hz, 6-H), 7.77 (1 H, d, $J = 8.0$ Hz, 4-H), 7.90 (1 H, s, 2-H), 8.05 (1 H, bs, NH); MS (FAB⁺) 195.1144 (MH⁺, 100) (C₁₀H₁₅N₂O₂ requires 195.1134).



3-(*N*-(2-hydroxyethyl)aminomethyl)benzonitrile **48**

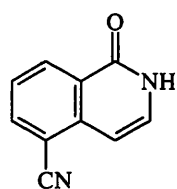
3-Bromomethylbenzonitrile (5.0 g, 26 mmol) was added in several portions to ethanolamine (5.0 ml, 5.1 g, 84 mmol) in ethanol (50 ml). The solution was stirred for 7 d. The solvent was evaporated and the residue, in dichloromethane, was washed twice with water, dried and concentrated. The product was recrystallised from ethyl acetate to give **48** (2.96 g, 66%) as colourless crystals; $R_f = 0.23$ (ethyl acetate / hexane, 1:1); mp 98-99°C; IR (KBr) 3250 (O-H), 2220 (C≡N); ¹H NMR (CDCl₃) δ 2.42 (2 H, bs, NH, OH), 2.78 (2 H, t, $J = 5.1$ Hz, CH₂CH₂OH), 3.69 (2 H, t, $J = 5.1$ Hz, CH₂CH₂OH), 3.85 (2 H, s, Ar-CH₂), 7.44 (1 H, t, $J = 7.7$ Hz, 5-H), 7.55 (2 H, m, 4,6-H₂), 7.65 (1 H, s, 2-H); MS (CI) 177.1028 (MH⁺, 100) (C₁₀H₁₂N₂O requires 177.1028), 145 (45); Anal. Calcd. for C₁₀H₁₂N₂O: C, 68.16; H, 6.86; N, 15.90: Found: C, 68.3; H, 6.69; N, 15.7.



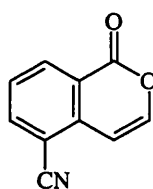
3-(Aziridin-1-ylmethyl)benzonitrile **50**

Method A: A solution of 3-[*N*-(2-Hydroxyethyl)methylamino]benzonitrile **48** (0.5 g, 2.8 mmol), dry carbon tetrachloride (0.29 ml, 2.8 mmol), triphenylphosphine (0.85 g, 3.2 mmol) and dry triethylamine (0.4 ml, 2.8 mmol) in dry acetonitrile (5 ml) was stirred at ambient temperature for 24 h. The

reaction mixture was filtered and the solid washed with acetonitrile. The filtrate was concentrated and the residue extracted four times with hot petroleum ether. The combined extracts were stored at 4°C for 48 h. The crystals of triphenylphosphine oxide that formed were filtered and the filtrate concentrated to give a slightly yellow oil. ¹H NMR analysis showed that this was a mixture of the desired aziridine **50**, the amino alcohol, **48**, 1,4-di-(3-cyanophenylmethyl)piperazine **54** and triphenyl phosphine oxide in the molar ratio; 12 : 4 : 2 : 4. However attempts to separate these products by flash chromatography (alumina (as above), hexane / ethyl acetate, 7:3), yielded only triphenylphosphine oxide (22 mg) and the piperazine **54** (82 mg, 18%) as white crystals; R_f = 0.8 (hexane / ethyl acetate, 1:1); mp 120-122°C; IR (KBr) 2230 (C≡N); ¹H NMR (CDCl₃) δ 2.48 (8 H, bs, piperazine CH₂), 3.54 (4 H, s, ArCH₂), 7.41 (2 H, t, *J* = 7.7 Hz, 5-H), 7.55 (4 H, m, 4, 6-H₂), 7.66 (2 H, s, 2-H); MS (CI) 317.1766 (MH⁺, 100) (C₂₀H₂₀N₄ requires 317.1766), 279 (68), 203 (72). The estimated, un-isolated yield of 3-(aziridin-1-ylmethyl)benzonitrile **50** was (130 mg, 29%); ¹H NMR (CDCl₃) δ 1.30 (2 H, def t, *trans*-H), 1.69 (2 H, def t, *cis*-H), 3.36 (2 H, s, ArCH₂), 7.55-7.8 (4 H, m, Ar H).



59



72

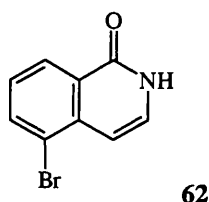
5-Cyanoisoquinolin-1-one **59**

Method A: ²²³ 2,6-Dicyanotoluene **71** (2.0 g, 14 mmol) in freshly distilled ethyl formate (50 ml) was stirred at 0-5°C with potassium *tert*-butoxide (8.7 g, 77 mmol) for 25 min. A yellow precipitate formed, diethyl ether was added and the suspension was filtered. The yellow solid was dissolved in water and the solution was acidified with acetic acid, saturated with sodium chloride and extracted with chloroform. The organic extract was dried and concentrated. Chromatography (twice) (chloroform / ethyl acetate, 2:1, hexane / ethyl acetate, 4:1) yielded:

5-Cyanoisoquinolin-1-one 59 (0.30 g, 12.5%); pale yellow solid; $R_f = 0.22$ (chloroform / ethyl acetate, 2:1); mp 296-300°C (lit.²²³ 275°C, sublimation at 265°C); IR (KBr) 3500, 3300 (N-H), 2230 (C≡N), 1690, 1660 (C=O); ^1H NMR ($(\text{CD}_3)_2\text{SO}$) δ 6.60 (1 H, $J = 7.0$ Hz, 4-H), 7.47 (1 H, d, $J = 7.0$ Hz, 3-H), 7.63 (1 H, t, $J = 7.7$ Hz, 7-H), 8.26 (1 H, d, $J = 7.7$ Hz, 6-H), 8.47 (1 H, d, $J = 7.7$ Hz, 8-H), 11.72 (1 H, bs, NH); MS (EI) 171.0512 (M^+ , 10) ($^{13}\text{CC}_9\text{H}_6\text{N}_2\text{O}$ requires 171.0514), 170.0480 (M^+ , 100) ($\text{C}_{10}\text{H}_6\text{N}_2\text{O}$ requires 170.0480).

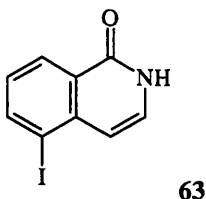
5-Cyanoisocoumarin 72 (0.33 g, 14%); colourless crystals; $R_f = 0.85$ (chloroform / ethyl acetate, 2:1); mp 212-214°C; IR (KBr) 2240 (C≡N), 1735 (C=O); ^1H NMR (CDCl_3) δ 6.88 (1 H, d, $J = 5.7$ Hz, 4-H), 7.46 (1 H, d, $J = 5.7$ Hz, 3-H), 7.64 (1 H, t, $J = 7.7$ Hz, 7-H), 8.05 (1 H, d, $J = 7.7$ Hz, 6-H), 8.52 (1 H, d, $J = 7.7$ Hz, 8-H); MS (EI) 171 (M^+ , 50), 143 (100); MS (EI) 172.0353 (M^+ , 5) ($^{13}\text{CC}_9\text{H}_5\text{NO}_2$ requires 172.0353), 171.0319 (M^+ , 47) ($\text{C}_{10}\text{H}_5\text{NO}_2$ requires 171.0320), 143 (100).

Method B: *E*-2-(2,6-Dicyanophenyl)-*N,N*-dimethylethenamine **81** (0.30 g, 1.5 mmol) in dry methanol (50 ml) was saturated with hydrogen chloride gas. The mixture was then boiled under reflux for 3 d. The solution was concentrated and stirred with 10% sodium carbonate solution for 30 min. The aqueous suspension was extracted several times with ethyl acetate and the extract was dried and concentrated. Recrystallisation of the residue from ethyl acetate and chromatography of the mother liquor (hexane / ethyl acetate, 4:1) gave **59** (141 mg, 55%) as an off-white solid; $R_f = 0.31$ (hexane / ethyl acetate, 1:1); mp 296-300°C; data identical to those above (see method A). Chromatography of the crude product also yielded 5-cyanoisocoumarin **72** (13 mg, 5%); data as above.



5-Bromoisoquinolin-1-one **62**

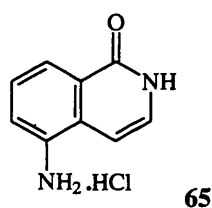
Triethylamine (2.2 ml, 1.6 g, 16 mmol), in dry acetone (3 ml), was added to **104** (3 g, 13 mmol), in dry acetone (35 ml) at 0°C. Ethyl chloroformate (1.5 ml, 1.72 g, 16 mmol), in dry acetone (3 ml) was added and the mixture was stirred at 0°C for 30 min. Sodium azide (1.2 g, 19 mmol), in water (3 ml), was added portionwise over 15 min. The mixture was poured on to ice and was extracted with dichloromethane. The extract was dried (calcium chloride) and was added carefully to boiling diphenyl ether (10 ml). The solution was boiled under reflux for 1 h. Evaporation, chromatography (diethyl ether) and recrystallisation (acetonitrile) gave **62** (305 mg, 10%) as white needles; $R_f = 0.1$ (hexane / ethyl acetate, 1:1); mp 242–244°C; IR (KBr) 3300, 3170 (N-H), 1680, 1660 (C=O); ^1H NMR ($(\text{CD}_3)_2\text{SO}$) δ 6.65 (1 H, d, $J = 7.3$ Hz, 4-H), 7.36 (1 H, t, $J = 7$ Hz, 7-H), 7.42 (1 H, d, $J = 7.3$ Hz, 3-H), 8.02 (1 H, d, $J = 7$ Hz, 6-H), 8.21 (1 H, d, $J = 7$ Hz, 8-H), 11.55 (1 H, bs, NH); MS (EI) 224.9628 ($[\text{}^{81}\text{Br}]\text{M}^+$, 100) ($\text{C}_9\text{H}_6\text{}^{81}\text{BrNO}$ requires 224.9612), 222.9635 ($[\text{}^{79}\text{Br}]\text{M}^+$, 100) ($\text{C}_9\text{H}_6\text{}^{79}\text{BrNO}$ requires 222.9633); Anal. Calcd. for $\text{C}_9\text{H}_6\text{BrNO}$: C, 48.25; H, 2.70; N, 6.25. Found: C, 47.9 ; H, 2.59; N, 6.14.



5-Iodoisoquinolin-1-one **63**

E-3-(2-Iodophenyl)propenoic acid **115** (4.00 g, 15 mmol) was stirred with thionyl chloride (10 ml) and dimethylformamide (5 μl) for 16 h. The thionyl chloride was removed by distillation at atmospheric pressure. The residue, in 1,4-dioxan

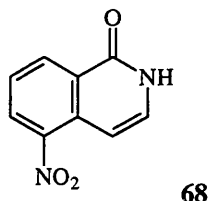
(5 ml), was added in portions to sodium azide (2.85 g, 44 mmol) in water (6 ml) and 1,4-dioxan (6 ml) over 15 min. The mixture was stirred for 45 min and water (11 ml) was added. The suspension was extracted three times with dichloromethane. The combined extracts were dried and the solvent was evaporated. The residue, in dichloromethane (10 ml), was added carefully to boiling dry bis(2-(2-methoxyethoxy)ethyl) ether (12 ml) in portions. The solution was boiled under reflux for 1 h. The precipitate that formed on cooling was recrystallised from acetone to give **63** (1.65 mg, 42%) as white needles; $R_f = 0.24$ (hexane / ethyl acetate, 1:1); mp 238-244°C (decomp.); IR (KBr) 3400 (N-H) 1660, 1630 (C=O); $^1\text{H NMR}$ ($(\text{CD}_3)_2\text{SO}$) δ 6.57 (1 H, d, $J = 7.7$ Hz, 4-H), 7.25 (1 H, t, $J = 7.7$ Hz, 7-H), 7.32 (1 H, d, $J = 7.3$ Hz, 3-H), 8.23 (2 H, m, 6,8-H₂), 11.5 (1 H, bs, NH); MS (EI) 270.9492 (M^+ , 100) ($\text{C}_9\text{H}_6\text{INO}$ requires 270.9494); Anal. Calcd. for $\text{C}_9\text{H}_6\text{INO}$: C, 39.88; H, 2.23; N, 5.17. Found: C, 39.8; H, 2.32; N, 5.06.



5-Aminoisoquinolin-1-one hydrochloride **65**

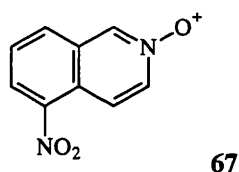
To a solution of 5-nitroisoquinolin-1-one **68** (160 mg, 0.84 mmol) in ethanol (10 ml) and concentrated hydrochloric acid (0.4 ml), a slurry of 10% palladium on charcoal (0.10 g) in ethanol (2 ml) was added. The mixture was stirred under H_2 for 1 h. The suspension was then filtered through Celite®. The Celite® pad and residue were suspended in water (200 ml) and heated. The hot suspension was filtered through a second Celite® pad. Concentration of the filtrate and drying gave **65** (110 mg, 66%) as white crystals; $R_f = 0.05$ (methanol / chloroform, 1:9); mp 250-260°C dec. (lit.²²³ 273-276°C dec. [blackening at 267°C]); IR (KBr) 3410, 3180, 3040-2850 (N-H), 1685, 1650 (C=O); $^1\text{H NMR}$ (D_2O) δ 6.76 (1 H, d, $J = 7.5$ Hz, 4-H), 7.39 (1 H, d, $J = 7.5$ Hz, 3-H), 7.59 (1 H, t, $J = 8.0$ Hz, 7-H),

7.79 (1 H, d, $J = 8.0$ Hz, 6-H), 8.27 (1 H, d, $J = 8.0$ Hz, 8-H); MS (EI) 161 (M^+ , 12), 160 (M^+ (free base), 100).



5-Nitroisoquinolin-1-one **68**

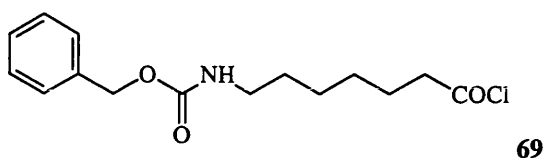
5-Nitroisoquinolin-1-one *N*-oxide **67** (8.6 g, 45 mmol) was suspended in acetic anhydride (150 ml) and stirred at 100°C for 7 d. The cooled solution was concentrated and the residue was boiled with 10% w/v sodium carbonate solution (400 ml) for 1 h. The suspension was filtered, the filtrate was concentrated, taken up in enough water to dissolve the inorganics and filtered again. The dark brown solid remaining was purified by extraction, several times, with hot toluene, which, on cooling, gave **68** (2.6, 30 %) as buff crystals; $R_f = 0.26$ (methanol / chloroform, 1:19); mp 250-252°C (softening at 230°C) (lit.²⁶⁷ 250°C); ^1H NMR ($(\text{CD}_3)_2\text{SO}$) δ 6.98 (1 H, d, $J = 7.7$ Hz, 4-H), 7.45 (1 H, d, $J = 7.7$ Hz, 3-H), 7.67 (1 H, t, $J = 8.0$ Hz, 7-H), 8.47 (1 H, d, $J = 7.7$ Hz, 8-H), 8.58 (1 H, d, $J = 8.0$ Hz, 6-H), 11.8 (1 H, bs, NH); MS (CI) 191 ($M\text{H}^+$, 100).



5-Nitroisoquinoline *N*-oxide **67**

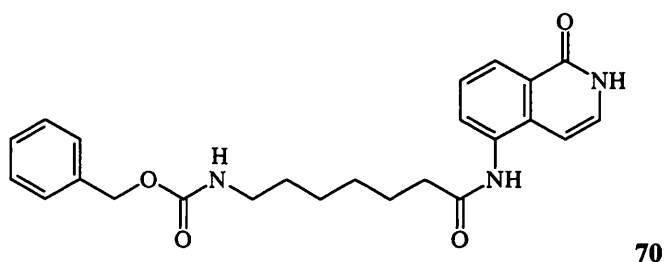
Finely divided 5-nitroisoquinolin-1-one (12.5 g, 72 mmol) was suspended in glacial acetic acid (125 ml) and 27.5% w/v hydrogen peroxide solution (45 ml, 364 mmol) was added. The solution was stirred at ambient temperature for 3 h and was heated to reflux for 36 h. The acetic acid was evaporated under reduced pressure and the residue was suspended in water, filtered, washed thoroughly with water and dried to give **67** (12.8 g, 94%) as a yellow solid; $R_f = 0.20$

(methanol / chloroform, 1:19); mp 221-223 (lit²⁶⁸ 220°C); IR (KBr) 1280 (N⁺-O); ¹H NMR (CD₃CO₂D) δ 7.93 (1 H, t, *J* = 7.5 Hz, 7-H), 8.40 (1 H, d, *J* = 7.5 Hz, 8-H), 8.61 (1 H, d, *J* = 7.5 Hz, 6-H), 8.5-8.7 (2 H, m, 3,4-H₂), 9.42 (1 H, s, 1-H); MS (EI) 190 (M⁺, 100).



6-(Phenylmethoxycarbonylamino)hexanoyl chloride **69**

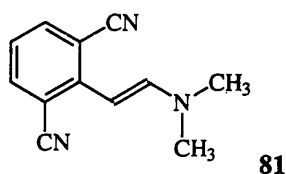
6-(Phenylmethoxycarbonylamino)hexanoic acid (187 mg, 0.71 mmol), 2.0 M oxalyl chloride solution in dichloromethane (0.7 ml, 1.41 mmol) and DMF (50 µl) were stirred in dichloromethane (2 ml) at ambient temperature for 3 h. The solvent was evaporated and the residue was taken up in dichloromethane which was then evaporated. This process was repeated. The yellow oil that remained was taken through to the next stage without further purification.



5-[6-(Phenylmethoxycarbonylamino)hexanoylamino]isoquinolin-1-one **70**

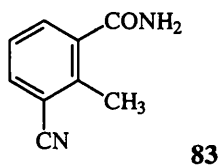
The freshly prepared 6-(phenylmethoxycarbonylamino)hexanoyl chloride **69** (201 mg, 0.71 mmol) and 5-aminoisoquinolin-1-one **68** (100 mg, 0.51 mmol) were stirred in pyridine (4 ml) for 24 h. The mixture was partitioned between 2 M hydrochloric acid and diethyl ether; a pale pink solid remained undissolved in both phases. This was collected and dried to give **70** (60 mg, 42%); *R*_f = 0.20 (methanol / chloroform, 1:9); mp 186-188°C; 1.5 (4 H, m, CH₂CH₂CH₂CO), 1.76

(2 H, qu, $J = 6.7$ Hz, NHCH_2CH_2), 2.48 (2 H, t, $J = 6.7$ Hz, $\text{CH}_2\text{CH}_2\text{CO}$), 3.15 (2 H, t, $J = 6.7$ Hz, NHCH_2), 5.05 (2 H, s, PhCH_2), 6.70 (1 H, d, $J = 7.4$ Hz, isoquinolinone 4-H), 7.20 (1 H, d, $J = 7.4$ Hz, isoquinolinone 3-H), 7.30 (5 H, m, Ph-H_5), 7.50 (1 H, t, $J = 8.0$ Hz, 7-H), 7.77 (1 H, d, $J = 8.0$ Hz, 8-H), 8.20 (1 H, d, $J = 8.0$ Hz, 6-H); MS (FAB⁺) 408.1908 (MH^+ , 24) ($\text{C}_{23}\text{H}_{26}\text{N}_3\text{O}_4$ requires 408.1923).



E*-2-(2,6-Dicyanophenyl)-*N,N*-dimethylethenamine **81*

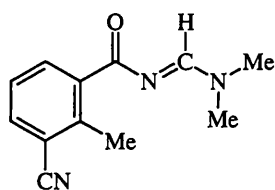
A suspension of 2,6-dicyanotoluene (1.0 g, 7.0 mmol) in dimethylformamide dimethylacetal (10 ml) was boiled under reflux for 4 d. The solvent was evaporated and the yellow-brown residue was recrystallised from ethanol to give **81** (0.973 g, 71%) as a bright yellow solid; $R_f = 0.65$ (hexane / ethyl acetate, 7:3); mp 117-119°C; ^1H NMR (CDCl_3) δ 3.00 (6 H, s, NMe_2), 5.36 (1 H, d, $J = 13.6$ Hz, $\text{ArCH}=\text{C}$), 6.94 (1 H, t, $J = 7.7$ Hz, 5-H), 7.63 (2 H, d, $J = 7.7$ Hz, 4,6-H), 7.77 (1 H, d, $J = 13.6$ Hz, $\text{C}=\text{CHN}$); MS (EI) 197.0960 (M^+ , 100) ($\text{C}_{12}\text{H}_{11}\text{N}_3$ requires 197.0953), 182 (25), 155 (30).



2-Cyano-2-methylbenzamide **83**

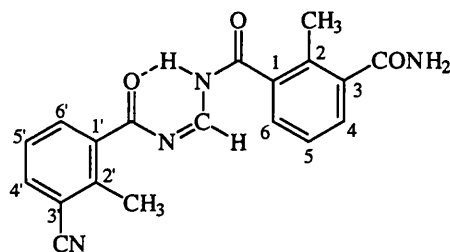
To 2,6-dicyanotoluene (13.0 g, 21 mmol) in ethanol (75 ml) and 0.5 M sodium hydroxide solution (10.5 ml), 27.5 % w/v hydrogen peroxide solution (7.0 ml, 57 mmol) was added in small portions. The solution was stirred for 1 h. and was extracted several times with ethyl acetate. The combined organic extracts were

dried and concentrated. The residue was recrystallised from ethyl acetate to give **83** (1.62 g, 48%) as a white crystalline solid; $R_f = 0.32$ (methanol / chloroform, 1:9); mp 186-188°C; IR (KBr) 3420, 3350 (N-H), 2218 (C≡N), 1680 (amide I), 1625 (amide II); ^1H NMR (CDCl_3 , $(\text{CD}_3)_2\text{SO}$) δ 2.65 (3 H, s, CH_3), 6.94 (1 H, bs, NH), 7.36 (1H, t, $J = 7.7$ Hz, 5-H), 7.52 (1 H, bs, NH), 7.65 (2 H, m, 4,6- H_2); MS (EI) 160.0634 (M^+ , 100) ($\text{C}_9\text{H}_8\text{N}_2\text{O}$ requires 160.0637), 144 (7).



3-Cyano-*N*-(dimethylaminomethylene)-2-methyl benzamide **84**

2-Cyano-2-methylbenzamide **83**, dimethylformamide dimethyl acetal (0.183 ml, 164 mg, 1.25 mmol) and dimethylformamide (1 ml) were boiled under reflux for 3 h. Water was added and the mixture was extracted with dichloromethane four times. The organic extracts were washed with water and saturated sodium chloride solution, dried and concentrated to give **84** (114 mg, 83%) as a yellow solid; $R_f = 0.57$ (methanol/ chloroform, 1:9); mp 98-100°C; ^1H NMR (CDCl_3) δ 2.81 (3 H, s, Ar- CH_3), 3.19 (3 H, s, NCH_3), 3.23 (3 H, s, NCH_3), 7.33 (1 H, t, $J = 7.7$ Hz, 5-H), 7.65 (1 H, d, $J = 7.7$ Hz, 4-H), 8.18 (1 H, d, $J = 7.7$ Hz, 6-H), 8.62 (1 H, s, $\text{N}=\text{CH}$); MS (FAB^+) 216.1139 (MH^+ , 100) ($\text{C}_{12}\text{H}_{14}\text{N}_3\text{O}$ requires 216.1137)

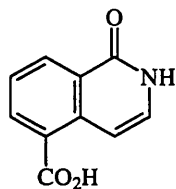


85

***N*-(3-Carbamoyl-2-methylbenzoyl)-*N'*-(3-cyano-2-methylbenzoyl)formamidine**

85

To anhydrous 4-methylbenzenesulphonic acid (0.361 g, 2.1 mmol) in toluene (10 ml), **84** (0.30 g, 1.4 mmol) was added and the resulting mixture was refluxed for 13 h. The solvent was evaporated and the residue, in dichloromethane, was washed with water and 10% sodium carbonate solution and was dried. Concentration and recrystallisation from dichloromethane gave **85** (132 mg, 27%) as white crystals; $R_f = 0.33$ (methanol / chloroform, 1:19); mp 160-162°C; IR (KBr) 3370, 3190 (N-H), 2210 (C≡N), 1735 (C=O), 1690 (amide I), 1655 (amide II); ^1H NMR ((CD₃)₂SO) δ 2.59 (3 H, s, Ar-CH₃), 2.63 (3 H, s, Ar-CH₃), 7.50 (1 H, t, $J = 7.7$ Hz, 5-H), 7.60 (1 H, t, $J = 7.7$ Hz, 5'-H), 7.71 (1 H, d, $J = 7.7$ Hz, 4'-H), 7.72 (1 H, bs, CONH₂), 7.90 (2 H, d, $J = 7.7$ Hz, 4, 6-H₂), 8.00 (1 H, bs, CONH₂), 8.04 (1 H, d, $J = 7.7$ Hz, 6'-H), 9.22 (1 H, s, CHC=N), 11.78 (1 H, bs, NHC=N); MS (CI) 349 (MH⁺, 40 %).

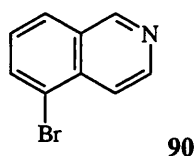


89

(1-Oxoisquinoline-5-carboxylic acid **89)**

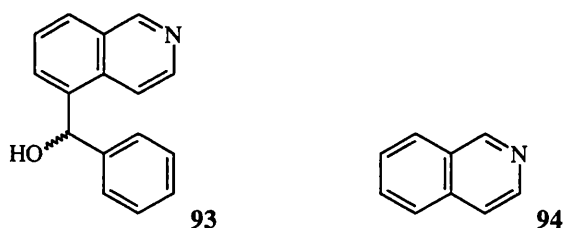
5-Cyanoisoquinolin-1-one **59** (0.427 g, 2.5 mmol) was boiled under reflux with potassium hydroxide in ethanol (20% w/v, 12 ml), under nitrogen, until the production of ammonia ceased (3 d). The mixture was acidified with

concentrated hydrochloric acid and the solvent was evaporated. The residue was taken up into methanol and filtered. Concentration of the filtrate gave **89** (0.394 g, 83%) as a pale yellow solid; $R_f = 0.02$ (chloroform / methanol / acetic acid, 100:10:1); mp $>300^\circ\text{C}$; IR (KBr) 3400 (N-H), 3400-2700 (O-H), 1705, 1655, 1625 (C=O); ^1H NMR (CD_3OD) δ 7.26 (1 H, d, $J = 7.7$ Hz, 4-H), 7.58 (1 H, t, $J = 7.7$ Hz, 7-H), 7.75 (1 H, d, $J = 7.7$ Hz, 3-H), 8.41 (1 H, d, $J = 7.7$ Hz, 8-H), 8.55 (1 H, d, $J = 7.7$ Hz, 6-H); MS (EI) 190.0458 (M^+ , 11) ($^{13}\text{C}_9\text{H}_7\text{NO}_3$ requires 190.0459), 189.0425 (M^+ , 100) ($\text{C}_{10}\text{H}_7\text{NO}_3$ requires 189.0426). (This compound has been reported²²³ but only as an intermediate and was not characterised.)



5-Bromoisoquinoline **90**

5-Aminoisoquinoline **91** (4.8 g, 33 mmol) was dissolved in 48% hydrobromic acid (12 ml), water (13 ml) was added and the solution was cooled to 0°C . The solution was diazotised with sodium nitrite (2.3 g, 33 mmol) in water (15 ml) and was added slowly to a solution of cuprous bromide (5.8 g, 40 mmol) in 48% hydrobromic acid (48 ml) at 75°C . The solution was then stirred at ambient temperature for 24 h. The reaction mixture was basified (2.5 M sodium hydroxide solution) and steam distilled. The aqueous distillate was extracted with ethyl acetate and the organic extracts were dried and concentrated to give **90** (2.67 g, 39%) as white crystals; $R_f = 0.58$ (hexane / ethyl acetate, 1:1); mp $81-83^\circ\text{C}$ (lit.²⁶⁹ $82-84^\circ\text{C}$); ^1H NMR (CDCl_3) δ 7.48 (1 H, t, $J = 7.8$ Hz, 7-H), 7.97 (3 H, m, 4,6,8- H_3), 8.65 (1 H, d, $J = 6.0$ Hz, 3-H), 9.24 (1 H, s, 1-H).



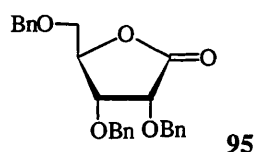
5-(1-Hydroxy-1-phenylmethyl)isoquinoline **93**

5-Bromoisoquinoline **90** (208 mg, 1.0 mmol) in dry tetrahydrofuran (6.25 ml) was stirred under nitrogen and cooled to -116°C (liquid N_2 / Et_2O). Butyllithium in hexane (2.5 M, 0.4 ml, 1.0 mmol) was added and stirring continued for a further 10 min. Benzaldehyde (0.1 ml, 104 mg, 0.98 mmol) in dry tetrahydrofuran (1.0 ml) was added and the mixture was allowed to reach ambient temperature. Ammonium chloride solution (20%, 1 ml) was added and after being stirred for 5 min, the solvent was evaporated. The residue, in dichloromethane, was basified (saturated sodium hydrogen carbonate solution). The organic extract was dried. Evaporation and chromatography (hexane / ethyl acetate, 3:2) gave:

Isoquinoline 94 (4 mg, 3 %); a pale yellow oil; $R_f = 0.54$ (hexane / ethyl acetate, 1:1); ^1H NMR (CDCl_3) δ 7.66 (3 H, m, 4,6,7- H_3), 7.82 (1 H, d, $J = 8.1$ Hz, 5-H), 7.98 (1 H, d, $J = 8.1$ Hz, 8-H), 8.53 (1 H, d, $J = 5.9$ Hz, 3-H), 9.26 (1 H, s, 1-H) (identical to an authentic sample).

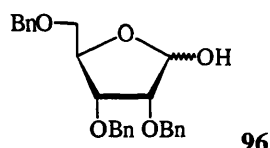
5-Bromoisoquinoline 90 (26 mg, 13 %); $R_f = 0.60$ (hexane / ethyl acetate, 1:1); ^1H NMR data was identical to those above.

5-(1-Hydroxy-1-phenylmethyl)isoquinoline 93 (79 mg, 34%); off-white crystals; $R_f = 0.24$ (hexane / ethyl acetate, 1:1); mp $124\text{--}126^{\circ}\text{C}$; ^1H NMR (CDCl_3) δ 1.7 (1 H, bs, OH), 6.48 (1 H, s, CHOH), 7.36 (5 H, m, Ph- H_5), 7.65 (1 H, t, $J = 7.7$ Hz, isoquinoline 7-H), 7.78 (1 H, d, $J = 6.1$ Hz, isoquinoline 4-H), 7.9 (2 H, m, isoquinoline 6,8-H), 8.41 (1 H, d, $J = 6.1$ Hz, isoquinoline 3-H), 9.20 (1 H, s, isoquinoline 1-H); MS (EI) 236.1030 (M^+ , 11) ($^{13}\text{C}^{12}\text{C}_{15}\text{H}_{13}\text{NO}$ requires 236.1030), 235.0993 (M^+ , 82) ($\text{C}_{16}\text{H}_{13}\text{NO}$ requires 235.0997).



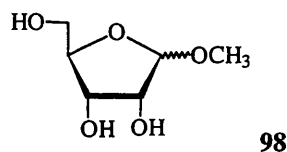
3*R*,4*S*,5*R*-3,4-Bis(phenylmethoxy)-5-phenylmethoxymethyltetrahydrofuran-2-one 95

To 2,3,5-tri-*O*-benzyl-*D*-ribose (4.81 g, 11.4 mmol) in dry dimethylsulphoxide (17 ml), acetic anhydride (11.5 ml) was added and the solution was stirred at ambient temperature for 24 h. The solution was poured onto ice-water and the mixture was extracted with dichloromethane. After washing with water, the organic extract was dried and concentrated to give a viscous yellow liquid. Chromatography (hexane / ethyl acetate, 17:3) gave **95** (3.56 g, 74%) as off-white crystals; R_f = 0.17 (hexane / ethyl acetate, 17:3); mp 50-52°C (lit.²⁴⁰ mp 54-55°C); ^1H NMR (CDCl_3) δ 3.55 (1 H, dd, J = 11.0, 2.6 Hz, 5- H_A), 3.66 (1 H, dd, J = 11.0, 2.8 Hz, 5- H_B), 4.08 (1 H, dd, J = 5.5, 2.0 Hz, 3-H), 4.4 (1 H, m, 2-H), 4.5 (3 H, m, Ph- CH_2), 4.55 (1 H, m, 4-H), 4.71 (2 H, m, Ph- CH_2), 4.94 (1 H, d, J = 11.9 Hz, Ph-CH), 7.3 (15 H, m, $3 \times$ Ph- H_5).



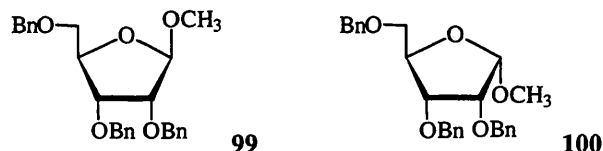
2,3,5-Tri-*O*-benzyl-*D*-ribose 96

To 2,3,5-tri-*O*-benzyl-*D*-riboside **99/100** (5.59 g, 13 mmol) in dioxane (125 ml), hydrochloric acid (0.1 M, 31 ml, 0.31 mmol) was added. The solution was boiled gently and the distillate was collected for 30 h. The mixture was then neutralised (1 M sodium hydroxide solution) and concentrated. The residue, in dichloromethane, was washed three times with water and was dried. Evaporation gave **96** (4.81 g, 89 %) as a colourless syrup; R_f = 0.18 (hexane / ethyl acetate, 4:1); ^1H NMR (CDCl_3) δ 3.5-3.6 (2 H, m, 5- H_2), 3.7-3.9 (3 H, m, 2,3,4- H_3), 4.5 (6 H, m, Ph- CH_2), 5.26 (1 H, s) and 5.31 (1 H, bs) (α , β 1-H), 7.3 (15 H, m, Ph-H).



Methyl *D*-ribofuranoside **98**

D-Ribose **97** (5 g, 33 mmol) in dry methanol was cooled to 0°C and treated with concentrated sulphuric acid (0.5 ml). After storage at 4°C for 14 h, the solution was neutralised by passage through a column of anion-exchange resin (Dowex 1×8-200) in the free base form. The eluate was concentrated to give **98** (5.5 g, 100%) as a syrup; attempts to crystallise this syrup were unsuccessful; the mixture of α and β isomers (α : β , 1:3) was used for the next stage; ^1H NMR ($(\text{CD}_3)_2\text{SO}$) δ 3.21 (3 H, s, β isomer OCH_3), 3.27 (3 H, s, α isomer OCH_3), 3.33 (1 H, dd, $J = 12, 5$ Hz, β 5- H_A O), 3.4 (2 H, m, α CH_2), 3.5 (1 H, m, β 5- H_B), 3.75 (3 H, m, α 2,3,4- H_3 and 3 H, m, β 2,3,4- H_3), 4.23 (1 H, d, $J = 8.4$ Hz, α OH), 4.6 (2 H, m, β 1-H, OH and 1 H, m, α OH), 4.7 (2 H, m, α 1-H, OH), 4.80 (1 H, d, $J = 6.6$ Hz, β OH), 5.01 (1 H, d, $J = 4.4$ Hz, β OH).

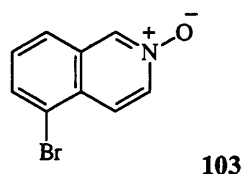


Methyl 2,3,5-tri-*O*-benzyl- β -*D*-ribose **99**

Methyl *D*-ribofuranoside **98** (5.42 g, 33 mmol) in dry tetrahydrofuran (40 ml) was stirred with powdered potassium hydroxide (22.5 g, 0.39 mol). Benzyl chloride (32.0 ml, 35.2 g, 278 mmol) was added and the mixture was heated under reflux for 36 h. The suspension was filtered and the residue was washed thoroughly with tetrahydrofuran. The filtrate was concentrated and the residue, in ethyl acetate, was washed with water, dried and concentrated. Distillation (56°C @ 0.2 Torr) to remove the excess benzyl chloride and chromatography (hexane / ethyl acetate, 9:1) of the remaining crude yellow liquid gave:

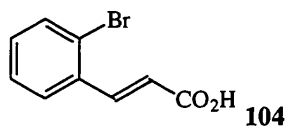
Methyl 2,3,5-tri-*O*-benzyl- α -*D*-ribose 100 (2.83 g, 20%) as a colourless syrup; $R_f = 0.10$ (hexane / ethyl acetate, 1:1); $^1\text{H NMR}$ (CDCl_3) δ 3.4 (2 H, m, 5- H_2), 3.46 (3 H, s, OCH_3), 3.8 (2 H, m, 2,3- H_2), 4.26 (1 H, q, $J = 4.0$ Hz, 4-H), 4.4-4.7 (6 H, m, $3 \times \text{Ph-CH}_2$), 4.88 (1 H, d, $J = 4.0$ Hz, 1-H), 7.2-7.4 (15 H, m, $3 \times \text{Ph-H}_5$). [The $^1\text{HNMR}$ agrees with a literature report²³⁹]

Methyl 2,3,5-tri-*O*-benzyl- β -*D*-ribose 99 (8.21, 57%) as a colourless syrup (lit.²³⁸ bp 235°C); $R_f = 0.27$ (hexane / ethyl acetate, 1:1); $^1\text{H NMR}$ (CDCl_3) δ 3.31 (3 H, s, OCH_3), 3.50 (1 H, dd, $J = 10.6, 5.9$ Hz, 5- H_A), 3.61 (1 H, dd, $J = 10.6, 3.8$ Hz, 5- H_B), 3.83 (1 H, dd, $J = 4.8, 1.0$ Hz, 2-H), 4.01 (1 H, dd, $J = 7.1, 4.8$ Hz, 3-H), 4.35 (1 H, m, 4-H), 4.55 (6 H, m, $3 \times \text{Ph-CH}_2$), 4.92 (1 H, bs, 1-H), 7.2-7.4 (15 H, m, $3 \times \text{Ph-H}_5$). [The $^1\text{HNMR}$ agrees with a literature report²³⁹]



5-Bromoisoquinoline *N*-oxide **103**

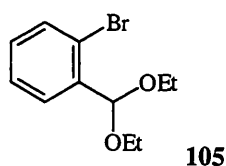
5-Bromoisoquinoline (0.30 g, 1.4 mmol), acetic acid (3 ml) and 27.5% w/v hydrogen peroxide solution (1.5 ml) were stirred for 14 d. The solvent was evaporated to give **103** (314 mg, 100%) as an off-white solid; $R_f = 0.13$ (methanol / chloroform, 1:19); mp $187\text{--}189^\circ\text{C}$; $^1\text{H NMR}$ ($(\text{CD}_3)_2\text{SO}$) δ 7.50 (1 H, t, $J = 7.8$ Hz, 7-H), 7.77 (1 H, d, $J = 7.7$ Hz, 6-H), 7.86 (1 H, d, $J = 7.7$ Hz, 8-H), 8.04 (1 H, d, $J = 7.0$ Hz, 4-H), 8.21 (1 H, d, $J = 7.0$ Hz, 3-H), 8.82 (1 H, s, 1-H); MS (EI) 224.9606 ($[\text{}^{81}\text{Br}]\text{M}^+$, 72) ($\text{C}_9\text{H}_6\text{}^{81}\text{BrNO}$ requires 224.9612), 222.9632 ($[\text{}^{79}\text{Br}]\text{M}^+$, 79) ($\text{C}_9\text{H}_6\text{}^{79}\text{BrNO}$ requires 222.9633).



E*-3-(2-Bromophenyl)propenoic acid **104*

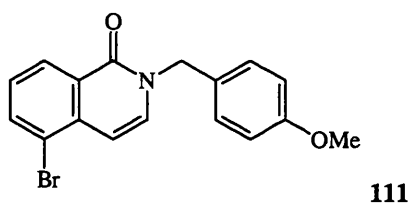
Method A: 2-(Diethoxymethyl)bromobenzene **105** (12.8 g, 50 mmol), propandioic acid (10.3 g, 99 mmol), pyridine (20 ml) and piperidine (1 ml) were heated at 100°C for 3 h and at 140°C for 30 min. The cooled mixture was poured onto a mixture of concentrated hydrochloric acid and ice. The white precipitate was filtered and the filtrate was extracted with diethyl ether. The organic extract was washed with 5% sodium carbonate solution. The aqueous layer was acidified and extracted with diethyl ether. The combined organic product, in diethyl ether, was dried and concentrated to give **104** (4.64 g, 41%) as an off-white solid; (data below).

Method B: 2-Bromiodobenzene **107** (14.05 g, 50 mmol), propenoic acid (4.5 ml, 4.73 g, 66 mmol), palladium (II) acetate (0.111 g, 0.49 mmol), triethylamine (17.3 ml, 12.55 g, 124 mmol) and propanenitrile (20 ml) were heated, to reflux, under nitrogen, for 1.5 h. Hydrochloric acid (2 M, 800 ml) was added to the cooled mixture. The precipitate, in hot ethanol, was filtered and the filtrate was allowed to cool slowly. The solid was collected and dried to give **104** (8.53 g, 76%) as white crystals; R_f = 0.58 (hexane / ethyl acetate, 1:1); mp 202-204°C (decomp.) (lit.²⁷⁰ 212-212.5°C); IR (KBr) 3000-2500 (O-H), 1690 (C=O); ¹H NMR ((CD₃)₂SO) δ 6.57 (1 H, d, J = 16.1 Hz, 2-H), 7.35 (1 H, td, J = 7.7, 1.5 Hz, Ar 4-H), 7.44 (1 H, t, J = 7.7 Hz, Ar 5-H), 7.71 (1 H, dd, J = 7.7, 1.5 Hz, Ar 6-H), 7.83 (1 H, d, J = 16.1 Hz, 3-H), 7.90 (1 H, dd, J = 7.7, 1.5 Hz, Ar 3-H), 12.66 (1 H, bs, CO₂H); MS (EI) 226 ([⁸¹Br]MH⁺, 25), 224 ([⁷⁹Br]M⁺, 25), 147 (100).



2-(Diethoxymethyl)bromobenzene **105**

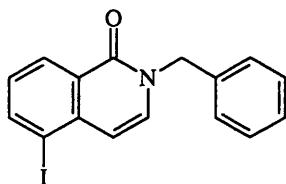
Thionyl chloride (2 ml) was added slowly to 2-bromobenzaldehyde **106** (10.0 g, 55.0 mmol) in triethyl orthoformate (16.9 g, 19.0 ml, 114 mmol) and dry ethanol (25 ml). The mixture was boiled under reflux for 4 h. The cooled mixture was stirred with sodium carbonate (8.0 g) for 15 min; it was then diluted with diethyl ether. Filtration, concentration and distillation gave **105** (152.97 g, 93%) as a colourless oil; bp_{2.5} 118°C; ¹H NMR (CDCl₃) δ 1.25 (6 H, t, *J* = 7.0 Hz, 2 × CH₃), 3.64 (4 H, m, 2 × CH₂), 5.66 (1 H, s, CH), 7.18 (1 H, td, *J* = 7.6, 1.8 Hz, 5-H), 7.32 (1 H, td, *J* = 7.6, 1.8 Hz, 4-H), 7.54 (1 H, dd, *J* = 7.6, 1.8 Hz, 3-H), 7.65 (1 H, dd, *J* = 7.6, 1.8 Hz, 6-H); MS (EI) 260.0227, ([⁸¹Br]M⁺, 92) (C₁₁H₁₅⁸¹BrO₂ requires 260.0234), 258.0248, ([⁷⁹Br]M⁺, 100) (C₁₁H₁₅⁷⁹BrO₂ requires 258.0255). (This is not a novel compound, however no spectroscopic data is reported in the literature.)



5-Bromo-2-(4-methoxyphenylmethyl)isoquinolin-1-one **111**

Lithium bis(trimethylsilyl)amide (1.0 M in tetrahydrofuran, 0.90 ml, 0.90 mmol) was added to a stirred suspension of **62** (100 mg, 0.45 mmol) in dry tetrahydrofuran (10 ml) under nitrogen. The mixture was stirred for 1.5 h. The solution was cooled to 0°C and 1-(chloromethyl)-4-methoxybenzene (0.1 ml, 0.12 g, 0.74 mmol) in dry tetrahydrofuran (10 ml) was added, followed by sodium iodide (7 mg, 47 μmol). The reaction mixture was stirred under nitrogen

for 4 d. The solvent was evaporated and the residue, in ethyl acetate, was washed with water and with saturated brine. The organic solution was dried and purified by chromatography (hexane / ethyl acetate, 7:3) to give **111** (156 mg, 100 %) as white crystals; R_f = 0.47 (hexane / ethyl acetate, 1:1); mp 98-100°C; ^1H NMR (CDCl_3) δ 3.78 (3 H, s, CH_3), 5.15 (2 H, s, CH_2), 6.84 (3 H, m, 4-H + Ph 3,5- H_2), 7.18 (1 H, d, J = 7.7 Hz, 3-H), 7.3 (3 H, m, 7-H + Ph 2,6- H_2), 7.87 (1 H, d, J = 7.7 Hz, 6-H), 8.43 (1 H, d, J = 8 Hz, 8-H); MS (CI) 346 ($[\text{Br}^{81}\text{Br}]^+\text{MH}^+$, 38), 344 ($[\text{Br}^{79}\text{Br}]^+\text{MH}^+$, 38), 121 (100); Anal. Calcd. for $\text{C}_{17}\text{H}_{14}\text{BrNO}_2$: C, 59.32; H, 4.10; N, 4.07. Found: C, 59.4; H, 4.18; N, 3.88.

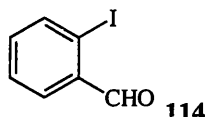


112

5-Iodo-2-(phenylmethyl)isoquinolin-1-one **112**

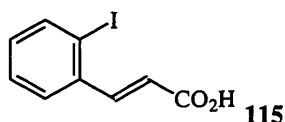
Lithium bis(trimethylsilyl)amide (1.0 M in tetrahydrofuran, 0.60 ml, 0.60 mmol) was added to a stirred suspension of **63** (100 mg, 0.37 mmol) in dry tetrahydrofuran (10 ml) under nitrogen. The mixture was stirred for 2 h. The solution was cooled to 0°C and chloromethylbenzene (55 μl , 61 mg, 0.48 mmol) in dry tetrahydrofuran (10 ml) was added, followed by sodium iodide (7 mg, 47 μmol). The reaction mixture was stirred at ambient temperature, under nitrogen, for 5 d. The solvent was evaporated and the residue, in ethyl acetate, was washed with water and with saturated brine. The organic solution was dried and purified by chromatography (hexane / ethyl acetate, 7:3) to give **112** (123 mg, 92 %) as white crystals; R_f = 0.52 (hexane / ethyl acetate, 1:1); mp 118-120°C; IR (KBr) 1650 ($\text{C}=\text{O}$), 1620 ($\text{C}=\text{O}$); ^1H NMR (CDCl_3) δ 5.22 (2 H, s, CH_2), 6.72 (1 H, d, J = 7.5 Hz, 4-H), 7.19 (2 H, m, 3,7- H_2), 7.33 (5 H, m, Ph- H_5), 8.15 (1 H, dd, J = 7.7, 1.3 Hz, 6-H), 8.47 (1 H, dd, J = 7.7, 1.3 Hz, 8-H); ^{13}C NMR (CDCl_3)

δ 51.90 (NCH₂), 96.29 (C_q), 109.91 (CH), 127.21 (C_q), 127.96 (CH), 128.14 (CH), 128.69 (CH), 128.86 (CH), 132.55 (CH), 136.41 (C_q), 139.02 (C_q), 143.01 (CH), 161.45 (C_q); MS (EI) 360.9960 (M⁺, 75) (C₁₆H₁₂INO requires 360.9964); Anal. Calcd. for C₁₆H₁₂INO: C, 53.21; H, 3.35; N, 3.88: C, 53.8; H, 3.46; N, 3.82.



2-Iodobenzaldehyde **114**

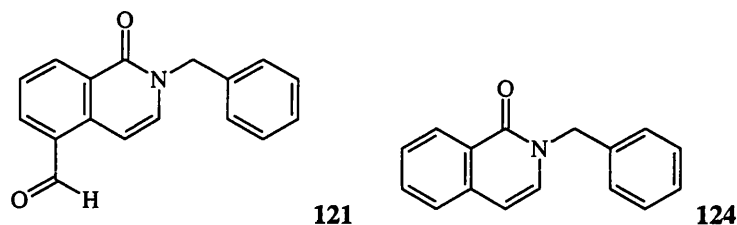
2-Iodobenzyl alcohol **113** (20.0 g, 86 mmol) in dichloromethane (55 ml) was added to a well stirred suspension of pyridinium dichromate (49.2 g, 130 mmol) in dichloromethane (140 ml). After 3 h, the mixture was diluted with diethyl ether (56 ml), filtered and distilled to give **114** (12.33 g, 62%) as a pale yellow wax; R_f = 0.58 (hexane / ethyl acetate, 9:1); bp_{1.1} 109°C (lit.²⁷¹ bp₁₄ 129°C @ 14 mmHg, lit.²⁷² mp 37°C); ¹H NMR (CDCl₃) δ 7.29 (1 H, td, J = 7.7, 1.8 Hz, 4-H), 7.46 (1 H, t, J = 7.7 Hz, 5-H), 7.88 (1 H, dd, J = 7.7, 1.8 Hz, 6-H), 7.96 (1 H, d, J = 7.7 Hz, 3-H), 10.07 (1 H, s, CHO); MS (EI) 232 (M⁺, 100).



E-3-(2-Iodophenyl)propenoic acid **115**

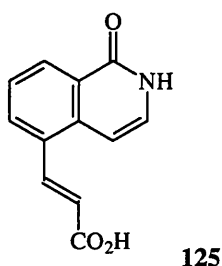
2-Iodobenzaldehyde **114** (8.29 g, 36 mmol), propanedioic acid (8.11 g, 78 mmol) and piperidine (0.3 ml) in pyridine (17 ml) were boiled under reflux for 2 h. Hydrochloric acid (2 M, 250 ml) was added to the cooled solution. The white precipitate was collected, recrystallised from hot ethanol and dried to give **115** (8.29 g, 85%) as colourless needles; R_f = 0.33 (hexane / ethyl acetate, 1:1); mp 219-220°C (lit.²⁷³ 212-214°C); ¹H NMR ((CD₃)₂SO) δ 6.48 (1 H, d, J = 15.8 Hz, 2-H), 7.16 (1 H, t, J = 8.1 Hz, Ar 4-H), 7.44 (1 H, t, J = 8.1 Hz, Ar 5-H), 7.63 (1

H, d, $J = 15.8$ Hz, 3-H), 7.83 (1 H, d, $J = 8.1$ Hz) and 7.95 (1 H, d, $J = 8.1$ Hz) (Ar 3,6-H₂), 12.67 (1 H, bs, CO₂H); MS (EI) 274 (M^+ , 20), 147 (100).



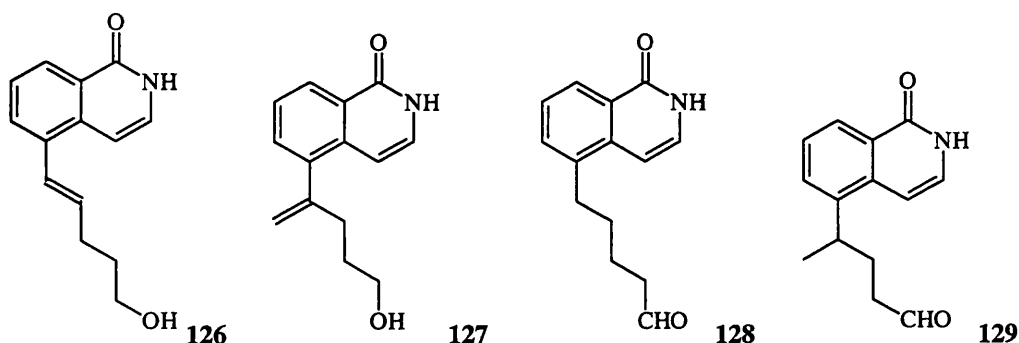
5-Formyl-2-phenylmethyloisoquinolin-1-one **121**

5-Iodo-2-(phenylmethyl)isoquinolin-1-one **112** (79 mg, 0.2 mmol) in dry tetrahydrofuran (2 ml) was stirred under nitrogen and cooled to -78°C (acetone / CO₂). Butyllithium in hexane (1.6 M, 0.15 ml, 0.24 mmol) was added and stirring was continued for a further 4 h. Dimethylformamide (0.028 ml, 0.029 g, 0.4 mmol) in dry tetrahydrofuran (0.1 ml) was added. Stirring was continued for 15 min before the mixture was allowed to reach ambient temperature. The reaction mixture was stirred for 1 h at ambient temperature and water (1 ml) was then added. The solution was stirred for 10 min and then extracted several times with ethyl acetate. The combined organic extracts were dried. Evaporation and chromatography gave only **124** (20 mg, 38%) as a colourless oil (lit²⁷⁴ mp 69–71 $^{\circ}\text{C}$); $R_f = 0.31$ (hexane / ethyl acetate, 4:1); ^1H NMR (CDCl₃) δ 5.23 (2 H, s, CH₂), 6.49 (1 H, d, $J = 7.5$ Hz, isoquinoline 4-H), 7.09 (1 H, d, $J = 7.5$ Hz, isoquinoline 3-H), 7.32 (5 H, m, Ph-H₅), 7.49 (2 H, m, isoquinoline 5,7-H₂), 7.66 (1 H, t, $J = 7.3$ Hz, isoquinoline 6-H), 8.48 (1 H, d, $J = 7.3$ Hz, isoquinoline 8-H); MS (EI) 235.0998 (M^+ , 100) (C₁₆H₁₃NO requires 235.0997), 91 (100).



E*-3-(1-Oxoisoquinolin-5-yl)propenoic acid **125*

5-Iodoisoquinolin-1-one **63** (100 mg, 0.37 mmol), propenoic acid (0.03 ml, 35 mg, 0.49 mmol), palladium (II) acetate (8 mg, 37 μ mol) and triethylamine (0.13 ml, 93 mg, 0.92 mmol) in propanenitrile (0.3 ml) were boiled under reflux for 1 h. Hydrochloric acid (2 M, 10 ml) was added and the precipitate was collected and dried to give **125** (76 mg, 97%) as a pale green solid; R_f = 0.05 (hexane / ethyl acetate, 1:1); mp 315-318°C; IR (KBr) 3550 (N-H), 1695, 1660 (C=O); ^1H NMR ($(\text{CD}_3)_2\text{SO}$) δ 6.57 (1 H, d, J = 15.8 Hz, 2-H), 6.76 (1 H, d, J = 7.3 Hz, isoquinoline 4-H), 7.28 (1 H, *ca.* t, isoquinoline 3-H), 7.52 (1 H, t, J = 7.7 Hz, isoquinoline 7-H), 8.10 (1 H, d, J = 15.8 Hz, 3-H), 8.12 (1 H, d, J = 7.7 Hz) and 8.27 (1 H, d, J = 7.7 Hz, isoquinoline 6,8-H₂), 11.47 (1 H, bs, NH), 12.60 (1 H, bs, CO₂H); MS (CI) 216 (MH^+ , 100); MS (FAB⁺) 216.0616 (MH^+ , 50) ($\text{C}_{12}\text{H}_{10}\text{NO}_3$ requires 216.0661), 215.0584 (M^+ , 24) ($\text{C}_{12}\text{H}_9\text{NO}_3$ requires 215.0582).



5-(1-Oxoisoquinolin-5-yl)-pent-4-enol **126**

5-Iodoisoquinolin-1-one **63** (400 mg, 1.5 mmol), pent-4-enol (0.2 ml, 0.17 g, 1.9 mmol), palladium (II) acetate (32 mg, 0.14 mmol), triethylamine (0.52 ml, 0.37 g, 3.7 mmol) and propanenitrile (1.5 ml) were boiled under reflux for 2 h. The

solvent was evaporated and the residue, in dichloromethane, was washed, successively, with hydrochloric acid (2 M), water and saturated brine. The organic extract was dried and concentrated. Chromatography (ethyl acetate / methanol, 99:1) gave the starting material, **63** (221 mg, 55%) and two mixtures of isomers with identical R_f values which could not, therefore, be separated

5-(1-Oxoisquinolin-5-yl)-pent-4-enol 126 (44 mg, 13%) as an off-white solid;

$R_f = 0.11$ (ethyl acetate / methanol, 99:1) [mixture with **127**]; ^1H NMR

$((\text{CD}_3)_2\text{SO})$ δ 1.6 (2 H, qu, $J = 6.8$ Hz, 2- H_2), 2.3 (2 H, m, 3- H_2), 3.5 (2 H, m, 1- H_2), 6.3 (1 H, dt, $J = 15.6, 7.2$ Hz, 4-H), 6.75 (1 H, d, $J = 7.5$ Hz, isoquinoline 4-H), 6.93 (1 H, d, $J = 15.6$ Hz, 5-H), 7.18 (1 H, m, isoquinoline 3-H), 7.48 (1 H, m, isoquinoline 7-H), 7.80 (1 H, d, $J = 7.5$ Hz, isoquinoline 6-H), 8.1 (1 H, m, 8-H).

4-(1-Oxoisquinolin-5-yl)-pent-4-enol 127 (37 mg, 11%) as an off-white solid;

$R_f = 0.11$ (ethyl acetate / methanol, 99:1) [mixture with **126**]; ^1H NMR

$((\text{CD}_3)_2\text{SO})$ δ 2.1 (2 H, m, 2-H), 2.5 (2 H, m, 3-H), 3.5 (2 H, m, 1-H), 5.5 (2 H, m, 4,5- H_2), 6.62 (1 H, d, $J = 7.7$ Hz, isoquinoline 4-H), 7.18 (1 H, m, 3-H), 7.48 (2 H, m, 6,7- H_2), 8.1 (1 H, m, 8-H).

MS (FAB $^+$) 230.1178 (MH^+ , 100) ($\text{C}_{14}\text{H}_{16}\text{NO}_2$ requires 230.1181).

5-(1-Oxoisquinolin-5-yl)pentanal 128 (14 mg, 5%) as an off-white solid; $R_f =$

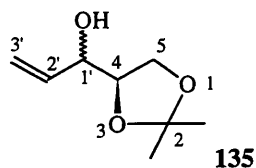
0.23 (ethyl acetate / methanol, 99:1) [mixture with **129**]; ^1H NMR $((\text{CD}_3)_2\text{SO})$ δ 1.7 (4 H, m, 3,4- H_4), 2.5 (2 H, m, 2- H_2), 2.9 (2 H, m, 5- H_2), 6.73 (1 H, d, $J = 7.7$ Hz, isoquinoline 4-H), 7.23 (1 H, d, $J = 7.7$ Hz, isoquinoline 3-H), 7.5 (2 H, m, isoquinoline 6,7- H_2), 8.3 (1 H, m, isoquinoline 8-H), 9.78 (1 H, s, CHO), 11.37 (1 H, bs, NH).

(\pm)-**4-(1-Oxo-isoquinolin-5-yl)pentanal 129** (7 mg, 2%) as an off-white solid;

$R_f = 0.23$ (ethyl acetate / methanol, 99:1) [mixture with **128**]; ^1H NMR

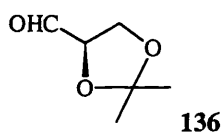
$((\text{CD}_3)_2\text{SO})$ δ 1.3 (5 H, m, 3,5- H_5), 2.4 (2 H, t, $J = 7.7$ Hz, 2- H_2), 3.4 (1 H, m, 4-H), 6.83 (1 H, d, $J = 7.7$ Hz, isoquinoline 4-H), 7.5 (3 H, m, isoquinoline 3,6,7- H_3), 8.3 (1 H, m, isoquinolinone 8-H), 9.74 (1 H, bs, CHO), 11.37 (1 H, bs, NH).

MS (FAB $^+$) 230.1184 (MH^+ , 100) ($\text{C}_{14}\text{H}_{16}\text{NO}_2$ requires 230.1181).



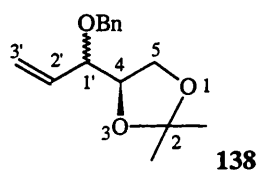
4*R*-2,2-Dimethyl-4-(1-hydroxyprop-2-enyl)-1,3-dioxolane 135

Freshly prepared (4*R*)-2,2-Dimethyl-1,3-dioxolan-4-carboxaldehyde **136** (3.89 g, 30 mmol) in dry tetrahydrofuran (10 ml) was added, over 30 min, to a 1 M solution of vinylmagnesium bromide in tetrahydrofuran (59 ml, 59 mmol) at -20°C (ice / sodium chloride). After 1 h, the solution was warmed to 0°C . Diethyl ether (15 ml) was added, followed by saturated ammonium chloride solution (25 ml). The precipitate was filtered and washed with diethyl ether (4×25 ml). The combined organic solutes were dried and concentrated and the residue was distilled to give **135** (2.79 g, 59%) as a colourless oil; ^1H NMR (CDCl_3) δ 1.37 (3 H, s, CH_3 both diastereomers), 1.45 (3 H, s, CH_3 , both diastereomers), 2.45 (1 H, bs, OH, diastereomer I), 2.62 (1 H, bs, OH, diastereomer II), 3.78 (1 H, m, 4-H, diastereomer II), 3.90-4.06 (3 H, m, 5- H_2 , 1'-H, diastereomer II), 3.90-4.06 (2 H, m, 5- H_2 , diastereomer I), 4.12 (1 H, m, 1'-H, diastereomer I), 4.26 (1 H, m, 4-H, diastereomer I), 5.24 (1 H, d, $J = 10$ Hz, *cis* 3'-H, both diastereomers), 5.40 (1 H, d, $J = 17$ Hz, *trans* 3'-H, both diastereomers), 5.8 (1 H, m, 2'-H, both diastereomers) (molar ratio of diastereomers, I:II, 1:1.5); ^{13}C NMR (CDCl_3) δ 25.06 (CH_3), 25.20 (CH_3), 26.35 (CH_3), 26.64 (CH_3), 64.74 (CH_2), 65.76 (CH_2), 71.84 (CH), 73.97 (CH), 78.52 (CH), 78.02 (CH), 109.35 (C_q), 109.74 (C_q), 116.83 ($=\text{CH}_2$), 117.71 ($=\text{CH}_2$), 135.79 ($=\text{CH}$), 136.15 ($=\text{CH}$).



(4R)-2,2-Dimethyl-1,3-dioxolan-4-carboxaldehyde 136

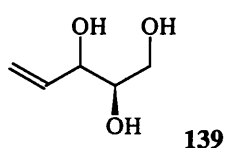
To 1,2,5,6-Di-*O*-isopropylidene-*D*-mannitol **137** (5.00 g, 19 mmol), in dichloromethane (75 ml), at 0°C, sodium carbonate (20.2 g, 191mmol) was added followed by lead (IV) acetate (8.87 g, 20 mmol). The reaction mixture was stirred for 10 min (oxidation was monitored using starch-iodide paper). The suspension was filtered through Celite® / magnesium sulphate and the residue was washed three times with dichloromethane. The filtrate was concentrated and the residue was distilled to give **136** (3.89 g, 78%) as a colourless oil; bp₃ 45°C (lit.²⁵⁸ bp₁₅ 39°C); IR (film) 1740 (C=O); ¹H NMR (CDCl₃) δ 1.43 (3 H, s, CH₃), 1.50 (3 H, s, CH₃), 4.16 (2 H, m, CH₂), 4.40 (1 H, m, CH), 9.73 (1 H, s, CHO).



(4R)-2,2-Dimethyl-4-(1-phenylmethoxyprop-2-enyl)-1,3-dioxolane 138

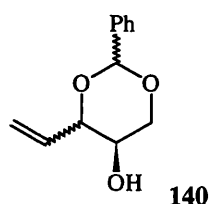
Method A: Lithium bis(trimethylsilyl)amide in dry tetrahydrofuran (1.0 M, 19.0 ml, 19 mmol) was added to **135** (1.5 g, 9.5 mmol) in dry tetrahydrofuran (150 ml) under nitrogen. The solution was stirred for 1.5 h, then cooled to 0°C. Bromomethylbenzene (2.6 g, 1.8 ml, 15 mmol) in dry tetrahydrofuran (100 ml) was added and the resulting mixture was stirred at ambient temperature for 7 d. The reaction mixture was then heated under reflux for 4 d. The solvent was evaporated and the residue, in ethyl acetate, was washed with water and saturated brine. The solution was dried, concentrated and purified by chromatography (hexane / ethyl acetate, 9:1) to give **138** (655 mg, 28%) as a yellow oil; R_f = 0.6 (hexane / ethyl acetate, 4:1); ¹H NMR (CDCl₃) δ 1.38 (3 H, s, CH₃), 1.41 (3 H, s, CH₃), 3.7-4.1 (4 H, m, 5-H₂, 4-H, 1'-H), 4.4 (1 H, m, PhOCH₂), 4.7 (1 H, m, PhOCH₂), 5.4 (2 H, m, 3'-H₂), 5.8 (1 H, m, 2'-H), 7.32 (5 H, m, Ph-H₅).

Method B: Sodium hydride (60 % in oil, 130 mg, 3.3 mmol) was added to **135** (0.52 g, 3.3 mmol) in dry dimethylformamide (20 ml) under nitrogen. The mixture was stirred for 1 h. Bromomethylbenzene (0.43 ml, 615 mg, 3.6 mmol) was added and the mixture was stirred for 3 d. The solvent was evaporated and the residue, in ethyl acetate, was washed with water and was dried. Concentration and chromatography (hexane / ethyl acetate, 4:1) gave **138** (154 mg, 19%); data identical to above.



(4R)-Pent-4-ene-1,2,3-triol 139

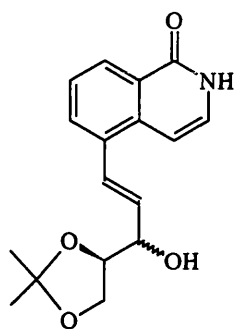
Hydrochloric acid (2 M, 4.5 ml) was added to a solution of **135** (0.50 g, 3.2 mmol) in tetrahydrofuran (4.5 ml). The resulting mixture was stirred at 60°C for 2 h. The cooled solution was neutralised with sodium hydroxide solution (2 M) and filtered. The solvents were evaporated and the residue was dried by adding successive aliquots of dry ethanol and removing the solvent by distillation at atmospheric pressure. The residue was used immediately without characterisation.



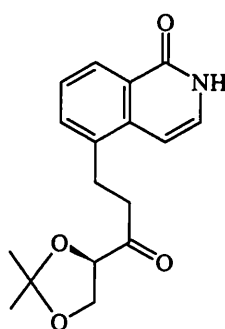
(5R)-4-Ethenyl-2-phenyl-1,3-dioxan-5-ol 140

To (4R)-Pentene-4-ene-1,2,3-triol **139** (0.37 g, 3.1 mmol) in dry dimethylformamide (3 ml), (dimethoxymethyl)benzene (0.50 ml, 3.3 mmol) and 4-methylbenzenesulphonic acid (1 mg) were added. The reaction vessel was fitted with an air condenser attached to a water pump *via* a three-way tap. The apparatus was evacuated and the system was stirred at 70°C until methanol ceased to condense (6 h). The cooled mixture was concentrated and the residue,

in diethyl ether, was washed with sodium carbonate solution (10%) and water. The organic solution was dried, concentrated and chromatographed (hexane / ethyl acetate) to give **140** (413 mg, 64%) as a yellow oil; $R_f = 0.26$; mixture of diastereomers; ^1H NMR (CDCl_3) δ 2.09 (1 H, bs, OH), 3.6-4.6 (4 H, m, 6- H_2 , 4,5- H_2), 5.4 (2 H, m, $\text{CH}_2=$), 5.5 (1 H, s, 2-H, diastereomer I), 5.92 (1 H, m, $\text{CH}=$), 6.0 (1 H, s, 2-H, diastereomer II), 7.35-7.53 (5 H, m, Ph-H_5).



141



142

5-(3-(4*R*-2,2-Dimethyl-1,3-dioxolan-4-yl)-3-hydroxyprop-1-enyl)isoquinolin-1-one **141**

5-Iodoisoquinolin-1-one **63** (400 mg, 1.5 mmol), (4*R*)-2,2-dimethyl-4-(1-hydroxyprop-2-enyl)-1,3-dioxolane **135** (315 mg, 1.9 mmol), triethylamine (0.52 ml, 0.37 g, 3.7 mmol) and palladium (II) acetate (32 mg, 0.14 mmol) in propanenitrile (1.5 ml) were heated under reflux for 2 h. The solvent was evaporated and the residue, in ethyl acetate, was washed with 2 M hydrochloric acid and saturated brine. The dried organic solution was concentrated and purified by chromatography (ethyl acetate, then acetone / hexane, 2:1) to give:

5-(3-(4*R*-2,2-Dimethyl-1,3-dioxolan-4-yl)-3-hydroxyprop-1-enyl)isoquinolin-1-one **141** (76 mg, 18%) as an off-white solid; $R_f = 0.18$ (ethyl acetate); mp 164-166°C; ^1H NMR (CDCl_3) δ 1.40 (3 H, s, CH_3), 1.50 (3 H, s, CH_3), 2.17 (1 H, bs, OH), 3.93 (1 H, dd, $J = 8.4, 5.5$ Hz, dioxolane 5- $\text{H}_\text{A}\text{H}_\text{B}$, diastereomer I), 4.04 (2 H, d, $J = 6.8$ Hz, dioxolane 5- H_2 , diastereomer II), 4.1 (1 H, dd, $J = 6.3, 8.4$ Hz, dioxolane 5- $\text{H}_\text{A}\text{H}_\text{B}$, diastereomer I), 4.20 (1 H, m, dioxolane 4-H, diastereomer I), 4.28 (1 H, m, dioxolane 4-H, diastereomer II), 4.34 (1 H, td, $J = 6.3, 1.5$ Hz,

CHOH, diastereomer I), 4.56 (1 H, td, $J = 5.5, 1.5$ Hz, CHOH, diastereomer II), 6.18 (1 H, m, =CHCH, diastereomers I and II), 6.82 (1 H, d, $J = 7.3$ Hz) and 6.81 (1 H, d, $J = 7.3$ Hz, isoquinoline 4-H, diastereomers I and II), 7.19 (1 H, d, $J = 7.3$ Hz, isoquinoline 3-H, diastereomers I and II), 7.24 (1 H, m, ArCH=, diastereomers I and II), 7.48 (1 H, t, $J = 7.8$ Hz, isoquinoline 7-H, diastereomers I and II), 7.78 (1 H, d, $J = 7.8$ Hz, isoquinoline 6-H, diastereomers I and II), 8.37 (1 H, d, $J = 7.8$ Hz, isoquinoline 8-H, diastereomers I and II), 10.6 (1 H, bs, NH) [The ratio of diastereomers was 1 : 1.8 (I : II)]; MS (FAB⁺) 302.1373 (MH⁺, 100) (C₁₇H₂₀NO₄ requires 302.1392).

5-(3-(4*R*-2,2-dimethyl-1,3-dioxolan-4-yl)-3-oxo-propyl)isoquinolin-1-one 142 (176 mg, 42%) as an off-white solid; $R_f = 0.25$ (ethyl acetate); mp 138-141°C; IR (KBr) 3300, 3160 (N-H), 1715 (ketone C=O), 1660, 1630 (isoquinolinone C=O); ¹H NMR (CDCl₃) δ 1.38 (3 H, s, CH₃), 1.43 (3 H, s, CH₃), 3.00 (2 H, td, $J = 7.6, 2.7$ Hz) and 3.20 (2 H, m) (2 \times CH₂), 3.96 (1 H, dd, $J = 8.5, 5.5$ Hz, dioxolane 5-H_AH_B), 4.19 (1 H, dd, $J = 8.5, 7.8$ Hz, dioxolane 5-H_AH_B), 4.45 (1 H, dd, $J = 7.8, 5.5$ Hz, dioxolane 4-H), 6.87 (1 H, d, $J = 7.3$ Hz, isoquinoline 4-H), 7.29 (1 H, d, $J = 7.3$ Hz, isoquinoline 3-H), 7.50 (1 H, t, $J = 7.9$ Hz, isoquinoline 7-H), 7.61 (1 H, d, $J = 7.9$ Hz, isoquinoline 6-H), 8.34 (1 H, d, $J = 7.9$ Hz, isoquinoline 8-H), 11.15 (1 H, bs, NH); MS (FAB⁺) 302.1384 (M⁺, 53) (C₁₇H₂₀NO₄ requires 302.1392), 149 (100).

References

1. W. A. Creasey, *Cancer, An Introduction*, Oxford University Press, New York, 1981, p. 162.
2. A. H. W. Nias in *Treatment of Cancer*, Chapman and Hall, London, 1982, p. 33.
3. M. M. Elkind and H. Sutton, *Nature*, 1959, **184**, 1293.
4. M. M. Elkind, H. Sutton-Gilbert, W. B. Moses and C. Kamper, *Nature*, 1967, **214**, 1088.
5. J. F. Ward, *Int. J. Radiat. Oncol. Biol. Phys.*, 1986, **12**, 1027.
6. L. R. Kelland and G. G. Steel, *Int. J. Radiat. Biol.*, 1988, **54**, 229.
7. R.B.Painter in *Radiation Biology in Cancer Research* ed. R. E. Meyn and H. R. Withers, Raven Press, New York, 1979, p.59.
8. N. L. Oleinick, *Radiat. Res.*, 1990, **124**, 1.
9. M. M. Elkind, *Radiat. Res.*, 1984, **100**, 425.
10. F. Ellis, *Clin. Radiol.*, **1969**, 20, 1.
11. M. M. Elkind and J. L. Redpath in *Cancer: A Comprehensive Treatise*, ed. F. F. Becker, Plenum Press, New York, 1977, **vol. 6**, p.59.
12. G. E. Adams in *Cancer: A Comprehensive Treatise*, ed. F. F. Becker, Plenum Press, New York, 1977, **vol.6**, 185.
13. T. C. Jenkins, M. A. Naylor, P. O'Niell, M. D. Threadgill, S. Cole, I. Stratford, G. E. Adams, E. M. Fielden, M. J. Suto and M. A. Stier, *J. Med. Chem.*, 1990, **33**, 2603.
14. M. J. Suto in *Annual Reports in Medicinal Chemistry*, ed. Plattner, Academic Press, New York, 1991, **vol. 26**, p.151.
15. J. L. Foster and R. L. Willson, *Br. J. Radiol.*, 1973, **46**, 234.
16. J. D. Chapman, R. G. Webb and J. Borsa, *Int. J. Radiat. Biol.*, 1971, **19**, 561.

17. J. M. Brown, N. Y. Yu, D. M. Brown, and W. Lee, *Int. J. Radiat. Oncol. Biol. Phys.*, 1981, **7**, 695.
18. P. J. Wood and D. J. Hirst, *Int. J. Rad. Oncol. Biol. Phys.*, **1989**, **16**, 1141.
19. D. G. Hirst and P. J. Wood, *Int. J. Radiat. Oncol. Biol. Phys.*, 1989, **16**, 1183.
20. J. F. Ward and W. F. Blakely, *Cancer Res.*, 1984, **44**, 59.
21. M. R. Purnell and W. J. D. Whish, *Biochem. J.*, 1980, **185**, 775.
22. S. Shall, *Adv. Radiat. Biol.*, 1984, **11**, 1.
23. K. Ueda, M. Kawaichi and O. Hayaishi in *ADP-Ribosylation Reactions*, ed. O. Hayaishi and K. Ueda, Academic Press, New York, 1982, p.117.
24. R. C. Benjamin and D. M. Gill, *J. Biol. Chem.*, 1980, **255**, 10493.
25. R. C. Benjamin and D. M. Gill, *J. Biol. Chem.*, 1980, **255**, 10502.
26. H. Mendoza-Alvarez and R. Alvarez-Gonzalez, *J. Biol. Chem.*, 1993, **268**, 22575.
27. P. L. Panzeter and F. R. Althaus, *Biochemistry*, 1994, **33**, 9600.
28. H. Okayama, C. M. Edson, M. Fukushima, K. Ueda and O. Hayaishi, *J. Biol. Chem.*, 1977, **252**, 7000.
29. H. M. Alkhatib, D. F. Chen, B. Cherney, K. Bahtia, V. Notario, C. Giri, G. Stein, E. Slattery, R. G. Roeder and M. E. Smulson, *Proc. Natl. Acad. Sci. USA*, 1987, **84**, 1224.
30. J. H. Küpper, M. Müller, M. K. Jacobson, J. Tatsumi-Miyajima, D. L. Coyle, E. L. Jacobson and A. Burkle, *Mol. Cell. Biol*, 1995, **15**, 3154.
31. B. W. Cherney, O. W. McBride, D. Chen, H. Alkhatib, K. Bhatia, P. Hensley and M. E. Smulson, *Proc. Natl. Acad. Sci. USA*, 1987, **84**, 8370.
32. I. Kameshita, Z. Matsuda, T. Tanigushi, and Y. Shizuta, *J. Biol. Chem.*, 1984, **259**, 4770.
33. G. de Murcia, J. Ménissier-de Murcia and V. Schreiber, *Bioessays*, 1991, **13**, 455.

34. G. Gradwohl, J. Menissier-de Murcia, M. Molinete, F. Simonin, M. Koken, J. H. J. Hoeijmakers and G. de Murcia, *Proc. Natl. Acad. Sci USA*, 1990, **87**, 2990.
35. E. Le Cam, F. Fack, J. Ménissier-de Murcia, J. A. H. Cognet, A. Barbin, V. Sarantoglou, B. Révet, E. Delain and G. de Murcia, *J. Mol. Biol.*, 1994, **235**, 1062.
36. P. Zahradka and K. Ebisuzaki, *Eur. J. Biochem.*, 1984, **142**, 503.
37. G. de Murcia, V. Schreiber, M. Molinete, B. Saulier, O. Poch, M. Masson, C. Niedergang and J. Ménissier-de Murcia, *Mol. Cell. Biochem.*, 1994, **138**, 15.
38. Y. Wei, P. Robins, K. Carter, K. Caldecott, D. J. C. Pappin, G. Yu, R. Wang, B. K. Shell, R. A. Nash, P. Schär, D. E. Barnes, W. A. Haseltine and T. Lindahl, *Mol. Cell. Biol.*, 1995, **15**, 3206.
39. T. Lindahl, M. Satoh, G. Poirier and A. Klungland, *TIBS*, 1995, **20**, 405.
40. G. T. Marsischky, B. A. Wilson and R. J. Collier, *J. Biol. Chem.*, 1995, **270**, 3247.
41. F. Simonin, O. Poch, M. Delarue and G. de Murcia, *J. Biol. Chem.*, 1993, **268**, 8529.
42. A. Ruf, J. Ménissier-de Murcia, G. de Murcia and G. E. Schulz, *Proc. Natl. Acad. Sci USA*, 1996, **93**, 7481.
43. K. Ueda and O. Hayaishi, *Ann. Rev. Biochem.*, 1985, **54**, 73.
44. O. Hayaishi and K. Ueda in *ADP-Ribosylation Reactions*, ed. O. Hayaishi and K. Ueda, Academic Press, New York, 1982, p.3.
45. V. S. Allured, R. J. Collier, S. F. Carroll and D. B. McKay, *Proc. Natl. Acad. Sci. USA*, 1986, **83**, 1320.
46. R. Alvarez-Gonzalez, *Mol. Cell. Biochem.*, 1994, **138**, 213.
47. T. Katada and M. Ui, *Proc. Natl. Acad. Sci. USA*, 1982, **79**, 3129.
48. S. Choe, M. J. Bennett, G. Fujii, P. M. G. Curmi, K. A. Kantardjieff, R. J. Collier and D. Eisenberg, *Nature*, 1992, **357**, 216.

49. R. Zhang, D. L. Scott, M. L. Westbrook, S. Nance, B. D. Spangler, G. G. Shipley and E. M. Westbrook, *J. Mol. Biol.*, 1995, **251**, 563.
50. P. Chambon, J. D. Weill, J. Doly, M. T. Strosser and P. Madel, *Biochem. Biophys. Res. Commun.*, 1966, **25**, 638.
51. M. Miwa, M. Ishihara, S. Takishima, N. Takasuka, M. Maeda, Z. Yamaizumi, T. Sugimura, S. Yokoyama and T. Miyazawa, *J. Biol. Chem.*, 1981, **256**, 2916.
52. N. Ogata, K. Ueda, M. Kawaichi and O. Hayaishi, *J. Biol. Chem.*, 1981, **256**, 4135.
53. A. M. Ferro and B. M. Olivera, *J. Biol. Chem.*, 1982, **257**, 7808.
54. F. Althaus, *J. Cell. Sci.*, 1992, **102**, 663.
55. K. Yoshihara, Y. Tanigawa, L. Burzio and S. S. Koide, *Proc. Natl. Acad. Sci. USA*, 1975, **72**, 289.
56. K. Yoshihara, A. Itaya, Y. Tanaka, Y. Ohashi, K. Ito, H. Teraoka, K. Tsukada, A. Matsukage and T. Kamiya, *Biochem. Biophys. Res. Commun.*, 1985, **128**, 61.
57. A. M. Ferro and B. M. Olivera, *J. Biol. Chem.* 1984, **259**, 547.
58. J. E. Cleaver and W. E. Morgan, *Mutation Res.*, 1991, **257**, 1.
59. M. K. Darby, B. Schmitt, J. Jongstra-Bilen and H. P. Vosenburg, *EMBO J.*, 1985, **4**, 2129.
60. T. Taniguchi, S. Suzuki and Y. Shizuta, *Biochem. Biophys. Res. Commun.*, 1985, **127**, 526.
61. H. Suzuki, P. Quesada, B. Farina and E. Leone, *J. Biol. Chem.*, 1986, **261**, 6048.
62. M. Z. Hussain, Q. P. Ghani and T. K. Hunt, *J. Biol. Chem.*, 1989, **264**, 7850
63. S. Tanuma, T. Yagi and G. S. Johnson, *Arch. Biochem. Biophys.*, 1985, **237**, 38.
64. N. Ogata, K. Ueda, H. Kagamiyama and O. Hayaishi, *J. Biol. Chem.*, 1980, **255**, 7616.

65. P. Adamietz and A. Rudolf, *J. Biol. Chem.*, 1984, **259**, 6841.
66. N. Goldman, M. Brown and G. Khoury, *Cell*, 1981, **24**, 567.
67. K. Hatekeyama, Y. Nemoto, K. Ueda, O. Hayaishi, *J. Biol. Chem.*, 1986, **261**, 14902.
68. H. Maruta, K. Inageda, T. Aoki, H. Nishima and S. Tanuma, *Biochemistry*, 1991, **30**, 5907.
69. G. Brochu, C. Duchaine, L. Thibeault, J. Lageux, G. M. Shah, G. G. Poirier, *Biochim. Biophys. Acta*, 1994, **1219**, 342.
70. J. T. Slama, N. Aboul-Ela, D. M. Goli, B.V. Cheeseman, A. M. Simmons and M. K. Jacobson, *J. Med. Chem.*, 1995, **38**, 389.
71. M. Ikejima, G. Marsischky and D. M. Gill, *J. Biol. Chem.*, 1987, **262**, 17641.
72. K. Uchida, S. Hanai, K. Ishikawa, Y. Ozawa, M. Uchida, T. Sugimura and M. Miwa, *Proc. Natl. Acad. Sci. USA*, 1993, **90**, 3481.
73. P. Zahradka and K. Ebisuzaki, *Eur. J. Biochem.*, 1982, **127**, 579.
74. H. Naegeli and F. R. Althaus, *J. Biol. Chem.*, 1991, **266**, 10596.
75. P. L. Panzeter, C. A. Realini and F. R. Althaus, *Biochemistry*, 1992, **31**, 1379.
76. C. A. Realini and F. R. Althaus, *J. Biol. Chem.*, 1992, **267**, 18858.
77. L. Ménard, L. Thibeault and G. G. Poirier, *Biochim. Biophys. Acta*, 1990, **1049**, 45.
78. H. Thomassin, L. Ménard, C. Hengartner, J. B. Kirkland and G. G. Poirier, *Biochim. Biophys. Acta*, 1992, **1137**, 171.
79. M. S. Satoh, G. G. Poirier and T. Lindahl, *Biochemistry*, 1994, **33**, 7099.
80. B. W. Durkacz, O. Omidiji, D. A. Gray and S. Shall, *Nature*, 1980, **283**, 593.
81. G. de Murcia, A. Huletsky, D. Lamarre, A. Gaudreau, J. Pouyet, M. Daune and G. G. Poirier, *J. Biol. Chem.*, 1986, **261**, 7011.
82. L. Thibeault, M. Hengartner, J. Lageux, G. G. Poirier and S. Muller, *Biochim. Biophys. Acta*, 1992, **1121**, 317.

83. M. Molinete, W. Vermeulen, A. Bürkle, J. Ménissier-de Murcia, J. H. Küpper, J. H. J. Hoeijmakers and G. de Murcia, *EMBO J.*, 1993, **12**, 2109.
84. R. Ding, Y. Pommier, V. H. Kang and M.E. Smulson, *J. Biol. Chem.*, 1992, **267**, 12804.
85. Z. Wang, B. Auer, L. Stingl, H. Berghammer, D. Haidacher, M. Schweiger and E. F. Wagner, *Genes Dev.*, 1995, **9**, 509.
86. T. Boulikas, *Anticancer Res.*, 1991, **11**, 489.
87. V. Schreiber, D. Hunting, C. Trucco, B. Gowans, D. Grunwald, G. de Murcia and J. Ménissier-de Murcia, *Proc. Natl. Acad. Sci. USA*, 1995, **92**, 4753.
88. R. Ding and M. Smulson, *Cancer Res.*, 1994, **54**, 4627.
89. S. Chatterjee, M. Cheng, R. B. Berger, S. J. Berger and N. A. Berger, *Cancer Res.*, 1995, **55**, 868.
90. C. M. G. Simbulan, M. Suzuki, S. Izuta, T. Sakurai, E. Savovsky, K. Kojima, K. Miyahara, Y. Shizuta and S. Yoshida, *J. Biol. Chem.*, 1993, **268**, 93.
91. T. Eki, *FEBS Lett.*, 1994, **356**, 261.
92. C. M. Simbulan-Rosenthal, D. S. Rosenthal, H. Hilz, R. Hickey, L. Malkas, N. Applegren, Y. Wu, G. Bers and M. E. Smulson, *Biochemistry*, 1996, **35**, 11622.
93. M. E. Smulson, V. H. Kang, J. M. Ntambi, D. S. Rosenthal, R. Ding and C. M. G. Simbulan, *J. Biol. Chem.*, 1995, **270**, 119.
94. A. P. Johnstone and G. T. Williams, *Nature*, 1982, **300**, 368.
95. J. A. Gäken, M. Tavassoli, S. Gan, S. Vallian, I. Giddings, D. C. Darling, J. Galea-Lauri, M. G. Thomas, H. Abedi, V. Schreiber, J. Ménissier, M. K. L. Collins, S. Shall and F. Farzaneh, *J. Virology*, 1996, **70**, 3992.
96. C. Nosseri, S. Coppola and L. Ghibelli, *Exp. Cell. Res.*, 1994, **212**, 367.
97. D. E. Fisher, *Cell*, 1994, **78**, 539.

98. W. S. T. Griffin, L. C. Stanley, C. Ling, L. White, V. MacLeod, L. J. Perrot, C. L. White III and C. Araoz, *Proc. Natl. Acad. Sci. USA*, 1989, **86**, 7611.
99. A. M. Ibrado, Y. Huang, G. Fang, L. Liu and K. Bhalla, *Cancer Res.*, 1996, **56**, 4743.
100. V. A. Soldatenkov, S. Prasad, V. Notario and A. Dritschillo, *Cancer Res.*, 1995, **55**, 4240.
101. D. A. Carson, S. Seto, D. B. Wasson and C. J. Carrera, *Exp. Cell. Res.*, 1986, **164**, 273.
102. S. H. Kaufmann, S. Desnoyers, Y. Ottaviano, N. E. Davidson and G. G. Poirier, *Cancer Res.*, 1993, **53**, 3976.
103. Y. A. Lazebnik, S. H. Kaufmann, S. Desnoyers, G. G. Poirier and W. C. Earnshaw, *Nature*, 1994, **371**, 346.
104. M. Tewari, L. T. Quan, K. O' Rourke, S. Desnoyers, Z. Zeng, D. R. Beidler, G. G. Poirier, G. S. Salvesen and V. M. Dixit, *Cell*, 1995, **81**, 801.
105. M. J. Smyth, D. K. Perry, J. Zhang, G. G. Poirier, Y. A. Hannun and L. M. Obeid, *Biochem. J.*, 1996, **316**, 25.
106. Y. A. Lazebnik, A. Takahashi, R. D. Moir, R. D. Goldman, G. G. Poirier, S. H. Kaufmann and W. C. Earnshaw, *Proc. Natl. Acad. Sci. USA*, 1995, **92**, 9042.
107. L. C. Penning, J. W. M. Lagerberg, J. H. VanDierendonck, C. J. Cornelisse, T. M. A. R. Dubbelman and J. VanSteveninck, *Cancer Res.*, 1994, **54**, 5561.
108. W. G. Rice, C. D. Hillyer, B. Harten, C. A. Schaeffer, M. Dorminy, D. A. Lackey III, E. Kirsten, J. Mendeleyev, K. G. Buki, A. Hakam and E. Kun, *Proc. Natl. Acad. Sci. USA*, 1992, **89**, 7703.
109. L. T. Quan, M. Tewari, K. O'Rourke, V. Dixit, S. J. Snipas, G. G. Poirier, C. Ray, D. J. Pickup and G. S. Salvesen, *Proc. Natl. Acad. Sci. USA*, 1996, **93**, 1972.

110. A. J. Darmon, D. W. Nicholson and R. C. Bleackley, *Nature*, 1995, **377**, 446.
111. U. K. Meßmer, D. M. Reimer, J. C. Reed and B. Brüne, *FEBS Lett.*, 1996, **384**, 162.
112. J. Hoshino, C. Koeppel and E. Westhäuser, *Biochim. Biophys. Acta*, 1994, **1201**, 516.
113. D. Monti, A. Cossarizza, S. Salvioli, C. Franceschi, G. Rainaldi, E. Straface, R. Rivabene and W. Malorni, *Biochem. Biophys. Res. Commun.*, 1994, **199**, 525.
114. S. Coppola, C. Nosseri, V. Maresca and L. Ghibelli, *Exp. Cell Res.*, 1995, **221**, 462.
115. B. Heller, Z. Wang, E. F. Wagner, J. Radons, A. Bürkle, K. Fehsel, V. Burkart and H. Kolb, *J. Biol. Chem.*, 1995, **270**, 11176.
116. W. J. D. Whish, M. I. Davies and S. Shall, *Biochem. Biophys. Res. Commun.*, 1975, **65**, 722.
117. M. Smulson, P. Stark, M. Gazzoli and J. Roberts, *Exp. Cell. Res.*, 1975, **90**, 175.
118. H. Juarez-Salinas, J. L. Sims, and M. K. Jacobson, *Nature*, 1979, **282**, 740.
119. G. Ahnström and M. Ljungman, *Mutation Res.*, 1988, **194**, 17.
120. M. R. James and A. R. Lehmann, *Biochemistry*, 1982, **21**, 4007.
121. J. E. Cleaver and W. J. Bodell, W. F. Morgan and B. Zelle, *J. Biol. Chem.*, 1983, **258**, 9059.
122. D. Creissen and S. Shall, *Nature*, 1982, **296**, 271.
123. Y. Ohashi, K. Ueda, M. Kawaichi and O. Hayaishi, *Proc. Natl. Acad. Sci. USA*, 1983, **80**, 3604.
124. V. Bohr and H. Klenow, *Biochem. Biophys. Res. Commun.*, 1981, **102**, 1254.
125. E. Ben-Hur, *Int. J. Radiat. Biol.*, 1984, **46**, 659.
126. E. Ben-Hur, H. Utsumi and M. M. Elkind, *Radiat. Res.*, 1984, **97**, 546.
127. A. M. Ueno, O. Tanaka and H. Matsudaira, *Radiat. Res.*, 1984, **98**, 574.

128. P. Thraves, K. L. Mossman, T. Brennan and A. Dritschilo, *Radiat. Res.*, 1985, **104**, 119.
129. E. Ben-Hur, C. Chen and M. M. Elkind, *Cancer Res.*, 1985, **45**, 2123.
130. J. E. Cleaver, K. M. Milam and W. F. Morgan, *Radiat. Res.*, 1985, **101**, 16.
131. T. Stevnsner, R. Ding, M. Smulson and V. A. Bohr, *Nucleic Acids Res.*, 1994, **22**, 4620.
132. M. S. Satoh, G. G. Poirier and T. Lindahl, *J. Biol. Chem.*, 1993, **268**, 5480.
133. M. S. Satoh, and T. Lindahl, *Cancer Res. (Suppl.)*, 1994, **54**, 1899s.
134. K. Mizumoto and J. L. Farber, *Arch. Biochem. Biophys.*, 1995, **319**, 512.
135. M. A. Babich and R. S. Day III, *Carcinogenesis*, 1988, **9**, 541.
136. R. L. Wells, M. L. Shibuya, E. Ben-Hur and M. M. Elkind, *Cancer Biochem. Biophys.*, 1990, **11**, 97.
137. S. R. Wedge, J. K. Porteous and E. S. Newlands, *Br. J. Cancer*, 1996, **74**, 1030.
138. S. Boulton, L. C. Pemberton, J. K. Porteous, N. J. Curtin, R. J. Griffin, B. T. Golding and B. W. Durkacz, *Br. J. Cancer*, 1995, **72**, 849.
139. K. Moses, A. L. Harris and B. W. Durkacz, *Biochem. Pharmacol.*, 1988, **37**, 2155.
140. K. Moses, A. L. Harris and B. W. Durkacz, *Cancer Res.*, 1988, **48**, 5650.
141. G. Chen and Q-C. Pan, *Cancer Chemother. Pharmacol.*, 1988, **22**, 303.
142. M. R. Horsman, D. M. Brown, D. G. Hirst and J. M. Brown, *Br. J. Cancer*, 1986, **53**, 247.
143. K. M. Milam, G. H. Thomas and J. E. Cleaver, *Exp. Cell Res.*, 1986, **165**, 260.
144. K. M. Milam, and J. E. Cleaver, *Science*, 1984, **223**, 589.
145. R. J. Griffin, N. J. Curtin, D. R. Newell, B. T. Golding, B. W. Durkacz and A. H. Calvert, *Biochimie*, 1995, **77**, 408.
146. G.G. Jonsson, E. Kjellén, R. W. Pero and R. Cameron, *Cancer Res.*, 1985, **45**, 3609.

147. M. R. Horsman, D. J. Chaplin and J. M. Brown, *Radiat. Res.*, 1989, **118**, 139.
148. H. Zheng and P. L. Olive, *Cancer Res.*, 1996, **56**, 2801.
149. J. B. Clark, G. M. Ferris and S. Pinder, *Biochim. Biophys. Acta*, 1971, **238**, 82.
150. M. R. Purnell, P. R. Stone and W. J. D. Whish, *Biochem. Soc. Trans.*, 1980, **8**, 215.
151. J. L. Sims, G. W. Sikorski, D. M. Catino, S. J. Berger and N. A. Berger, *Biochemistry*, 1982, **21**, 1813.
152. S. Shall, *J. Biochem. (Tokyo)*, 1975, **77**, 2p.
153. M. R. Purnell and W. J. D. Whish, *Biochem. Soc. Trans.*, 1980, **8**, 175.
154. P. W. Rankin, E. L. Jacobson, R. C. Benjamin, J. Moss and M. K. Jacobson, *J. Biol. Chem.*, 1989, **264**, 4312.
155. P. Sestili, C. Balsamini, G. Spadoni, F. Cattabeni and O. Cantoni, *Pharmacol. Res. Commun.*, 1988, **20**, 613.
156. O. Cantoni, P. Sestili, G. Spadoni, C. Balsamini, L. Cucchiaroni and F. Cattabeni, *Biochem. Int.*, 1987, **15**, 329.
157. A. E. Shinkwin, M. D. Threadgill and W. J. D. Whish, poster presented at the 211th American Chemical Society Meeting, New Orleans, 1996.
158. M. J. Suto, W. R. Turner, C. M. Arundel-Suto, L. M. Werbel and J. S. Sebolt-Leopold, *Anti-Cancer Drug Design*, 1991, **7**, 107.
159. S. Yoshida, T. Aoyagi, S. Harada, N. Matsude, T. Ikeda, H. Naganawa, M. Hamada and T. Takeuchi, *J. Antibiotics*, 1991, **44**, 111.
160. R. J. Griffin, L. C. Pemberton, D. Rhodes, C. Bleasdale, K. Bowman, A. H. Calvert, N. J. Curtin, B. W. Durkacz, D. R. Newell, J. K. Porteous and B. T. Golding, *Anti-Cancer Drug Design*, 1995, **10**, 507.
161. M. Banasik, H. Komura, M. Shimoyama and K. Ueda, *J. Biol. Chem.*, 1992, **267**, 1569.
162. K. Krohn, H. Heins and K. Wielkens, *J. Med. Chem.*, 1992, **35**, 511.

163. A. D. Pivazyan, E. M. Birks, T. G. Wood, T-S. Lin and W. H. Prusoff, *Biochem. Pharmacol.*, 1992, **44**, 947.
164. C. E. Bell and D. Eisenberg, *Biochemistry*, 1996, **35**, 1137.
165. J. T. Slama and A. M. Simmons, *Biochemistry*, 1988, **27**, 183.
166. J. T. Slama and A. M. Simmons, *Biochemistry*, 1989, **28**, 7688.
167. J. March, *Advanced Organic Chemistry: Reactions, Mechanisms and Structure*, McGraw-Hill, Tokyo, 1977, second edition, p. 661.
168. E. N. Jacobsen, I. Markó, W. S. Mungall, G. Schröder and K. B. Sharpless, *J. Am. Chem. Soc.*, 1988, **110**, 1968.
169. B. B. Lohray, *Tetrahedron Asymm.*, 1992, **3**, 1317.
170. K. B. Sharpless, W. Amberg, Y. L. Bennai, G. A. Crispino, J. Hartug, K-S. Jeong, H-L. Kwong, K. Morikawa, Z-M. Wang, D. Xu and X-L. Zhang, *J. Org. Chem.*, 1992, **57**, 2768.
171. N. Sperber, D. Papa and E. Schwenk, *J. Am. Chem. Soc.*, 1948, **70**, 3091.
172. C. R. Hauser and D. S. Hoffenberg, *J. Org. Chem.*, 1955, **20**, 1448.
173. W. Roberts and M. C. Whiting, *J. Chem. Soc.*, 1965, 1290.
174. C. R. Noller, W. W. Hartman and L. A. Smith, *Org Synth.*, Wiley, New York, 1943, Coll. Vol. II, 586.
175. A. L. Beckwith in *The Chemistry of Amides*, ed. J. Zabicky, Wiley-Interscience, London, 1970, 123.
176. C. S. Marvel and C. G. Overberger, *J. Am. Chem. Soc.*, 1945, **67**, 2250.
177. S. Servi, *Synthesis*, 1990, 1.
178. D. D. Ridley and M. Stralow, *J. Chem. Soc., Chem. Commun.*, 1975, 400.
179. A. Manzocchi, A. Fiecchi and E. Santaniello, *J. Org. Chem.*, 1988, **53**, 4405.
180. P. Ferraboschi, P. Grisenti, A. Manzocchi and E. Santaniello, *Tetrahedron*, 1994, **50**, 10539.
181. R. M. Moriarty, B. A. Berglund and R. Penmasta, *Tetrahedron Lett.*, 1992, **33**, 6065.

182. T. Kometani, Y. Morita, H. Furui, H. Yoshii and R. Matsuno, *Chem. Lett.*, 1993, 2123.
183. V. Prelog, *Pure Appl. Chem.*, 1964, **9**, 119.
184. P. A. Levene and A. Walti, *Org. Synth.*, Wiley, New York, 1943, Coll. Vol. II, 545.
185. P. Ferraboschi, P. Grisenti, A. Manzocchi and E. Santiello, *J. Chem. Soc., Perkin Trans. 1*, 1990, 2469.
186. M. H. Holshouser and M. Kolb, *J. Pharm. Sci.*, 1986, **75**, 619.
187. A. Kaufmann and H. Müller, *Ber. Dtsch. Chem. Ges.*, 1918, **51**, 123.
188. S. Yamaguchi in *Asymmetric Synthesis*, ed. J. D. Morrison, Academic Press, New York, 1983, vol. 1, p.125.
189. D. Parker, *Chem. Rev.*, 1991, **91**, 1441.
190. J. A. Dale, D. L. Dull and H. S. Mosher, *J. Org. Chem.*, 1969, **34**, 2543.
191. N. Kato, *J. Am. Chem. Soc.*, 1990, **112**, 254.
192. H. Gerlach and B. Zagalak, *J. Chem. Soc., Chem. Commun.*, 1973, 274.
193. R. R. Fraser in *Asymmetric Synthesis*, ed. J. D. Morrison, Academic Press, New York, 1983, vol. 1, p.173.
194. R. R. Fraser, M. A. Petit and J. K. Saunders, *J. Chem. Soc., Chem. Commun.*, 1971, 1450.
195. S. Li and W. C. Purdy, *Chem. Rev.*, 1992, **92**, 1457.
196. D. D. MacNicol, *Tetrahedron Lett.*, 1975, **38**, 3325.
197. D. Greatbanks and R. Pickford, *Magn. Reson. Chem.*, 1987, **25**, 208.
198. W. H. Pirkle and J. Finn in *Asymmetric Synthesis*, ed. J. D. Morrison, Academic Press, New York, 1983, vol. 1, p.87.
199. J. A. Dale and H. S. Mosher, *J. Org. Chem.*, 1970, **35**, 4002.
200. B.B. Lohray, *Synthesis*, 1992, 1035.
201. M. S. Berridge, M. P. Franceschini, E. Rosenfeld and T. J. Tewson, *J. Org. Chem.*, 1990, **55**, 1211.
202. S. E. Denmark, *J. Org. Chem.*, 1981, **46**, 3144.
203. Y. Gao and K. B. Sharpless, *J. Am. Chem. Soc.*, 1988, **110**, 7538.

204. B. M. Kim and K. B. Sharpless, *Tetrahedron Lett.*, 1990, **31**, 4317.
205. B. E. Rossiter, T. Katsuki and K. B. Sharpless, *J. Am. Chem. Soc.*, 1981, **103**, 464.
206. G. Berti, *Top. Stereochem.*, 1973, **7**, 93.
207. B. T. Golding, D. R. Hall and S. Sakrikar, *J. Chem. Soc., Perkin Trans. I*, 1973, 1214.
208. K. Mori, *Tetrahedron*, 1976, **32**, 1101.
209. M. K. Ellis and B. T. Golding in *Org. Synth.*, ed. G. Saucy, Wiley, New York, 1985, vol. 63, 140.
210. J. C. Martin, J.A. Franz and R. J. Arhart, *J. Am. Chem. Soc.*, 1974, **96**, 4604.
211. J. A. Franz and J. C. Martin, *J. Am. Chem. Soc.*, 1973, **95**, 2017.
212. O. C. Dermer and G. E. Ham, *Ethylenimine and Other Aziridines*, Academic Press, New York, 1969.
213. J.A. Deyrup in *Small Ring Heterocycles*, ed. A. Hassner, Wiley-Interscience, New York, 1983, Part 1, p.2.
214. H. Wenker, *J. Am. Chem. Soc.*, 1935, **57**, 2328.
215. E. L. Stogryn and S. J. Bois, *J. Org. Chem.*, 1965, **30**, 88.
216. J. P. Freeman and P. J. Mondron, *Synthesis*, 1974, 894.
217. I. Okada, K. Ichimura and R. Sudo, *Bull. Chem. Soc., Japan*, 1970, **43**, 1185.
218. R. Appel and R. Kleinstück, *Chem. Ber.*, 1974, **107**, 5.
219. J. R. Pfister, *Synthesis*, 1984, 969.
220. A. G. Giumanini, *J. Org. Chem.*, 1972, **37**, 513.
221. M. M. Ponpipom and S. Hanessian, *Carbohydrate Res.*, 1971, **18**, 342.
222. S. Kappus and W. J. D. Whish, *Biochem. Soc. Trans.*, 1996, **24**, 120S.
223. E. Wenkert, D. B. R. Johnston and K. G. Dave, *J. Org. Chem.*, 1964, **29**, 2534.
224. W-C. Lin and T. H. Morton, *J. Org. Chem.*, 1991, **56**, 6850.

225. T. Sakamoto, M. An-naka, Y. Kondo and H. Yamanaka, *Chem. Pharm. Bull.*, 1986, **34**, 2754.
226. T. Sakamoto, Y. Kondo and H. Yamanaka, *Chem. Pharm. Bull.*, 1985, **33**, 626.
227. T. Sakamoto, N. Miura, Y. Kondo and H. Yamanaka, *Chem. Pharm. Bull.*, 1986, **34**, 2760.
228. G. S. Ponticello and J. J. Baldwin, *J. Org. Chem.*, 1979, **44**, 4003.
229. J. March, *Advanced Organic Chemistry*, McGraw-Hill, Tokyo, 1977, second edition, p. 813.
230. K. Edo, T. Sakamoto and H. Yamanaka, *Chem. Pharm. Bull.*, 1979, **27**, 193.
231. T. Sakamoto, M. Shiraiwa, Y. Kondo, H. Yamanaka, *Synthesis*, 1983, 312.
232. L. N. Pridgen, *J. Heterocycl. Chem.*, 1980, **17**, 1289.
233. K. Tamao, S. Kodama, I. Nakajima, M. Kumada, A. Minato and K. Suzuki, *Tetrahedron*, 1982, **38**, 3347.
234. H. Gilman and T. S. Soddy, *J. Org. Chem.*, 1957, **22**, 565.
235. J. B. Wommack, T. G. Barbee, Jr, D. J. Thoennes, M. A. McDonald and D. E. Pearson, *J. Heterocyclic Chem.*, 1969, **6**, 243.
236. R. D. J. Clipperton, Ph. D. Thesis, University of Bath, 1969.
237. W. E. Parham and R. M. Piccirilli, *J. Org. Chem.*, 1977, **42**, 257.
238. R. Barker and H. G. Fletcher, Jnr, *J. Org. Chem.*, 1961, **26**, 4605.
239. M. Kawana, H. Kuzuhara and S. Emoto, *Bull. Chem. Soc. Jpn.*, 1981, **54**, 1492.
240. W. Timpe, K. Dax, N. Wolf, and H. Weidmann, *Carbohydr. Res.*, 1975, **39**, 53.
241. M. M. Robison and B. L. Robison, *J. Am. Chem. Soc.*, 1958, **80**, 3443.
242. E. Ochiai and Y. Kawazoe, *Chem. Pharm. Bull.*, 1957, **5**, 289.
243. E. Ochiai and Y. Kawazoe, *Chem. Pharm. Bull.*, 1960, **8**, 24.
244. H. Win and K. Koshinuma, *J. Org. Chem.*, 1967, **32**, 59.
245. F. Eloy and A. Deryckere, *Helv. Chim. Acta*, 1969, **52**, 1755.

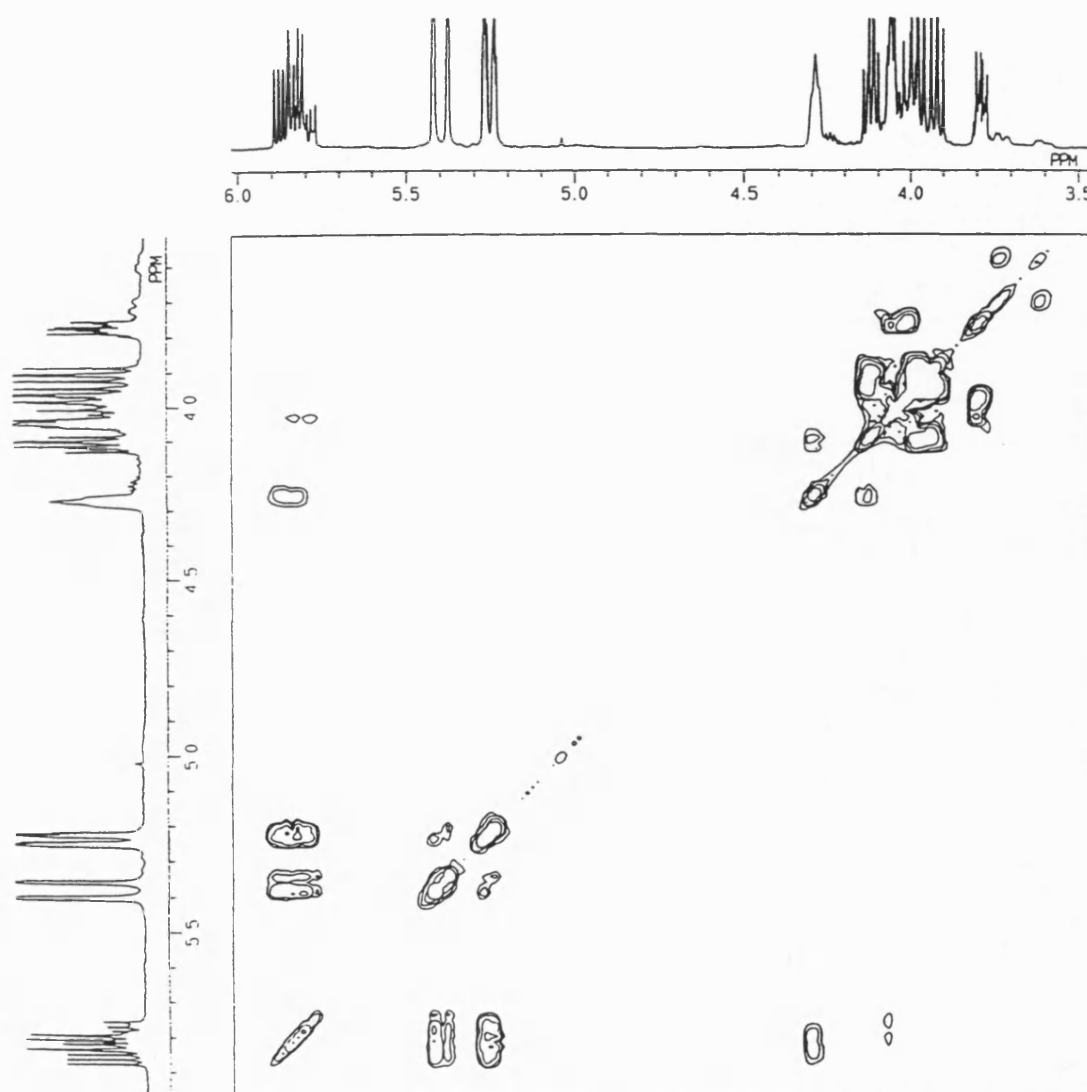
246. J. Klein and E. D. Bergman, *J. Am. Chem. Soc.*, 1957, **79**, 3452.
247. J. E. Plevyak, J. E. Dickerson and R. F. Heck, *J. Org. Chem.*, 1979, **44**, 4078.
248. R. F. Heck, *Organic Reactions*, 1982, **27**, 345.
249. R. F. Heck in "Comprehensive Organic Synthesis" ed. B. M. Trost, Pergamon Press, Oxford, 1991, vol. 4, 833.
250. C. Kaneko, N. Katagiri, K. Uchiyama and T. Yamada, *Chem. Pharm. Bull.*, 1985, **33**, 4160.
251. L. W. Deady, W. L. Finlayson and C. H. Potts, *Aust. J. Chem.*, 1977, **30**, 1349.
252. T. Matsui, T. Sugiura, H. Nakai, S. Iguchi, S. Shigeoka, H. Takada, Y. Odagaki, Y. Nagao, Y. Ushio, K. Ohmoto, H. Iwamura, S. Yamazaki, Y. Arai and M. Kawamura, *J. Med. Chem.*, 1992, **35**, 3307.
253. E. J. Corey and G. Schmidt, *Tetrahedron Lett.*, 1979, 399.
254. R. M. Acheson and G. C. M. Lee, *J. Chem. Soc., Perkin Trans. 1*, 1987, 2321.
255. J. B. Melpolder and R. F. Heck, *J. Org. Chem.*, 1976, **41**, 265.
256. A. J. Clark and S. A. Magennis, *J. Org. Chem.*, 1976, **41**, 1206.
257. J. Nokami, H. Ogawa, S. Miyamoto, T. Mandai, S. Wakabayashi and J. Tsuji, *Tetrahedron Lett.*, 1988, **29**, 5181.
258. R. Dumont and H. Pfander, *Helv. Chim. Acta*, 1983, **66**, 814.
259. V. Jäger, D. Schröter and B. Koppenhoeffler, *Tetrahedron*, 1991, **47**, 2195.
260. L. C. Pemberton, C. Bleasdale, A. H. Calvert, N. J. Curtin, B. W. Durkacz, B. T. Golding, R. J. Griffin, D. R. Newell and D. Rhodes, presented at NCI/EORTC New Drug Symposium, Amsterdam. 1994.
261. M. V. R. Reddy, S. Vijayalakshmi, D. B. Reddy and P. V. R. Reddy, *Phosphorus, Sulfur and Silicon*, 1991, **60**, 209.
262. *Aldrich catalogue*, 1993.
263. J. Bromilow, R. T. C. Brownlee, D. J. Craik, P. R. Fiske, J. E. Rowe and M. Sadek, *J. Chem. Soc., Perkin Trans. 2*, 1981, 753.

264. A. A. Morozov, *Zh. Obshch. Khim.*, 1989, **59**, 215.
265. E. Gryszkiewicz-Trochimowski, W. Schmidt and O. Gryszkiewicz-Trochimowski, *Bull. Soc. Chim. France*, 1948, 593.
266. A. A. Santilli, A. C. Scotese, R. L. Morris and S. C. Bell, *J. Heterocyclic Chem.*, 1991, **28**, 2025.
267. B. Elpern and C. S. Hamilton, *J. Am. Chem. Soc.*, 1946, **68**, 1436.
268. E. Ochiai and M. Ikehara, *J. Pharm. Soc. Japan*, 1953, **73**, 666.
269. A. R. Osborn, K. Schofield and L. N. Short, *J. Chem. Soc.*, 1956, 4191.
270. W. Miersch, *Chem. Ber.*, 1882, **25**, 2109.
271. W. S. Rapson and R. G. Shuttleworth, *J. Chem. Soc.*, 1941, 487
272. R. G. R. Bacon and W. S. Lindsay, *J. Chem. Soc.*, 1958, 1375.
273. S. Gabriel and M. Herzberg, *Ber. Deut. Chem. Ges.*, 1883, **16**, 2036.
274. M. Noguchi, S. Kakimoto, H. Kawakami and S. Kajigaeshi, *Bull. Chem. Soc. Jpn.*, 1986, **59**, 1355.

APPENDIX A

^1H NMR COSY Spectrum (399.65 MHz, CDCl_3)

4*R*-2,2-Dimethyl-4-(1-hydroxyprop-2-enyl)-1,3-dioxolane **135**



^1H NMR COSY Spectrum (399.65 MHz, CDCl_3)

3-(3-(4*R*-2,2-Dimethyl-1,3-dioxolan-4-yl)-3-hydroxyprop-1-en-yl)isoquinolin-1-one **141**.

